

UNIVERSIDADE FEDERAL DE MINAS GERAIS
INSTITUTO DE CIÊNCIAS BIOLÓGICAS
DEPARTAMENTO DE MORFOLOGIA
PROGRAMA DE PÓS-GRADUAÇÃO EM BIOLOGIA CELULAR

Camila Ferreira Sales

**ESTUDO DA INTER-RELAÇÃO DAS VIAS AUTOFÁGICAS E APOPTÓTICAS
DURANTE A ESPERMATOGÊNESE E REGRESSÃO OVARIANA DA TILÁPIA DO
NILO *OREOCHROMIS NILOTICUS* EM CONDIÇÕES DE CULTIVO.**

Belo Horizonte
2020

Camila Ferreira Sales

**ESTUDO DA INTER-RELAÇÃO DAS VIAS AUTOFÁGICAS E
APOPTÓTICAS DURANTE A ESPERMATOGÊNESE E REGRESSÃO
OVARIANA DA TILÁPIA DO NILO *OREOCHROMIS NILOTICUS* EM
CONDIÇÕES DE CULTIVO.**

Versão final

Tese apresentada ao Programa de Pós-graduação em Biologia Celular da Universidade Federal de Minas Gerais, como requisito parcial para a obtenção do título de doutora em Biologia Celular

Orientadora: Dra. Elizete Rizzo

Co-orientador: Dr. Ronald Kennedy Luz

Belo Horizonte
2020

043

Sales, Camila Ferreira.

Estudo da inter-relação das vias autofágicas e apoptóticas durante a espermatogênese e regressão ovariana da tilápia do Nilo *Oreochromis niloticus* em condições de cultivo [manuscrito] / Camila Ferreira Sales. – 2020.

113 f. : il. ; 29,5 cm.

Orientadora: Dra. Elizete Rizzo. Co-orientador: Dr. Ronald Kennedy Luz.
Tese (doutorado) – Universidade Federal de Minas Gerais, Instituto de Ciências Biológicas. Programa de Pós-Graduação em Biologia Celular.

1. Biologia Celular. 2. Apoptose. 3. Autofagia. 4. Atresia Folicular. 5. Ciclídeos. 6. Espermatogênese. 7. Jejum. I. Bazzoli, Elizete Rizzo. II. Luz, Ronald Kennedy. III. Universidade Federal de Minas Gerais. Instituto de Ciências Biológicas. IV. Título.

CDU: 576



ATA DA DEFESA DE TESE DE DOUTORADO DE

CAMILA FERREIRA SALES

223/2020
entrada
1º/2016
2016686302

Às nove horas do dia 20 de fevereiro de 2020, reuniu-se, no Instituto de Ciências Biológicas da UFMG, a Comissão Examinadora da Tese, indicada pelo Colegiado do Programa, para julgar, em exame final, o trabalho final intitulado: "ESTUDO DA INTER-RELAÇÃO DAS VIAS AUTOFÁGICAS E APOPTÓTICAS DURANTE A ESPERMATOGÊNESE E REGRESSÃO OVARIANA DA TILÁPIA DO NILO OREOCHROMIS NILOTICUS EM CONDIÇÕES DE CULTIVO", requisito final para obtenção do grau de Doutora em Biologia Celular. Abrindo a sessão, a Presidente da Comissão, **Dra. Elizete Rizzo Bazzoli**, após dar a conhecer aos presentes o teor das Normas Regulamentares do Trabalho Final, passou a palavra à candidata, para apresentação de seu trabalho. Seguiu-se a arguição pelos examinadores, com a respectiva defesa da candidata. Logo após, a Comissão se reuniu, sem a presença da candidata e do público, para julgamento e expedição de resultado final. Foram atribuídas as seguintes indicações:

Prof./Pesq.	Instituição	Indicação
Dra. Elizete Rizzo Bazzoli	UFMG	APROVADA
Dr. Ralph Gruppi Thomé	UFSJ	APROVADA
Dr. Guilherme Mattos Jardim Costa	UFMG	APROVADA
Dr. Hélio Batista dos Santos	UFSJ	APROVADA
Dr. Vinicius de Toledo Ribas	UFMG	APROVADA

Pelas indicações, a candidata foi considerada: APROVADA
O resultado final foi comunicado publicamente à candidata pela Presidente da Comissão. Nada mais havendo a tratar, a Presidente encerrou a reunião e lavrou a presente ATA, que será assinada por todos os membros participantes da Comissão Examinadora. **Belo Horizonte, 20 de fevereiro de 2020.**

Dr^a. Elizete Rizzo Bazzoli (Orientadora)

Dr. Ralph Gruppi Thomé

Dr. Guilherme Mattos Jardim Costa

Dr. Hélio Batista dos Santos

Dr. Vinicius de Toledo Ribas

Obs: Este documento não terá validade sem a assinatura e carimbo do Coordenador

Prof. Vanessa Pinho da Silva
Sub-Coordenadora do Programa de
Pós Graduação em Biologia Celular ICB/UFMG

Dedico este trabalho primeiramente a Deus, aos meus pais, Antônio e Maria e ao meu noivo Marley, pelo apoio, compreensão e carinho e por sempre acreditarem em meus sonhos, principalmente nos momentos mais difíceis.

AGRADECIMENTOS

A DEUS por toda força e saúde, por sempre colocar pessoas especiais em meu caminho e por me acompanhar sempre.

A minha orientadora Dra. Elizete Rizzo pelos ensinamentos, disponibilidade e amizade durante esses quatro anos.

A todos os meus familiares que foram meu alicerce.

Ao professor Dr. Rafael pelos materiais cedidos para realização do capítulo 1, pelo apoio e ajuda na condução deste trabalho.

Aos colegas de laboratório, Yves, Davidson, André, Alessandro, Lourenço, Camila, Marina, Samuel, Thaís e Chico pelo apoio, amizade e ajuda em todos os momentos desta caminhada, em especial a Ana Paula pela parceria e essencial contribuição neste trabalho.

Aos alunos do Laboratório de Aquacultura (LAQUA), pela ajuda na manutenção dos tanques e durante as coletas, em especial ao Cristiano.

As instituições de fomento Conselho Nacional de Desenvolvimento Científico e Tecnológico (CNPq), Fundação de Amparo à Pesquisa do Estado de Minas Gerais (FAPEMIG) e Coordenação de Aperfeiçoamento de Pessoal de Nível Superior (CAPES).

Aos professores e funcionários do Programa de Pós-graduação.

Àqueles que de alguma forma contribuíram não apenas para a realização deste sonho, mas acima de tudo, para o meu crescimento enquanto pessoa.

MUITO OBRIGADA.

RESUMO

Apoptose e autofagia são vias de sinalização altamente conservadas e são essenciais em diversos processos fisiológicos. Apesar dos avanços recentes, ainda há muitas lacunas no conhecimento das suas interações, especialmente em vertebrados não mamíferos. Neste sentido, o objetivo do presente estudo foi investigar a interação das vias autofágica e apoptótica na atresia folicular e na espermatogênese de tilápia do Nilo, *Oreochromis niloticus*, em condições de cultivo. Para isso, o projeto foi desenvolvido em três etapas. Na primeira etapa, para investigar a interação das vias autofágica e apoptótica na atresia folicular, animais recém desovados foram mantidos em condição de cultivo e amostras de ovários foram coletadas para análises morfológicas, técnica de TUNEL e imunohistoquímica. A atresia folicular nos ovários de *O. niloticus* foi analisada em três estágios de regressão: folículos atrésicos iniciais (AF_E), avançados (AF_A) e tardios (AF_L). Nos folículos atrésicos iniciais e avançados as células foliculares apresentaram grandes lisossomos e autofagossomos contendo mitocôndrias em degeneração, restos de organelas e grânulos elétron-densos. Além disso, foram observados aumentos significativos nas imunomarcações de Bcl-2, Catepsina-D, Beclin-1 e LC3. Nos folículos atrésicos tardios, as células foliculares apresentaram um citoplasma elétron-lúcido e apoptose aumentada com imunorreatividade para Bax e muitas células positivas para TUNEL. Além disso, a colocalização entre LC3 e Caspase-3 em AF_L e LAMP-1 e Catepsina-D em AF_E e AF_A mostrou pontos de interação entre autofagia e apoptose durante atresia folicular de tilápia do Nilo. Na segunda e terceira etapa desse trabalho, nós avaliamos a atuação das vias autofágica e apoptótica durante a espermatogênese em animais submetidos ao sistema de realimentação e a restrição alimentar total por 7, 14, 21 e 28 dias. A análise dos efeitos do jejum sobre os parâmetros bioquímicos, hormonais e morfológicos mostrou que após 7 dias de jejum, os níveis glicêmicos e lipídicos foram significativamente reduzidos, seguidos pela redução plasmática de testosterona (T) e 11-ketotestosterona (11-KT). Além disso, foi observado a proliferação reduzida de espermatogônias e aumento da apoptose em espermatócitos, espermatídes e espermatozoides. Nos grupos de realimentação, os esteroides sexuais e a proporção de células germinativas não apresentaram alterações significativas em relação ao grupo controle, exceto pela redução de espermatozoides. A atuação da via autofágica durante a espermatogênese foi evidenciada pela imunomarcação de LC3 e Beclin-1 e pela presença de estruturas autofágicas como autofagossomos, autolisossomos e corpos multilamelares em espermatócitos secundários, espermatídes, células de Sertoli e de Leydig. A apoptose foi identificada principalmente em espermatócitos e espermatídes, com aumento significativo após 21 e 28 dias de jejum. Em conjunto, nossos dados mostraram a atuação da autofagia na manutenção da viabilidade celular

no estágio inicial da atresia folicular e durante a espermatogênese da tilápia do Nilo. No estágio final da atresia folicular, a via autofágica e a liberação de catepsina-D no citoplasma atuaram em cooperação com a apoptose para remodelação tecidual característica da atresia. Nos machos submetidos ao jejum prolongado, houve redução progressiva de T e 11-TK redução da autofagia e aumento significativo da apoptose das células germinativas resultando em danos à produção de células espermatogênicas.

Palavras-chave: Testosterona. Células Germinativas. Marcadores Autofágicos. Teleósteos. Restrição Alimentar.

ABSTRACT

Apoptosis and autophagy are highly conserved signaling pathways between species, essential in several physiological. Despite recent advances, there are still many gaps in the knowledge of their interactions, and especially in non-mammalian vertebrates. In this sense, the aim of the present study was to investigate the interaction between autophagy and apoptosis in follicular atresia and spermatogenesis of Nile tilapia *Oreochromis niloticus* under cultivation conditions, and, for this, the project was developed in three stages. In the first stage, to investigate the interaction of autophagic and apoptotic pathways in follicular atresia, freshly spawned animals were kept in culture condition and ovarian samples were collected for morphological analysis, TUNEL technique and immunohistochemistry. The follicular atresia in the ovaries of *O. niloticus* was analyzed in 3 stages of regression: early (AF_E), advanced (AF_A) and late (AF_L) atretic follicles. Early and advanced atretic follicles presented autophagy in follicular cells by the presence of large lysosomes and autophagosomes with degenerating mitochondria, organelles debris and electron-dense granules. Moreover, it were observed significant increases of immunoreactivity for Bcl-2, Cathepsin-D, Beclin-1 and LC3. In late atretic follicles, the follicular cells presented a markedly electron-lucid cytoplasm and increased apoptosis, with immunoreactivity for Bax and many TUNEL positive cells. In addition, the colocalization between LC3 and Caspase-3 in AF_L and LAMP-1 and Cathepsin-D in AF_E and AF_A showed points of interaction between autophagy and apoptosis during follicular atresia of Nile tilapia. In the second and third stage of this work, we evaluated the performance of the autophagic and apoptotic pathways during spermatogenesis in animals submitted to system of refeeding and total food restriction for 7, 14, 21 and 28 days. Analysis of the effects of starvation on biochemical, hormonal and morphological parameters showed that, glycemic and lipid levels were significantly reduced, followed by plasma reduction of testosterone (T) and 11-ketotestosterone (11-KT). In addition, reduced proliferation of spermatogonia and increased apoptosis of spermatocytes, spermatids and spermatozoa were observed. In the refeeding groups, the sex steroids and the proportion of germ cells had no significant alterations compared to the control group, except for reduction of spermatozoa. The performance of the autophagic pathway during spermatogenesis was evidenced by immunostaining of LC3 and Beclin-1 and by the presence of autophagic structures, such as autophagosomes, autolysosomes and multilamellar bodies in secondary spermatocytes, spermatids and Sertoli and Leydig cells. However, after 21 days of starvation apoptosis increased mainly in spermatocytes and

spermatids. Together, our data showed the role of autophagy in maintaining cell viability was evidenced in the early stages of follicular atresia and during spermatogenesis of Nile tilapia. In the final stage of follicular atresia, the autophagic pathway and the release of cathepsin-D in the cytoplasm acted in cooperation with apoptosis for tissue remodeling characteristic of atresia. In males submitted to prolonged fasting, there was a progressive reduction in T and 11-TK reduction in autophagy and a significant increase in germ cell apoptosis resulting in damage to sperm cell production.

Keywords: Testosterone. Germ Cells. Autophagic Markers. Teleost. Food Restriction.

LISTA DE ILUSTRAÇÕES

Figura 1 - Principais tipos de autofagia e caminhos que convergem aos lisossomas	11
Figura 2 - Conexões entre os processos autofágico e apoptótico	15
Figura 3 - Vias de morte celular por permeabilização da membrana lisossomal (LMP)	17

LISTA DE ABREVIATURAS E SIGLAS

A_{UND}: Espermatogônias do tipo A Indiferenciada

A_{DIFF}: Espermatogônias do tipo A diferenciada

A_{FE}: Folículo atrésico inicial

A_{FA}: Folículo atrésico avançado

A_{FL}: Folículo atrésico final

AF: Autofagossomo

AL: Autolisossomo

ATG: Autophagy-related genes

BAX: BCL 2 homologous antagonista

BCL-2: B-CELL LYMPHOMA-2

B: Espermatogônias do tipo B

C: Espermatócitos

DAPI: 4',6'-Diamino-2-fenil-indol

DAB: 3,3-Diaminobenzidina

DISC: Complexo de sinalização indutor de morte

FA: Folículo atrésico

FADD: Domínio de morte associado ao faz

FLIP: Proteína inibidora do tipo flice

FC: Células foliculares

FPO: Folículo pós-ovulatório

FSH : Folículo estimulante

HE: Hematoxilina e eosina

IGS: Índice gonadossomático

LH : Hormônio luteinizante

LE: Células de Leydig

LMP: Permeabilização da membrana lisossomal

SE: Células de sertoli

TUNEL: Terminal deoxynucleotidyl transferase dutp nick end labeling

T: Testosterona

Z: Espermatozóides

11KT 11 Ketotetosterona

SUMÁRIO

1.0. INTRODUÇÃO	11
1.1. Autofagia	11
1.2. Apoptose.....	13
1.3. Inter-relação das vias autofágicas e apoptóticas.....	14
1.4. Lisossomos e morte celular.....	16
1.5. Gametogênese.....	18
1.5.1. Ovogênese.....	18
1.5.2. Espermatogênese.....	19
1.6. Restrição alimentar.....	21
1.7. Tilápia de Nilo.....	21
2.0. JUSTIFICATIVA.....	22
3.0. OBJETIVOS.....	23
3.1. OBJETIVO GERAL.....	23
3.2. OBJETIVOS ESPECÍFICOS.....	23
4.0. RESULTADOS.....	23
4.1. CAPÍTULO 1: (artigo publicado na revista Molecular Reproduction and Development.....	25
4.2. CAPÍTULO 2: (artigo publicado na revista Molecular and Cellular Endocrinology)	37
4.3. CAPÍTULO 3: Autophagy and apoptosis during fish spermatogenesis: insights from Nile tilapia	48
5.0 DISCUSSÃO GERAL.....	65
6.0. CONCLUSÕES.....	69
7.0. REFERÊNCIAS BIBLIOGRÁFICAS.....	70
8.0. ANEXOS (ARTIGOS PUBLICADOS DURANTE O DOUTORADO) E CO-ORIENTAÇÃO DE MONOGRAFIA.....	81

1.0. INTRODUÇÃO

1.1. Autofagia

Autofagia se refere à via catabólica lisossomal de degradação de componentes intracelulares, essencial no desenvolvimento, diferenciação e manutenção da homeostasia celular podendo levar à sobrevivência ou morte celular (Ryter *et al.*, 2013, 2014; Agnello and Chiarelli, 2016). A via autofágica é conservada entre as espécies e ocorre praticamente em todas as células. Essa via é finamente regulada por proteínas codificadas por genes ATG, e apresenta proteínas homólogas em levedo e mamíferos como, por exemplo, ATG6/Beclin 1 e ATG8/LC3 (Uchiyama *et al.*, 2008). A autofagia pode ser classificada em três principais tipos de acordo com a função fisiológica e ao modo de entrega da carga ao lisossomo: 1) microautofagia, 2) autofagia mediada por chaperonas e 3) macroautofagia (Fig 1).

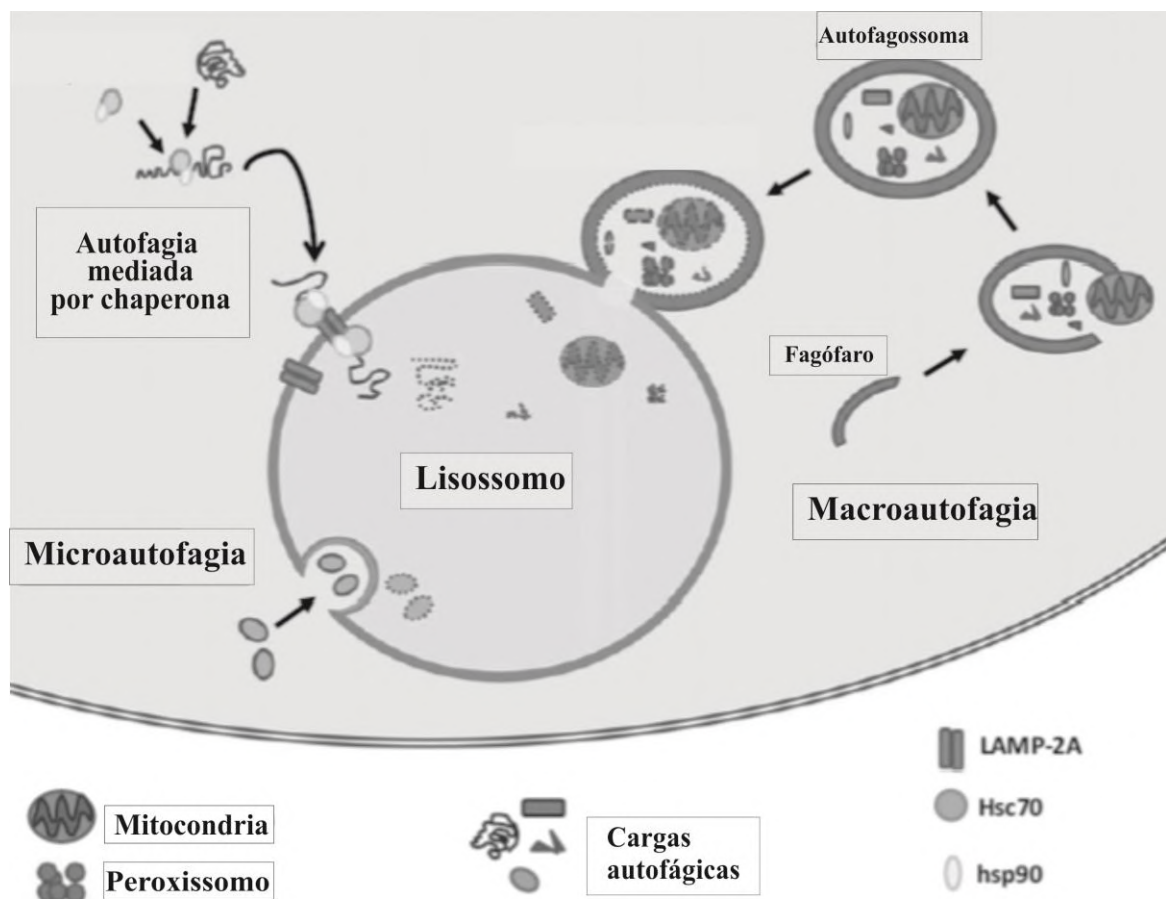


Figura 1: Principais tipos de autofagia e caminhos que convergem aos lisossomos (Mrschtik and Ryan 2015; adaptado)

Na microautofagia ocorre a incorporação seletiva ou não seletiva de componentes citosólicos diretamente em lisossomos através de invaginações da membrana lisossomal (Mizushima and Komatsu, 2011). Na autofagia mediada por chaperonas, proteínas citoplasmáticas marcadas com a sequência de aminoácidos KFERQ ligam-se a chaperonas, como Hsp73, e são transportadas aos lisossomos através da interação com receptor LAMP-2 (Alerting, 2007). A macroautofagia usualmente chamada de autofagia é a via melhor estudada de degradação lisossomal. Durante a autofagia, estruturas de membrana com dupla bicamada lipídica (autofagossomos) são capazes de englobar e isolar vários constituintes celulares e até organelas inteiras (Gómez-Sintes *et al.*, 2016).

Na fase inicial da autofagia, ocorre a formação do fagóforo (ou membrana de isolamento) onde componentes citoplasmáticos são sequestrados no início da autofagia. O fagóforo expande-se através da aquisição de lipídeos, formando o autofagossomo (Soto-Burgos *et al.*, 2018). Em mamíferos, estudos recentes mostraram que autofagossomos são formados na interface retículo endoplasmático-mitocôndria (Hamasaki *et al.*, 2013). A proteína beclin-1 (homóloga a Atg6 de levedo) que compõe o complexo PI3 kinase classe III (PI3K) apresenta um papel central na formação do fagóforo, coordenando e regulando a mobilização de membranas para a formação do autofagossomo (Kang *et al.*, 2011).

A fase de alongamento, onde ocorre a expansão da membrana do autofagossomo, requer o recrutamento de proteínas como a proteína de cadeia leve 3 associada a microtúbulos (LC3). LC3 é produto do gene homólogo MAP1LC3 e após um estímulo autofágico, LC3-I sofre lipidação por conjugação com fosfatidiletanolamina e então é convertida em LC3-II que passa a integrar a membrana interna e externa do autofagossomo (He *et al.*, 2015). LC3-II é responsável pela seleção do substrato a ser degradado pela autofagia e possui um domínio que interage e recruta outras proteínas para a membrana do autofagossomo (Kabeya, 2000; He *et al.*, 2015). LC3 II é exclusivamente expressa durante a autofagia, sendo usado no monitoramento desse processo (Klionsky *et al.*, 2016). Outro importante marcador de fluxo autofágico é a proteína p62. Esta proteína é capaz de reconhecer e interagir com proteínas ubiquitinadas por meio de associação ao domínio ubiquitina. Posteriormente, p62 interage com LC3 sendo assim incorporada ao lúmen do autofagossomo e degradada pela autofagia (Hansen and Johansen, 2011). Devido a sua degradação, p62 atua como um marcador inverso da atividade autofágica (Mizushima and Komatsu, 2011; Pan *et al.*, 2011)

O processo de maturação do autofagossomo inclui a fusão com endossomo tardio e/ou com lisossomo formando estrutura conhecida como autolisossomo, onde o material interno e a

membrana autofagossomal serão completamente degradados pelas hidrolases ácidas lisossomais. A fusão desses componentes ocorre por atuação de diversas proteínas, dentre elas destaca-se as proteínas de membrana lisossomal, denominadas Lamp-1 e Lamp-2 (Huynh *et al.*, 2007). Além de fusão entre as membranas, essas proteínas são altamente glicosiladas, sendo responsáveis pela manutenção da integridade estrutural da membrana lisossomal, protegendo-a do ambiente luminal hostil (Eskelinen, 2005; Huynh *et al.*, 2007).

1.2. Apoptose

Apoptose é altamente conservada durante a evolução, sendo um processo fisiológico essencial para a manutenção do desenvolvimento e do número apropriado de células no tecido (Kerr *et al.*, 1972). Este processo é descrito como o principal mecanismo de morte celular programada, entretanto outras formas de morte celular programada podem também ocorrer em diferentes condições (Kroemer *et al.*, 2009; Galluzzi *et al.*, 2018). As células apoptóticas apresentam características morfológicas típicas tais como: retração celular, perda de adesão célula-célula e célula-matriz extracelular, condensação da cromatina em um padrão crescente subjacente ao envelope nuclear e formação de corpos apoptóticos (Robertson and Orrenius, 2000). Externalização de fosfatidilserina na membrana plasmática leva a estimulação de fagócitos e células vizinhas saudáveis, que fagocitam os corpos apoptóticos sem desencadear reação inflamatória (Wyllie *et al.*, 1980). Além disso, durante apoptose, ocorre a clivagem do DNA em regiões internucleossomais gerando múltiplos fragmentos de 180 a 200 pares de bases nucleotídicas (padrão em escada do DNA apoptótico) (Gavrieli *et al.*, 1992).

A apoptose requer uma maquinaria proteica especializada, envolvendo caspases iniciadoras (caspase-2, -8, -9, -10) e efetoras (caspase-3, -6, -7) e pode ser desencadeada por via extrínseca ou intrínseca (Antonsson, 2001; Takle and Andersen, 2007). A interação de ligantes (FasL, TNF e proteínas relacionadas) com receptores de morte (via Fas) desencadeia a via extrínseca e ativa a cascata das caspases (Elmore, 2007). Estes receptores interagem com moléculas conhecidas como FADD/MORT-1 recrutando caspase-8, que por sua vez irá ativar caspases efetoras, executando a morte por apoptose por clivagem de respectivos substratos celulares (Tripathi *et al.*, 2009). Em mamíferos, diversas proteínas celulares, incluindo DNAases, proteínas do citoesqueleto, reguladores do ciclo celular, moléculas de sinalização e reparo, assim como enzimas constitutivas, foram identificadas como substrato de uma ou mais caspases efetoras ativas (Elmore, 2007).

A via intrínseca pode ser ativada por estresse intra- ou extracelular tais como: danos no DNA, privação de fatores de crescimento e hipóxia. Alterações na permeabilidade da membrana mitocondrial são apontadas como principal mediadora dessa via apoptótica e as proteínas da família Bcl-2 participam ativamente da sua regulação (Shimizu *et al.*, 2000; Youle and Strasser, 2008). A proteína antiapoptótica Bcl-2 está localizada na membrana mitocondrial externa, onde atua no bloqueio da liberação de citocromo *c* pela mitocôndria após estímulo apoptogênico. A ligação de Bcl-2 com a proteína pro-apoptótica Bax forma um heterodímero (Bax/Bcl-2) suprimindo a morte celular. Entretanto o homodímero Bax/Bax promove a formação de poros na membrana mitocondrial e consequente liberação de citocromo *c* para o citosol (Polcic *et al.*, 2015; Delbridge *et al.*, 2016). O citocromo *c* associa-se com Apaf-1 (apoptotic protease activation factor-1) e pro-caspase-9 para a formação do apoptossomo, complexo que ativa a caspase-9, e por conseguinte caspase-3, levando a apoptose (Wu *et al.*, 2014).

Entre os diversos substratos das caspases pode-se citar a mdm-2 (murine double minute), uma proteína que se liga à p53, mantendo-a no citoplasma. A clivagem de mdm-2 pelas caspases libera a p53, que se desloca para o núcleo ativando a transcrição de genes pró-apoptóticos como *Bax* (Danial and Korsmeyer, 2004; Galluzzi *et al.*, 2018). A morte celular independente de caspases também pode ocorrer envolvendo moléculas da rota mitocondrial e proteases não-caspases, tais como catepsinas, granzimas e endonuclease G, que podem induzir apoptose de forma independente ou cooperativamente com caspases (Zhang *et al.*, 2003).

1.3. Inter-relação das vias autofágicas e apoptóticas

A interação entre as vias autofágica e apoptótica vem despertando grande interesse, principalmente na área médica, pois alterações nestas vias estão relacionadas à doenças neurodegenerativas como Alzheimer, Parkinson, e à vários tipos de tumores (Ghavami *et al.*, 2014; Aufschnaiter *et al.*, 2017; Bischof *et al.*, 2017). Embora o mecanismo de autofagia esteja gradualmente sendo elucidado, diversas proteínas e interações possuem ainda função desconhecida (Gump and Thorburn, 2011; Song *et al.*, 2017). Além disso, a complexa interação entre estas vias de sinalização dificulta sua total elucidação, mesmo com crescente número de estudos. Múltiplos pontos de interação direta e indireta entre essas vias de sinalização evidenciam a participação de algumas proteínas como, por exemplo, p62 e p53 na

regulação da autofagia e da apoptose (Mathew *et al.*, 2009; Hou *et al.*, 2010; Nikolettou *et al.*, 2013). A ação de p62 é moldada pela interação com caspase-8 que pode ser ativada por p62 ou promover a clivagem desta em resposta a um estímulo de morte celular (Jin *et al.*, 2009; Pan *et al.*, 2011). Por outro lado a atuação de p53 nas vias autofágicas e apoptóticas é dependente de sua localização. Evidências mostram que a translocação de p53 para o núcleo leva a indução da autofagia enquanto condições de estresse celular extremo resulta no deslocamento de p53 citosólica para a matriz mitocondrial, promovendo a abertura de poros na membrana mitocondrial externa, assim levando a apoptose (Crichton *et al.*, 2006; Tasdemir *et al.*, 2008; Lu *et al.*, 2017). A proteína anti-apoptótica Bcl-2 é um importante regulador da autofagia uma vez que interage diretamente com Beclin-1, tornando-o incapaz de ativar a autofagia. Outro mecanismo pelo qual apoptose pode inibir a autofagia é através da clivagem por caspase-3 de Beclin-1 e outras proteínas essenciais da autofagia (Gump and Thorburn, 2011) (Fig.2).

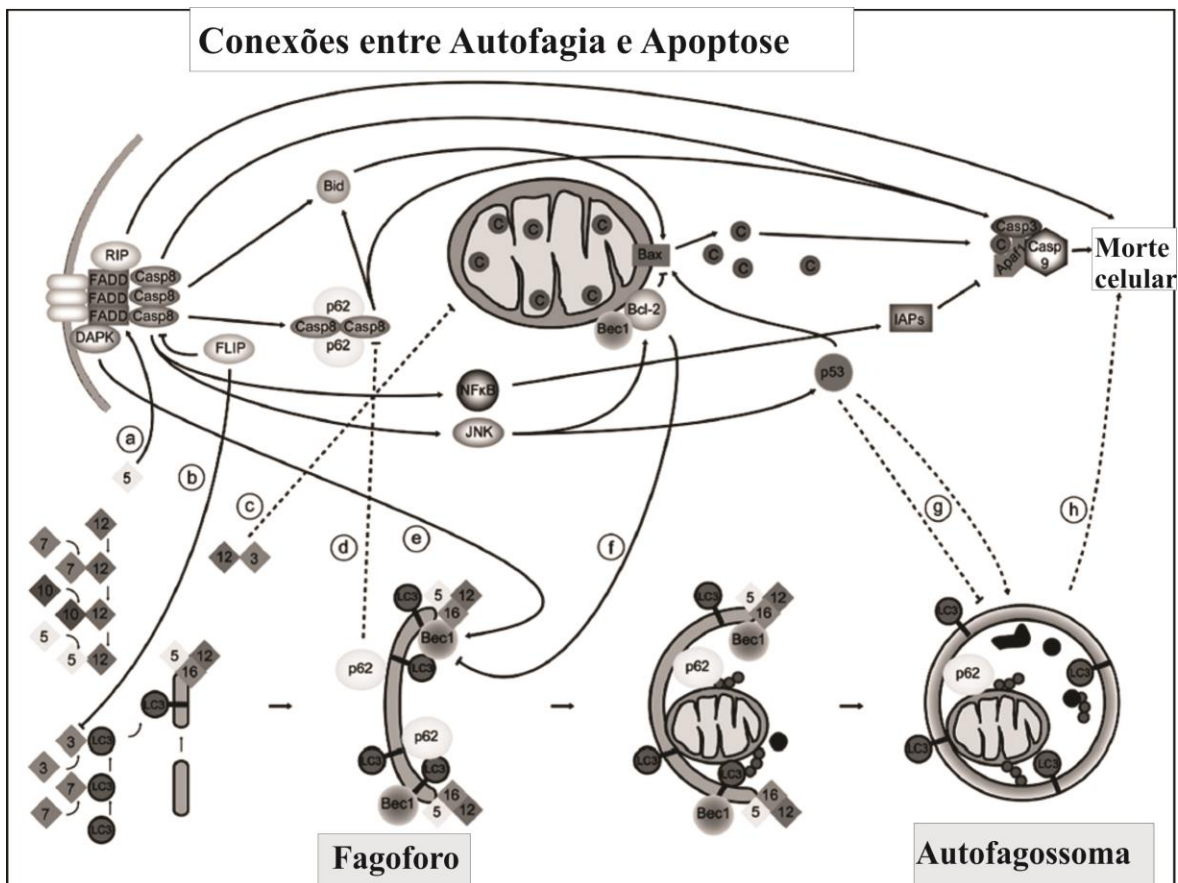


Figura 2: Conexões entre os processos autofágico e apoptótico. A. Atg5 ativa o DISC (Complexo de sinalização indutor de morte) através da interação com FADD (Domínio de morte associado ao FAS). B. O FLIP (Proteína inibidora do tipo FLICE) inibe a associação

Atg3-LC3 e, portanto, a indução de autofagia. C. A conjugação Atg12-Atg3 inibe a fissão mitocondrial e a apoptose, independente de autofagia. D. p62 promove a agregação e ativação de Caspase-8 que, paradoxalmente, é degradada pela autofagia, provavelmente através de sua interação com p62. E. A fosforilação de Beclin-1 pela Dap cinase promove a autofagia. F. Interação Bcl-2 com Beclin-1 inibe a autofagia. G. p53 pode tanto promover como inibir a autofagia, dependendo do contexto. H. Morte celular autofágica. Links bem estabelecidos são representados com linhas sólidas e links menos estabelecidos são mostrados com traços (Gump and Thorburn, 2011).

1.4. Lisossomos e morte celular

Os lisossomos são organelas formadas por membrana simples presentes em todos os organismos eucariotos. Geralmente, endossomos iniciais ou precoces (pH 6,0 - 6,6) encontrados próximo à membrana celular originam estruturas encontradas mais profundas no citoplasma denominadas de endossomos tardios (pH~5). Esses últimos tipicamente amadurecem em estruturas com pH mais ácido pH~4,5 denominados lisossomos (de Duve *et al.*, 1955; Replik *et al.*, 2012). O termo 'lisossoma' é derivado da palavra grega 'corpo digestivo' sendo descrita pela primeira vez por de Duve et al. (1955). A principal função dos lisossomos é a degradação de componentes externos (via endocitose) ou de dentro da própria célula (via autofágica) (Fig. 1). Os produtos de degradação dos lisossomos são ativamente transportados para o citosol podendo ser reutilizados pela célula. Para exercer sua função, esta organela contém hidrolases fosfatases, nucleases, glicosidases, proteases, peptidases, sulfatases e lipases cuja função é dependente do pH ácido lisossomal (Replik *et al.*, 2012). Os lisossomos e as proteases lisossomais também estão envolvidos no processo de morte celular (Mrschtik and Ryan, 2015). Quando as proteases lisossomais se encontram dentro do compartimento lisossomal não podem afetar outros componentes citosólicos. Em contraste, o extravasamento do conteúdo lisossomal está associado a vias de morte celular como a apoptose (Johansson *et al.*, 2010). Entre as hidrolases lisossomais, a protease catepsina-D apresenta um papel importante na degradação de proteínas durante a morte celular. Catepsina-D é a principal protease aspártica endolisossômica sendo sintetizada como proenzima. A enzima madura possui dois domínios, uma cadeia pesada (34 kDa) e uma cadeia leve (14 kDa) não ligados covalentemente (Turk *et al.*, 2012). Estudos recentes demonstram que a catepsina-D pode atuar em diferentes vias de morte celular, incluindo apoptose, autofagia e

necroptose (Repnik *et al.*, 2012; Mrschik and Ryan, 2015). A liberação desta protease para o citoplasma após a desestabilização da membrana lisossomal pode resultar em morte celular independente ou dependente de caspase, com ou sem envolvimento de mitocôndrias. Além disso, proteínas como caspases-2 e 8 e as proteínas da família Bcl-2 como Bid, Bcl-2, Bcl-XL e Mcl-1 podem ser alvos de catepsinas (Fig.3) (Boya and Kroemer, 2008).

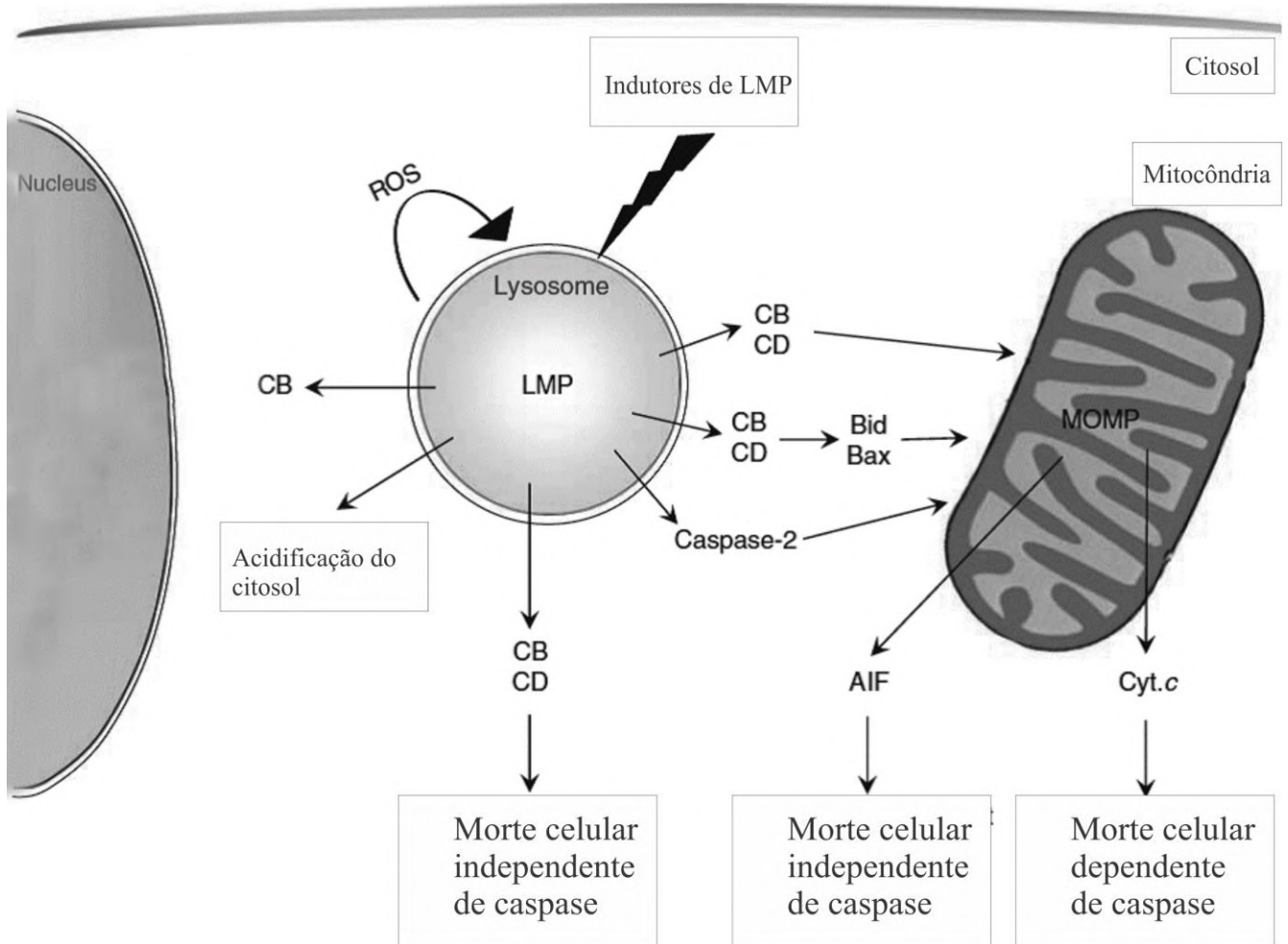


Figura 3: Vias de morte celular por permeabilização da membrana lisossomal (LMP). AIF, fator indutor de apoptose; CB, catepsina B; CD, catepsina D; Cyt.c, citocromo c; MOMP, permeabilização da membrana externa mitocondrial (Boya and Kroemer, 2008)

1.5. Gametogênese

1.5.1. Ovogênese

A gametogênese é um processo altamente ordenado controlado por fatores ambientais e hormonais do eixo hipotálamo-hipófise-gônada e depende do equilíbrio entre proliferação, diferenciação e morte celular de células germinativas (Gawriluk *et al.*, 2011). Em teleósteos, autofagia e apoptose participam da regressão folicular e podem garantir uma regressão ovariana mais eficiente após a desova (Santos *et al.*, 2008; Morais *et al.*, 2012). Entretanto, os mecanismos e interações desses processos não são completamente elucidados. Neste sentido, gônadas de peixes constituem um excelente modelo de estudo para apoptose e autofagia, principalmente em peixes com intensa atividade reprodutiva e de fácil cultivo em laboratório, como a tilápia do Nilo.

A ovogênese em teleósteos tem sido dividida em três fases principais: 1) crescimento primário, independente de gonadotrofinas, compreende a divisão das ovogônias e diferenciação em ovócitos perinucleolares, 2) crescimento secundário, dependente de gonadotrofinas, envolve a formação de alvéolos corticais (ovócitos pré-vitelogênicos) e a incorporação de vitelo nos folículos vitelogênicos e 3) maturação ovocitária, quando ocorre a retomada da meiose e o desenvolvimento final do ovócito tornando-o apto à fertilização (Grier *et al.*, 2007; Quagio-Grassiotto *et al.*, 2011). Durante o crescimento secundário, o fígado produz vitelogenina e coreogenina que são proteínas essenciais na formação do vitelo e da zona pelúcida, respectivamente (Rizzo e Bazzoli, 2014, 2020).

Após a desova, os ovários apresentam estruturas remanescentes dos folículos ovarianos ovulados denominados de folículos pós-ovulatórios, além de ovócitos vitelogênicos em degeneração, folículos atrésicos, ovogônias e ovócitos perinucleolares nas lamelas ovulíferas. Folículos pós-ovulatórios não têm atividade hormonal e são rapidamente reabsorvidos após a regressão do ovário (Santos *et al.*, 2005, 2008). Diferente dos folículos pós-ovulatórios, atresia folicular ocorre em condições naturais ou experimentais e pode ser induzida por fatores tais como estresse, jejum, agentes tóxicos, luz, temperatura, confinamento e níveis hormonais inadequados (Saidapur, 1978). Em mamíferos, apesar do grande número de folículos presentes nos ovários, cerca de 99 % destes sofrem atresia folicular logo após o nascimento e são reabsorvidos pelos ovários (Hsueh *et al.*, 1994). Em decorrência do processo de atresia folicular somente cerca de 1% dos folículos podem ser

ovulados durante a vida reprodutiva, neste sentido, a atresia folicular atua como um mecanismo de seleção natural dos folículos que serão ovulados (Hughes and Gorospe, 1991).

Em teleósteos, a atresia folicular é frequentemente observada na fase vitelogênica, entretanto folículos pré-vitelogênicos e perinucleolares também podem sofrer atresia (Rizzo and Bazzoli, 1995; Habibi and Andreu-Vieyra, 2007). Diversos fatores exógenos podem induzir atresia folicular em ovários peixes, tais como hipofisectomia, irradiação, aplicação de substâncias anti-gonadotróficas, estresse térmico e confinamento (Linares-Casenave *et al.*, 2002; Sato *et al.*, 2005). Diversos eventos caracterizam a atresia folicular tais como: fragmentação do envelope nuclear com liberação do material genético para o ooplasma, liquefação do vitelo, formação de fendas na zona radiata, hipertrofia das células foliculares, seguido por reabsorção progressiva do vitelo, fragmentos da zona radiata e remanescentes do ovócito (Saidapur, 1982; Santos *et al.*, 2005).

A eliminação dos folículos atrésicos é um processo coordenado por hormônios, envolvendo morte celular por apoptose (Hsueh *et al.*, 1994; Kaipia and Hsueh, 1997). Estudos com diferentes espécies de peixes relatam apoptose como um evento tardio da atresia folicular, uma vez que nas fases iniciais, as células foliculares estão ativamente envolvidas na reabsorção do vitelo e remanescentes do ovócito em degeneração (Santos *et al.*, 2008; Morais *et al.*, 2012). Além da via apoptótica, a autofagia pode ser uma via alternativa para a eliminação celular na atresia folicular (Choi *et al.*, 2010; Escobar *et al.*, 2012; Cassel *et al.*, 2017). Entretanto, ainda há lacunas no conhecimento quanto a interação da autofagia e apoptose na manutenção e morte das células foliculares durante a regressão folicular.

1.5.2. Espermatogênese

Diferentemente dos mamíferos, a espermatogênese em peixes ocorre no interior de estruturas denominadas cistos onde células de Sertoli estão em contato com clones de células germinativas em uma mesma fase de desenvolvimento (Nóbrega *et al.*, 2009; Schulz *et al.*, 2010a). Os cistos se formam quando uma espermatogônia tipo A indiferenciada (GA_{ind}) é completamente envolvida pelos prolongamentos das células de Sertoli. As GA_{ind} podem permanecer em estado quiescente, autorrenovarem-se e dar origem a espermatogônias tipo A_{dif} (GA_{dif}). As GA_{dif} através de sucessivas divisões mitóticas originarão espermatogônias secundárias (G_B), obtendo assim, um aumento geométrico de células germinativas com redução do diâmetro nuclear (Grier, 1981; Schulz *et al.*, 2012). Os clones das células

germinativas resultantes das divisões mitóticas permanecem ligados entre si por pontes citoplasmáticas, devido à citocinese incompleta responsável pelo desenvolvimento sincrônico destas células (Schulz and Nóbrega, 2011). As G_B diferenciam-se em espermatócitos primários (C_1) e durante a prófase meiótica (leptóteno, zigóteno, paquíteno, diplóteno) ocorrem os processos de recombinação e segregação gênica, importantes para a diversidade da espécie e produção de RNAm essenciais para a fase espermiogênica (Cobb and Handel, 1998; Schulz *et al.*, 2010a). Após a segunda divisão meiótica, os espermatócitos secundários (C_2) darão origem às espermátides (T).

Na espermiogênese, uma série de alterações morfológicas tais como condensação da cromatina, eliminação de corpos residuais, formação da peça intermediária e do flagelo levam à diferenciação das espermátides (T) em espermatozóides (Z). Ao final do processo espermatogênico, as pontes citoplasmáticas entre as células germinativas e as junções das células de Sertoli são rompidas, culminado com a liberação dos espermatozóides recém-formados no lúmen dos túbulos seminíferos (Batlouni *et al.*, 2009).

Os eventos observados durante a espermatogênese são fortemente regulados pelo eixo hipotálamo-hipófise-gônada. Assim, estímulos ambientais como chuva, fotoperíodo e temperatura estimulam o hipotálamo a produzir os fatores liberadores de hormônios gonadotróficos (GnRH), que por sua vez induzem a hipófise a produzir e liberar hormônio folículo estimulante (FSH) e hormônio luteinizante (LH) (Weltzien *et al.*, 2004). O FSH atua nas células de Leydig estimulando a conversão de 17α - hidroxiprogesterona em testosterona (T), a qual posteriormente será substrato para produção de 11-ketotestosterona (11-KT), ambos atuando durante a maturação testicular principalmente na divisão mitótica, diferenciação das espermatogônias e na espermição (de Waal *et al.*, 2009).

A apoptose durante a espermatogênese é essencial à manutenção da homeostase, e modificações nas proteínas chave desta via estão associados a alterações no desenvolvimento normal da espermatogênese (Russell *et al.*, 2002). Estudos recentes em mamíferos mostram que sob condições de estresse (jejum, calor, exposição a produtos químicos ambientais e radiação) a autofagia aumenta para manter a sobrevivência destas células germinativas e inibir a apoptose (Zhang *et al.*, 2012; Yin *et al.*, 2017). Em peixes, o conhecimento da função e interação das vias de sinalização da autofagia e apoptose é limitado, especialmente na espermatogênese.

1.6. Restrição alimentar

Durante o ciclo de vida, algumas espécies de peixes enfrentam longos períodos de privação alimentar devido a escassez de alimento, como ocorre nos meses de inverno. Durante a migração para reprodução e no estágio de pré-desova os peixes utilizam as reservas armazenadas durante o verão (período chuvoso) (Navarro e Gutiérrez, 1995). Entretanto, sabe-se que longos períodos de jejum podem afetar negativamente o crescimento, a reprodução e a saúde dos animais (Jobling, 2015).

Os níveis metabólicos de carboidratos, proteínas e lipídeos são afetados pela restrição alimentar de modo variável entre as espécies e podem ainda apresentar diferença intraespecífica, de acordo com alguns fatores, como idade do animal e sua condição nutricional (Wang *et al.*, 2006; Furné e Sanz, 2017). Espécies carnívoras, por exemplo, podem apresentar melhor tolerância aos efeitos da restrição alimentar. Já as espécies de hábito alimentar herbívoro e onívoro, onde a ingestão de alimentos ocorre com maior periodicidade (como a tilápia) são menos tolerantes a longos períodos de jejum (McCue, 2010). Além disso, as consequências da restrição alimentar são mais pronunciadas em larvas e juvenis do que em peixes adultos, que apresentam maior quantidade de reservas energéticas (Gadomski and Petersen, 1988).

A tilápia do Nilo pode passar por períodos de restrição alimentar em função da oscilação natural na disponibilidade de alimento ou durante o cuidado parental (Barreto *et al.*, 2003). Na aquicultura, essa espécie pode sofrer inanição na fase de pré-despesca, durante o transporte, seleção, estocagem ou em dietas onde se utiliza uma estratégia alimentar com ciclos de restrição e realimentação, para a otimização do desempenho produtivo, por meio do crescimento compensatório, mecanismo observado em algumas espécies incluindo *O. niloticus* (Palma *et al.*, 2010).

1.7. Tilápia de Nilo

As tilápias são o segundo grupo de peixes de água doce mais cultivado no mundo, logo após a carpa (Food and Agriculture Organization of the United Nations (FAO), 2016). A espécie *Oreochromis niloticus* também conhecida por tilápia do Nilo é oriunda das bacias do rio Nilo, Níger e Senegal (leste e oeste da África), sendo introduzida no Brasil em 1971, inicialmente na região nordeste e, a partir de então distribuída pelo país (Castagnoli, 1992). Espécie onívora, a tilápia do Nilo se alimenta de algas, fitoplâncton, zooplâncton, ovos e larvas de peixes e detritos. A fêmea apresenta comportamento de cuidado parental incubando

ovos fertilizados na cavidade bucal até a liberação dos alevinos. Durante a incubação dos ovos, a fêmea não se alimenta, mantendo-se por um período de 10 a 12 dias em jejum até a liberação dos alevinos (Barreto *et al.*, 2003). Em cultivo, a tilápia desova de 1.500 a 2.000 ovos com intervalos de 28 dias entre desovas consecutivas em temperatura da água acima de 24°C (Zanoni *et al.*, 2000). Além disso, esta espécie se adapta facilmente a sistemas de produção e a diferentes condições ambientais, apresenta facilidade de reprodução e rápido crescimento corporal (Castagnolli, 1992). Esse conjunto de qualidades altamente positivas torna a tilápia do Nilo um modelo experimental interessante para estudos morfofisiológicos da gametogênese em condições de cultivo.

2.0 . JUSTIFICATIVA

Autofagia e apoptose são processos fisiológicos fundamentais para o desenvolvimento correto e manutenção dos tecidos em organismos multicelulares (Mizushima and Komatsu, 2011; Romano, 2013; Ryter *et al.*, 2013; Song *et al.*, 2017). Atualmente tem se observado um interesse crescente da comunidade acadêmica no melhor entendimento das vias autofágicas e apoptóticas e suas complexas interações. A disfunção desses processos tem sido associada ao aparecimento e desenvolvimento de muitas patologias crônicas humanas, como doenças cardiovasculares, metabólicas e neurodegenerativas, além do câncer, e o conhecimento exato dos alvos que inibem e induzem a autofagia auxilia no desenvolvimento de novos fármacos. Estudos recentes em outros vertebrados como peixes (Han *et al.*, 2019; Sales *et al.*, 2019; Xia *et al.*, 2019), aves (Gong, 2019; Shi *et al.*, 2019) e reptéis (Chen *et al.*, 2019; Vistro *et al.*, 2019) reportam a participação autofagia em diferentes processos fisiológicos. Neste trabalho nos utilizamos a tilápia do Nilo para o estudo dessas vias e suas interações durante a gametogênese e regressão folicular. A tilápia do Nilo se destaca como modelo experimental por apresentar características apreciáveis como: rápido crescimento corporal, fácil reprodução, adaptação a uma ampla faixa de condições ambientais, resistência a doenças e infecções, e tolerância ao estresse (Little e Hulata, 2000). Além disso, em fêmeas desta espécie o estudo da interação entre autofagia e apoptose durante a regressão ovariana se torna apreciável, pois nos ovários da tilápia do Nilo as três fases (inicial, avançada e tardia) da atresia folicular são encontradas simultaneamente nos ovários paralelamente ao desenvolvimento dos folículos, desta forma permitindo a avaliação da dinâmica das proteínas autofágica e apoptótica durante todo o ciclo reprodutivo (Melo et al. al 2014, 2015). Nestes

animais, a rápida recuperação ovariana após desova (3 a 4 semanas, intervalo entre desovas) é também ponto favorável para o estudo da regressão folicular (Melo et al., 2014). Além disso, o conhecimento do papel e dos mecanismos pelos quais a via autofágica atua durante a espermatogênese de peixes ainda é incipiente. Neste sentido, o uso da restrição alimentar, como indutor da via autofágica durante a espermatogênese de tilápia do Nilo e as características favoráveis da estrutura testicular dessa espécie são ferramentas interessantes para o melhor conhecimento da sinalização autofágica nos testículos de peixes.

3.0. OBJETIVOS

3.1. OBJETIVO GERAL

Investigar a interação entre os processos de autofagia e apoptose na atresia folicular e na espermatogênese da tilápia do Nilo *Oreochromis niloticus* em condições de cultivo.

3.2. OBJETIVOS ESPECÍFICOS

- Analisar os padrões de expressão de proteínas e a interação das vias autofágica/lisossomal (Beclin-1, LC3 e catepsina-D) e apoptótica (Bcl-2 e Bax) em diferentes fases da atresia folicular;
- Avaliar os efeitos da restrição alimentar total e intermitente sobre a espermatogênese, níveis plasmáticos de esteroides sexuais e de cortisol, e parâmetros bioquímicos do sangue (glicose, triglicérides, colesterol e proteína total);
- Investigar a expressão e interação de proteínas das vias autofágica/lisossomal e apoptótica durante espermatogênese em condições nutricionais distintas

4.0. RESULTADOS

4.1. CAPÍTULO 1: (artigo publicado na revista *Molecular Reproduction and Development*)

Autophagy and Cathepsin D mediated apoptosis contributing to ovarian follicular atresia in the Nile tilapia: Sales CF, Melo RMC, Pinheiro APB, Luz RK, Bazzoli N, Rizzo E. *Mol Reprod Dev.* 2019 Nov;86(11):1592-1602. doi: 10.1002/mrd.23245.

4.2. CAPÍTULO 2: (artigo publicado na revista *Molecular and Cellular Endocrinology*)

Effects of starvation and refeeding cycles on spermatogenesis and sex steroids in the Nile tilapia *Oreochromis niloticus*: Sales CF, Pinheiro APB, Ribeiro YM, Weber AA, Paes-Leme FO, Luz RK, Bazzoli N, Rizzo E, Melo RMC. *Molecular and Cellular Endocrinology* 500 (2020) 110643. doi.org/10.1016/j.mce.2019.110643

4.3. CAPÍTULO 3: Autophagy and apoptosis during fish spermatogenesis: insights from Nile tilapia

4.1. CAPÍTULO 1: Autophagy and Cathepsin D mediated apoptosis contributing to ovarian follicular atresia in the Nile tilapia: Sales CF, Melo RMC, Pinheiro APB, Luz RK, Bazzoli N, Rizzo E. Mol Reprod Dev. 2019 Nov;86(11):1592-1602. doi: 10.1002/mrd.23245.

RESEARCH ARTICLE

Autophagy and Cathepsin D mediated apoptosis contributing to ovarian follicular atresia in the Nile tilapia

Camila Ferreira Sales¹ | Rafael Magno Costa Melo¹ | Ana Paula Barbosa Pinheiro¹ |
Ronald Kennedy Luz² | Nilo Bazzoli³ | Elizete Rizzo¹ 

¹Departamento de Morfologia, Instituto de Ciências Biológicas, Universidade Federal de Minas Gerais, Belo Horizonte, Minas Gerais, Brazil

²Laboratório de Aquacultura, Escola de Veterinária, Universidade Federal de Minas Gerais, Belo Horizonte, Minas Gerais, Brazil

³Programa de Pós-graduação em Biologia de Vertebrados, Pontifícia Universidade Católica de Minas Gerais, Belo Horizonte, Minas Gerais, Brazil

Correspondence

Elizete Rizzo, Departamento de Morfologia, Instituto de Ciências Biológicas, Universidade Federal de Minas Gerais, Belo Horizonte, Minas Gerais, 31270-901 Brazil.
Email: ictio@icb.ufmg.br and elizeterizzo@gmail.com

Funding information

Fundação de Amparo à Pesquisa do Estado de Minas Gerais, Grant/Award Number: CRA-PPM-00394-13; Coordenação de Aperfeiçoamento de Pessoal de Nível Superior, Grant/Award Number: 001; Conselho Nacional de Desenvolvimento Científico e Tecnológico, Grant/Award Numbers: 482756/2012-8, 306792/2011-7

Abstract

Follicular atresia is a hormonally controlled degenerative process involving apoptosis of the somatic and germ cells. Since different signaling pathways can induce cell death, the aim of the present study was to investigate cell death signaling and crosstalk between autophagic, apoptotic, and lysosomal proteins during follicular atresia in Nile tilapia. For this, females were kept in controlled conditions for 21 days, and ovary samples were collected weekly. The atretic follicles (AF) were analyzed in three regression phases: Early, advanced, and late. Under electron microscopy, the follicular cells exhibited numerous protein synthesis organelles in the early AF. Immunoreactivity for Bcl2, Beclin1, Lc3, and Cathepsin D increased significantly in advanced AF ($p < .001$), when follicular cells were in intense yolk phagocytosis. In this phase, autophagosomes and autolysosomes were frequently observed. In the late AF, follicular cells had a markedly electron-lucid cytoplasm and immunoreactivity for Bax and TUNEL assay indicated an elevated apoptosis rate. Colocalisation of Lamp1/Cathepsin D and Lc3/Caspase-3 suggests dynamic crosstalk between the autophagy, apoptosis, and lysosome pathways. Taken together, the data indicate that autophagy plays a role in the homeostasis and clearance of the follicular cells preceding Cathepsin D mediated apoptosis during follicular atresia in Nile tilapia.

KEYWORDS

Bcl2 family, Beclin1, Cathepsin D, Lamp1, Lc3

1 | INTRODUCTION

Follicular atresia is a natural degenerative process that occurs at different stages of development and is essential for ovarian homeostasis in vertebrates (Zhou, Peng, & Mei, 2019). This process is finely regulated by a hormonal balance and expression of proliferation, differentiation, and cell death factors (Craig et al., 2007; Kaipia & Hsueh, 1997; Lin et al., 2012). During follicular atresia, a drastic tissue remodeling occurs in the ovaries, with morphological changes of the somatic and germ cells followed by cell death by apoptosis (Hsueh, Billig, & Tsafirri, 1994; Santos et al., 2008). However, non-apoptotic processes, such as autophagy, can contribute to the efficient elimination of granulosa cells in mammals (Repnik Meng

et al., 2018). In teleost fish, recent studies indicate that autophagy can be involved in follicular atresia (Cassel, Camargo, Jesus, & Borella, 2017; Morais, Thomé, Lemos, Bazzoli, & Rizzo, 2012; Morais, Thomé, Santos, Bazzoli, & Rizzo, 2016; Thomé et al., 2009), but the interactions between these signaling pathways are not fully elucidated.

Apoptosis is a programmed cell death pathway that requires specialised protein machinery and can be triggered by endogenous and exogenous factors (Elmore, 2007; Takle & Andersen, 2007). Proteins of the Bcl2 family actively participate in the regulation of this pathway, acting as inducers or repressors of apoptosis (Polcic, Jaka, & Mentel, 2015; Shimizu, Narita, & Tsujimoto, 2000). Bcl2 protein has an antiapoptotic function by inhibiting the action of

proapoptotic proteins such as Bax, which can form pores in the outer mitochondrial membrane with the release of cytochrome *c* that triggers the activation of caspases (Antonsson, 2001; Zamorano et al., 2012). In some cell types, autophagy may play a role in inducing apoptosis signaling (Nikoletopoulou, Markaki, Palikaras, & Tavernarakis, 2013; Tsujimoto & Shimizu, 2005).

Autophagy is a complex catabolic mechanism involving the transport of cytoplasmic components to the lysosome (Sever & Demir, 2017). Key proteins of the autophagic pathway, such as Beclin1 and microtubule-associated protein light chain 3 (Lc3), are conserved among species and are widely used as autophagic markers (Chifenti et al., 2013; Mathai, Meijer, & Simonsen, 2017). Beclin1 promotes autophagic nucleation and the recruitment of cytosolic proteins essential for autophagosome formation (Kang, Zeh, Lotze, & Tang, 2011). The Lc3 protein can be found in the cytosolic form (Lc3I) and lipid form (Lc3II), which is conjugated to the phosphatidylethanolamine of the cell membranes. The lipid form (Lc3II) is required for autophagosome membrane elongation, thus characterizing the autophagic flow (Klionsky et al., 2012). Lysosome-associated membrane proteins (Lamp1 and 2) are required in the fusion of the autophagosome with the lysosome and the formation of a hybrid organelle, autolysosome, enriched in hydrolytic enzymes, reactive oxygen species, and antimicrobial peptides (Huynh et al., 2007).

Recent studies indicate that lysosomes may actively contribute and/or amplify cell death response (Serrano-Puebla & Boya, 2018; Zhou et al., 2017). To perform this function, hydrolytic enzymes such as Cathepsin D (Ctsd) are released from lysosomes into cytosol. Ctsd is the major endolysosomal hydrolytic enzyme, and it is widely associated with the intrinsic and extrinsic apoptotic pathways when free in the cytoplasm, acting on the degradation of antiapoptotic proteins, permeabilization of the mitochondrial membrane, and induction of caspase-dependent or independent cell death (Gómez-Sintes, Ledesma, & Boya, 2016).

The signaling pathways of apoptosis and autophagy have converging points with proteins that can act in both processes. Under nonlethal stress, autophagy may precede apoptosis, avoiding local inflammation, but in some conditions, autophagy may lead to cell death by apoptosis with caspase-8 activation and degradation of apoptosis inhibitors (Doherty & Baehrecke, 2018; Nikoletopoulou et al., 2013). When apoptosis is triggered, there is a caspase-mediated cleavage of essential proteins for autophagy (Kang et al., 2011; Sever & Demir, 2017). Among the caspases, Caspase-3 (Casp3) is a key effector molecule of the apoptotic program, which is responsible for the proteolytic cleavage of a wide range of cellular proteins that lead to the characteristic morphological changes of apoptosis (Huettenbrenner et al., 2003).

The Nile tilapia *Oreochromis niloticus* (Linnaeus, 1758) is one of the most cultivated fish species in the world and has often been used in experimental studies on reproductive physiology and development, due to its ease of breeding in captivity (Coward & Bromage, 2000; FAO, 2018). As well as in other teleost species, follicular atresia in Nile tilapia occurs during follicular growth but is more frequent in vitellogenic follicles that were not spawned in the

reproductive season (Miranda, Bazzoli, Rizzo, & Sato, 1999; Santos et al., 2008). In this species, the follicular atresia is a good model to study the cell death pathways since females breed every three to 4 weeks under optimum cultivation conditions, and atretic follicles (AF) are present throughout the reproductive cycle (Melo, Martins, Luz, Rizzo, & Bazzoli, 2015; Melo et al., 2014). To improve the knowledge of cell death mechanisms regulating follicular atresia, we investigated the expression, interaction, and dynamics existing between key proteins of autophagy and apoptosis pathways and the crosstalk with lysosomal proteins in different phases of follicular atresia in Nile tilapia.

2 | RESULTS

2.1 | Morphological dynamics of follicular regression

Follicular atresia in the ovaries of *O. niloticus* was analyzed in three phases of regression, according to morphological characteristics of the AF: Early ($AF_E = 530.90 \pm 30.26 \text{ mm}^2$), advanced ($AF_A = 341.25 \pm 19.73 \text{ mm}^2$), and late ($AF_L = 186.96 \pm 21.70 \text{ mm}^2$). During follicular regression, there was a progressive reduction of the yolk and a gradual increase in the proportion (%) of follicular cells and theca (Table 1). Histologically, early atretic follicles (AF_E) presented folds and fine slits in the zona radiata, degradation of the yolk, and a fine connective theca (Figure 1a). In the ultrastructure, follicular cells exhibited protein synthesis organelles, electron-dense granules, and lysosomes (Figure 1b,c). At this stage, the follicular cells remained intimately attached to the basal lamina and exhibited cell-cell adhesion (Figure 1d). In advanced atretic follicles (AF_A), the follicular cells became hypertrophied and presented intense phagocytic activity, especially engulfing the yolk and remains of the zona radiata (Figure 1e). In addition to yolk phagocytosis, the follicular cells had numerous autophagic structures, that is, autophagosomes with degenerating organelles, autolysosomes, and large lysosomes (Figure 1f-h). The late atretic follicles (AF_L) exhibited follicular cells in degeneration and complete reabsorption of yolk and zona radiata (Figure 1i). Under electron microscopy, some follicular cells showed highly electron-lucid cytoplasm with degenerating organelles (Figure 1j). The typical nuclear pattern of apoptosis, large

TABLE 1 Proportion (%) of the atretic follicle components during follicular atresia in the Nile tilapia, *Oreochromis niloticus*

	AF_E	AF_A	AF_L
Follicular cell	6.85 ± 0.21^c	33.22 ± 0.85^b	70.60 ± 1.18^a
Theca cells	4.00 ± 0.10^b	6.50 ± 0.20^a	5.30 ± 0.24^a
Zona radiata	4.51 ± 0.09^c	9.56 ± 0.34^a	7.82 ± 0.44^b
Yolk	84.50 ± 0.31^a	50.44 ± 0.80^b	16.78 ± 0.64^c

Note: Values represent mean \pm standard error of 50 atretic follicles. In the same line, different letters indicate significant differences ($p < .05$).

Abbreviations: AF_A : advanced atretic follicles; AF_E : early atretic follicles; AF_L : late atretic follicles.

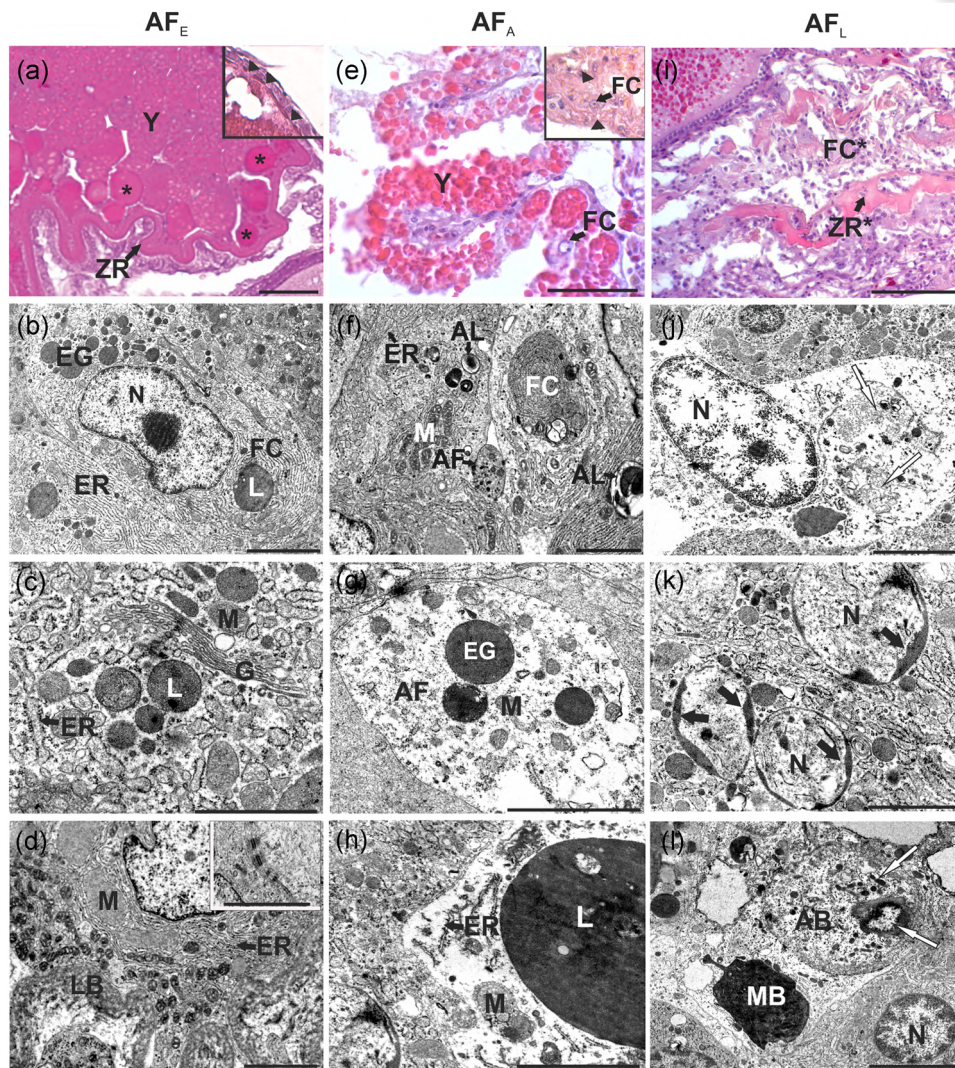


FIGURE 1 Histological sections stained with hematoxylin–eosin (a, e, i) and electron microscopy (b–d, f–h, j–l) of ovaries during early (a–d), advanced (e–h), and late (i–l) regression of the atretic follicle (AF) in *O. niloticus*. (a) Early atretic follicle (AF_E) with irregular shape, yolk (Y) at the beginning of liquefaction (*) and ripples in the zona radiata (ZR) black arrowhead (a-inset). (b) Follicular cell (FC) with euchromatic nucleus (N) and cytoplasm filled with electron-dense granules (EG) and lysosomes (L). (c) FC with numerous endoplasmic reticulum (ER), mitochondria (M), Golgi (G), and L in the cytoplasm. (d) FC connected to the basal lamina (LB) and adjacent cells by desmosomes (d-inset). (e) In advanced atretic follicle (AF_A), the zona radiata (ZR) black arrowhead (e-inset) and yolk (Y) were engulfed by FC. (f, g, h) FC with autophagosomes (AF) containing organelles debris (mitochondria, electron-dense granules, and other cytoplasmic materials), autolysosomes (AL) and large lysosomes (L). (i) Late atretic follicle (AF_L) showing residual ZR* and FC* in regression. (j) Highly electron-lucid FC with degenerated organelles (white arrows). (k) Apoptotic nuclei (N) with chromatin attached to the nuclear envelope in FC. (l) Multilamellar body (MB) and apoptotic body (AB) with degenerate nucleus and other organelles debris (white arrows). Scale bars: (a, e, i) 100 μ m, (b–d, f–h, j–l), 0.5 μ m [Color figure can be viewed at wileyonlinelibrary.com]

multilamellar, and apoptotic bodies were frequently observed in the follicular layer (Figure 1k,l).

2.2 | Labeling pattern of autophagy proteins and CtSD

Beclin1, Lc3, and CtSD showed a similar pattern of immunostaining during follicular regression. In AF_E, the reactivity for these proteins was found in granules dispersed mainly around the nucleus of follicular cells, while the theca cells exhibited sparse positive immunostaining in the cytoplasm. (Figure 2a–c). During advanced follicular atresia, some follicular

cells presented autophagic activity concomitant with yolk phagocytosis (Figure 2d–f). At this stage, theca cells were also positive for autophagic proteins and weakly labeled for CtSD (Figure 2f). In AF_L, immunostaining for autophagic proteins was less intense in follicular cells (Figure 2g–i). Morphometric analysis of the immunoreactions showed a peak of Lc3, Beclin1, and CtSD in follicular cells in AF_A ($p < .001$; Figure 2j–l). In theca cells, the expression of Lc3 and Beclin1 followed the same pattern displayed by follicular cells, however, with reduced labeling. Lc3I to Lc3II conversion was detected by Western blot analysis in ovaries of *O. niloticus*, and Lc3II labeling was higher in ovaries with AF than in ovaries without AF (Figure 2m).

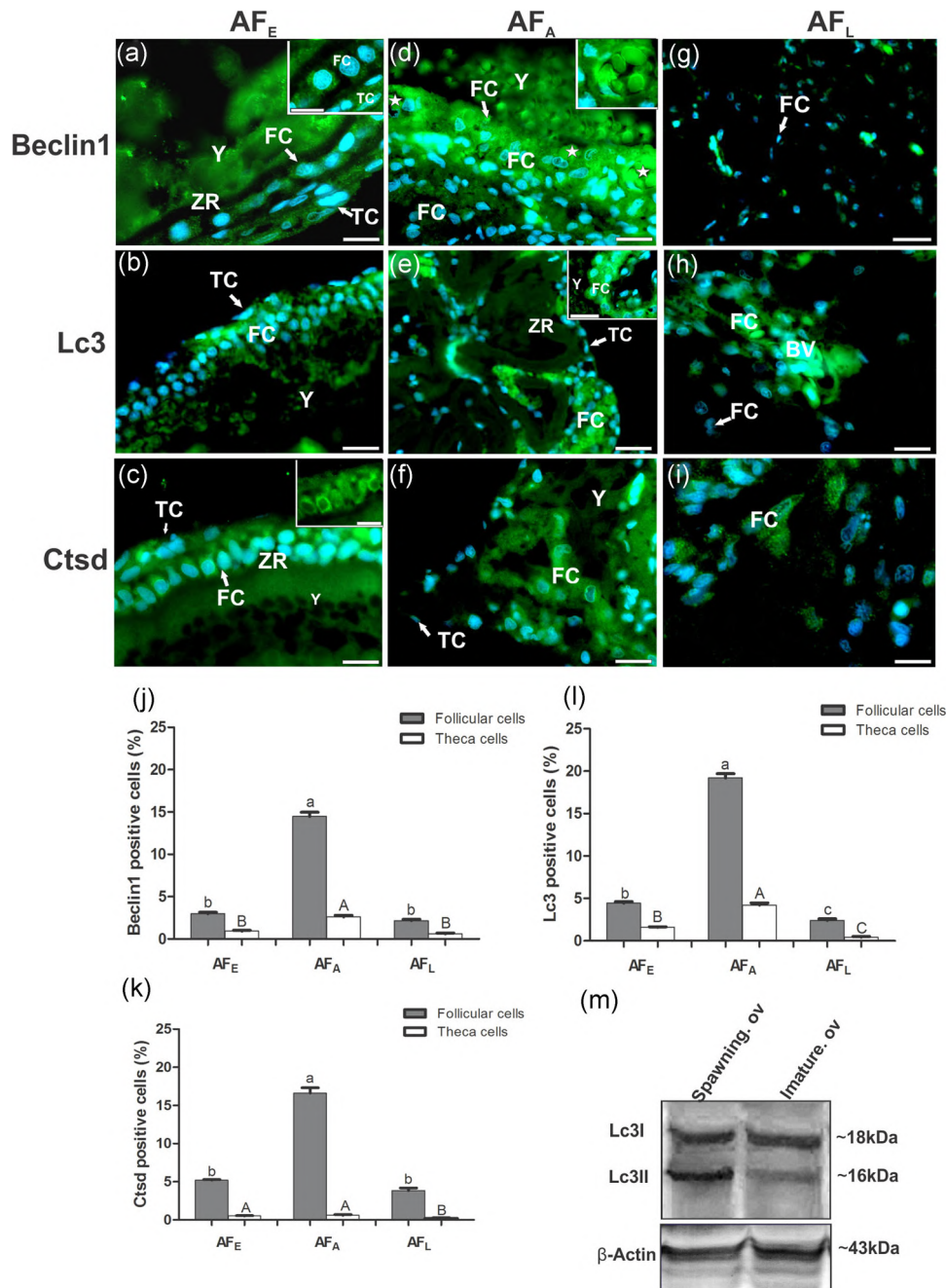


FIGURE 2 Immunofluorescence for Beclin1, Lc3, and Cathepsin D (Ctsd; green) during follicular atresia in the Nile tilapia. Nuclei are stained with 4',6-diamidine-2'-phenylindole dihydrochloride (DAPI; blue). (a–f) Follicular and theca cells (FC, TC) showing intense cytoplasmic immunoreactivity for Beclin1, Lc3, and Ctsd in the early atretic follicle (AF_E) and advanced atretic follicle (AF_A), (f) except TC labeled for Ctsd. (d) FC with heterophagic vacuoles (star) in AF_A. (g, h, i) Weak and punctual immunostaining in FC in the late atretic follicle (AF_L). (j–l) Relative proportion (%) of follicular and theca cells positive for Beclin1, Lc3, and Ctsd during follicular atresia in *O. niloticus*. Values are mean ± SEM. Different letters indicate significant differences ($p < .001$; Kruskal–Wallis, Dunn’s post hoc) between the phases of the follicular atresia. (m) Conversion of Lc3I to Lc3II in immature ovaries (Immature. ov) which presented only perinucleolar follicles and spawned ovaries (Spawning. ov) which presented several atretic follicles in different regression phases. Scale bars (a, d–h) 15 μm (b) 20 μm (c, i) 10 μm. SEM: standard error of the mean [Color figure can be viewed at wileyonlinelibrary.com]

2.3 | Apoptosis

The labeling of antiapoptotic Bcl2 and proapoptotic Bax was observed in the cytoplasm of follicular and theca cells throughout follicular regression; however, the expression pattern and intensity of the

immunostaining changed throughout the follicular regression (Figure 3). Although Bcl2 was expressed in all phases of the regression, morphometric analyses demonstrated a significant increase during AF_A ($p < .001$) compared to AF_E, followed by a significant reduction in

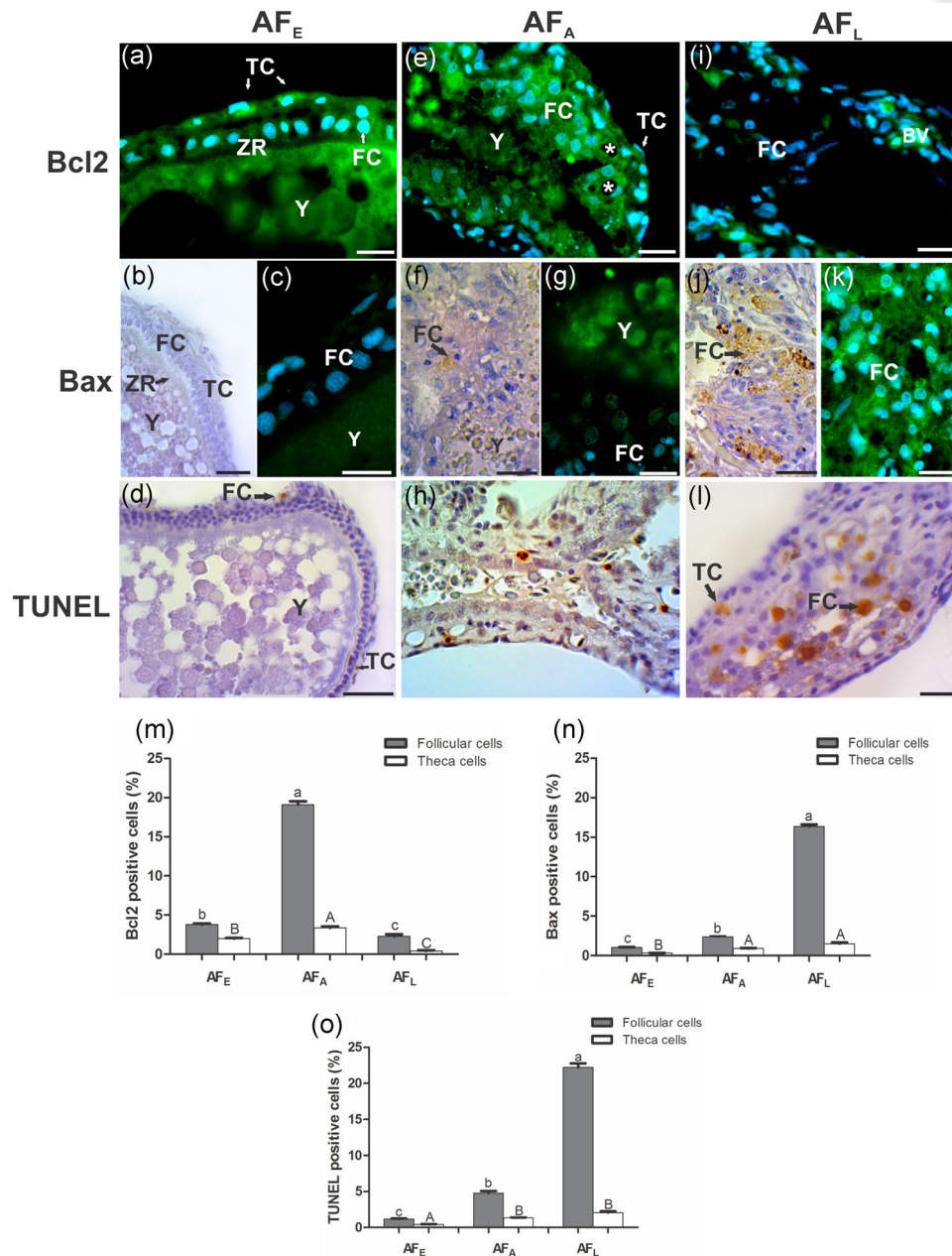


FIGURE 3 Immunofluorescence for Bcl2 and Bax (green) (a, c, e, g, i, k), Terminal Deoxynucleotidyl Transferase (TdT) dUTP nick-end labeling (TUNEL) assay (d, h, l) and immunoperoxidase for Bax (b, f, j) during follicular atresia in the Nile tilapia. Nuclei are stained with 4',6-diamidino-2'-phenylindole dihydrochloride (DAPI) (blue). (a, e) Bcl2 positive follicular cells (FC) with autophagic vacuoles (asterisks) and theca cells (TC) showing intense cytoplasmic immunoreactivity in the early atretic follicle (AF_E) and advanced atretic follicle (AF_A). (b-d and f-h) AF_E and AF_A presented FC and TC with weak and punctual immunolabelling for Bax and TUNEL reaction. (j-l) late atretic follicle (AF_L) presented a strong reaction for Bax and many TUNEL-positive cells. (m-o) Relative proportion (%) of follicular and theca positive cells for Bcl2, Bax, and TUNEL during follicular atresia in *O. niloticus*. Values are expressed as mean \pm SEM. Different letters indicate significant differences ($p < .001$) (Kruskal-Wallis, Dunn's post hoc) between the phases of follicular atresia. Scale bars (c, g, k) 10 μ m, (a, e, i) 15 μ m, (b, f, j, h, l) 20 μ m, and (d) 50 μ m. SEM: standard error of the mean [Color figure can be viewed at wileyonlinelibrary.com]

the AF_L (Figure 3m). In contrast, immunostaining for Bax and Terminal Deoxynucleotidyl Transferase (TdT) dUTP Nick-End Labeling (TUNEL) assay showed a gradual increase, which was significantly higher in AF_L ($p < .001$; Figure 3n,o).

2.4 | Crosstalk between autophagy, apoptosis, and Cttd

To verify the interaction between autophagy and apoptosis, we colocalized Lc3/Casp3. In AF_E, positive cells for Casp3 (red) were rarely

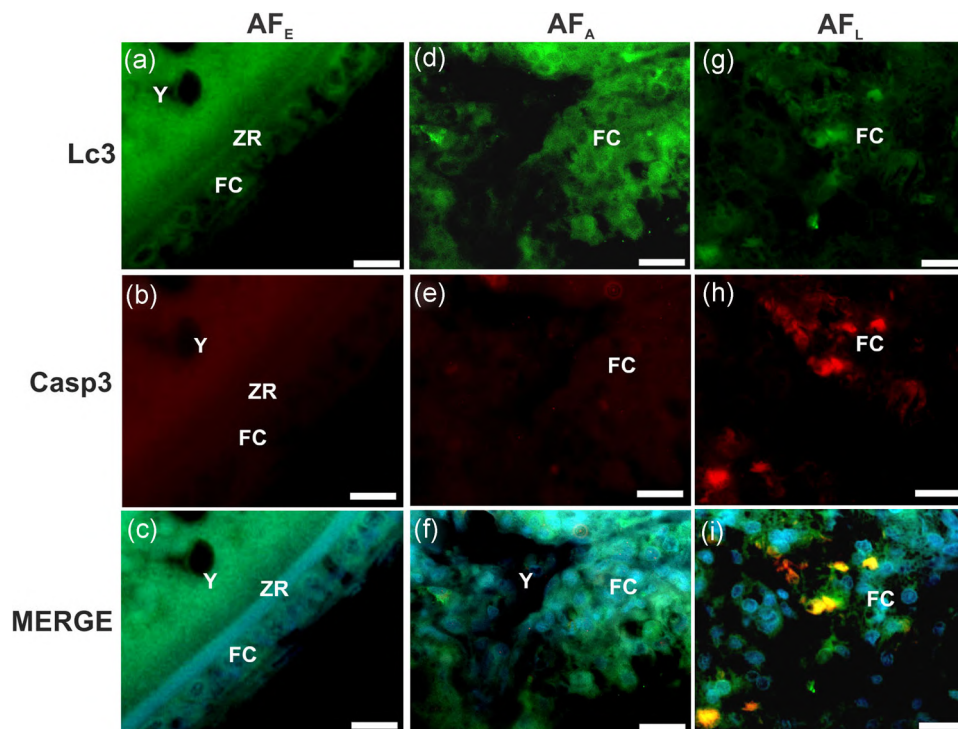


FIGURE 4 Double-labeling for Lc3 (green) and Caspase-3 (Casp3) (red) during follicular atresia in the Nile tilapia. Nuclei are stained with 4',6-diamidino-2'-phenylindole dihydrochloride (DAPI) (blue). (a–f) Follicular cells (FC) with poor immunostaining for Casp3, in contrast to the strong reaction for Lc3 in the early atretic follicle (AF_E) and advanced atretic follicle (AF_A). (g–i) Punctual colocalization between Lc3 and Casp3 (yellow) in late atretic follicle (AF_L) (g–i). Scale bars (a–i) 15 μm [Color figure can be viewed at wileyonlinelibrary.com]

observed while positive cells for Lc3 (green) were predominant, and there was no colocalization between these proteins (Figure 4a–c). In AF_A , the frequency and intensity of the labeling increased for both proteins, and colocalization regions were eventually found (Figure 4d–f). In AF_L , Lc3/Casp3 colocalization was clearly evident (yellow) in the cytoplasm of follicular cells (Figure 4g–i).

Ctsd/Lamp1 colocalization was evaluated to verify whether Ctsd was in the lysosomal compartment or in the cytosol (Figure 5). Immunostaining for Lamp1 (red) and Ctsd (green), as well as the colocalization of these proteins (yellow), occurred in thin granules in the cytoplasm of follicular cells, indicating the presence of Ctsd inside the lysosomal compartment in AF_E and AF_A (Figure 5a–f). In AF_L , Ctsd/Lamp1 colocalization (yellow) became restricted to specific areas in the follicular cells. In these cells, positive areas for Ctsd (green) were found, suggesting partial translocation of Ctsd from lysosomes to the cytosol (Figure 5g–i).

3 | DISCUSSION

In this study, we report the immunolabelling of key proteins of the autophagic (Lc3 and Beclin1) and apoptotic (Bax, Bcl2, and Casp3) pathways and the interaction of these pathways with lysosomal proteins (Lamp1 and Ctsd) in different phases of ovarian follicular atresia in Nile tilapia. The results showed that these cellular mechanisms act

cooperatively for an efficient regression and elimination of AF and are essential processes in the ovarian remodeling in teleost fish.

The presence of abundant rough endoplasmic reticulum and a developed Golgi complex detected in the follicular cells of AF_E can be related to the protein synthesis of autophagic and apoptotic machinery (Kishi-Itakura, Koyama-Honda, Itakura, & Mizushima, 2014; Lamb, Yoshimori, & Tooze, 2013). The presence of autophagic vacuoles labeling for Beclin1 and Lc3 as well as conversion of Lc3I to Lc3II suggest that autophagy is intensely active during advanced follicular atresia. In addition, this period is also marked by intense phagocytosis of the yolk and oocyte remnants by the follicular cells. Thus, autophagy and phagocytosis convergence account for efficient elimination of extracellular and intracellular components of the AF.

In the AF_A , theca cells showed increased labeling for autophagic proteins, but they were weakly stained for Ctsd, possibly because these cells did not perform phagocytosis. The low vascularization of the theca during most of the follicular regression (Miranda et al., 1999) may justify the induction of autophagy to maintain cell homeostasis through clearance and selective removal of protein aggregates and dysfunctional organelles (Ryter, Cloonan, & Choi, 2013; Sever & Demir, 2017). However, under prolonged metabolic stress, autophagy may contribute to the provision of energy for apoptotic execution (Chiarelli, Agnello, Bosco, & Roccheri, 2014; Kriel & Loos, 2019). In support of this hypothesis, we observed follicular cells with highly electron-lucid cytoplasm and a shortage of organelles under the electron microscope. In some models, an

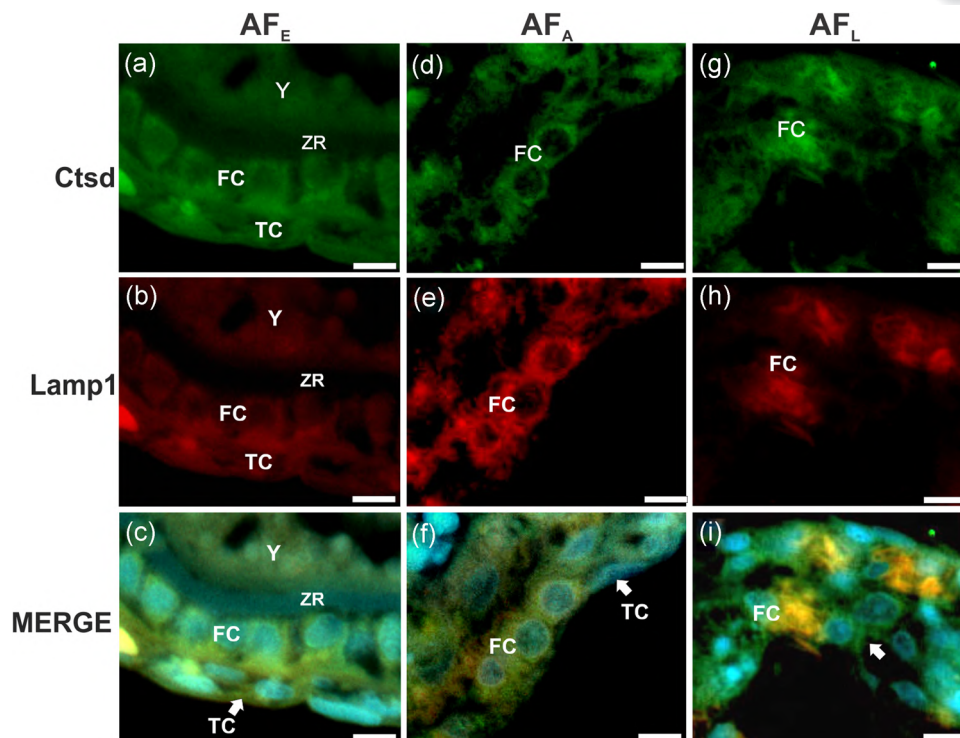


FIGURE 5 Double-labeling for Cathepsin D (Ctsd) (green) and Lamp1 (red) during follicular atresia in the Nile tilapia. Nuclei are stained with 4',6-diamidino-2'-phenylindole dihydrochloride DAPI (blue). (a–f) FC with colocalization between Ctsd and Lamp1 (yellow) in the early atretic follicle (AF_E) and advanced atretic follicle (AF_A). (g–i) late atretic follicle (AF_L) with colocalization limited to specific areas of the cytoplasm and positive areas only for Ctsd (green labeling and white arrow). Scale bars = 10 μ m [Color figure can be viewed at wileyonlinelibrary.com]

exacerbated autophagy can lead to excessive cleavage of prosurvival molecules and organelles essential for cellular viability, inducing autophagy-dependent cell death (Gómez-Sintes et al., 2016). In *Drosophila*, autophagy may induce activation of Casp3 and DNA fragmentation during oogenesis (Nezis et al., 2010). Similarly, after the increase of the autophagic proteins in AF_A, our results showed a significant increase of TUNEL-positive cells and Casp3 expression during late follicular atresia.

Apoptosis can be identified through typical morphological characteristics such as chromatin condensation around the nuclear envelope, loss of cell–cell and cell–basal lamina adhesion, and cell fragmentation into apoptotic bodies (Drummond, Bazzoli, Rizzo, & Sato, 2000; Elmore, 2007; Morais et al., 2016; present study). The internucleosomal DNA cleavage pattern (DNA ladder) in apoptosis was also found in atretic ovaries (Santos et al., 2008). Moreover, we found a significant increase of follicular and theca cells labeled for Bax and TUNEL reaction, in addition to immunostaining for Casp3 in the AF_L. Thus, the data obtained on Casp3-dependent apoptosis in follicular atresia are highly consistent. In addition, the significant increase in the labeling for antiapoptotic Bcl2 protein in AF_A suggests a crucial role for the follicular cells in the maintenance of cell viability during yolk and oocyte remnants resorption. Therefore, Bcl2 expression is capable of inhibiting the expression of proapoptotic proteins, such as Bax (Polcic et al., 2015).

The interplay between autophagy and apoptosis signaling pathways has attracted increasing attention in recent years, although

little is known about the interaction points between them (Gump & Thorburn, 2011; Mariño, Niso-Santano, Baehrecke, & Kroemer, 2014). The concomitant increase of Beclin1 and Bcl2 observed in AF_A suggests the interaction of these pathways during follicular atresia in the Nile tilapia. Studies show that the binding of Bcl2 to the BH3 domain of Beclin1 inactivates the autophagy (Kang et al., 2011; Zalckvar et al., 2009). However, high levels of Bcl2 in the context presented in this study may contribute to the maintenance of autophagy and follicular cell survival in AF_A. In the AF_L, Lc3/Casp3 colocalization may be due to cleavage of Lc3 by Casp3 and activation of apoptosis. In fact, recent evidence demonstrates that the caspases may act on the cleavage of autophagic proteins such as Beclin1 and Atg3, inhibiting the pro-autophagic activity of these proteins (Cassel et al., 2017; Luo & Rubinsztein, 2010; Oral et al., 2012; Zhu et al., 2010).

In this study, we also reported the dynamics of Ctsd lysosomal protease through colocalization with Lamp1, a lysosomal membrane protein. The peak of Ctsd in AF_A may be related to yolk degradation and removal of cell remnants (Carnevali, Cionna, Tosti, Lubzens, & Maradonna, 2006). Hence, Ctsd/Lamp1 colocalization in the follicular cells indicates that Ctsd is located inside the lysosomal compartment in AF_A. The partial release of Ctsd to the cytosol occurred in AF_L, since Ctsd/Lamp1 colocalization was restricted to some cytoplasmic areas. The destabilization of the lysosomal membrane leads to the release of Ctsd into the cytosol with mitochondrial membrane disturbance, activation of effector caspases, and apoptosis

(Gómez-Sintes et al., 2016; Repnik, Stoka, Turk, & Turk, 2012). In this sense, the release of CtSD into the cytosol in the follicular cells during late follicular atresia of Nile tilapia can amplify the cell death response by apoptosis. Similarly, in cells cultured under serum deprivation, the inhibition of autophagy protects cells against apoptosis, and the overexpression of CtSD accelerates apoptosis, suggesting that cell death is regulated by lysosomal proteinases and cathepsins, downstream autophagy (Uchiyama, 2001). In contrast, reduced CtSD labeling and increased autophagy were related to autophagic cell death in lymphoma cells under infection by the Epstein–Barr virus (Hasui et al., 2011).

Taken together, our data suggest a complex network of interactions between the autophagy and apoptosis signaling pathways with lysosomal protease regulating follicular atresia in fish ovaries. Autophagy is essential to maintain follicular cell homeostasis during yolk phagocytosis in the advanced phase of follicular atresia, while Cathepsin D-dependent apoptosis may contribute to follicular cell death during late follicular atresia.

4 | MATERIALS AND METHODS

4.1 | Experimental design and fish sampling

The experiment was carried out at the Aquaculture Laboratory (LAQUA) of the Federal University of Minas Gerais (UFMG), Southeastern Brazil, and the research was approved by the Ethics Committee on Animal Use (CEUA 97/2011) of UFMG.

For breeding, adult specimens of *O. niloticus* were kept under cultivation conditions at the ratio of three females to one male with a water temperature of $28 \pm 1^\circ\text{C}$. After 3 days of stocking, females were examined for egg incubation in the oral cavity. Following removal of the offspring from the buccal cavity, 12 females were transferred to a 5 m^3 tank under controlled conditions with a photoperiod of 12 hr:dark/12 hr light. Throughout the experiment, the fish were fed ad libitum twice daily with commercial feed, and the physicochemical parameters of the water were kept within the optimal levels for tilapia cultivation (temperature: $29.5 \pm 1.5^\circ\text{C}$, dissolved oxygen: $6.70 \pm 1.46\text{ mg l}^{-1}$, pH: 7.68 ± 0.31 , conductivity: $0.28 \pm 0.05\text{ mS cm}^{-1}$, total dissolved solids: $0.16 \pm 0.03\text{ g l}^{-1}$, salinity: $0.12 \pm 0.02\text{ ppt}$, and turbidity: $1.71 \pm 0.38\text{ NTU}$).

To study the follicular atresia, three females were collected weekly until 21 days after spawning, making a total of 12 individuals. For this, the specimens were euthanized with a 285 mg/L eugenol solution according to the ethical principles established by the Brazilian College of Animal Experimentation (COBEA). Samples of the middle region of the ovaries of each specimen were collected for analysis by various techniques.

4.2 | Light and electron microscopy

Histology analyses were performed on ovary samples fixed in Bouin's fluid for 24 hr at room temperature, embedded in paraffin, cut into $5\text{ }\mu\text{m}$ thickness, and stained with haematoxylin–eosin. For electron

microscopy analysis, small fragments were fixed in Karnovsky solution (2.5% glutaraldehyde and 2% paraformaldehyde) in 0.01 M sodium phosphate buffer pH 7.3 for 24 hr at 4°C , postfixed in 1% osmium tetroxide with 1.5% potassium ferrocyanide for 2 hr, and then embedded in plastic resin Epon/Araldite. The ultrathin sections were contrasted with uranyl acetate and lead citrate and examined under a Tecnai G2-135 12 Spirit 120 kV Transmission Electron Microscope (FEI Company, Hillsboro).

4.3 | In situ TUNEL assay

Ovarian samples were fixed in buffered 4% paraformaldehyde for 24 hr at 4°C , embedded in paraffin, sectioned at $5\text{ }\mu\text{m}$ thickness, and submitted to the in situ TUNEL assay using the ApopTag Plus Peroxidase S7101 Apoptosis Detection Kit (Millipore, Burlington). In summary, the ovary sections were washed in phosphate-buffered saline (PBS) pH 7.4 and treated with $20\text{ }\mu\text{g/ml}$ proteinase K in PBS for 15 min. To inactivate the endogenous peroxidase, 3% H_2O_2 was used in PBS for 10 min. Then, sections were incubated with TdT and biotinylated deoxynucleotides for 1 hr at 37°C and, subsequently, with anti-digoxigenin solution conjugated for 30 min at room temperature. The reaction was revealed with 3,3'-diaminobenzidine (DAB) for approximately 1 min, and the sections were counterstained with haematoxylin. The negative control excluded treatment with TdT and labeled deoxynucleotides.

4.4 | Immunohistochemistry

Immunofluorescence was used to localize the proteins of apoptosis, autophagy, and lysosomes in the ovaries of the Nile tilapia. Serial ovarian sections were also submitted to immunoperoxidase to evaluate the immunoreactions following similar procedures used for immunofluorescence. Ovarian samples were fixed in buffered 4% paraformaldehyde for 24 hr at 4°C and the sections were submitted to a boiling water bath for 20 min in 10 mM sodium citrate buffer pH 6.0 for antigen retrieval. Nonspecific binding block was performed with blocking buffer (2% bovine serum albumin + 0.05% Tween 20) for 45 min. Then, the sections were incubated with primary antibodies (Table 2) in a humid chamber overnight at 4°C . Subsequently, sections

TABLE 2 Primary antibodies with dilution used in the immunohistochemical reactions

Primary antibodies	Origin	Dilution
Bcl2 polyclonal rabbit	Santa Cruz Biotechnology	1:50
Bax polyclonal rabbit	Santa Cruz Biotechnology	1:100
Casp3 monoclonal mouse	Abcam	1:200
Beclin1 polyclonal rabbit	Santa Cruz Biotechnology	1:100
CtSD polyclonal rabbit	Abcam	1:100
Lamp1 monoclonal mouse	Abcam	1:200
Lc3 polyclonal rabbit	Santa Cruz Biotechnology	1:200
Actin polyclonal mouse	Sigma–Aldrich	1:500

were incubated with anti-rabbit IgG secondary antibody conjugated to Alexa Fluor 488 (1:500) or anti-mouse IgG conjugated to Alexa fluor 568 (1:500; Life Technologies, Carlsbad). Nuclear DNA labeling was performed using 4',6-diamidino-2-phenylindole (DAPI; 1:2000; Sigma-Aldrich, St. Louis). Sections were examined using an Axio Imager Z2-ApoTome 2 fluorescence microscope. For immunoperoxidase, the sections were incubated in a dark chamber with 3% H₂O₂ for 30 min for inactivation of the endogenous peroxidase. After treatment with primary antibody, the sections were incubated with biotinylated secondary antibody LSAB 2 System-HRP (Dako, Santa Clara) for 1 hr, followed by streptavidin conjugated with peroxidase for 1 hr. The reactions were revealed with DAB, and the sections were counterstained with hematoxylin. For negative control, the primary antibody was omitted.

4.5 | Western blot analysis

For detection of Lc3I to Lc3II conversion and to confirm the specificity of the antibodies used in the present study, the ovaries from three females of the Nile tilapia were submitted to Western blot analysis technique. Frozen ovary samples were sonicated in lysis buffer with aprotinin and phenylmethylsulfonyl fluoride protease inhibitors and centrifuged at 150,000g for 1 hr. The protein dosage was performed on the supernatant according to Bradford (1976). For each sample, 80 µg of protein in sample buffer was added to 15% polyacrylamide gel electrophoresis and subsequently transferred to polyvinylidene difluoride membrane. After transfer, nonspecific reactions were blocked with skimmed milk powder for 1 hr at room temperature. Then, the membrane was incubated with primary antibody (1:500; Table 2) overnight at 4°C. Finally, the membrane was incubated with anti-rabbit IgG or anti-mouse IgG secondary antibody peroxidase-conjugated dilution 1:750 (Sigma-Aldrich) for 2 hr and the reaction was revealed using DAB. The specificity of the primary antibodies for Nile tilapia was confirmed by a Western blot: Bcl2 ~29 kDa, Bax ~20 kDa, Casp~15 kDa, Beclin1 ~57 kDa, CtSD ~29 kDa, Lamp1 ~100 kDa, Actin ~43 kDa, Lc3I ~18 kDa, and Lc3II ~16 kDa.

4.6 | Morphometry

The area of AF was determined by the measurement of 50 follicles at three regression phases: Early (AF_E), advanced (AF_A), and late (AF_L) using AxioVision image analysis software coupled to a Zeiss AxioPlan 2 microscope. For quantification, the proportion (%) of the follicular components (yolk, zona radiata, follicular cells, and theca) of 50 AF from each regression phase were quantified at ×400 magnification using the ImageJ software with 690 grid points. This proportion was determined considering the number of points on the follicular components multiplied by 100 and divided by the total number of points on the tissue. The immunoperoxidase reaction and TUNEL assay were quantified for 20 representative AF from each regression phase, and the proportion (%) of labeled follicular and theca cells was calculated using the ImageJ software (Morais et al., 2016).

4.7 | Statistical analysis

Minitab 16.1 and GraphPad Prism 6.03 software was used in the statistical analyses. The data did not show a normal distribution, and therefore, the Kruskal-Wallis test followed by Dunn's post hoc test was used. Values were expressed as mean ± standard error of the mean and considered significant with a 95% confidence interval.

ACKNOWLEDGMENTS

The authors would like to thank Mônica Cândida Pereira Ricardo for preparing the histological slides, the technicians at the Laboratory of Aquaculture (LAQUA) of the UFMG for their assistance in handling of the fishes, Dr. Priscila Divina Diniz Alves for helping in immunofluorescence procedures and to Stephen Latham for the valuable suggestions with the English language. The work was supported by Brazilian funding agencies: Conselho Nacional de Desenvolvimento Científico e Tecnológico (CNPq, grant numbers: 482756/2012-8, 306792/2011-7), Fundação de Amparo à Pesquisa no Estado de Minas Gerais (FAPEMIG, grant number: CRA-PPM-00394-13) and Coordenação de Aperfeiçoamento de Pessoal de Nível Superior (CAPES Finance Code 001).

CONFLICT OF INTEREST

The authors declare that there is no conflict of interest.

ORCID

Elizete Rizzo  <http://orcid.org/0000-0001-8601-0856>

REFERENCES

- Antonsson, B. (2001). Bax and other pro-apoptotic Bcl-2 family "killer-proteins" and their victim the mitochondrion. *Cell and Tissue Research*, 306(3), 347–361. <https://doi.org/10.1007/s00441-001-0472-0>
- Bradford, M. M. (1976). A rapid and sensitive method for the quantitation of microgram quantities of protein utilizing the principle of protein-dye binding. *Analytical Biochemistry*, 72, 248–254.
- Carnevali, O., Cionna, C., Tosti, L., Lubzens, E., & Maradonna, F. (2006). Role of cathepsins in ovarian follicle growth and maturation. *General and Comparative Endocrinology*, 146(3), 195–203. <https://doi.org/10.1016/j.ygcen.2005.12.007>
- Cassel, M., de paiva camargo, M., Oliveira de Jesus, L. W., & Borella, M. I. (2017). Involution processes of follicular atresia and post-ovulatory complex in a characid fish ovary: A study of apoptosis and autophagy pathways. *Journal of Molecular Histology*, 48(3), 243–257. <https://doi.org/10.1007/s10735-017-9723-6>
- Chiarelli, R., Agnello, M., Bosco, L., & Roccheri, M. C. (2014). Sea urchin embryos exposed to cadmium as an experimental model for studying the relationship between autophagy and apoptosis. *Marine Environmental Research*, 93, 47–55. <https://doi.org/10.1016/j.marenvres.2013.06.001>
- Chifenti, B., Locci, M. T., Lazzeri, G., Guagnozzi, M., Dinucci, D., Chiellini, F., ... Battini, L. (2013). Autophagy-related protein LC3 and Beclin-1 in the first trimester of pregnancy. *Clinical and Experimental Reproductive Medicine*, 40(1), 33–37. <https://doi.org/10.5653/cerm.2013.40.1.33>
- Coward, K., & Bromage, N. R. (2000). Reproductive physiology of female tilapia broodstock. *Reviews in Fish Biology and Fisheries*, 10(1), 1–25. <https://doi.org/10.1023/A:1008942318272>

- Craig, J. (2007). Gonadotropin and intra-ovarian signals regulating follicle development and atresia: The delicate balance between life and death. *Frontiers in Bioscience*, 12(1), 3628–3639. <https://doi.org/10.1093/geront/gns169>
- Doherty, J., & Baehrecke, E. H. (2018). Life, death and autophagy. *Nature Cell Biology*, 20(10), 1110–1117. <https://doi.org/10.1038/s41556-018-0201-5>
- Drummond, C. D., Bazzoli, N., Rizzo, E., & Sato, Y. (2000). Postovulatory follicle: A model for experimental studies of programmed cell death or apoptosis in teleosts. *The Journal of Experimental Zoology*, 287(2), 176–182.
- Elmore, S. (2007). Apoptosis: A review of programmed cell death. *Toxicologic Pathology*, 35(4), 495–516. <https://doi.org/10.1080/01926230701320337>
- Food and Agriculture Organization of the United Nations (2018). *Cultured aquatic species information programme: Oreochromis niloticus (Linnaeus, 1758)*. Retrieved from: http://www.fao.org/fishery/culturedspecies/Oreochromis_niloticus/en
- Gómez-Sintes, R., Ledesma, M. D., & Boya, P. (2016). Lysosomal cell death mechanisms in aging. *Ageing Research Reviews*, 32, 150–168. <https://doi.org/10.1016/j.arr.2016.02.009>
- Gump, J. M., & Thorburn, A. (2011). Autophagy and apoptosis: What is the connection? *Trends in Cell Biology*, 21(7), 387–392. <https://doi.org/10.1016/j.tcb.2011.03.007>
- Hasui, K., Wang, J., Jia, X., Tanaka, M., Nagai, T., Matsuyama, T., & Eizuru, Y. (2011). Enhanced autophagy and reduced expression of Cathepsin D are related to autophagic cell death in Epstein-Barr virus-associated nasal natural killer/T-cell lymphomas: An Immunohistochemical analysis of Beclin-1, LC3, Mitochondria (AE-1), and Cathepsin D in nasopharyngeal lymphomas. *Acta Histochemica et Cytochemica*, 44(3), 119–131. <https://doi.org/10.1267/ahc.10024>
- Hsueh, A. J. W., Billig, H., & Tsafiriri, A. (1994). Ovarian follicle atresia: A hormonally controlled apoptotic process. *Endocrine Reviews*, 15(6), 707–724. <https://doi.org/10.1210/edrv-15-6-707>
- Huettenbrenner, S., Maier, S., Leisser, C., Polgar, D., Strasser, S., Grusch, M., & Krupitza, G. (2003). The evolution of cell death programs as prerequisites of multicellularity. *Mutation Research*, 543(3), 235–249. [https://doi.org/10.1016/S1383-5742\(02\)00110-2](https://doi.org/10.1016/S1383-5742(02)00110-2)
- Huynh, K. K., Eskelinen, E. L., Scott, C. C., Malevanets, A., Saftig, P., & Grinstein, S. (2007). LAMP proteins are required for fusion of lysosomes with phagosomes. *EMBO Journal*, 26(2), 313–324. <https://doi.org/10.1038/sj.emboj.7601511>
- Kaipia, A., & Hsueh, A. J. (1997). Regulation of ovarian follicle atresia. *Annual Review of Physiology*, 59, 349–363.
- Kang, R., Zeh, H. J., Lotze, M. T., & Tang, D. (2011). The Beclin 1 network regulates autophagy and apoptosis. *Cell Death and Differentiation*, 18(4), 571–580. <https://doi.org/10.1038/cdd.2010.191>
- Kishi-Itakura, C., Koyama-Honda, I., Itakura, E., & Mizushima, N. (2014). Ultrastructural analysis of autophagosome organization using mammalian autophagy-deficient cells. *Journal of Cell Science*, 127(22), 4984–4984. <https://doi.org/10.1242/jcs.164293>
- Klionsky, D. J., Abdalla, F. C., Abeliovich, H., Abraham, R. T., Acevedo-Arozena, A., Adeli, K., ... Zuckerbraun, B. (2012). Guidelines for the use and interpretation of assays for monitoring autophagy. *Autophagy*, 8(4), 445–544. <https://doi.org/10.4161/auto.19496>
- Kriel, J., & Loos, B. (2019). The good, the bad and the autophagosome: Exploring unanswered questions of autophagy-dependent cell death. *Cell Death and Differentiation*, 26, 640–652.
- Lamb, C. A., Yoshimori, T., & Tooze, S. A. (2013). The autophagosome: Origins unknown, biogenesis complex. *Nature Reviews Molecular Cell Biology*, 14(12), 759–774. <https://doi.org/10.1038/nrm3696>
- Lin, F., Li, R., Pan, Z., Zhou, B., Yu, D., Wang, X., ... Liu, H. (2012). miR-26b promotes granulosa cell apoptosis by targeting ATM during follicular atresia in porcine ovary. *PLoS One*, 7(6), e38640. <https://doi.org/10.1371/journal.pone.0038640>
- Luo, S., & Rubinsztein, D. C. (2010). Apoptosis blocks Beclin 1-dependent autophagosome synthesis: An effect rescued by Bcl-xL. *Cell Death and Differentiation*, 17(2), 268–277. <https://doi.org/10.1038/cdd.2009.121>
- Mariño, G., Niso-Santano, M., Baehrecke, E. H., & Kroemer, G. (2014). Self-consumption: The interplay of autophagy and apoptosis. *Nature Reviews Molecular Cell Biology*, 15(2), 81–94. <https://doi.org/10.1038/nrm3735>
- Mathai, B., Meijer, A., & Simonsen, A. (2017). Studying autophagy in zebrafish. *Cells*, 6(3), 21. <https://doi.org/10.3390/cells6030021>
- Melo, R. M. C., Martins, Y. S., de Alencar Teixeira, E., Luz, R. K., Rizzo, E., & Bazzoli, N. (2014). Morphological and quantitative evaluation of the ovarian recrudescence in Nile Tilapia (*Oreochromis niloticus*) after spawning in captivity. *Journal of Morphology*, 275(3), 348–356. <https://doi.org/10.1002/jmor.20214>
- Melo, R. M. C., Martins, Y. S., Luz, R. K., Rizzo, E., & Bazzoli, N. (2015). PCNA and apoptosis during post-spawning ovarian remodeling in the teleost *Oreochromis niloticus*. *Tissue and Cell*, 47(6), 541–549. <https://doi.org/10.1016/j.tice.2015.10.002>
- Miranda, A. C. L., Bazzoli, N., Rizzo, E., & Sato, Y. (1999). Ovarian follicular atresia in two teleost species: A histological and ultrastructural study. *Tissue and Cell*, 31(5), 480–488. <https://doi.org/10.1054/tice.1999.0045>
- Morais, R. D., Thomé, R. G., Lemos, F. S., Bazzoli, N., & Rizzo, E. (2012). Autophagy and apoptosis interplay during follicular atresia in fish ovary: A morphological and immunocytochemical study. *Cell and Tissue Research*, 347, 467–478. <https://doi.org/10.1007/s00441-012-1327-6>
- Morais, R. D., Thomé, R. G., Santos, H. B., Bazzoli, N., & Rizzo, E. (2016). Relationship between bcl-2, bax, beclin-1, and cathepsin-D proteins during postovulatory follicular regression in fish ovary. *Theriogenology*, 85(6), 1118–1131. <https://doi.org/10.1016/j.theriogenology.2015.11.024>
- Nezis, I. P., Shrivage, B. V., Sagona, A. P., Johansen, T., Baehrecke, E. H., & Stenmark, H. (2010). Autophagy as a trigger for cell death: Autophagic degradation of inhibitor of apoptosis dBruce controls DNA fragmentation during late oogenesis in *Drosophila*. *Autophagy*, 6(8), 1214–1215. <https://doi.org/10.4161/auto.6.8.13694>
- Nikoletopoulou, V., Markaki, M., Palikaras, K., & Tavernarakis, N. (2013). Crosstalk between apoptosis, necrosis and autophagy. *Biochimica et Biophysica Acta—Molecular Cell Research*, 1833(12), 3448–3459. <https://doi.org/10.1016/j.bbamcr.2013.06.001>
- Oral, O., Oz-Arslan, D., Itah, Z., Naghavi, A., Deveci, R., Karacali, S., & Gozuacik, D. (2012). Cleavage of Atg3 protein by caspase-8 regulates autophagy during receptor-activated cell death. *Apoptosis*, 17(8), 810–820. <https://doi.org/10.1007/s10495-012-0735-0>
- Polcic, P., Jaka, P., & Mentel, M. (2015). Yeast as a tool for studying proteins of the Bcl-2 family. *Microbial Cell*, 2(3), 74–87. <https://doi.org/10.15698/mic2015.03.193>
- Repnik, U., Stoka, V., Turk, V., & Turk, B. (2012). Lysosomes and lysosomal cathepsins in cell death. *Biochimica et Biophysica Acta - Proteins and Proteomics*, 1824(1), 22–33. <https://doi.org/10.1016/j.bbapap.2011.08.016>
- Repnik Meng, L., Jan, S. Z., Hamer, G., Van Pelt, A. M., Van Der Stelt, I., Keijer, J., & Teerds, K. J. (2018). Preantral follicular atresia occurs mainly through autophagy, while antral follicles degenerate mostly through apoptosis. *Biology of Reproduction*, 99(4), 853–863. <https://doi.org/10.1093/biolre/iox116>
- Ryter, S. W., Cloonan, S. M., & Choi, A. M. K. (2013). Autophagy: A critical regulator of cellular metabolism and homeostasis. *Molecules and Cells*, 36(1), 7–16. <https://doi.org/10.1007/s10059-013-0140-8>
- Santos, H. B., Thomé, R. G., Arantes, F. P., Sato, Y., Bazzoli, N., & Rizzo, E. (2008). Ovarian follicular atresia is mediated by heterophagy, autophagy, and apoptosis in *Prochilodus argenteus* and *Leporinus taeniatus* (Teleostei: Characiformes). *Theriogenology*, 70, 1449–1460. <https://doi.org/10.1016/j.theriogenology.2008.06.091>
- Serrano-Puebla, A., & Boya, P. (2018). Lysosomal membrane permeabilization as a cell death mechanism in cancer cells. *Biochemical Society Transactions*, 46, 207–215. <https://doi.org/10.1042/BST20170130>
- Sever, O. N., & Demir, O. G. (2017). Autophagy: Cell death or survive mechanism. *Journal of Oncological Sciences*, 3(2), 37–44. <https://doi.org/10.1016/j.jons.2017.07.001>

- Shimizu, S., Narita, M., & Tsujimoto, Y. (2000). Bcl-2 family proteins regulate the release of apoptogenic cytochrome c by the mitochondrial channel VDAC. *Nature*, *66*(1992), 1–5.
- Take, H., & Andersen, Ø. (2007). Caspases and apoptosis in fish. *Journal of Fish Biology*, *71*, 326–349. <https://doi.org/10.1111/j.1095-8649.2007.01665.x>
- Thomé, R. G., Santos, H. B., Arantes, F. P., Domingos, F. F. T., Bazzoli, N., & Rizzo, E. (2009). Dual roles for autophagy during follicular atresia in fish ovary. *Autophagy*, *5*(1), 117–119. <https://doi.org/10.4161/auto.5.1.7302>
- Tsujimoto, Y., & Shimizu, S. (2005). Another way to die: Autophagic programmed cell death. *Cell Death and Differentiation*, *12*, 1528–1534. <https://doi.org/10.1038/sj.cdd.4401777>
- Uchiyama, Y. (2001). Autophagic cell death and its execution by lysosomal cathepsins. *Archives of Histology and Cytology*, *64*(3), 233–246. <https://doi.org/10.1679/aohc.64.233>
- Zalckvar, E., Berissi, H., Mizrachy, L., Idelchuk, Y., Koren, I., Eisenstein, M., ... Kimchi, A. (2009). DAP-kinase-mediated phosphorylation on the BH3 domain of beclin 1 promotes dissociation of beclin 1 from Bcl-XL and induction of autophagy. *EMBO Reports*, *10*(3), 285–292. <https://doi.org/10.1038/embor.2008.246>
- Zamorano, S., Rojas-Rivera, D., Lisbona, F., Parra, V., Court, F. A., Villegas, R., ... Hetz, C. (2012). A BAX/BAK and cyclophilin D-independent intrinsic apoptosis pathway. *PLoS One*, *7*(6), e37782. <https://doi.org/10.1371/journal.pone.0037782>
- Zhou, J., Peng, X., & Mei, S. (2019). Autophagy in ovarian follicular development and atresia. *International Journal of Biological Sciences*, *15*(4), 726–737. <https://doi.org/10.7150/ijbs.30369>
- Zhou, X. Y., Luo, Y., Zhu, Y. M., Liu, Z. H., Kent, T. A., Rong, J. G., ... Zhang, H. L. (2017). Inhibition of autophagy blocks cathepsins-tBid-mitochondrial apoptotic signaling pathway via stabilization of lysosomal membrane in ischemic astrocytes. *Cell Death and Disease*, *8*(2), e2618. <https://doi.org/10.1038/cddis.2017.34>
- Zhu, Y., Zhao, L., Liu, L., Gao, P., Tian, W., Wang, X., ... Chen, Q. (2010). Beclin 1 cleavage by caspase-3 inactivates autophagy and promotes apoptosis. *Protein and Cell*, *1*(5), 468–477. <https://doi.org/10.1007/s13238-010-0048-4>

How to cite this article: Sales CF, Melo RMC, Pinheiro APB, Luz RK, Bazzoli N, Rizzo E. Autophagy and Cathepsin D mediated apoptosis contributing to ovarian follicular atresia in the Nile tilapia. *Mol Reprod Dev.* 2019;1–11. <https://doi.org/10.1002/mrd.23245>

4.2. CAPÍTULO 2: Effects of starvation and refeeding cycles on spermatogenesis and sex steroids in the Nile tilapia *Oreochromis niloticus*: Sales CF, Pinheiro APB, Ribeiro YM, Weber AA, Paes-Leme FO, Luz RK, Bazzoli N, Rizzo E, Melo RMC. *Molecular and Cellular Endocrinology* 500 (2020) 110643. doi.org/10.1016/j.mce.2019.110643



Effects of starvation and refeeding cycles on spermatogenesis and sex steroids in the Nile tilapia *Oreochromis niloticus*



Camila Ferreira Sales^a, Ana Paula Barbosa Pinheiro^a, Yves Moreira Ribeiro^a, André Alberto Weber^a, Fabíola de Oliveira Paes-Leme^b, Ronald Kennedy Luz^b, Nilo Bazzoli^c, Elizete Rizzo^a, Rafael Magno Costa Melo^{a,*}

^a Departamento de Morfologia, Instituto de Ciências Biológicas, Universidade Federal de Minas Gerais, 31270-901, Belo Horizonte, Minas Gerais, Brazil

^b Laboratório de Aquacultura, Escola de Veterinária, Universidade Federal de Minas Gerais, 31270-901, Belo Horizonte, Minas Gerais, Brazil

^c Pontifícia Universidade Católica de Minas Gerais, Programa de Pós-graduação em Biologia de Vertebrados, 30535-610, Belo Horizonte, Minas Gerais, Brazil

ARTICLE INFO

Keywords:

Germ cells
Apoptosis
Ki-67
Cholesterol
Testosterone
Cortisol

ABSTRACT

Food restriction is part of the life cycle of many fish species; however, nutritional deficiency may negatively influence gametogenesis and gonadal maturation. The aim of this study was to evaluate the effects of food restriction on the spermatogenesis of Nile tilapia. For this, adult males were submitted to starvation and refeeding cycles (alternating periods of starvation and feeding) for 7, 14, 21, and 28 days. After 7 days of starvation, glycaemic and lipid levels were significantly reduced, followed by reduction of plasma testosterone (T) and 11-ketotestosterone (11-KT). In addition, reduced proliferation of spermatogonia and increased apoptosis of spermatocytes, spermatids, and spermatozoa was observed in starvation groups. In the refeeding groups, the sex steroids and the proportion of germ cells had no significant alterations compared to the control group, except for spermatozoa. In this sense, the present study suggests that starvation after 7 days progressively reduces T and 11-TK, resulting in damage to the production of spermatogenic cells, while refeeding may delay spermatogenesis but does not lead to testicular impairment.

1. Introduction

Nutritional deficiency is associated with metabolic changes that may be reflected in the circulating concentrations of hormones such as testosterone and gonadotrophins, which regulate spermatogenesis and testicular maturation (Cheah and Yang, 2011; Churchill et al., 2019; Gilad et al., 2018; Grizard et al., 1997). In addition to hormonal impairment, nutrient deficiencies interfere with spermatogenesis, especially deficiency of ions and vitamins that act protecting the testis from oxidative damage and improve sperm quality, as well as are related with the differentiation of spermatogonia (Alonge et al., 2019; Chung et al., 2009). In fish, long fasting periods can also negatively influence the reproductive potential depending on the species, sex, age of the animal, and its capacity to mobilise the energy reserves (Jobling, 2016; Luquet and Watanabe, 1986). However, the mechanisms by which spermatogenesis is influenced by starvation remain unknown.

Fish spermatogenesis is a cyclic process finely regulated by endocrine, paracrine, and autocrine factors involving complex interactions

between somatic and germ cells (Batlouni et al., 2009; Schulz et al., 2010). The germ cells development can be divided into three main phases: spermatogonial or proliferative, when undifferentiated spermatogonia originate type A and type B spermatogonia; spermatocytary or meiotic phase, when meiotic division originates primary and secondary spermatocytes; and spermiogenesis, when a series of morphological changes leads to the differentiation of spermatids into spermatozoa (Schulz et al., 2010). Follicle stimulating hormone (FSH) and luteinizing hormone (LH) regulate the production of sex steroids, testosterone, and 11-ketotestosterone by Leydig cells, and these hormones mainly act on the mitotic proliferation and differentiation of spermatogonia and spermiation (de Waal et al., 2009; Haider, 2007).

In testes, a complex and well organised balance between proliferation and cell death maintains tissue homeostasis (Ribeiro et al., 2017; Russell et al., 2002; Wang et al., 2012). During spermatogenesis, apoptosis is responsible for maintaining the appropriate number of germ cells supported by the Sertoli cells and for elimination of defective germ cells (Barnes et al., 1998; Richburg, 2000; Shaha et al., 2010).

* Corresponding author. Departamento de Morfologia, Instituto de Ciências Biológicas, Universidade Federal de Minas Gerais, Av. Antônio Carlos 6627, 31270-901, Belo Horizonte, Minas Gerais, Brazil.

E-mail address: rafaelmelo@icb.ufmg.br (R.M.C. Melo).

<https://doi.org/10.1016/j.mce.2019.110643>

Received 3 October 2019; Received in revised form 7 November 2019; Accepted 7 November 2019

Available online 08 November 2019

0303-7207/ © 2019 Elsevier B.V. All rights reserved.

Stressors such as thermal shock, exposure to toxic substances, hormonal changes, and starvation increase germ cells apoptosis, impairing sperm production (Cheah and Yang, 2011; Lascarez-Lagunas et al., 2014; Shaha et al., 2010; Wang et al., 2012, 2017).

Food deprivation and fasting are common in the life cycle of many fish species in response to environmental fluctuations under both natural and farming conditions. The physiological and metabolic response to fasting is variable among species, with carnivorous fish being better adapted to periods of food restriction than herbivores and omnivores (Gadomski and Petersen, 1988). Nile tilapia *Oreochromis niloticus* is a omnivorous fish that is very attractive for aquaculture due to its large size, rapid body growth, flesh palatability, ease of reproduction, adaptability to a wide range of environmental conditions, resistance to diseases and infections, and stress tolerance (Little and Hulata, 2000). In addition, males have favourable features to study the structure and function of the testes since they present cystic organisation of germ cells that allows a reliable analysis of spermatogenesis (Melo et al., 2016; Vilela et al., 2003). Although studies have associated food deprivation with reduced reproductive potential in fish species (Pérez-Jiménez et al., 2007; Píkle et al., 2017), knowledge about the consequences of food restriction at metabolic, hormonal, and morphological levels is still incipient. In this sense, the goal of this study was to evaluate the effects of refeeding cycles (alternating periods of starvation and feeding) and starvation on blood biochemical parameters, androgens concentration, and spermatogenesis of Nile tilapia.

2. Material and methods

2.1. Experimental design and fish sampling

The experiment was conducted at the Laboratory of Aquaculture (LAQUA) of the Universidade Federal de Minas Gerais (UFMG), and the study was approved by the Ethics Committee on Animal Use (CEUA, UFMG 67/2017). For acclimation, a breeding stock of 94 adult males of *O. niloticus* (GIFT lineage, age between 6 and 8 months, 24.31 ± 0.31 cm total length, 268.37 ± 11.21 g body weight) were equally distributed in six 1 m^3 culture tanks and kept for 30 days with a mechanical and biological filtration system under controlled conditions. The culture conditions of the experiment were maintained by heaters with thermostat for stabilization of temperature, continuous supplementary aeration by an air diffuser and the photoperiod was kept at 12 h light to 12 h dark. Throughout the experiment period, the water parameters of the tanks were monitored once a week using a Horiba U51 multi-parameter probe and the average values were obtained: temperature 29.06 ± 0.04 °C, dissolved oxygen 7.06 ± 0.02 mg/l, pH 7.31 ± 0.04 , conductivity 0.87 ± 0.11 mS/cm, total dissolved solids 0.51 ± 0.02 g/l, and salinity 0.36 ± 0.02 (values represent mean \pm SEM).

During the experiment, the fish were divided into three groups (control $n = 30$ fish, refeeding $n = 32$, and starvation $n = 32$) with a duplicate tank for each group. In the control group, fish were fed *ad libitum* with commercial feed containing 32% crude protein, and three/four animals per tank were collected at the following sampling times (7, 14, 21 and 28 days). In the refeeding group, four animals per tank were collected at the following sampling times: refeeding 1 (day 14, after a week of starvation, followed by a week of *ad libitum* feeding), refeeding 2 (day 21, after a week of starvation, followed by a week of feeding, and another week of starvation), refeeding 3 (day 28, after alternating two weeks of starvation and feeding). In the starvation group, fish were submitted to total food restriction, and four animals per tank were collected with 7, 14, 21 and 28 days (starvation 7D, 14D, 21D and 28D). The fish were euthanized with 285 mg/l eugenol solution following the ethical principles established by the National Council for Animal Experimentation Control (CONCEA). From these animals, the body weight (BW), total length (TL), and gonad weight (GW) were obtained and the gonadosomatic index ($\text{GSI} = 100\text{GW}/\text{BW}$) and Fulton

condition factor ($K = 100\text{BW}/\text{TL}^3$) were calculated. Blood plasma and testis samples were obtained for analyses using different techniques.

2.2. Light and electron microscopy

For histology, the middle section of the testis of each specimen were fixed in Bouin's fluid for 24 h, embedded in paraffin, sectioned at $5\ \mu\text{m}$ thickness, and stained with haematoxylin-eosin. For electron microscopy, testis samples were fixed in Karnovsky solution (2.5% glutaraldehyde and 2% paraformaldehyde) in 0.1 M sodium phosphate buffer pH 7.3 for 24 h at 4 °C and post-fixed in 1% osmium tetroxide with 1.5% potassium ferrocyanide for 2 h and then embedded in Epon/Araldite plastic resin. The ultrathin sections were contrasted with uranyl acetate and lead citrate and examined under a Tecnai G2-135 12 Spirit 120 kV transmission electron microscope (FEI Company, Hillsboro, OR, USA).

2.3. Blood biochemical parameters

For biochemical analyses, blood samples of each fish were collected in a heparinized syringe and transferred to Eppendorf tubes at 4 °C, also heparinized. The Accu-Chek kit with a minimum detection limit of 10 mg/dl and satisfactory accuracy according to European standard EN ISO 15197 was used for determination of glucose. Then, 2 ml blood samples were centrifuged for 4 min at 3000 rpm and stored in a freezer at -80 °C. Concentrations of total cholesterol and triglycerides were determined using BioTechnique kits following the manufacturer's recommendations.

2.4. TUNEL in situ assay

In order to detect the apoptotic DNA fragmentation, testis samples of each fish were fixed in 4% paraformaldehyde solution for 24 h at 4 °C, embedded in paraffin, and sectioned at $5\ \mu\text{m}$ thickness. The sections were subjected to the terminal deoxynucleotidyl transferase dUTP nick end labelling (TUNEL) assay using the FragEL DNA fragmentation detection kit QIA 33 (Calbiochem, San Diego, CA, USA), following the manufacturer's protocol. For this, the sections were washed in phosphate buffered saline (PBS) pH 7.4, treated with $20\ \mu\text{g}/\text{ml}$ proteinase K in PBS for 15 min, and then treated with and 3% hydrogen peroxide (H_2O_2) in PBS for 15 min to inactivate the endogenous peroxidase. Next, the sections were incubated with terminal deoxynucleotidyl transferase (TdT) and biotinylated deoxynucleotides for 90 min at 37 °C. After this, the sections were incubated with anti-digoxigenin antibody conjugated with peroxidase for 30 min at room temperature and revealed with diaminobenzidine (DAB, Sigma Aldrich's Corp., St. Louis, MO, USA) in PBS for 2 min and counterstained with haematoxylin. In the negative control, treatment with TdT/deoxynucleotides was omitted.

2.5. Immunohistochemistry

Testis samples were submitted to immunohistochemistry reaction for detection of the antibody Ki67 (Sigma), a marker of cell proliferation/mitosis. For this, samples were fixed in 4% paraformaldehyde solution for 24 h at 4 °C, embedded in paraffin, and sectioned at $5\ \mu\text{m}$ thickness. For endogenous peroxidase blocking, the sections were incubated with 3% H_2O_2 in PBS for 30 min at room temperature. Subsequently, the sections were subjected to antigen recovery with 10 mM sodium citrate buffer pH 6.0 for 20 min at 96 °C. Non-specific binding was blocked with 2% bovine albumin in PBS buffer for 30 min at room temperature. Then, the sections were incubated with the primary antibody Ki67 in a humid chamber at 4 °C overnight at 1:100 dilution. Following, the sections were submitted to the Dako EnVision™ + Dual Link System-HRP (kit K4063 Dako), revealed with DAB, and counterstained with haematoxylin. For the negative control, one of the sections did not receive the primary antibody.

2.6. Plasma sex steroids

For the determination of testosterone, 11-ketotestosterone and cortisol, plasma samples of each fish were stored at -80°C . The samples were submitted in duplicate to ELISA assay using 11-ketotestosterone kit (Cayman Chemical, Michigan, USA), testosterone kit (Cayman, Instruments GmbH, Marburg, German), and cortisol kit (DRG Instruments GmbH, Marburg, German) following the manufacturers' protocols, as described previously (Weber et al., 2019). The sensitivity of the assays was 3.9 pg/ml (testosterone), 0.8 pg/ml (11-ketotestosterone), and 2.5 ng/ml (cortisol).

2.7. Morphometry

For morphometry of spermatogenesis, four animals per sampling/group were randomly chosen and digital histological images were obtained using an image analysis system with Zeiss Axiovision software coupled to an Axioplan 2 Zeiss Microscope. To evaluate the proportion of the testicular components and positive cells for Ki67 and TUNEL, 30 randomly chosen fields per animal were photographed at $400\times$ magnification. Spermatogenic cells were identified according to features previously established (Schulz et al., 2010). The images were analysed in ImageJ software using a grid of 540 points. The proportion of somatic and germ cells was determined based on the number of points on the testicular cells in relation to the total points analysed in each field (Melo et al., 2016; Ribeiro et al., 2017).

2.8. Statistical analyses

Data were statistically analysed using Minitab 16.1 and GraphPad Prism 6.03 software. The data did not present normal distribution, so Kruskal-Wallis test followed by Dunn's *post-hoc* test were used. The results were considered significant at 95% confidence interval and values were expressed as mean \pm S.E.M.

3. Results

3.1. Testicular alterations and biological indices

During the experiment, animals from the control and refeeding groups did not present relevant histological alterations in the testes (Fig. 1A). However, after 7 days of starvation, germ cells at different stages of development had highly compacted chromatin (Fig. 1B), and type A undifferentiated spermatogonia (A_{und}) with cytoplasmic vacuolization were observed (Fig. 1C). In the fish collected with 14, 21, and 28 days of starvation, inflammatory infiltrate, spermatogonia and spermatocytes in the tubular lumen, and hyperplasia of Leydig cells was also detected (Fig. 1D and E). Furthermore, the animals submitted to 28 days of starvation had testicular regions with disorganisation and degeneration of the seminiferous tubules (Fig. 1F). In the ultrastructure, the sampling times starvation 7D, 14D, 21D, and 28D showed spermatocytes with vacuolated cytoplasm and degenerate mitochondria being released into the lumen together with cellular debris and apoptotic bodies (Fig. 1G–I). At this time, the spermatids presented abnormalities in the chromatin compaction, degeneration of the midpiece with inefficient elimination of cytoplasm material (Fig. 1J–L). In addition to the histological and ultrastructural changes described above, the animals submitted to starvation and refeeding cycles presented testes with a significantly lower GSI when compared to the control group ($p < 0.05$), although the Fulton condition factor did not show any variation among groups (Fig. 1M and N).

3.2. Morphometry of the germ and somatic cells

In the spermatogonial phase, the proportion (%) of type A undifferentiated and differentiated spermatogonia (A_{und} and A_{diff}) was

reduced in the starvation 21D and 28D when compared to the other sampling times. In contrast, the proportion of type B spermatogonia did not show a significant difference between the treatments (Fig. 2A). Starvation for 7, 14, 21 and 28 days affected the spermatocytary phase, leading to a significant reduction ($p < 0.05$) in the proportion of spermatocytes (Fig. 2B), but no significant variation was detected in the sampling times refeeding 1, 2 and 3 compared to the control. During spermiogenesis, no significant variation was found in the proportion of spermatids, but a significant reduction in spermatozoa ratio ($p < 0.01$) was observed in all treatments when compared to the control (Fig. 2B).

The proportion of Leydig cells was significantly higher at all the sampling times in animals submitted to starvation when compared to the control group ($p < 0.01$) (Fig. 2C). In the animals collected in the sampling times refeeding 1, 2 and 3, an increase in the Leydig cells ratio was also observed, but without statistical difference when compared to the control group. In addition, there was a significant reduction in the proportion of Sertoli cells in the starvation 21D (Fig. 2C). Interstitial tissue did not show significant changes in the treated groups compared to the control, except on 14 days of total food restriction (starvation 14D) when there was a significant increase ($p < 0.05$) in relation to the other groups (Fig. 2C).

3.3. Blood biochemical parameters

In the sampling times starvation 7D, 14D, 21D, 28D and refeeding 2 the blood glucose was significantly lower than that observed in the control group ($p < 0.05$) (Table 1). Plasma levels of total cholesterol and triglycerides were higher in the control group when compared to the experimental groups, except for refeeding 1 ($p < 0.05$).

3.4. Plasma concentrations of androgens and cortisol

The animals submitted to 7, 14, 21, and 28 days of starvation presented a significant reduction ($p < 0.05$) in plasma concentrations of 11-ketotestosterone and testosterone compared to the control group, with a drastic reduction of these hormones at 28 days of total food restriction (Fig. 3A and B). The sampling times refeeding 1 and 3 did not show significant variations for both androgens when compared to the control, while the sampling time refeeding 2 presented a significant reduction for both androgens. Plasma cortisol levels were significantly higher in the starvation 7D, 14D and refeeding 2 when compared to the control ($p < 0.05$) but no significant variation was found between the starvation 28D and control group. During starvation, a cortisol peak was found at 7 days after starting the treatment, and it was gradually reducing until reaching values close to the control group after 21 days of total food restriction (Fig. 3C).

3.5. Cell proliferation and apoptosis

Since the refeeding group showed few alterations in the morphological analyses compared to the control, cell proliferation and apoptosis were only evaluated in the control and starvation groups. The proportion of A_{und} , A_{diff} , and Sertoli cells positive for Ki67 showed a significant decrease after 21 and 28 days of total food restriction when compared to the control group (Fig. 4 A, B and E). In addition, after 7 days of starvation, a significant increase of Leydig cells labelled by Ki67 was observed. In the sampling times starvation 14D, 21D, and 28D, the proportion of TUNEL-positive spermatocytes, spermatids, and spermatozoa increased significantly and progressively over the course of total food restriction (Fig. 4 C, D, and F).

4. Discussion

Response to nutritional stress encompasses metabolic and hormonal changes, which negatively reflect on fish spermatogenesis, as also reported in mammals (Grizard et al., 1997; Yu et al., 2016). In general,

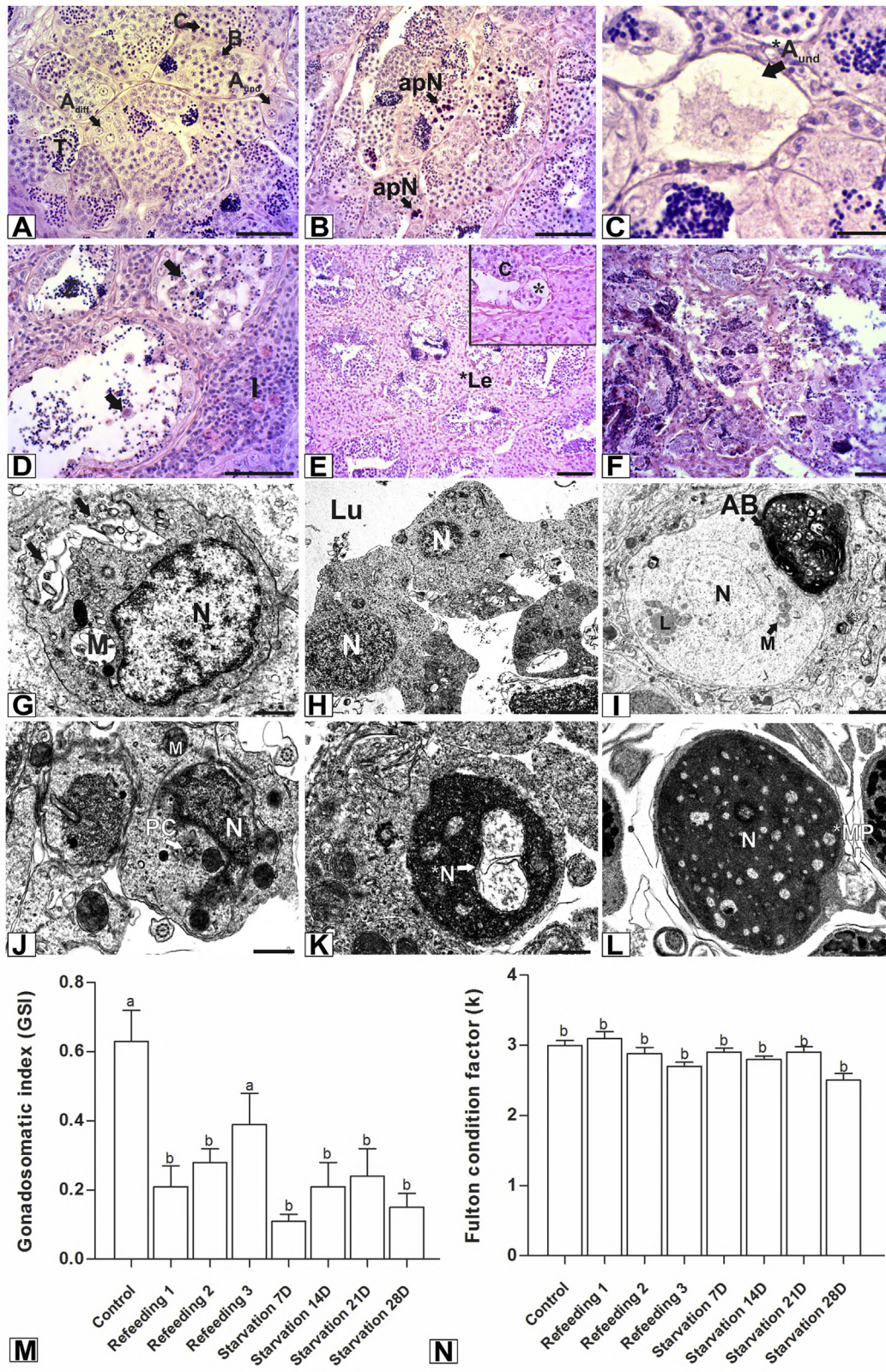


Fig. 1. Histological sections stained with haematoxylin-eosin (A–F), ultrastructural sections (G–L), and biological indices (M, N) of testes of Nile tilapia. A: Control group containing type A undifferentiated spermatogonia (A_{und}), type A differentiated spermatogonia (A_{dir}), type B spermatogonia (B), spermatocytes (C) and spermatids (T) without morphological alterations. B: Cysts containing cell clusters with apoptotic nucleus (apN). C: A_{und} with dilatation and cytoplasmic vacuolization. D: Spermatogonia inside the lumen of the seminiferous tubule (black arrow) and inflammatory infiltrate with acidophilic granulocytes in the interstitial tissue (I). E: Hypertrophy and hyperplasia of Leydig cells (*Le) and empty cysts (*). F: Seminiferous tubules in degeneration. G–H: Spermatocytes in degeneration with vacuolization in the cytoplasm (black arrow) being released in the tubular lumen together with cellular debris. I: Apoptotic body (AB) next to a spermatogonia. J–L: Anomalies in the compaction of chromatin and degeneration of the midpiece (*MP) in spermatids. Nucleus (N); mitochondria (M); proximal centriole (PC); lumen (Lu); lysosome (L). Different letters indicate significant difference among sampling times. Scale bars (A, B, D–F) 50 μ m, (C) 20 μ m, (G, J–L) 500 nm, (H) 1 μ m and (I) 2 μ m.

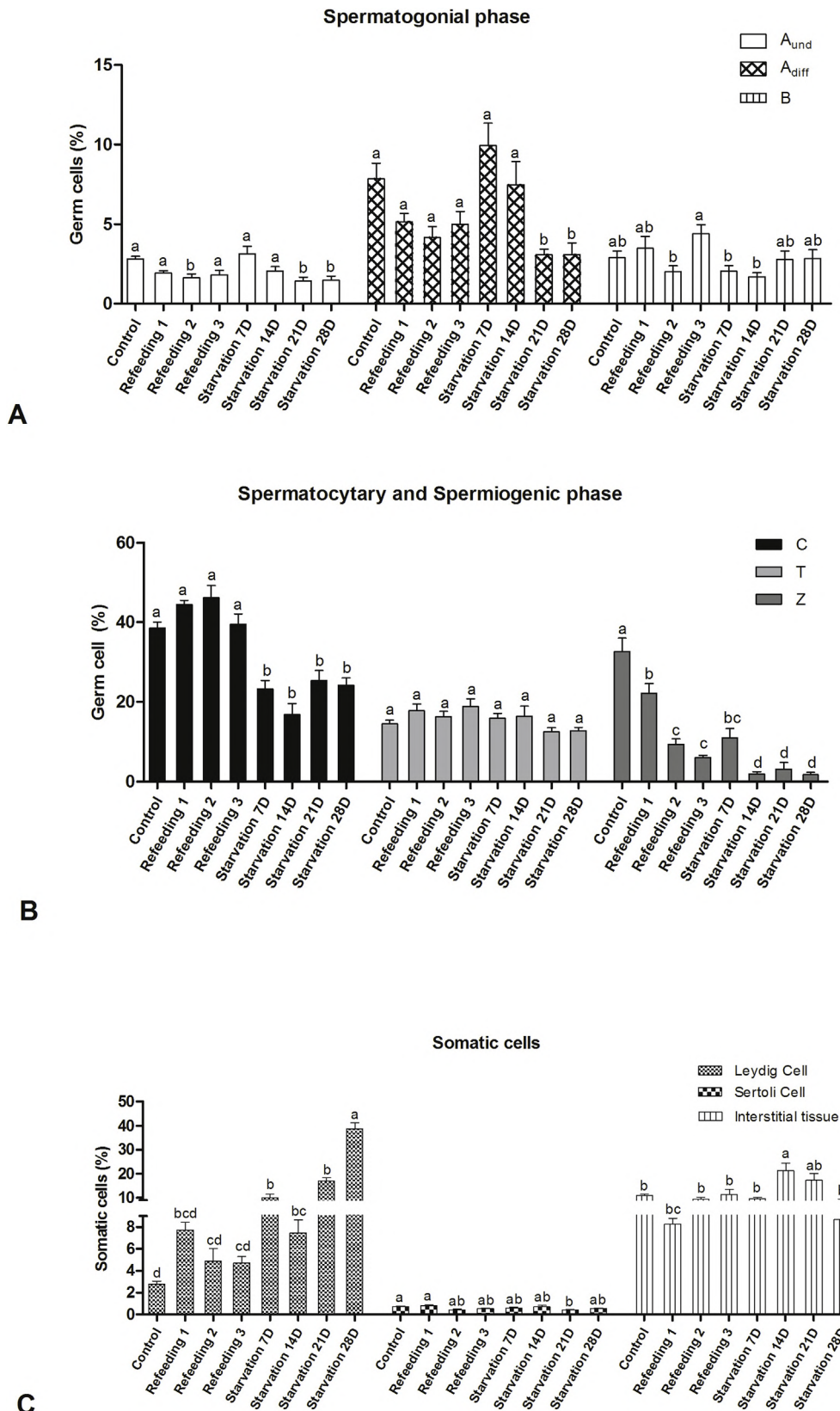


Fig. 2. Proportion of germ and somatic cells during spermatogenesis of Nile tilapia submitted to refeeding cycles and starvation (A–C). Type A undifferentiated spermatogonia (A_{und}), type A differentiated spermatogonia (A_{diff}), type B spermatogonia (B), spermatocytes (C), spermatids (T) and spermatozoa (Z). In each spermatogenic germ cell, different letters indicate significant difference among sampling times ($p < 0.05$).

Table 1

Blood biochemical parameters (mg/dL) in Nile tilapia submitted to refeeding and total food restriction.

Groups	Glucose	Total cholesterol	Triglycerides
Control	56.7 ± 5.10 ^a	238.1 ± 33.23 ^a	228.05 ± 22.39 ^a
Refeeding 1	68.0 ± 2.90 ^a	175.0 ± 9.45 ^b	141.55 ± 26.39 ^b
Refeeding 2	20.6 ± 1.70 ^b	107.5 ± 10.15 ^{bc}	88.59 ± 6.18 ^b
Refeeding 3	34.7 ± 3.00 ^a	102.3 ± 11.45 ^{bc}	112.52 ± 11.67 ^b
Starvation 7D	18.5 ± 0.80 ^b	83.1 ± 4.30 ^c	95.05 ± 12.39 ^b
Starvation 14D	27.3 ± 2.90 ^b	81.7 ± 6.90 ^c	93.33 ± 6.39 ^b
Starvation 21D	20.6 ± 1.60 ^b	84.10 ± 13.23 ^c	131.51 ± 1.79 ^b
Starvation 28D	20.6 ± 1.60 ^b	73.41 ± 9.70 ^c	93.42 ± 5.39 ^b

Different letters in the same columns represent significant difference between the sampling groups for each biochemical parameter ($p < 0.05$).

females are more sensitive than males to the effects of food restriction (Grone et al., 2012; Ridelman et al., 1984), but few studies have been reported the effects of fasting on fish spermatogenesis (Pikle et al., 2017). In the Nile tilapia, severe morphological changes were observed in the germ cells development during starvation, and there was a decrease in the percentage of spermatogonia, spermatocytes, and spermatozoa that may be related to increased apoptosis and reduced cell proliferation.

The gonadosomatic index (GSI) is an indicator of the gonadal development widely used to evaluate the effects of different environmental stressors on fish reproduction (Collins and Anderson, 2002; Duston and Saunders, 1999; Frantzen et al., 2004; Grone et al., 2012). Studies have shown that GSI is negatively affected by nutrient deprivation in both sexes as observed in the European seabass *Dicentrarchus labrax*, amago salmon *Oncorhynchus masou ishikawae*, and catfish *Clarias gariepinus* (Chatzifotis et al., 2011; Silverstein and Shimma, 1994; Suchiang and Gupta, 2011). In addition, findings of the present study show that GSI reduction during food restriction is associated with changes in testicular morphology. Although the tissue response to nutritional deficiency varies among fish species depending on the exposure period and their capacity to mobilise energy reserves, severe tissue changes such as cell degeneration and structural disorganisation have been reported after long periods of food restriction (Pikle et al., 2017; Suchiang and Gupta, 2011). These changes may be related to the poor nutritional status, culminating in the reduction of androgens and elevation of cortisol, as detected in the Nile tilapia of this study.

Short periods of food restriction cause nutritional deficiencies that increase the plasma lipid levels. However, after long periods of food restriction, in addition to lipid deficiency, lipogenesis is depressed while lipolysis is accelerated (Yu et al., 2016). The reduction of lipid levels, mainly cholesterol during food restriction, has been observed in several fish species (Pérez-Jiménez et al., 2007; Prasad, 2015; Rossi et al., 2015). Cholesterol is required for testosterone synthesis in the Leydig cells (Wayne Hou et al., 1990). In this sense, the reduction of testosterone levels as well as 11-ketotestosterone after 7 days of starvation found in this study may be due to the reduction of plasma total cholesterol levels, which has been well documented in humans and other mammalian species (Eacker et al., 2008; Morrison et al., 2002; Velasco-Santamaría et al., 2011).

In addition to sex steroids, glucocorticoids, especially cortisol, may act negatively at all stages of spermatogenesis in both fish and mammals (Dey et al., 2010; Milla et al., 2009; Weber et al., 2002). High plasma levels of cortisol are related to the reduction of the steroidogenic potential of Leydig cells by reducing their sensitivity to the luteinizing hormone (LH) (Orr and Mann, 1992; Whirledge and Cidlowski, 2010). In this study, high levels of cortisol are apparently related to decreased 11-ketotestosterone, increased apoptosis, and decreased of germ cell proliferation.

Proliferation of Leydig cells along with a higher proportion of these cells after 7 days of starvation may be a compensatory mechanism to

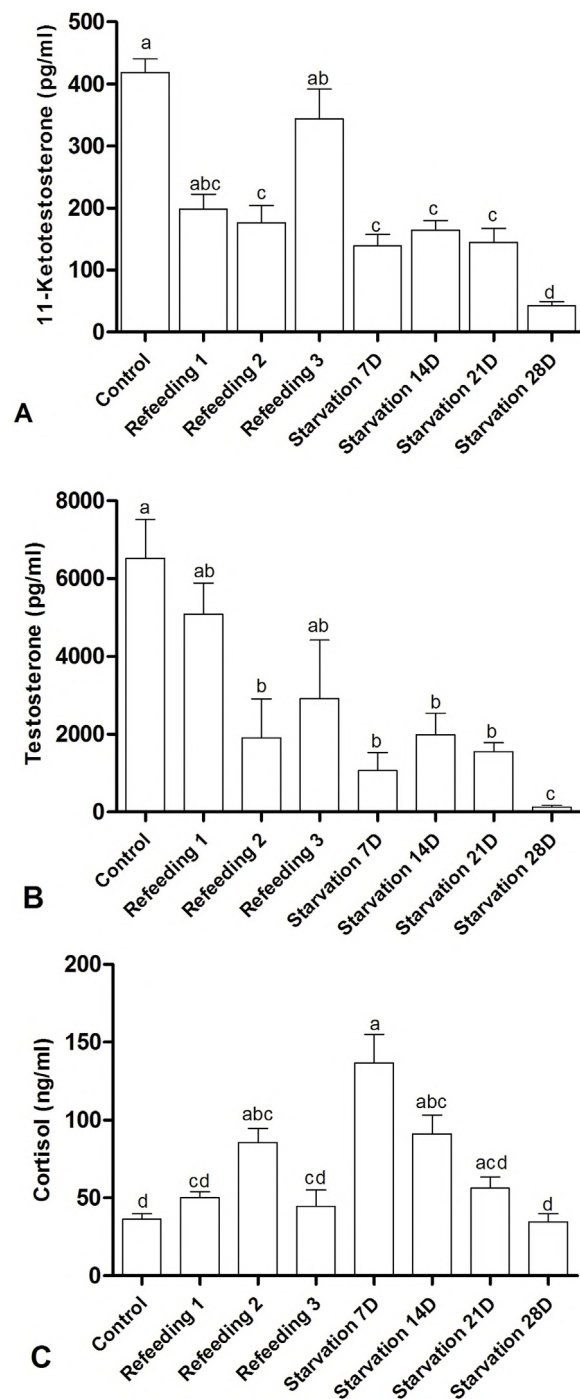


Fig. 3. Effect of refeeding cycles and starvation on androgen and cortisol concentrations in Nile tilapia. Plasma levels of 11-ketotestosterone (A), testosterone (B) and cortisol (C). Different letters indicate statistical difference among sampling times ($n = 8$ per sampling, $p < 0.05$).

increase steroidogenesis and androgen production in order to support the spermatogenesis and sperm production in the Nile tilapia under starvation conditions. Leydig cells proliferation in response to low testosterone concentration was observed in rats during the fetal period (Mylchreest et al., 2002). In fish testes, testosterone is converted to 11-ketotestosterone, the main androgen during fish spermatogenesis (Gazola and Borella, 1997; Ohta et al., 2007). The 11-ketotestosterone acts by suppressing the release of anti-Müllerian hormone (AMH) and stimulating the production of activin B by the Sertoli cells, and these molecules act antagonistically, as activin B being a stimulator and AMH

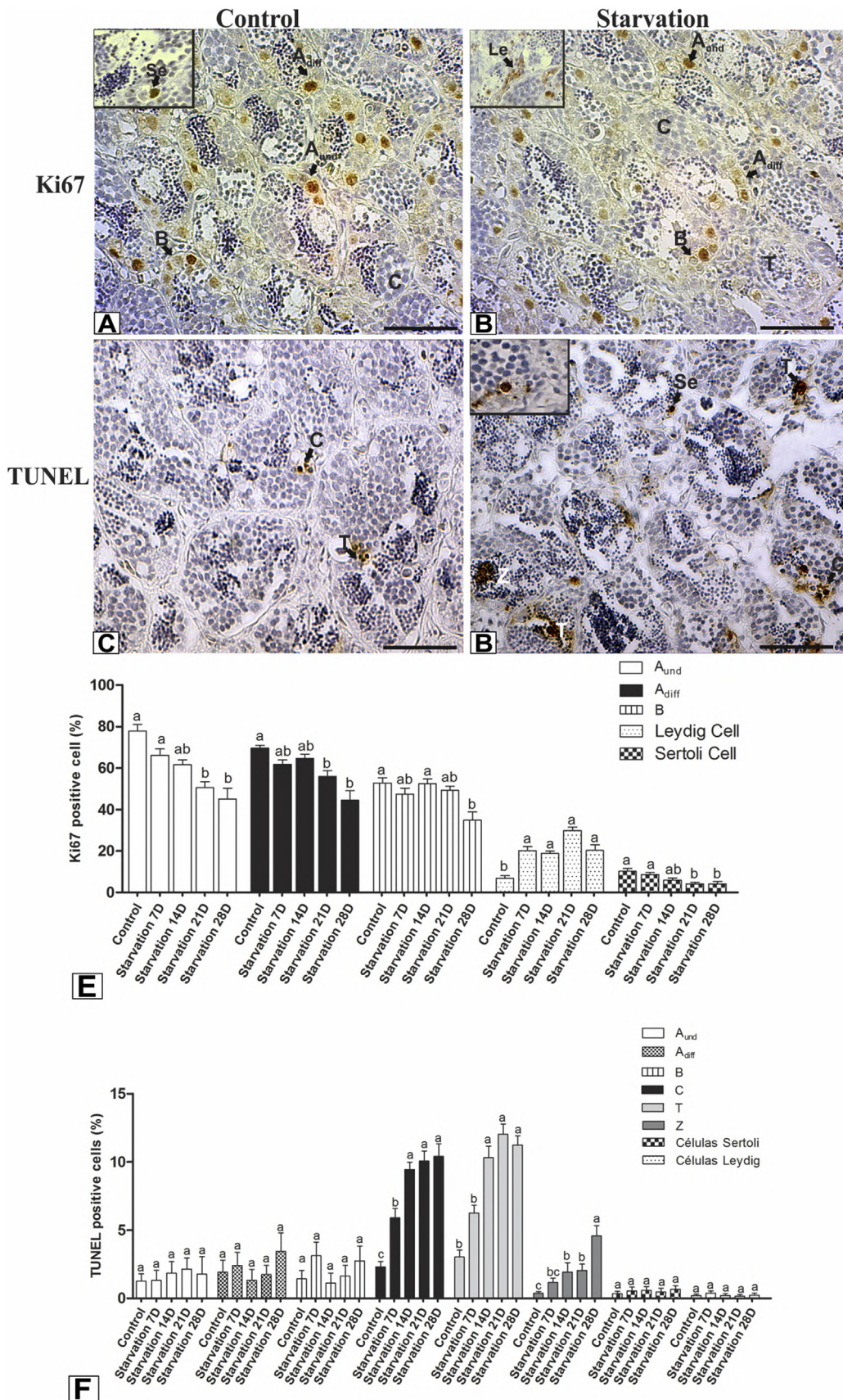


Fig. 4. Immunohistochemistry for Ki67 (A–B) and TUNEL assay (C–D) in testes of Nile tilapia from control and starvation groups. Type A undifferentiated spermatogonia (A_{und}), type A differentiated spermatogonia (A_{diff}), type B spermatogonia (B), spermatocytes (C), spermatids (T), spermatozoa (Z), Leydig cells (Le) and Sertoli cells (Se). Proportion of Ki67 and TUNEL positive cells in control and starvation groups (E–F). Different letters indicate statistical differences among sampling times ($p < 0.05$). Scale bars (A–D) 50 μ m.

Refeeding	=		=		=		=		= ↑		↓ =	
Starvation	KI67 ↓ ↓ ↓ =		Tunel ↑ ↓		Tunel ↑ = ↓		KI67 ↑ ↑ ↓		↓ ↓ ↓ ↑		↓ ↓	
Cells	Aund Adiff B		Spermatocytes		T Z		Leydig cells Sertoli cells		11KT T CT		CH TG Glucose	
	Spermatogonial phase		Spermatocitary phase		Spermiogenic phase							

= No significant difference compared to control ↓ Significantly lower than control ↑ Significantly higher than control

Fig. 5. Effects of refeeding cycles and starvation in Nile tilapia spermatogenesis and its relationship with sexual hormones and biochemical parameters. 11-ketotestosterone (11KT); Testosterone (T); Cortisol (C); Cholesterol (CH) Triglycerides (TG), Type A undifferentiated spermatogonia (A_{und}), type A differentiated spermatogonia (A_{diff}), type B spermatogonia (B), spermatocytes (C), spermatids (T) and spermatozoa (Z).

an inhibitor of spermatogonial proliferation (Ohta et al., 2007; Schulz et al., 2010; Skaar et al., 2011). Moreover, 11-ketotestosterone induces the synthesis of 17α , 20β -dihydroxy-4-pregnen-3-one (DHP) that is required for early meiosis and spermiation (Milla et al., 2009; Ozaki et al., 2006). In this sense, the low concentration of testosterone and 11-ketotestosterone observed in this study may be associated with a reduction in the spermatogonial proliferation (Ki67-positive cells) and a reduction in the proportion of spermatogonia, spermatocytes, and spermatozoa after 7 days of starvation. In addition, the survival and development of germ cells depend on their association with Sertoli cells, which showed a significant reduction in proliferation at 21 days of starvation.

Due to reproductive strategies or low food availability, some animals experience lifelong feeding and fasting periods (Pérez-Jiménez et al., 2007). In addition, alternating fasting and feeding periods may induce compensatory growth and decrease the loss of water quality and fish farming costs (Jobling, 2016; Morshedi et al., 2017). Our data suggest that refeeding changes the metabolic levels of carbohydrates and lipids as also reported by Pérez-Jiménez et al. (2007); however, the animals submitted to refeeding 1 3 did not present a marked reduction in the analysed androgen levels and kept their testicular architecture and germ cell morphology. The high proportion of spermatocytes observed in the refeeding group suggests a delay in germ cells recruitment to spermatogenesis progression. Indeed, changes in temperature, fasting, or exposure to xenobiotics may induce breakdown of DNA in primary spermatocytes and delay the progression of the meiotic phase of spermatogenesis (Alvarenga and França, 2009; Liu et al., 2013; Peñaranda et al., 2016).

During spermatogenesis, apoptosis maintains tissue homeostasis, regulating the production of spermatozoa and preventing the formation of abnormal gametes (Baum et al., 2005; Kaptaner and Kankaya, 2013; Ribeiro et al., 2017). However, external stimuli, such as nutrient deprivation, are associated with increased apoptosis during spermatogenesis in amphibians and mammals (González et al., 2018; Wang et al., 2012). In fish, the relationship between nutrient deprivation and its influence on apoptosis during fish spermatogenesis is poorly studied. In Nile tilapia, our findings show that starvation significantly increased the proportion of TUNEL-positive germ cells in the testes. In addition, the ultrastructural changes found in these cells may indicate that nutritional deficiency negatively affects spermatogenesis, culminating in abnormal cell elimination by apoptosis. These findings may justify the reduction in the proportion of spermatocytes and spermatozoa in animals submitted to starvation. Corroborating our results, Escobar et al. (2014) also observed a strong relationship between food restriction and increased apoptosis of spermatogenic cells in *Dicentrarchus labrax*.

Taken together, our results suggest that starvation can progressively

reduce testosterone and 11-ketotestosterone levels, with consequent morphological changes in the Nile tilapia spermatogenesis. In addition, prolonged total food restriction is associated with severe damage to testicular function and germ cell death (Fig. 5). Although refeeding cycles may delay spermatogenesis, they do not result in permanent damage to the testicular function and can be recommended for maintenance of breeding stock in the fish farming.

Funding

The research was supported by Brazilian funding agencies: Conselho Nacional de Desenvolvimento Científico e Tecnológico (CNPq, 40778/2016-0 and 305132/2015-6); Fundação de Amparo à Pesquisa no Estado de Minas Gerais (FAPEMIG, CVZ-PPM-00898-15 and APQ-00219-19) and Coordenação de Aperfeiçoamento de Pessoal de Nível Superior (CAPES Finance Code 001).

Declaration of competing interest

The authors declare that there is no conflict of interest that could be perceived as prejudicing the impartiality of the research reported.

Acknowledgments

The authors would like to thank the technicians at the Laboratory of Aquaculture (LAQUA) of the UFMG for their assistance in handling of the fishes, the technicians at the Center of Microscopy of the UFMG for preparing the biological material for the electron microscope and to Stephen Latham for the valuable suggestions with the English language.

References

- Alonge, S., Melandri, M., Leoci, R., Lacalandra, G.M., Caira, M., Aiudi, G.G., 2019. The effect of dietary supplementation of Vitamin E, Selenium, Zinc, Folic Acid, and N-3 polyunsaturated fatty acids on sperm motility and membrane properties in dogs. *Animals* 9, 34. <https://doi.org/10.3390/ani9020034>.
- Alvarenga, E.R., França, L.R., 2009. Effects of different temperatures on testis structure and function, with emphasis on somatic cells, in sexually mature Nile tilapias (*Oreochromis niloticus*). *Biol. Reprod.* 80, 537–544. <https://doi.org/10.1095/biolreprod.108.072827>.
- Barnes, C.J., Covington IV, B.W., Cameron, I.L., Lee, M., 1998. Effect of aging on spontaneous and induced mouse testicular germ cell apoptosis. *Aging Clin. Exp. Res.* 10, 497–501.
- Batlouni, S.R., Nóbrega, R.H., França, L.R., 2009. Cell junctions in fish seminiferous epithelium. *Fish Physiol. Biochem.* 35, 207–217. <https://doi.org/10.1007/s10695-008-9253-y>.
- Baum, J.S., St George, J.P., McCall, K., 2005. Programmed cell death in the germline. *Semin. Cell Dev. Biol.* 16, 245–259. <https://doi.org/10.1016/j.semcdb.2004.12.008>.
- Chatzifotis, S., Papadaki, M., Despoti, S., Roufidou, C., Antonopoulou, E., 2011. Effect of starvation and re-feeding on reproductive indices, body weight, plasma metabolites

- Wang, Y.Y., Sun, Y.C., Sun, X.F., Cheng, S.F., Li, B., Zhang, X.F., De Felici, M., Shen, W., 2017. Starvation at birth impairs germ cell cyst breakdown and increases autophagy and apoptosis in mouse oocytes. *Cell Death Dis.* 8, 1–10. <https://doi.org/10.1038/cddis.2017.3>.
- Wayne Hou, J., Collins, D.C., Schleicher, R.L., 1990. Sources of cholesterol for testosterone biosynthesis in murine leydig cells. *Endocrinology* 127, 2047–2055. <https://doi.org/10.1210/endo-127-5-2047>.
- Weber, L.P., Kiparissis, Y., Hwang, G.S., Niimi, A.J., Janz, D.M., Metcalfe, C.D., 2002. Increased cellular apoptosis after chronic aqueous exposure to nonylphenol and quercetin in adult medaka (*Oryzias latipes*). *Comp. Biochem. Physiol. C Toxicol. Pharmacol.* 131, 51–59. [https://doi.org/10.1016/S1532-0456\(01\)00276-9](https://doi.org/10.1016/S1532-0456(01)00276-9).
- Weber, A.A., Moreira, D.P., Melo, R.M.C., Ribeiro, Y.M., Bazzoli, N., Rizzo, E., 2019. Environmental exposure to oestrogenic endocrine disruptors mixtures reflecting on gonadal sex steroids and gametogenesis of the neotropical fish *Astyanax rivularis*. *Gen. Comp. Endocrinol.* 279, 99–108. <https://doi.org/10.1016/j.ygcen.2018.12.016>.
- Whirledge, S., Cidlowski, J.A., 2010. Glucocorticoids, stress, and fertility. *Minerva Endocrinol.* 35, 109–125.
- Yu, X., Peng, Q., Luo, X., An, T., Guan, J., Wang, Z., 2016. Effects of starvation on lipid metabolism and gluconeogenesis in Yak. *AJAS (Asian-Australas. J. Anim. Sci.)* 29, 1593–1600. <https://doi.org/10.5713/ajas.15.0868>.

4.3. CAPÍTULO 3: Autophagy and apoptosis during fish spermatogenesis: insights from Nile tilapia

Abstract

Autophagy and apoptosis are indispensable mechanisms for the normal development of the germ cells, and the deficiency of these processes results in functional changes that can lead to male infertility. In this study, we investigated the role of autophagy and apoptosis during spermatogenesis of Nile tilapia submitted to total food restriction. For this, adult specimens were subject to total food restriction during 7, 14, 21 and 28 days. The animals subjected to starvation showed a significant reduction in the gonadosomatic index, diameter of the seminiferous tubules and number of spermatozoa when compared to the control group. The immunofluorescence analysis showed secondary spermatocytes, spermatids, Sertoli and Leydig cells with strong immunostaining for autophagic proteins LC3 and Beclin-1. At electron microscopy, autophagosomes, autolysosomes and multilamellar bodies were detected, however, after 21 days of starvation autophagy decreased significantly. The apoptosis was identified in spermatocytes and spermatids and increased with 21 and 28 days of starvation. In conclusion, our data show that the autophagy acts in combination with the apoptosis in the germ and somatic cells of Nile tilapia, and a significant decrease of the autophagy and increase of apoptosis can be related to reduction of the sperm production after 21 days of starvation.

KEYWORDS: leydig cells, spermatogenic cell, autophagosomes, autophagic flux, starvation.

INTRODUCTION

Germ cell development is a complex and highly organized process involving the balance between proliferation, differentiation and cell death (Schulz et al., 2010). Apoptosis is essential for maintaining testicular homeostasis during germ cell development, and alterations in this pathway are associated with changes in the spermatogenesis (Shaha et al., 2010). In addition, studies in mammals show that autophagy and apoptosis may act together in the germ cell elimination (Yin et al., 2017; Zhang et al., 2012).

Apoptosis is the main and best known mechanism of cell death in fish testes. In addition to maintaining cellular homeostasis during spermatogenesis, apoptosis eliminates potentially

defective germ cells for production of healthy gametes (Barnes et al., 2014; Richburg, 2000; Shaha et al., 2010). The apoptotic pathway is highly conserved in vertebrates and requires a specialized protein machinery that can be activated by extrinsic and intrinsic factors (Elmore, 2007; Mariño et al., 2014; Takle and Andersen, 2007). The proteins of the Bcl-2 family, such as Bax and Bcl2 actively participate in the regulation of apoptosis, acting as inducers and repressors of the process, respectively (Antonsson, 2001; Youle and Strasser, 2008). Activation of cell death effector proteins such as caspase-3 culminates in the cleavage of specific substrates leading to cell death (Wang et al., 2005; Wu et al., 2014). In rats and mice, studies indicate that both intrinsic and extrinsic pathways are involved in the cell death during the first wave of spermatogenesis (Russell et al., 2002; Tripathi et al., 2009). In addition, alterations in expression of Bcl-2 family proteins lead to spermatogenesis damage (Russell et al. 2002). External stressors such as nutritional deficiency or starvation are also associated with disruption in the germ cell apoptosis, which can cause severe damage to sperm production (Cheah and Yang, 2011; Cheng et al., 2015; Lascarez-Lagunas et al., 2014; Shaha et al., 2010; Wang et al., 2017).

In addition to apoptosis, the autophagy may also act to eliminate germ cells during spermatogenesis (Aslani et al., 2017; González et al., 2018; Zhang et al., 2012). Autophagy is a complex evolutionarily conserved catabolic mechanism in the eukaryotic cells (Codogno and Meijer, 2005; Russell et al., 2014; Ryter et al., 2013). It involves sequestration and delivery of cytosolic components, including organelles and macromolecules to the lysosome, where they will be degraded and their products recycled and reused by the cell. For the recruitment and isolation of components to be degraded by autophagy, autophagosome formation is required (Soto-Burgos et al., 2018). Beclin-1 and LC3 proteins coordinate and regulate the membrane formation and mobilization to form autophagosome and are widely used as autophagy markers (He et al., 2015; Klionsky et al., 2016). In mammals, autophagy plays a protective role for germ cells by acting on spermatid differentiation into spermatozoa, on formation of acrosome and uptake of cholesterol by the Leydig cells for testosterone biosynthesis (Gao et al., 2018; Wang et al., 2014; Yin et al., 2017). In fish, knowledge about the role of autophagy during spermatogenesis is limited, and few studies addressing this issue are available (Herpin et al., 2015).

Given the lack of knowledge about the role of autophagy in fish spermatogenesis and that food deprivation and nutritional deficiency are strong inducers of autophagy, the aim of the present

study was to investigate the interaction of autophagic and apoptotic pathways during spermatogenesis of Nile tilapia submitted to prolonged starvation and under normal food condition.

MATERIAL AND METHODS

Experimental assay and sampling of fish

The experiment was realized at the Laboratory of Aquaculture (LAQUA) of the Universidade Federal de Minas Gerais (UFMG), and it was approved by the Ethics Committee on Animal Use (CEUA, UFMG 67/2017). For acclimation, 62 adult males of *O. niloticus* of the GIFT lineage (24.66 ± 0.40 cm total length, 282.26 ± 14.84 g body weight) were equally distributed in four 1m³ culture tanks and kept for 30 days with a mechanical and biological filtration system under controlled conditions of temperature, luminosity and water quality (temperature, mean \pm SEM: 29.06 ± 0.04 °C, dissolved oxygen: 7.06 ± 0.02 mg/L, pH: 7.31 ± 0.04 , conductivity: 0.87 ± 0.11 mS/cm, total dissolved solids: 0.51 ± 0.02 g/l, salinity: 0.36 ± 0.02 ppt and photoperiod of at 12 h light to 12 h dark).

During the experiment, the fish were subjected to 2 treatments: control group (n = 30) and starvation group (n = 32), in duplicate. In the control group, fish were fed *ad libitum* with commercial feed containing 32% crude protein. In the starvation group, fish were submitted to total food restriction. From each tank, four animals were collected at the following sampling times: 7, 14, 21 and 28 days. During the samplings, fish were euthanized with 285 mg/l eugenol solution following the ethical principles established by the National Council for Animal Experimentation Control (CONCEA). From these animals, body weight (BW), total length (TL), and gonad weight (GW) were obtained and the gonadosomatic index ($GSI=100GW/BW$) was calculated.

Light and electron microscopy

For histology, testis samples were fixed in Bouin's liquid for 24 h, embedded in paraffin, sectioned at 5 μ m thickness and stained with haematoxylin-eosin. For electron microscopy, the samples were fixed in Karnovsky solution (2.5% glutaraldehyde and 2% paraformaldehyde) in 0.1M sodium phosphate buffer pH 7.3 for 24 h at 4 °C and post-fixed in 1% osmium tetroxide for 2 h and, later embedded in Epon/Araldite plastic resin. The ultrathin sections were contrasted with uranyl acetate and lead citrate and examined under a Tecnai G2-135 12 Spirit 120 kV transmission electron microscope (FEI Company, Hillsboro, OR, EUA).

Immunohistochemistry

For analysis of autophagic and apoptotic proteins, testis sections from 4 animals of each group were randomly chosen and subjected to immunohistochemistry. For this, testis samples were fixed in 4% paraformaldehyde solution for 24 h at 4 °C, embedded in paraffin, and sectioned at 5 µm thickness. The sections were submitted to antigen retrieval with 10mM sodium citrate buffer pH 6.0 for 20 min at 96 °C. The blocking of non-specific binding was made with 2% bovine albumin in PBS buffer for 30 min at room temperature. Then, the sections were incubated with the primary antibody (Table 1) in a humid chamber at 4 °C overnight. Subsequently, for immunofluorescence, the sections were incubated with secondary anti-rabbit IgG antibody conjugated to Alexa Fluor 488 (1: 500) or anti-mouse IgG conjugated to Alexa fluorine 568 (1: 500; Life Technologies). Nuclear DNA staining was performed with 4', 6-diamino-2-phenylindole (DAPI; 1: 2000; Sigma Aldrich). The sections were examined using an Axio Imager Z2-ApoTome 2 fluorescence microscope.

For quantification of labelled cells, the sections were subjected to immunoperoxidase. For this, the sections were incubated in dark chamber with 3% H₂O₂ for 30 min for inactivation of endogenous peroxidase before the blocking of non-specific binding. After treatment with primary antibodies (Table 1), sections were incubated with biotinylated secondary antibody LSAB 2 System - HRP (Dako, Santa Clara) for 1 h, followed by streptavidin conjugated with peroxidase for 1 h, revealed with DAB (Dako EnVision™ + Dual Link System-HRP), and contrasted with hematoxylin. For negative control, one of the sections did not receive the primary antibody.

Western blot

Testes samples were frozen at -80 °C, sonicated in lysis buffer (150 mM NaCl, 0.5% sodium deoxycholate, 0.1% SDS e 50 mM Tris pH 8.0) with aprotinin and phenylmethylsulfonyl fluoride protease inhibitors and centrifuged at 150,000 x g for 1 h. The protein dosage was performed on the supernatant according to Bradford (1976). For each sample, 80 µg of protein in sample buffer was added to 12% polyacrylamide gel electrophoresis and subsequently transferred to a nitrocellulose membrane. After transfer, nonspecific reactions were blocked with skimmed milk powder for 1 h at room temperature. The membrane was incubated with the antibodies previously listed in the Table 1 at a concentration of 1: 500 overnight at 4 °C. Finally, the membrane was incubated with secondary antibody peroxidase - conjugated (IgG, dilution 1:750) for 2 h and the

reaction was revealed with DAB (Dako EnVision™ + Dual Link System-HRP). Densitometry of autophagic and apoptotic proteins was performed using the ImageJ software (NIH) and the relative optical density of the bands was normalized to constitutive protein calculated by dividing the study proteins and the control (β actin).

Morphometry

In order to assess the proportion of cells marked by Beclin-1, Cathepsin D, Caspase-3, Bax and Bcl2, digital images of histological cross sections of 4 animals per group were obtained using the Zeiss Axiovision image analysis system coupled to the Zeiss Microscope Axioplan 2. For each study protein, 10 randomly chosen fields were photographed at 400x magnification. The images were analysed in ImageJ software using a grid of 540 points placed on the tissue. The percentage of marked cells was determined considering the total number of points on the cells of interest. The area of the seminiferous tubules was determined by measuring the cross sections of 30 tubules per animal with a magnification of 200 x and the proportion of sperm was obtained in 10 seminiferous tubules per animal totaling 40 seminiferous tubules per group.

Statistical analyses

Data were statistically analysed using Minitab 16.1 and GraphPad Prism 6.03 software. The data showed a normal distribution, and hence, a one-way ANOVA followed by Tukey's post hoc test was used to compare the mean values. The results were considered significant at 95% confidence interval and values were expressed as mean \pm SEM.

RESULTS AND DISCUSSION

Influence of starvation on testicular morphology and function

The animals of the control group and of the group submitted to starvation presented germ cells in different stages of development (Fig.1 A and B). However, animals subjected to starvation showed a significant reduction ($p < 0.05$) in the area of the seminiferous tubules and in the number of spermatozoa per seminiferous tubules (Fig. 1 C and D). In addition, the GSI in animals of the control group (0.63 ± 0.09) was significantly higher ($p < 0.05$) than animals of groups 7 (0.11 ± 0.02), 14 (0.21 ± 0.02), 21 (0.24 ± 0.08) and 28 (0.15 ± 0.04) days of starvation. In the freshwater

shrimp *Macrobrachium rosenbergii*, short periods of starvation induced autophagy and, consequently, there was an increase in the gonadosomatic index and number of spermatozoa (Wanichanon and Isidoro, 2019).

Autophagy during spermatogenesis

To detect autophagy in the testes of the Nile tilapia, we used electron microscopy and immunohistochemistry, and the expression of key proteins was evaluated by western blot. Autophagy was found in the germ and somatic cells of both experimental groups. Autophagosomes and multilamellar bodies were detected in spermatogonia, spermatocytes and spermatids (Fig.2 A-C). In addition, spermatocytes with scarce cytoplasmic organelles were observed (Fig.2 D). Sertoli and Leydig cells showed also autophagosomes, autolysosomes and multilamellar bodies (Fig.2 E and F).

Immunofluorescence analysis showed secondary spermatocytes, spermatids, and Sertoli and Leydig cells with strong immunostaining for LC3 and Beclin-1 (Fig.2 G-L) in both groups. Moreover, in these cells there was a colocalization between LC3 and the lysosomal membrane protein Lamp-1, indicating the fusion of autophagosomes with lysosomes (Fig.3 A-D). Immunostaining for Cathepsin-D was predominant in spermatogonia, Leydig and Sertoli cells (Fig.2 M-O), with colocalization between Cathepsin-D and Lamp-1 (Fig.3 E-H). The autophagic protein Beclin-1 and apoptotic Bcl2 were identified in all cells of the spermatogenic lineage. However, there was no colocalization of these proteins in secondary spermatocytes, spermatids and Leydig cells (Fig.3 I-L). These results indicate that autophagy act in the sperm production in the Nile tilapia as reported in some mammalian species (Ozturk et al., 2017; Yin et al., 2017). In mice, the specific knockout of gene 7 related to autophagy (Atg7) in germ cells causes infertility and is related to failures in acrosome biogenesis (Wang et al., 2014). Furthermore, studies suggest the role of autophagy in the biogenesis of spermatozoa flagella and the removal of cytoplasm during spermiogenesis (Aparicio et al., 2016). Autophagic activity in the spermatids supports the possible involvement of autophagy in espermiogenic phase of the Nile tilapia. In medaka, Herpin et al. (2015) suggest that autophagy is required for the reduction of cytoplasmic organelles during spermatozoa differentiation.

The autophagic pathway is also required for hormonal synthesis in the testes, and the deficiency of this process in the Leydig cells is associated with low levels of testosterone in mice

(Gao et al., 2018). In this study, the strong immunostaining of proteins required for initiation (Beclin-1) and elongation (LC3) of autophagosomes in the Leydig cells suggests that the autophagic pathway acts in the Nile tilapia on the synthesis of testosterone through the mobilization of cholesterol,

Western blot quantification of the autophagic proteins Beclin-1 and LC3II was significantly higher at 7 and 14 days with subsequent reduction at 21 and 28 days of starvation (Fig.5 B-C). In addition, P62 increased significantly at times 21 and 28 days (Fig 5D) indicating a reduction of the autophagic flux with accumulation of p62 in the cells. During autophagy, p62 interacts with LC3, is incorporated to the autophagosome and degraded by the lysosomal hydrolases (Hansen and Johansen, 2011). Thus, our results demonstrate that starvation of up to two weeks induces the autophagic pathway in the Nile tilapia and, after this period, there is a reduction in testicular autophagic activity. In mammals, autophagy is an indispensable mechanism for the sperm production, and the deficiency of this process results in male infertility (Ozturk et al., 2017; Yin et al., 2017). The quantification of Cathepsin-D during starvation did not show any significant difference between the study groups (Fig. 5E). Cathepsin-D can act on degradation of cellular components via autophagy when located within lysosomes, however, the release of this protein may be related to the lysosomal death and induction of the apoptotic pathway (Kavčič et al., 2017; Repnik et al., 2012). In this study, no evidence of cytosolic Cathepsin-D was found in the testicular cells, thus reinforcing the relevancy of the apoptosis in the testicular physiology.

Apoptosis during spermatogenesis

For apoptosis, we used immunohistochemistry and western blot. In both study groups, the anti-apoptotic protein Bcl2 was identified in the cytoplasm of all germ cells, however, spermatocytes and spermatids were strongly positive for this protein (Fig.4 A-C). The pro-apoptotic proteins (Bax and Caspase-3) used in this study showed strong cytoplasmic immunostaining in spermatogonia and spermatids, especially after 7 days of starvation (Fig.4 D-I). In addition, spermatocytes with condensed nucleus were positive for Bax (Fig.4 D-F). Bcl-2 family proteins are expressed in distinct germ cell compartments, suggesting a specific role for these proteins in the maturation and differentiation processes (Oldereid et al., 2001). In addition, the balance between anti and pro apoptotic proteins guarantees successful spermatogenesis. In the Nile tilapia, the strong immunostaining of Bcl2 in spermatids is possibly related to the protective role of Bcl2,

since positive spermatids for Bax and Caspase-3 were frequently observed during starvation. In birds, Bcl2 expression was able to inhibit apoptosis, especially in spermatogonia (Vilagrassa et al., 1997).

After 14 days of starvation, the quantification of pro-apoptotic proteins (Caspase-3 and Bax) showed a significant increase ($p > 0.05$) when compared to the control group (Fig.5 H and F). However, the quantification of Bcl2 did not show any significant difference, except between the control and starvation groups for 28 days (Fig. 5G). The reduction of spermatozoa in seminiferous tubules is possibly associated with increased expression of Bax and Caspase-3 and decreased expression of Bcl2, leading to an increase in apoptosis during food restriction.

In addition to apoptosis, autophagy induced by food restriction may have contributed to the death of germ cells observed in Nile tilapia, since the positive regulation of autophagy by prolonged starvation may have led to excessive degradation of cellular structures and consequent autophagic cell death. During the spermatogenesis of mice, autophagy of germ cells induced by hyperthermia was evidenced by the formation of autophagosomes and the conversion of LC3-I into LC3-II, leading to cell death along with apoptosis (Zhang et al., 2012).

In conclusion, our data showed, for the first time, the presence of autophagic markers, LC3 and Beclin-1, and autophagic structures in different germ and somatic cells of Nile tilapia males. In addition, total food restriction reduces the autophagic flow and increases the apoptosis after 21 days treatment, with consequent reduction in the sperm production. These data suggest an essential role for autophagy controlling the apoptosis of the germ cells during the fish spermatogenesis.

References

- Antonsson, B., 2001. Bax and other pro-apoptotic Bcl-2 family “killer-proteins” and their victim, the mitochondrion. *Cell Tissue Res.* 306, 347–361. <https://doi.org/10.1007/s00441-001-0472-0>
- Aslani, F., Sebastian, T., Keidel, M., Fröhlich, S., Elsässer, H.P., Schuppe, H.C., Klug, J., Mahavadi, P., Fijak, M., Bergmann, M., Meinhardt, A., Bhushan, S., 2017. Resistance to apoptosis and autophagy leads to enhanced survival in sertoli cells. *Mol. Hum. Reprod.* 23, 370–380. <https://doi.org/10.1093/molehr/gax022>
- Barnes, C.J., Covington, B.W., Cameron, I.L., Lee, M., 2014. Effect of aging on spontaneous and induced mouse testicular germ cell apoptosis. *Aging Clin. Exp. Res.* <https://doi.org/10.1007/bf03340164>
- Cheah, Y., Yang, W., 2011. Functions of essential nutrition for high quality spermatogenesis. *Adv.*

- Biosci. Biotechnol. 02, 182–197. <https://doi.org/10.4236/abb.2011.24029>
- Cheng, C., Yang, F., Liao, S., Miao, Y., Ye, C., Wang, A., Tan, J., Chen, X., 2015. High temperature induces apoptosis and oxidative stress in puffer fish (*Takifugu obscurus*) blood cells. *J. Therm. Biol.* 53, 172–179. <https://doi.org/10.1016/j.jtherbio.2015.08.002>
- Codogno, P., Meijer, A.J., 2005. Autophagy and signaling: Their role in cell survival and cell death. *Cell Death Differ.* 12, 1509–1518. <https://doi.org/10.1038/sj.cdd.4401751>
- Elmore, S., 2007. Apoptosis: A Review of Programmed Cell Death. *Toxicol. Pathol.* 35, 495–516. <https://doi.org/10.1080/01926230701320337>
- Gao, F., Li, G., Liu, C., Gao, H., Wang, H., Liu, W., Chen, M., Shang, Y., Wang, L., Shi, J., Xia, W., 2018. Autophagy regulates testosterone synthesis by facilitating cholesterol uptake in Leydig cells 217, 2103–2119.
- González, C.R., Muscársel Isla, M.L., Vitullo, A.D., 2018. The balance between apoptosis and autophagy regulates testis regression and recrudescence in the seasonal-breeding South American plains vizcacha, *Lagostomus maximus*. *PLoS One* 13, 1–15. <https://doi.org/10.1371/journal.pone.0191126>
- Hansen, T.E., Johansen, T., 2011. Following autophagy step by step. *BMC Biol.* 9, 2–5. <https://doi.org/10.1186/1741-7007-9-39>
- He, R., Peng, J., Yuan, P., Xu, F., Wei, W., 2015. Divergent roles of BECN1 in LC3 lipidation and autophagosomal function. *Autophagy* 11, 740–747. <https://doi.org/10.1080/15548627.2015.1034404>
- Herpin, A., Englberger, E., Zehner, M., Wacker, R., Gessler, M., Scharl, M., 2015. Defective autophagy through *epg5* mutation results in failure to reduce germ plasm and mitochondria 1–17. <https://doi.org/10.1096/fj.14-265462>
- Kavčič, N., Pegan, K., Turk, B., 2017. Lysosomes in programmed cell death pathways: from initiators to amplifiers. *Biol. Chem.* 398, 289–301. <https://doi.org/10.1515/hsz-2016-0252>
- Klionsky, D., Agholme, L., Agnello, M., Agostinis, P., Aguirre-ghiso, J.A., Ahn, H.J., Ait-mohamed, O., Brown, E.J., Brumell, J.H., Brunetti-pierri, N., Brunk, U.T., Bulman, D.E., Bultman, S.J., Bultynck, G., Burbulla, L.F., Bursch, W., Butchar, J.P., Buzgariu, W., Bydlowski, S.P., Cadwell, K., Cahová, M., Cai, D., Cai, J., Cai, Q., Calabretta, B., Calvo-garrido, J., Camougrand, N., Campanella, M., Campos-salinas, J., Candi, E., Cao, L., Caplan, A.B., Carding, S.R., Cardoso, S.M., Carew, J.S., Carlin, C.R., Carmignac, V., Carneiro, L.A.M., Carra, S., Caruso, R.A., Casari, G., Casas, C., Castino, R., Cebollero, E., Cecconi, F., Celli, J., Chaachouay, H., Chae, H., Chai, C., Chan, D.C., Chan, E.Y., Chang, R.C., Che, C., Chen, C., Chen, G., Chen, G., Chen, M., Chen, Q., Chen, S.S., Chen, W., Chen, X., Chen, X., Chen, X., Chen, Y., Chen, Y., Chen, Y., Chen, Y., Chen, Y., Chen, Z., Cheng, A., Cheng, C.H.K., Cheng, Y., Cheong, H., Cheong, J., Cherry, S., Chess-williams, R., Cheung, Z.H., Chevet, E., Chiang, H., Chiarelli, R., Chiba, T., Chu, C.T., Chuang, T., Chueh, S., Chun, T., Chwae, Y., Chye, M., Codogno, P., Collier, H.A., Colombo, M.I., Comincini, S., Condello, M., Condorelli, F., Costes, S., Coto-montes, A., Couve, E., Coxon, F.P., Cregg, J.M., Crespo, J.L.,

- Fésüs, L., Feuer, R., Figueiredo-pereira, M.E., Fimia, G.M., Fingar, D.C., Finkbeiner, S., 2016. Guidelines for the use and interpretation of assays for monitoring autophagy. *Autophagy* 8, 445–544. <https://doi.org/10.4161/autophagy.19496>
- Lascarez-Lagunas, L.I., Silva-Garcia, C.G., Dinkova, T.D., Navarro, R.E., 2014. LIN-35/Rb Causes Starvation-Induced Germ Cell Apoptosis via CED-9/Bcl2 Downregulation in *Caenorhabditis elegans*. *Mol. Cell. Biol.* 34, 2499–2516. <https://doi.org/10.1128/mcb.01532-13>
- Mariño, G., Niso-Santano, M., Baehrecke, E.H., Kroemer, G., 2014. Self-consumption: The interplay of autophagy and apoptosis. *Nat. Rev. Mol. Cell Biol.* <https://doi.org/10.1038/nrm3735>
- Ozturk, N., Steger, K., Schagdarsurengin, U., 2017. The impact of autophagy in spermiogenesis 5, 617–618. <https://doi.org/10.4103/1008-682X.190324>
- Repnik, U., Stoka, V., Turk, V., Turk, B., 2012. Lysosomes and lysosomal cathepsins in cell death. *Biochim. Biophys. Acta - Proteins Proteomics* 1824, 22–33. <https://doi.org/10.1016/j.bbapap.2011.08.016>
- Richburg, J.H., 2000. The relevance of spontaneous- and chemically-induced alterations in testicular germ cell apoptosis to toxicology, in: *Toxicology Letters*. [https://doi.org/10.1016/S0378-4274\(99\)00253-2](https://doi.org/10.1016/S0378-4274(99)00253-2)
- Russell, L.D., Chiarini-Garcia, H., Korsmeyer, S.J., Knudson, C.M., 2002. Bax-dependent spermatogonia apoptosis is required for testicular development and spermatogenesis. *Biol. Reprod.* 66, 950–958. <https://doi.org/10.1095/biolreprod66.4.950>
- Russell, R.C., Yuan, H.X., Guan, K.L., 2014. Autophagy regulation by nutrient signaling. *Cell Res.* 24, 42–57. <https://doi.org/10.1038/cr.2013.166>
- Ryter, S.W., Cloonan, S.M., Choi, A.M.K., 2013. Autophagy: A critical regulator of cellular metabolism and homeostasis. *Mol. Cells* 36, 7–16. <https://doi.org/10.1007/s10059-013-0140-8>
- Schulz, R.W., de França, L.R., Lareyre, J.J., LeGac, F., Chiarini-Garcia, H., Nobrega, R.H., Miura, T., 2010. Spermatogenesis in fish. *Gen. Comp. Endocrinol.* 165, 390–411. <https://doi.org/10.1016/j.ygcen.2009.02.013>
- Shaha, C., Tripathi, R., Prasad Mishra, D., 2010. Male germ cell apoptosis: Regulation and biology. *Philos. Trans. R. Soc. B Biol. Sci.* 365, 1501–1515. <https://doi.org/10.1098/rstb.2009.0124>
- Soto-Burgos, J., Zhuang, X., Jiang, L., Bassham, D.C., 2018. Dynamics of Autophagosome Formation. *Plant Physiol.* 176, 219–229. <https://doi.org/10.1104/pp.17.01236>
- Takle, H., Andersen, 2007. Caspases and apoptosis in fish. *J. Fish Biol.* <https://doi.org/10.1111/j.1095-8649.2007.01665.x>
- Tripathi, R., Mishra, D.P., Shaha, C., 2009. Male germ cell development: turning on the apoptotic pathways. *J. Reprod. Immunol.* <https://doi.org/10.1016/j.jri.2009.05.009>

- Wang, H., Wan, H., Li, X., Liu, W., Chen, Q., Wang, Y., Yang, L., Tang, H., Zhang, X., Duan, E., Zhao, X., Gao, F., Li, W., 2014. Atg7 is required for acrosome biogenesis during spermatogenesis in mice. *Cell Res.* 24, 852–869. <https://doi.org/10.1038/cr.2014.70>
- Wang, Y.Y., Sun, Y.C., Sun, X.F., Cheng, S.F., Li, B., Zhang, X.F., De Felici, M., Shen, W., 2017. Starvation at birth impairs germ cell cyst breakdown and increases autophagy and apoptosis in mouse oocytes. *Cell Death Dis.* 8, 1–10. <https://doi.org/10.1038/cddis.2017.3>
- Wang, Z.B., Liu, Y.Q., Cui, Y.F., 2005. Pathways to caspase activation. *Cell Biol. Int.* 29, 489–496. <https://doi.org/10.1016/j.cellbi.2005.04.001>
- Wanichanon, C., Isidoro, C., 2019. Starvation Promotes Autophagy- Associated Maturation of the Testis in the Giant Freshwater Prawn , *Macrobrachium rosenbergii* 10. <https://doi.org/10.3389/fphys.2019.01219>
- Wu, H., Che, X., Zheng, Q., Wu, A., Pan, K., Shao, A., Wu, Q., Zhang, J., Hong, Y., 2014. Caspases: A molecular switch node in the crosstalk between autophagy and apoptosis. *Int. J. Biol. Sci.* 10, 1072–1083. <https://doi.org/10.7150/ijbs.9719>
- Yin, J., Ni, B., Tian, Z., Yang, F., Liao, W., Gao, Y., 2017. Regulatory effects of autophagy on spermatogenesis. *Biol. Reprod.* 96, 525–530. <https://doi.org/10.1095/biolreprod.116.144063>
- Youle, R.J., Strasser, A., 2008. The BCL-2 protein family: Opposing activities that mediate cell death. *Nat. Rev. Mol. Cell Biol.* <https://doi.org/10.1038/nrm2308>
- Zhang, M., Jiang, M., Bi, Y., Zhu, H., Zhou, Z., Sha, J., 2012. Autophagy and apoptosis act as partners to induce germ cell death after heat stress in mice. *PLoS One* 7. <https://doi.org/10.1371/journal.pone.0041412>

TABLE 1: Primary antibodies with dilution used in the immunohistochemical reactions.

Primary antibodies	Origin	Dilution
Bcl2 polyclonal rabbit	ABCAM	1:50
Bax polyclonal rabbit	ABCAM	1:100
Caspase-3 polyclonal rabbit	Sigma	1:200
Beclin1 monoclonal mouse	ABCAM	1:100
Cathepsin-D polyclonal rabbit	ABCAM	1:50
Lamp1 monoclonal mouse	ABCAM	1:200
LC3 polyclonal rabbit	Santa Cruz Biotechnology	1:200
P62 polyclonal rabbit	ABCAM	1:100

FIGURE CAPTIONS

Figure 1. Histological sections stained with haematoxylin-eosin (A and B) spermatozoa for seminiferous tubules (C) and area of the seminiferous tubules (D) of testes of Nile tilapia. **A:** Control group containing type A undifferentiated spermatogonia (Aund), type A differentiated spermatogonia (Adif), type B spermatogonia (B), spermatocytes (C), spermatids (T) and spermatozoa (Z). **B:** Starvation group 28 days with numerous Leydig cells. Different letters indicate significant difference among sampling times. Scale bars (A and B) 50 μ m.

Figure 2. Ultrastructural sections (A-F) and immunofluorescence (G-O) of testes of Nile tilapia. Nuclei are stained with 4',6-diamidino-2'-phenylindole dihydrochloride (DAPI; blue). **A:** spermatogonia **B and D:** spermatocytes **C:** spermatids **E:** Sertoli cell **F:** Leydig cell; with autophagosome (AF); autolysosomes (AL) and multilamellar bodies in formation (*CM) **G-L:** Leydig cells (Le) insert, Secondary spermatocytes (C2) and spermatids (T) showing intense immunoreactivity for LC3 and Beclin-1. **M-O** type A spermatogonia with strong and punctual immunolabelling for Cathepsin-D of the animals of control and starvation 7D and 14D groups. Scale bars (A-F) 500 nm, (G-I and M-O) 50 μ m, (J-I) 75 μ m.

Figure 3. Autophagy, lysosomal and apoptotic proteins colocalization in testes of Nile tilapia. **A-D:** colocalization of between Lc3 and Lamp-1 indicating the autophagosome and lysosomes fusion **E-H:** cathepsin-D and lamp-1 colocalized during spermatogenesis of Nile tilapia mainly in spermatogonia and Leydig cells **I-L:** LC3 and Beclin-1 was not show colocalization of the animals starvation 7D group. Nuclei are stained with 4',6-diamidino-2'-phenylindole dihydrochloride (DAPI) (blue). Scale bars (A-I) 50 μ m

Figure 4. Immunofluorescence for Bcl2, Bax (green) and Caspase-3 (red). Nuclei are stained with 4',6-diamidino-2'-phenylindole dihydrochloride (DAPI) (blue). **A-C:** Secondary spermatocytes (C2) and spermatids (T) showing strong immunolabelling for Bcl2 mainly in the control, 7 and 14 starvation groups **D-I:** After 21 days of starvation, type A undifferentiated spermatogonia (Aund), type A differentiated spermatogonia (Adiff) and spermatids with strongly marked to Bax and

caspase-3 were frequently observed and primary spermatocytes with condensed nucleus were positive for Bax. Scale bars (A-I) 50 μm

Figure 5. Western blotting images of autophagic and apoptotic proteins in testes of Nile tilapia. Actin β was used as internal standard. Data represent the results obtained from 3 animals per experimental group.

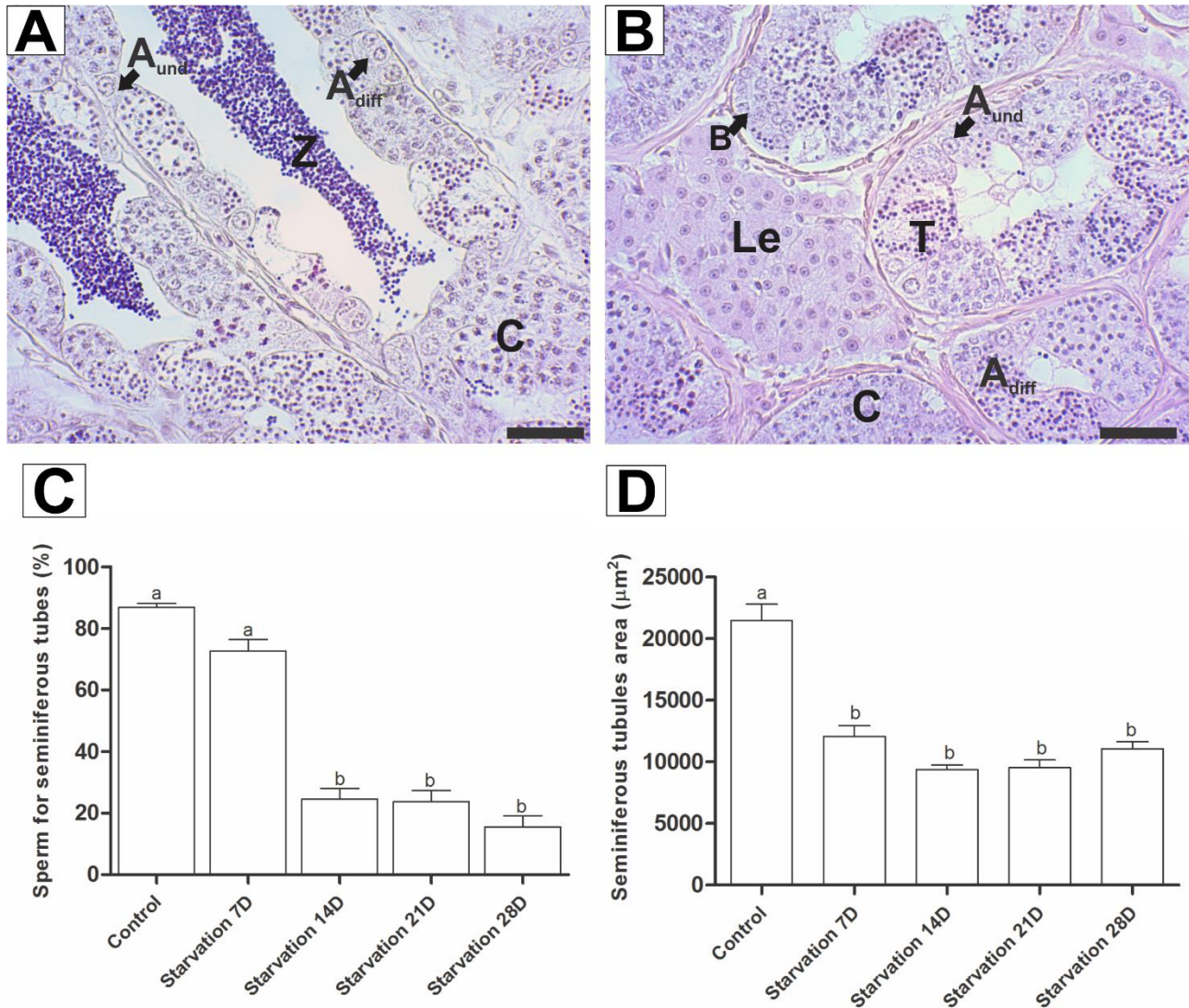


Figure.1

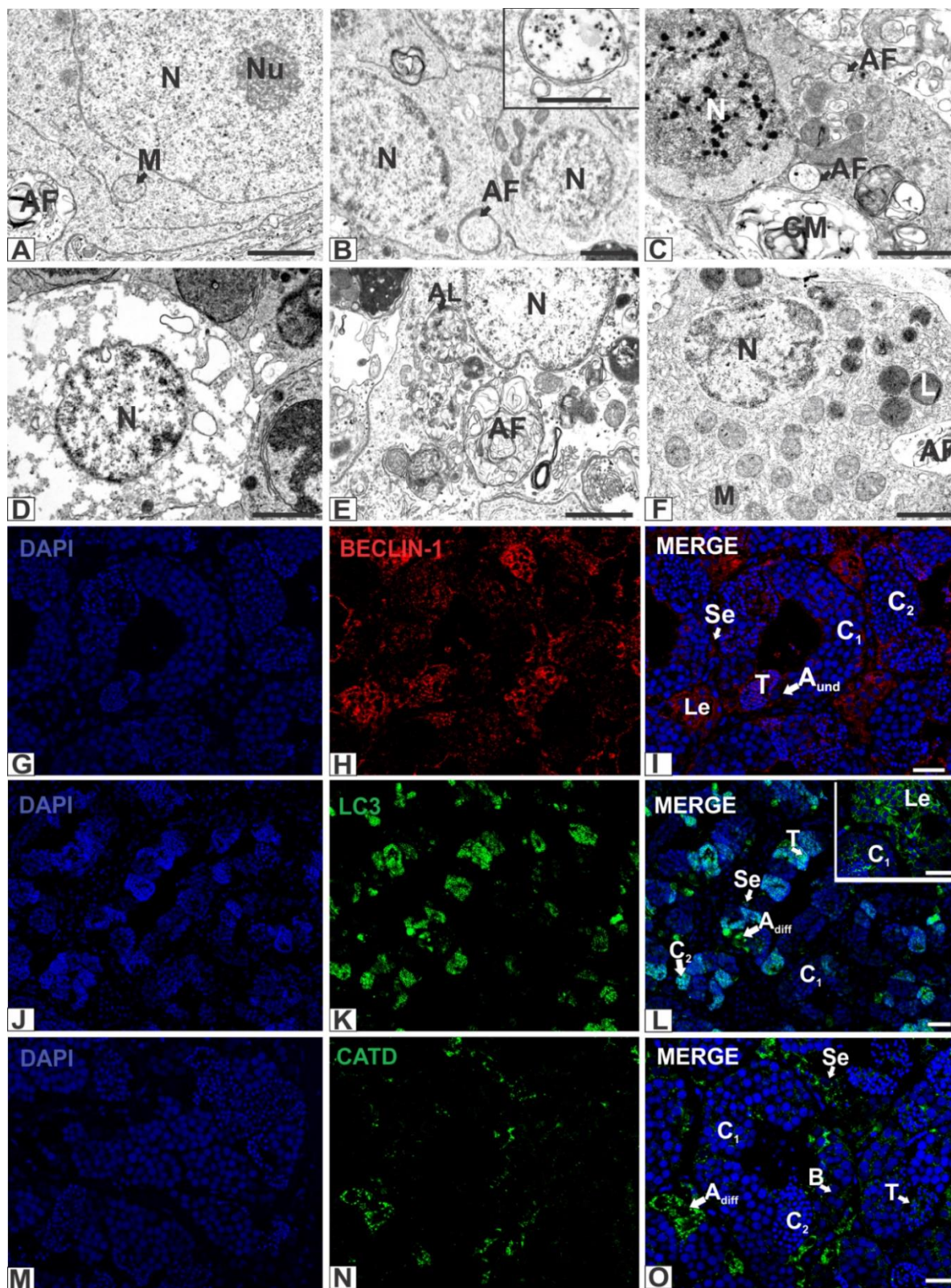


Figure.2

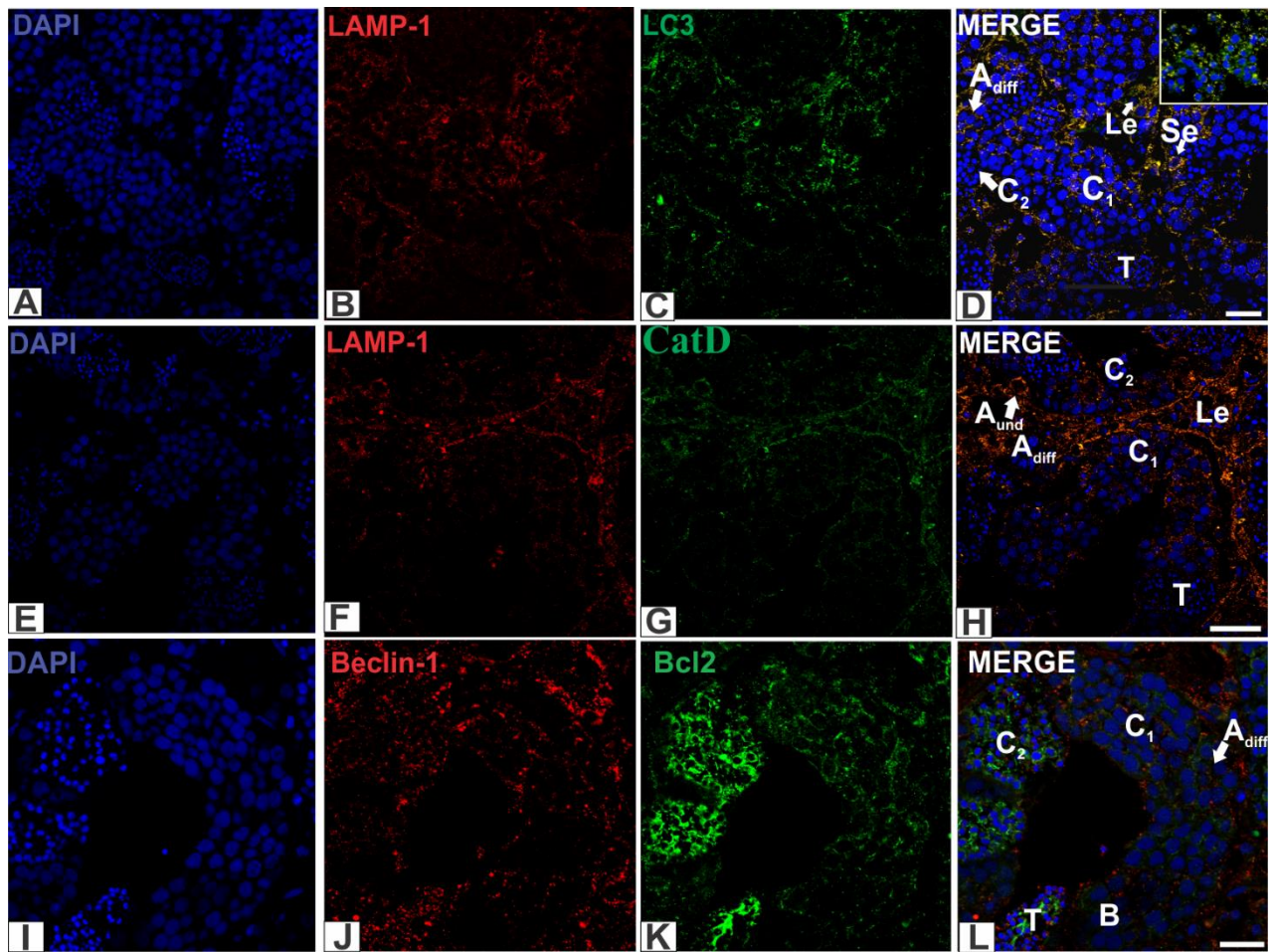


Figure.3

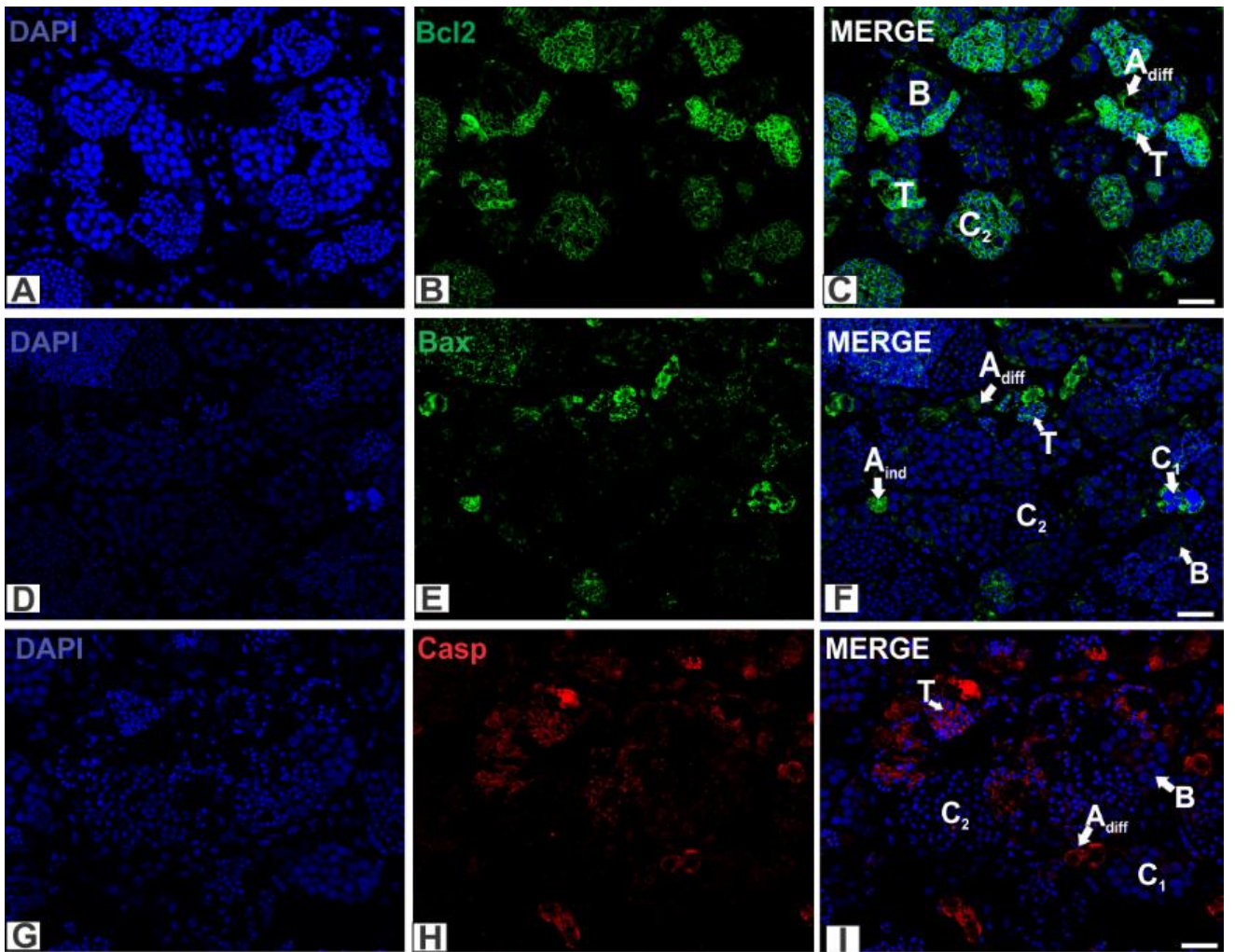


Figure.4

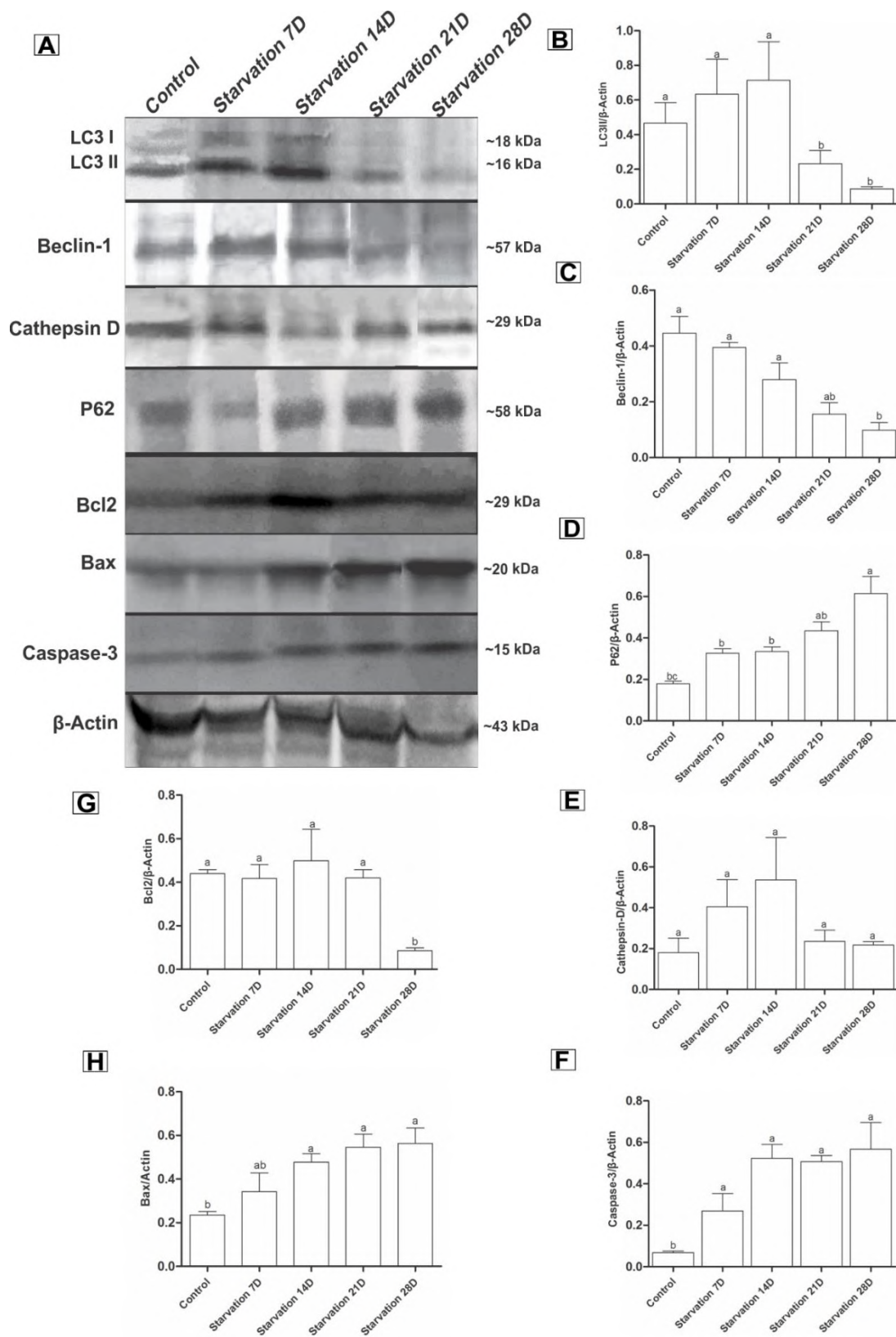


Figure.5

5.0 DISCUSSÃO GERAL

A interação entre autofagia e apoptose ocorre em diversos processos fisiológicos e alterações nessas vias estão associadas ao desenvolvimento de doenças como câncer e doenças neurodegenerativas em humanos. Ambas vias de sinalização são conservadas entre as espécies, e em consequência disso, houve um grande avanço do conhecimento sobre autofagia e apoptose em diferentes grupos de animais. Neste sentido, o presente trabalho foi realizado em três etapas, utilizando a tilápia do Nilo como modelo experimental. Na primeira etapa, nós avaliamos a expressão, interação e dinâmica existentes entre as proteínas chave da autofagia e apoptose durante a atresia folicular uma vez que, esses processos apresentam um importante papel na remodelação ovariana após desova (Thomé *et al.*, 2009, Moraes *et al.*, 2012, 2016; Cassel *et al.*, 2017). Para avaliar a autofagia e apoptose durante a espermatogênese, exemplares adultos da tilápia do Nilo foram submetidos à restrição alimentar, pois sabe-se que a deficiência alimentar e a falta de nutrientes como proteínas e glicose está associado a indução da via autofágica e apoptótica (Ryter *et al.*, 2013; Mejlvang *et al.*, 2018). Assim, na segunda etapa desse trabalho, nós avaliamos os efeitos de dois regimes de restrição alimentar na morfofisiologia da espermatogênese e, posteriormente, na terceira etapa, a expressão de proteínas e a inter-relação da autofagia e apoptose foi investigada.

Para estudar a dinâmica e a interação das vias de morte celular envolvidas na regeneração ovariana de tilápia do Nilo, os folículos atresicos foram divididos em três estágios: Folículo atrésico inicial (AF_E), Folículo atrésico avançado (AF_A) e Folículo atrésico final (AF_L). Nos AF_E, células foliculares apresentam intensa atividade de síntese com numerosas mitocôndrias, retículo endoplasmático e Complexo de Golgi. Essas organelas podem estar relacionadas à síntese de proteínas da maquinaria autofágica e no fornecimento de energia ao processo apoptótico (Lamb *et al.*, 2013; Chiarelli *et al.*, 2014).

No folículo atrésico avançado (AF_A) análises ultraestruturais evidenciaram estruturas autofágicas, como corpos multilamelares, autofagossomos e autolisossomos, caracterizando a intensa atividade autofágica das células foliculares nesta fase. O acúmulo dessas estruturas é uma das principais características morfológicas da autofagia (Hariri *et al.*, 2000; Kishi-Itakura *et al.*, 2014), sendo frequentemente observadas em doenças neurodegenerativas (Nixon, 2005). Ademais, células foliculares positivas para LC3 e Beclin-1 apresentaram intensa atividade de fagocitose do vitelo e zona radiata. Estudos recentes indicam a atuação da autofagia durante a fagocitose (heterofagia) e demonstram que esses processos podem atuar concomitantemente (Oczypok *et al.*, 2013, Lutz *et al.*, 2017). Neste sentido, nossos resultados sugerem a atuação

da autofagia durante a fase avançada da atresia folicular, atuando na manutenção das células foliculares envolvidas na fagocitose do vitelo. Embora os conhecimentos sobre a morte celular autofágica sejam incipientes, acredita-se que a autofagia pode levar à morte celular pela degradação proteolítica do volume de massa celular ou pela alta degradação de fatores de sobrevivência celular, o que pode induzir a ativação de um programa alternativo de morte celular (Nezis *et al.*, 2010; Nikolettou *et al.*, 2013). Nas fases finais da atresia folicular de *O. niloticus*, as células foliculares apresentaram citoplasma eletrólucido e escasso em organelas, devido possivelmente a intensa degradação e depuração de organelas e debris celulares promovidos pela alta atividade autofágica nos AF_A.

A interação entre as vias autofágicas e apoptóticas foi evidenciada no presente estudo pelo aumento concomitante na expressão de Beclin-1 e Bcl-2 durante a atresia avançada em tilápia do Nilo. Estudos mostram que Beclin-1 pode interagir com Bcl-2 através da ligação de Bcl-2 ao domínio BH3 de Beclin-1, inativando assim o processo autofágico (Gump and Thorburn, 2011; Mariño *et al.*, 2014). Entretanto, os altos níveis de Bcl-2 no contexto apresentado neste estudo podem estar contribuindo para a manutenção da autofagia e a sobrevivência das células foliculares no AF_A. Além disso, nós evidenciamos a interação entre as proteínas autofágica LC3 e apoptótica caspase-3 pela co-localização na fase final da atresia folicular, possivelmente indicando a clivagem de LC3 por caspase-3. Evidências recentes demonstram que caspases podem atuar clivando proteínas autofágicas como Beclin-1 e Atg 3 (Kang *et al.*, 2011; Wu *et al.*, 2014).

Ademais, nós relatamos em primeira mão a co-localização entre catepsina-D e a proteína específica de membrana lisossomal LAMP-1 durante a atresia folicular inicial e avançada. Estes dados indicam que catepsina-D se encontra dentro do compartimento lisossomal/autolisossomal atuando na degradação dos produtos fagocitados (heterofagia) e na via autofágica principalmente na fase avançada da atresia folicular. Em mamíferos, a hidrolase ácida catepsina-D está associada à autofagia atuando na degradação de componentes celulares e à heterofagia, atuando na degradação lisossomal de materiais extracelulares fagocitados (Vidoni *et al.*, 2016). Ao final da atresia, a co-localização entre estas duas proteínas foi pouco frequente e restrita a áreas celulares isoladas. A desestabilização da membrana lisossômica leva à liberação de catepsinas para o citosol iniciando a via lisossomal de morte celular através da degradação de proteínas anti-apoptóticas como as pertencentes à família Bcl-2. Frequentemente a permeabilização da membrana lisossomal causa perturbação na membrana mitocondrial, levando a ativação de caspases e consequente apoptose (Repnik *et al.*, 2012; Nilsson *et al.*, 2005; Kroemer and Jäättelä 2005; Gómez-Sintes *et al.*, 2016). Neste sentido, nossos achados

sugerem que a permeabilidade da membrana lisossomal em células foliculares ao final da regressão folicular pode levar à morte celular via apoptose, evidenciada pelo aumento da expressão de Bax, caspase-3 e células TUNEL positivas.

Estudos em mamíferos demonstram que a restrição alimentar é um potente indutor da via autofágica, inclusive durante a espermatogênese (Wang *et al.*, 2017; Wanichanon and Isidoro, 2019). Além disso, condições nutricionais desfavoráveis influenciam negativamente todos os aspectos da reprodução em vertebrados, das fases iniciais da gametogênese à viabilidade dos ovos e produção espermática (Luquet and Watanabe, 1986; Cheah and Yang, 2011; Escobar *et al.*, 2014; Jobling, 2016; Gilad *et al.*, 2018; Churchill *et al.*, 2019).

No presente trabalho, a restrição alimentar total afetou negativamente o índice gonadossomático (IGS) e o diâmetro dos túbulos seminíferos, e foi associada a alterações graves na morfologia testicular como desorganização e degeneração do testículo, levando a aumento da apoptose e diminuição da proliferação das espermatogônias. O IGS é um importante indicador da saúde geral e capacidade reprodutiva de um organismo (Collins, 2002; Frantzen *et al.*, 2004; Duston and Saunders, 2011; Grone *et al.*, 2012) sendo afetado negativamente pela privação de nutrientes como observado em algumas espécies de peixes (Silverstein and Shimma, 1994; Chatzifotis *et al.*, 2011; Suchiang and Gupta, 2011). Alterações teciduais severas como as observadas neste estudo também foram relatadas após longos períodos de restrição alimentar total em outras espécies de peixes (Suchiang and Gupta, 2011; Pikle *et al.*, 2017). Por outro lado, animais submetidos a jejum intermitente, com períodos de realimentação mantiveram a arquitetura e morfologia tecidual e das células germinativas, porém foi observado redução de espermatozoides e dos níveis plasmáticos de carboidratos e lipídios. Corroborando esses achados, a tilápia Moçambique apresentou resposta similar as do presente estudo com preservação do tecido testicular após ciclos de 6 dias de alimentação e 6 dias de jejum (Pikle *et al.*, 2017).

Assim como em mamíferos, a restrição alimentar em peixes está associada a redução dos níveis plasmáticos e teciduais de lipídios, principalmente de colesterol, molécula requerida para síntese de testosterona nas células de Leydig (Pérez-Jiménez *et al.*, 2007; Prasad, 2015; Rossi *et al.*, 2015). A redução dos níveis de testosterona e 11-ketotestosterona observada neste estudo após 7 dias de restrição total pode estar relacionada à redução dos níveis de colesterol total plasmático, como observado em humanos, outros mamíferos e em peixes (Morrison *et al.*, 2002; Eacker *et al.*, 2007; Velasco-Santamaría *et al.*, 2011). O pico de cortisol observado aos 7 dias na tilápia do Nilo coincidiu com a redução dos níveis plasmáticos de testosterona e 11 ketotestosterona. De fato, os glicocorticoides, em especial o cortisol, podem atuar

negativamente em todas as fases da espermatogênese tanto em peixes quanto em mamíferos (Weber *et al.*, 2002; Milla *et al.*, 2009; Dey *et al.*, 2010). Estudos sugerem que os altos níveis plasmáticos de cortisol estão relacionados a redução do potencial esteroidogênico das células de Leydig por reduzir a sensibilidade destas células ao hormônio luteinizante (LH) (Orr and Mann, 1992; Whirledge and Cidlowski, 2010).

Em peixes as células de Leydig são responsáveis pela conversão de testosterona em 11-ketotestosterona, o principal andrógeno durante a espermatogênese (Gazola and Borella, 1997; Ohta *et al.*, 2007). No presente estudo, o aumento progressivo na proliferação de células de Leydig juntamente com maior proporção destas células em animais submetidos a restrição alimentar total sugerem um mecanismo compensatório para aumentar a esteroidogênese e suprir os baixos níveis plasmáticos de testosterona e 11-ketotestosterona. Estudos recentes têm demonstrado a atuação da via autofágica na captação e utilização de colesterol pelas células de Leydig para síntese de testosterona (Gao *et al.*, 2018). Neste sentido, a redução significativa da expressão de proteínas autofágicas nos testículos de tilápia do Nilo pode ter contribuído para o aumento compensatório do número de células de Leydig, que embora aumentadas podem não estar totalmente funcionais. A baixa concentração de testosterona e 11-ketotestosterona pode estar associada à redução da proporção de A_{und} e A_{diff} positivas para Ki67, uma vez que a 11-ketotestosterona reprime a liberação de hormônio anti-mülleriano (AMH), que atua inibindo o processo proliferativo (Ohta *et al.*, 2007; Schulz *et al.*, 2010b; Skaar *et al.*, 2011).

A restrição alimentar total em tilápias do Nilo aumentou significativamente a proporção de espermátócitos, espermátides e espermatozoides TUNEL positivos e aumentou significativamente a expressão de Bax e Caspase-3 nos testículos, estes achados podem justificar a redução de espermátócitos e espermatozoides nos grupos tratados. Além disso, análises ultraestruturais de espermátócitos e espermátides evidenciaram alterações morfológicas que podem culminar em células anormais eliminadas por apoptose. A apoptose participa da homeostase celular do testículo, entretanto, estímulos externos como a privação de nutrientes, estão associados ao aumento da apoptose durante a espermatogênese em anfíbios e em mamíferos (Wang *et al.*, 2012; Gonzalez *et al.*, 2018). Em peixes, o aumento da apoptose em células germinativas foram associadas a altos níveis de cortisol e a diminuição de 11-ketotestosterona (Pickering *et al.*, 1987; Carragher *et al.*, 1989; Pottinger *et al.*, 1996; Goos and Consten, 2002; Milla *et al.*, 2009).

Estudos recentes evidenciaram o importante papel de autofagia durante a espermatogênese, atuando no remodelamento citoplasmático e removendo estruturas desnecessárias durante a diferenciação das espermátides (Herpin *et al.*, 2015; Shang *et al.*,

2016) e na formação do acrossoma e do flagelo (Wang *et al.*, 2014; Shang *et al.*, 2016) e na síntese de testosterona por promover a captação e utilização de colesterol pelas células de Leydig (Gao *et al.*, 2018). Nos últimos anos é notável o avanço do conhecimento sobre o papel da autofagia durante a espermatogênese, entretanto a atuação da via autofágica e os mecanismos moleculares envolvidos na espermatogênese são pouco conhecidos principalmente durante a espermatogênese de peixes. Nossos dados evidenciaram, pela primeira vez, a presença de marcadores autofágicos como LC3 e Beclin-1 e autofagossomos em diferentes células da linhagem germinativa assim como nas células de Leydig e de Sertoli. Além disso, nossos dados sugerem que a redução de espermatozoides nos túbulos seminíferos está relacionada a redução da autofagia e aumento da apoptose após 21 dias de restrição alimentar total.

6.0. CONCLUSÕES

- Na fase avançada da atresia folicular, a autofagia é essencial para a manutenção da homeostase das células foliculares durante a fagocitose de vitelo;
- A apoptose dependente de catepsina-D pode contribuir para a eliminação das células foliculares no final da atresia folicular;
- A restrição alimentar total reduz progressivamente os níveis de testosterona e 11 ketotestosterona e leva a danos nos testículos de tilápia do Nilo
- Animais submetidos ao sistema de realimentação apresentaram atraso na espermatogênese;
- Células germinativas e somáticas da tilápia do Nilo expressam proteínas autofágicas e apoptóticas e alteração dessas vias pode comprometer a progressão da espermatogênese.
- Após 21 dias de restrição alimentar total, a diminuição da autofagia e aumento da apoptose compromete significativamente a espermatogênese e produção espermática da tilápia do Nilo.

7.0 REFERÊNCIAS BIBLIOGRÁFICAS

- Agnello M and Chiarelli R** (2016) The role of autophagy and apoptosis during embryo development *The Role of Autophagy and Apoptosis During Embryo*.
- Alerting E** (2007) Autophagy : process and function. 2861–2873.
- Antonsson B** (2001) Bax and other pro-apoptotic Bcl-2 family ‘killer-proteins’ and their victim, the mitochondrion. *Cell and Tissue Research* **306** 347–361.
- Arantes FP, Santos HB, Rizzo E, Sato Y and Bazzoli N** (2011) General and Comparative Endocrinology Influence of water temperature on induced reproduction by hypophysation , sex steroids concentrations and final oocyte maturation of the ‘ curimatã-pacu’ *Prochilodus argenteus* (Pisces : Prochilodontidae). **172** 400–408.
- Aufschnaiter A, Kohler V and Büttner S** (2017) Taking out the garbage: Cathepsin D and calcineurin in neurodegeneration. *Neural Regeneration Research* **12** 1776–1779.
- Barreto RE, Moreira PSA and Carvalho RF** (2003) Sex-specific compensatory growth in food-deprived Nile tilapia. *Brazilian Journal of Medical and Biological Research* **36** 477–483.
- Batlouni SR, Nóbrega RH and França LR** (2009) Cell junctions in fish seminiferous epithelium. *Fish Physiology and Biochemistry* **35** 207–217.
- Bischof J, Westhoff M-A, Wagner JE, Halatsch M-E, Trentmann S, Knippschild U, Wirtz CR and Burster T** (2017) Cancer stem cells: The potential role of autophagy, proteolysis, and cathepsins in glioblastoma stem cells. *Tumor Biology* **39** 101042831769222.
- Boya P and Kroemer G** (2008) Lysosomal membrane permeabilization in cell death. *Oncogene* **27** 6434–6451.
- Carragher JF, Sumpter JP, Pottinger TG and Pickering AD** (1989) The deleterious effects of cortisol implantation on reproductive function in two species of trout, *Salmo trutta* L. and *Salmo gairdneri* Richardson. *General and Comparative Endocrinology*.
- Cassel M, Paiva M De, Lázaro C and Oliveira W** (2017) Involution processes of follicular atresia and post-ovulatory complex in a characid fish ovary : a study of apoptosis and autophagy pathways. *Journal of Molecular Histology* **48** 243–257.
- Chatzifotis S, Papadaki M, Despoti S, Roufidou C and Antonopoulou E** (2011) Effect of starvation and re-feeding on reproductive indices, body weight, plasma metabolites and oxidative enzymes of sea bass (*Dicentrarchus labrax*). *Aquaculture* **316** 53–59.
- Cheah Y and Yang W** (2011) Functions of essential nutrition for high quality spermatogenesis. *Advances in Bioscience and Biotechnology* **02** 182–197.

- Chen H, Huang Y, Yang P, Shi Y, Ahmed N, Liu T, Bai X, Haseeb A and Chen Q** (2019) Theriogenology Autophagy enhances lipid droplet development during spermiogenesis in Chinese soft-shelled turtle , *Pelodiscus sinensis*. *Theriogenology* 1–12.
- Choi JY, Jo MW, Lee EY, Yoon BK and Choi DS** (2010) The role of autophagy in follicular development and atresia in rat granulosa cells. *Fertility and Sterility* **93** 2532–2537.
- Churchill ER, Dytham C and Thom MDF** (2019) Differing effects of age and starvation on reproductive performance in *Drosophila melanogaster*. *Scientific Reports* **9** 4–11.
- Cobb J and Handel MA** (1998) Dynamics of meiotic prophase I during spermatogenesis: From pairing to division. *Seminars in Cell and Developmental Biology* **9** 445–450.
- Collins A** (2002) The role of food availability in regulating reproductive development in female golden perch. *Journal of Fish Biology* **55** 94–104.
- Crighton D, Wilkinson S, O’Prey J, Syed N, Smith P, Harrison PR, Gasco M, Garrone O, Crook T and Ryan KM** (2006) DRAM, a p53-Induced Modulator of Autophagy, Is Critical for Apoptosis. *Cell* **126** 121–134.
- Danial NN and Korsmeyer SJ** (2004) Cell Death: Critical Control Points. *Cell* **116** 205–219.
- Delbridge ARD, Grabow S, Strasser A and Vaux DL** (2016) Thirty years of BCL-2: Translating cell death discoveries into novel cancer therapies. *Nature Reviews Cancer* **16** 99–109.
- Dey CJ, O’Connor CM, Gilmour KM, Van Der Kraak G and Cooke SJ** (2010) Behavioral and physiological responses of a wild teleost fish to cortisol and androgen manipulation during parental care. *Hormones and Behavior* **58** 599–605.
- Duston J and Saunders RL** (2011) Effect of winter food deprivation on growth and sexual maturity of Atlantic salmon (*Salmo salar*) in seawater . *Canadian Journal of Fisheries and Aquatic Sciences*.
- de Duve C, Pressman BC, Gianetto R, Wattiaux R and Appelmans F** (1955) Tissue fractionation studies. 6. Intracellular distribution patterns of enzymes in rat-liver tissue. *Biochemical Journal* **60** 604–617.
- Eacker SM, Agrawal N, Qian K, Dichek HL, Gong E-Y, Lee K and Braun RE** (2007) Hormonal Regulation of Testicular Steroid and Cholesterol Homeostasis. *Molecular Endocrinology* **22** 623–635.
- Elmore S** (2007) Apoptosis: A Review of Programmed Cell Death. *Toxicologic Pathology* **35** 495–516.
- Escobar MLS, Echeverría Martínez OM and Vázquez-Nin GH** (2012) Immunohistochemical and ultrastructural visualization of different routes of oocyte

- elimination in adult rats. *European Journal of Histochemistry* **56** 102–110.
- Escobar S, Felip A, Salah M, Zanuy S and Carrillo M** (2014) Long-term feeding restriction in prepubertal male sea bass (*Dicentrarchus labrax*) increases the number of apoptotic cells in the testis and affects the onset of puberty and certain reproductive parameters. *Aquaculture* **433** 504–512.
- Eskelinen EL** (2005) Maturation of autophagic vacuoles in Mammalian cells. *Autophagy* **1** 1–10.
- Frantzen M, Damsgård B, Tveiten H, Moriyama S, Iwata M and Johnsen HK** (2004) Effects of fasting on temporal changes in plasma concentrations of sex steroids, growth hormone and insulin-like growth factor I, and reproductive investment in Arctic charr. *Journal of Fish Biology* **65** 1526–1542.
- Galluzzi L, Vitale I, Aaronson SA, Abrams JM, Adam D, Agostinis P, Alnemri ES, Altucci L, Amelio I, Andrews DW et al.** (2018) Molecular mechanisms of cell death: Recommendations of the Nomenclature Committee on Cell Death 2018. *Cell Death and Differentiation* **25** 486–541.
- Gao F, Li G, Liu C, Gao H, Wang H, Liu W, Chen M, Shang Y, Wang L, Shi J et al.** (2018) Autophagy regulates testosterone synthesis by facilitating cholesterol uptake in Leydig cells. **217** 2103–2119.
- Gavrieli Y, Sherman Y and Ben-Sasson SA** (1992) Identification of programmed cell death in situ via specific labeling of nuclear DNA fragmentation. *Journal of Cell Biology* **119** 493–501.
- Gawriluk TR, Hale AN, Flaws JA, Dillon CP, Green DR and Rucker EB** (2011) Autophagy is a cell survival program for female germ cells in the murine ovary. *Reproduction* **141** 759–765.
- Gazola R and Borella MI** (1997) Plasma testosterone and 11-ketotestosterone levels of male pacu *Piaractus mesopotamicus* (Cypriniformes, Characidae). *Brazilian Journal of Medical and Biological Research* **30** 1485–1487.
- Gadomski DM and Petersen JH** (1988). Effects of food deprivation on the larvae of two flatfishes. *Marine Ecology Progress Series*, 44(2), 103–111
- Ghavami S, Shojaei S, Yeganeh B, Ande SR, Jangamreddy JR, Mehrpour M, Christofferson J, Chaabane W, Moghadam AR, Kashani HH et al.** (2014) Autophagy and apoptosis dysfunction in neurodegenerative disorders. *Progress in Neurobiology* **112** 24–49.
- Gilad T, Koren R, Moalem Y, Subach A and Scharf I** (2018) Effect of continuous and

- alternating episodes of starvation on behavior and reproduction in the red flour beetle. *Journal of Zoology* **305** 213–222.
- Gómez-Sintes R, Ledesma MD and Boya P** (2016) Lysosomal cell death mechanisms in aging. *Ageing Research Reviews* **32** 150–168.
- Gong Y** (2019) Effect of Gpx3 gene silencing by siRNA on apoptosis and autophagy in chicken cardiomyocytes. 7828–7838.
- Goos HJT and Consten D** (2002) Stress adaptation, cortisol and pubertal development in the male common carp, *Cyprinus carpio*. *Molecular and Cellular Endocrinology* **197** 105–116.
- Grier HJ** (1981) Cellular organization of the testis and spermatogenesis in fishes. *Integrative and Comparative Biology* **21** 345–357.
- Grier HJ, Uribe MC and Parenti LR** (2007) Germinal epithelium, folliculogenesis, and postovulatory follicles in ovaries of rainbow trout, *Oncorhynchus mykiss* (Walbaum, 1792) (Teleostei, Protacanthopterygii, Salmoniformes). *Journal of Morphology* **268** 293–310.
- Grone BP, Carpenter RE, Lee M, Maruska KP and Fernald RD** (2012) Food deprivation explains effects of mouthbrooding on ovaries and steroid hormones, but not brain neuropeptide and receptor mRNAs, in an African cichlid fish. *Hormones and Behavior* **62** 18–26.
- Gump JM and Thorburn A** (2011) NIH Public Access. *Trends Cell Biol* **21** 387–392.
- Habibi HR and Andreu-Vieyra C V.** (2007) Hormonal regulation of follicular atresia in teleost fish. In *The Fish Oocyte: From Basic Studies to Biotechnological Applications*, pp 235–253.
- Hamasaki M, Furuta N, Matsuda A, Nezu A, Yamamoto A, Fujita N, Oomori H, Noda T, Haraguchi T, Hiraoka Y et al.** (2013) Autophagosomes form at ER-mitochondria contact sites. *Nature* **495** 389–393.
- Han S, Wang J, Zhang Y, Qiao F, Chen L, Zhang M and Du Z** (2019) Comparative Biochemistry and Physiology , Part A Inhibited autophagy impairs systemic nutrient metabolism in Nile tilapia. *Comparative Biochemistry and Physiology, Part A* **236** 110521.
- Hansen TE and Johansen T** (2011) Following autophagy step by step. *BMC Biology* **9** 2–5.
- Hariri M, Millane G, Guimond MP, Guay G, Dennis JW and Nabi IR** (2000) Biogenesis of multilamellar bodies via autophagy. *Molecular Biology of the Cell* **11** 255–268.
- He R, Peng J, Yuan P, Xu F and Wei W** (2015) Divergent roles of BECN1 in LC3 lipidation

and autophagosomal function. *Autophagy* **11** 740–747.

- Herpin A, Englberger E, Zehner M, Wacker R, Gessler M and Scharl M** (2015) Defective autophagy through *epg5* mutation results in failure to reduce germ plasm and mitochondria. *The FASEB Journal*. **29** :4145-61.
- Hou W, Han J, Lu C, Goldstein LA and Rabinowich H** (2010) Autophagic degradation of active caspase-8: A crosstalk mechanism between autophagy and apoptosis. *Autophagy* **6** 891–900.
- Hsueh AJW, Billig H and Tsafiriri A** (1994) Ovarian Follicle Atresia: A Hormonally Controlled Apoptotic Process. *Endocrine Reviews* **15** 707–724.
- Hughes FM and Gorospe WC** (1991) Biochemical identification of apoptosis (Programmed cell death) in granulosa cells: Evidence for a potential mechanism underlying follicular atresia. *Endocrinology* **129** 2415–2422.
- Huynh KK, Eskelinen EL, Scott CC, Malevanets A, Saftig P and Grinstein S** (2007) LAMP proteins are required for fusion of lysosomes with phagosomes. *EMBO Journal* **26** 313–324.
- Jin Z, Li Y, Pitti R, Lawrence D, Pham VC, Lill JR and Ashkenazi A** (2009) Cullin3-Based Polyubiquitination and p62-Dependent Aggregation of Caspase-8 Mediate Extrinsic Apoptosis Signaling. *Cell* **137** 721–735.
- Jobling M** (2016) Fish nutrition research: past, present and future. *Aquaculture International* **24** 767–786.
- Johansson A-C, Hanna A, Nilsson C, Kagedal K, Roberg K and Karin L** (2010) Regulation of apoptosis-associated lysosomal membrane permeabilization. *Apoptosis* **15** 527–540.
- Kabeya Y** (2000) LC3, a mammalian homologue of yeast Apg8p, is localized in autophagosome membranes after processing. *The EMBO Journal* **19** 5720–5728.
- Kaipia A and Hsueh AJW** (1997) Regulation of ovarian follicle atresia. *Annu. Rev. Physiol* **59** 349–363.
- Kang R, Zeh HJ, Lotze MT and Tang D** (2011) The Beclin 1 network regulates autophagy and apoptosis. *Cell Death and Differentiation* **18** 571–580.
- Kerr JFR, Wyllie AH and Curriar AR** (1972) Apoptosis: a basic biological phenomenon with wide- ranging implications in tissue kinetics. *Journal of Internal Medicine* **258** 479–517.
- Kishi-Itakura C, Koyama-Honda I, Itakura E and Mizushima N** (2014) Ultrastructural analysis of autophagosome organization using mammalian autophagy-deficient cells. *Journal of Cell Science* **127** 4984–4984.
- Klionsky D, Agholme L, Agnello M, Agostinis P, Aguirre-ghiso JA, Ahn HJ, Ait-mohamed**

- O, Brown EJ, Brumell JH, Brunetti-pierri N et al.** (2016) Guidelines for the use and interpretation of assays for monitoring autophagy. *Autophagy* **8** 445–544.
- Linares-Casenave J, Van Eenennaam JP and Doroshov SI** (2002) Ultrastructural and histological observations on temperature-induced follicular ovarian atresia in the white surgeon. *Journal of Applied Ichthyology* **18** 382–390.
- Lu Z, Chen C, Wu Z, Miao Y, Muhammad I, Ding L, Tian E, Hu W, Ni H, Li R et al.** (2017) A dual role of P53 in regulating colistin-induced autophagy in PC-12 cells. *Frontiers in Pharmacology* **8**.
- Luquet P and Watanabe T** (1986) Interaction “nutrition-reproduction” in fish. *Fish Physiology and Biochemistry* **2** 121–129.
- Mathew R, Karp CM, Beaudoin B, Vuong N, Chen G, Chen HY, Bray K, Reddy A, Bhanot G, Gelinas C et al.** (2009) Autophagy Suppresses Tumorigenesis through Elimination of p62. *Cell* **137** 1062–1075.
- Mejlvang J, Olsvik H, Svenning S, Bruun JA, Abudu YP and Larsen KB** (2018) Starvation induces rapid degradation of selective autophagy receptors by endosomal microautophagy. **217** 3640–3655.
- Melo RMC, Martins YS, de Alencar Teixeira E, Luz RK, Rizzo E and Bazzoli N** (2014) Morphological and quantitative evaluation of the ovarian recrudescence in Nile Tilapia (*Oreochromis niloticus*) after spawning in captivity. *Journal of Morphology* **275** 348–356.
- Melo RMC, Martins YS, Luz RK, Rizzo E and Bazzoli N** (2015) PCNA and apoptosis during post-spawning ovarian remodeling in the teleost *Oreochromis niloticus*. *Tissue and Cell* **47** 541–549.
- McCue MD** (2010) Starvation physiology: Reviewing the different strategies animals use to 1172 survive a common challenge. *Comparative Biochemistry and Physiology - A Molecular and Integrative Physiology* **1173** 156, 1–18.
- Milla S, Wang N, Mandiki SNM and Kestemont P** (2009) Corticosteroids: Friends or foes of teleost fish reproduction? *Comparative Biochemistry and Physiology - A Molecular and Integrative Physiology* **153** 242–251.
- Mizushima N and Komatsu M** (2011) Autophagy: Renovation of cells and tissues. *Cell* **147** 728–741.
- Morais RDVS, Thomé RG, Lemos FS, Bazzoli N and . ER** (2012) Autophagy and apoptosis interplay during follicular atresia in fish ovary : a morphological and immunocytochemical study. *Cell Tissue Res* **347** 467–478.
- Morrison JA, Sprecher DL, Biro FM, Apperson-Hansen C and DiPaola LM** (2002) Serum

- testosterone associates with lower high-density lipoprotein cholesterol in black and white males, 10 to 15 years of age, through lowered apolipoprotein AI and AII concentrations. *Metabolism: Clinical and Experimental* **51** 432–437.
- Mrschik M and Ryan KM** (2015) Lysosomal proteins in cell death and autophagy. *FEBS Journal* **282** 1858–1870.
- Nikoletopoulou V, Markaki M, Palikaras K and Tavernarakis N** (2013) Crosstalk between apoptosis, necrosis and autophagy. *Biochimica et Biophysica Acta - Molecular Cell Research* **1833** 3448–3459.
- Nixon RA, Wegiel J, Kumar A, Yu WH, Peterhoff C, Cataldo A, Cuervo AM.**(2005) Extensive involvement of autophagy in Alzheimer disease: an immuno-electron microscopy study. *J Neuropathol Exp Neurol.* **64**:113-22.
- Nóbrega RH, Batlouni SR and França LR** (2009) An overview of functional and stereological evaluation of spermatogenesis and germ cell transplantation in fish. *Fish Physiology and Biochemistry* **35** 197–206.
- Ohta T, Miyake H, Miura C, Kamei H, Aida K and Miura T** (2007) Follicle-Stimulating Hormone Induces Spermatogenesis Mediated by Androgen Production in Japanese Eel, *Anguilla japonica*1. *Biology of Reproduction.*
- Orr TE and Mann DR** (1992) Role of glucocorticoids in the stress-induced suppression of testicular steroidogenesis in adult male rats. *Hormones and Behavior.*
- Pan J-A, Ullman E, Dou Z and Zong W-X** (2011) Inhibition of Protein Degradation Induces Apoptosis through a Microtubule-Associated Protein 1 Light Chain 3-Mediated Activation of Caspase-8 at Intracellular Membranes. *Molecular and Cellular Biology* **31** 3158–3170.
- Palma, E. H. da et al.** (2010) Estratégia alimentar com ciclos de restrição e realimentação no 1185 desempenho produtivo de juvenis de tilápia do Nilo da linhagem GIFT. *Ciência 1186 Rural* **40**, 391–396.
- Pérez-Jiménez A, Guedes MJ, Morales AE and Oliva-Teles A** (2007) Metabolic responses to short starvation and refeeding in *Dicentrarchus labrax*. Effect of dietary composition. *Aquaculture* **265** 325–335.
- Pickering AD, Pottinger TG, Carragher J and Sumpter JP** (1987) The effects of acute and chronic stress on the levels of reproductive hormones in the plasma of mature male brown trout, *Salmo trutta* L. *General and Comparative Endocrinology.*
- Pikle RP, Jatiger RM and Ganesh CB** (2017) Food-deprivation-induced suppression of pituitary–testicular-axis in the tilapia *Oreochromis mossambicus*. *International Aquatic Research* **9** 203–213.

- Polcic P, Jaka P and Mentel M** (2015) Yeast as a tool for studying proteins of the Bcl-2 family. *Microbial Cell* **2** 74–87.
- Pottinger TG, Carrick TR, Hughes SE and Balm PHM** (1996) Testosterone, 11-ketotestosterone, and estradiol-17 β modify baseline and stress-induced interrenal and corticotropic activity in trout. *General and Comparative Endocrinology*.
- Prasad NK** (2015) Effects of Prolonged Starvation on Cholesterol Content of Gonads in *Clarias batrachus*. *Our Nature* **13** 26–30.
- Quagio-Grassiotto I, Grier H, Mazzoni TS, Nóbrega RH and De Arruda Amorim JP** (2011) Activity of the ovarian germinal epithelium in the freshwater catfish, *Pimelodus maculatus* (Teleostei: Ostariophysi: Siluriformes): Germline cysts, follicle formation and oocyte development. *Journal of Morphology* **272** 1290–1306.
- Repnik U, Stoka V, Turk V and Turk B** (2012) Lysosomes and lysosomal cathepsins in cell death. *Biochimica et Biophysica Acta - Proteins and Proteomics* **1824** 22–33.
- Rizzo E and Bazzoli N** (1995) Follicular atresia in curimatá-pioa *Prochilodus affinis* Reinhardt, 1874 (Pisces, Characiformes). 697–703.
- Robertson JD and Orrenius S** (2000) Molecular mechanisms of apoptosis induced by cytotoxic chemicals. *Critical Reviews in Toxicology* **30** 609–627.
- Romano PS** (2013) Autophagy - A Double-Edged Sword - Cell Survival or Death?
- Rossi A, Cazenave J, Bacchetta C, Campana M and Parma MJ** (2015) Physiological and metabolic adjustments of *Hoplosternum littorale* (Teleostei, Callichthyidae) during starvation. *Ecological Indicators* **56** 161–170.
- Russell LD, Chiarini-Garcia H, Korsmeyer SJ and Knudson CM** (2002) Bax-dependent spermatogonia apoptosis is required for testicular development and spermatogenesis. *Biology of Reproduction* **66** 950–958.
- Ryter SW, Cloonan SM and Choi AMK** (2013) Autophagy: A critical regulator of cellular metabolism and homeostasis. *Molecules and Cells* **36** 7–16.
- Ryter SW, Mizumura K and Choi AMK** (2014) The impact of autophagy on cell death modalities. *International Journal of Cell Biology* **2014** 17–19.
- Saidapur SK** (1978) Follicular Atresia in the Ovaries of Nonmammalian Vertebrates. *International Review of Cytology* **54** 225–244.
- Sales CF, Luz RK, Magno R, Melo C, Paula A and Pinheiro B** (2019) Autophagy and Cathepsin D mediated apoptosis contributing to ovarian follicular atresia in the Nile tilapia. 1–11.
- Santos HB, Rizzo E, Bazzoli N, Sato Y and Moro L** (2005) Ovarian regression and apoptosis

- in the South American teleost *Leporinus taeniatus* Lütken (Characiformes, Anostomidae) from the São Francisco Basin. *Journal of Fish Biology* **67** 1446–1459.
- Santos HB, Sato Y, Moro L, Bazzoli N and Rizzo E** (2008) Relationship among follicular apoptosis, integrin β 1 and collagen type IV during early ovarian regression in the teleost *Prochilodus argenteus* after induced spawning. *Cell and Tissue Research* **332** 159–170.
- Sato Y, Bazzoli N, Rizzo E, Boschi MB and Miranda MOT** (2005) Influence of the Abaeté River on the reproductive success of the neotropical migratory teleost *Prochilodus argenteus* in the São Francisco River, downstream from the Três Marias Dam, southeastern Brazil. *River Research and Applications* **21** 939–950.
- Schulz RW and Nóbrega RH** (2011) The reproductive organs and processes | Anatomy and Histology of Fish Testis. In *Encyclopedia of Fish Physiology*, pp 616–626.
- Schulz RW, de França LR, Lareyre JJ, LeGac F, Chiarini-Garcia H, Nobrega RH and Miura T** (2010) Spermatogenesis in fish. *General and Comparative Endocrinology* **165** 390–411.
- Schulz RW, van Dijk W, Chaves-Pozo E, García-López Á, de França LR and Bogerd J** (2012) Sertoli cell proliferation in the adult testis is induced by unilateral gonadectomy in African catfish. *General and Comparative Endocrinology* **177** 160–167.
- Shang Y, Wang H, Jia P, Zhao H, Liu C, Liu W, Song Z, Xu Z, Yang L, Wang Y et al.** (2016) Autophagy regulates spermatid differentiation via degradation of PDLIM1. *Autophagy* **12** 1575–1592.
- Shi Q, Jin X, Fan R, Xing M, Guo J, Zhang Z, Zhang J and Xu S** (2019) Chemosphere Cadmium-mediated miR-30a-GRP78 leads to JNK-dependent autophagy in chicken kidney. *Chemosphere* **215** 710–715.
- Shimizu S, Narita M and Tsujimoto Y** (2000) Bcl-2 family proteins regulate the release of apoptogenic cytochrome c by the mitochondrial channel VDAC Bcl-2 family proteins regulate the release of apoptogenic cytochrome c by the. *Nature* **66** 1–5.
- Silverstein JT and Shimma H** (1994) Effect of restricted feeding on early maturation in female and male amago salmon, *Oncorhynchus mason ishikawae*. *Journal of Fish Biology*.
- Skaar KS, Nóbrega RH, Magaraki A, Olsen LC, Schulz RW and Male R** (2011) Proteolytically activated, recombinant anti-Müllerian hormone inhibits androgen secretion, proliferation, and differentiation of spermatogonia in adult zebrafish testis organ cultures. *Endocrinology* **152** 3527–3540.
- Song S, Tan J, Miao Y, Li M and Zhang Q** (2017) Crosstalk of autophagy and apoptosis: Involvement of the dual role of autophagy under ER stress. *Journal of Cellular Physiology*

232 2977–2984.

- Soto-Burgos J, Zhuang X, Jiang L and Bassham DC** (2018) Dynamics of Autophagosome Formation. *Plant Physiology* **176** 219–229.
- Suchiang P and Gupta BBP** (2011) Effects of Partial and Full Feed Restriction on the Plasma Levels of Thyroid Hormones and Testicular Activity in the Male Air-breathing Catfish, *Clarias gariepinus* during Different Phases of the Breeding Cycle. *International Journal of Biology* **3** 32–42.
- Take H and Andersen** (2007) Caspases and apoptosis in fish. *Journal of Fish Biology* **71** 326–349.
- Tasdemir E, Maiuri MC, Morselli E, Criollo A, D’Amelio M, Djavaheri-Mergny M, Cecconi F, Tavernarakis N and Kroemer G** (2008) A dual role of p53 in the control of autophagy. *Autophagy* **4** 810–814.
- Tripathi R, Mishra DP and Shaha C** (2009) Male germ cell development: turning on the apoptotic pathways. *Journal of Reproductive Immunology* **83** 31–35.
- Turk V, Stoka V, Vasiljeva O, Renko M, Sun T, Turk B and Turk D** (2012) Cysteine cathepsins: From structure, function and regulation to new frontiers. *Biochimica et Biophysica Acta - Proteins and Proteomics* **1824** 68–88.
- Uchiyama Y, Shibata M, Koike M, Yoshimura K and Sasaki M** (2008) Autophagy-physiology and pathophysiology. *Histochemistry and Cell Biology* **129** 407–420.
- Velasco-Santamaría YM, Korsgaard B, Madsen SS and Bjerregaard P** (2011) Bezafibrate, a lipid-lowering pharmaceutical, as a potential endocrine disruptor in male zebrafish (*Danio rerio*). *Aquatic Toxicology* **105** 107–118.
- Vistro WA, Zhang Y, Bai X, Yang P, Huang Y and Qu W** (2019) In Vivo Autophagy Up-Regulation of Small Intestine Enterocytes in Chinese Soft-Shell Turtles during Hibernation. 1–17.
- de Waal PP, Leal MC, García-López Á, Liarte S, de Jonge H, Hinfrey N, Brion F, Schulz RW and Bogerd J** (2009) Oestrogen-induced androgen insufficiency results in a reduction of proliferation and differentiation of spermatogonia in the zebrafish testis. *Journal of Endocrinology* **202** 287–297.
- Wang H, Wan H, Li X, Liu W, Chen Q, Wang Y, Yang L and Tang H** (2014) Atg7 is required for acrosome biogenesis during spermatogenesis in mice. *Nature Publishing Group* 1–18.
- Wang YY, Sun YC, Sun XF, Cheng SF, Li B, Zhang XF, De Felici M and Shen W** (2017) Starvation at birth impairs germ cell cyst breakdown and increases autophagy and

apoptosis in mouse oocytes. *Cell Death and Disease* **8** 1–10.

- Wanichanon C and Isidoro C** (2019) Starvation Promotes Autophagy Associated Maturation of the Testis in the Giant Freshwater Prawn, *Macrobrachium rosenbergii*. *Frontiers in Physiology*. **27** 10:1219.
- Weber LP, Kiparissis Y, Hwang GS, Niimi AJ, Janz DM and Metcalfe CD** (2002) Increased cellular apoptosis after chronic aqueous exposure to nonylphenol and quercetin in adult medaka (*Oryzias latipes*). *Comparative Biochemistry and Physiology - C Toxicology and Pharmacology* **131** 51–59.
- Whirledge S and Cidlowski JA** (2010) Glucocorticoids, stress, and fertility. *Minerva Endocrinologica* **35** 109–125.
- Wu H, Che X, Zheng Q, Wu A, Pan K, Shao A, Wu Q, Zhang J and Hong Y** (2014) Caspases: A molecular switch node in the crosstalk between autophagy and apoptosis. *International Journal of Biological Sciences* **10** 1072–1083.
- Wyllie AH, Kerr JFR and Currie AR** (1980) Cell Death: The Significance of Apoptosis. *International Review of Cytology* **68** 251–306.
- Xia X, Wang X, Qin W, Jiang J and Cheng L** (2019) Emerging regulatory mechanisms and functions of autophagy in fish. *Aquaculture* **511** 734212.
- Yin J, Ni B, Tian Z, Yang F, Liao W and Gao Y** (2017) Regulatory effects of autophagy on spermatogenesis. *Biology of Reproduction* **96** 525–530.
- Youle RJ and Strasser A** (2008) The BCL-2 protein family: Opposing activities that mediate cell death. *Nature Reviews Molecular Cell Biology* **9** 47–59.
- Zanoni MA, Caetano M and Hermann J** (2000) Performance de crescimento de diferentes linhagens de tilápia- do - nilo , *Oreochromis niloticus* (Linnaeus ,1757), em gaiolas. **22** 683–687.
- Zhang JH, Zhang Y and Herman B** (2003) Caspases, apoptosis and aging. *Ageing Research Reviews* **2** 357–366.
- Zhang M, Jiang M, Bi Y, Zhu H, Zhou Z and Sha J** (2012) Autophagy and apoptosis act as partners to induce germ cell death after heat stress in mice. *PLoS ONE* **7**.

8.0 ANEXOS (ARTIGOS PUBLICADOS DURANTE O DOUTORADO) E CO-ORIENTAÇÃO DE MONOGRAFIA

- **Sales, CF; Santos, KPS, Rizzo,E; Ribeiro, RIMA; Santos, HB; Thome, RG (2017). Proliferation, survival and cell death in fish gills remodeling: From injury to recovery.** Fish & Shellfish Immunology 68-10-18.
- **Sales CF*, Lemos FS*, Morais RDVS, Thomé RG, Santos HB, Pinheiro APB, Bazzoli N, Rizzo E, 2019. Thermal stress induces HSP70 and apoptosis during embryo 2 development in a Neotropical freshwater fish.** Reprod Fertil Dev. 2019 Mar;31(3):547-556. doi: 10.1071/RD18217.
- **Weber AA, Sales CF, de Souza Faria F, Melo RMC, Bazzoli N, Rizzo. E Effects of metal contamination on liver in two fish species from a highly impacted neotropical river: A case study of the Fundão dam, Brazil.** Ecotoxicol Environ Saf. 2020 Mar 1;190:110165. doi: 10.1016/j.ecoenv.2020.110165. Epub 2020 Jan 6.

Co-orientação de Monografia

- **Francisco de Souza Faria (Co-orientação). 2018. Trabalho de Conclusão de Curso. Título: Efeitos da restrição alimentar sobre parâmetros hematológicos e histologia hepática da tilápia do Nilo (*Oreochromis Niloticus*) em condições de cultivo. (Graduação em Ciências Biológicas) - Universidade Federal de Minas Gerais. Co-orientadora: **Camila Ferreira Sales.****



Full length article

Proliferation, survival and cell death in fish gills remodeling: From injury to recovery



Camila Ferreira Sales ^{a,b}, Keiza Priscila Enes dos Santos ^a, Elizete Rizzo ^b,
Rosy Iara Maciel de Azambuja Ribeiro ^c, Hélio Batista dos Santos ^a,
Ralph Gruppi Thomé ^{a,*}

^a Universidade Federal de São João Del Rei, Campus Centro Oeste, Laboratório de Processamento de Tecidos – LAPROTEC, Rua Sebastião Gonçalves Coelho, 400, 35501-296, Divinópolis, Minas Gerais, Brazil

^b Universidade Federal de Minas Gerais, Instituto de Ciências Biológicas, Departamento de Morfologia, Laboratório de Ictiohistologia, Avenida Presidente Antônio Carlos, 6627, 31270-901, Belo Horizonte, Minas Gerais, Brazil

^c Universidade Federal de São João Del Rei, Campus Centro Oeste, Laboratório de Patologia Experimental - LAPATEX, Rua Sebastião Gonçalves Coelho, 400, 35501-296, Divinópolis, Minas Gerais, Brazil

ARTICLE INFO

Article history:

Received 28 March 2017

Received in revised form

30 June 2017

Accepted 1 July 2017

Available online 1 July 2017

Keywords:

PCNA

iNOS

HSP70

Bax

Teleost

ABSTRACT

Pollutants found dispersed in water can cause irritations on the gills, challenge the immune system and prejudice the welfare of the fish. Here we investigated molecules linked to proliferation, survival, and cell death, as well as inflammatory and vascular control, in a model of fish gill remodeling, from injury to recovery. We assessed the gill histology and immunohistochemistry for PCNA, iNOS, HSP70, and Bax in *Hypostomus francisci* obtained from a river subjected to chronic anthropic influences and then after they were placed in water of good quality. A total of 30 *H. francisci* adult individuals were collected and distributed into two groups: euthanized on the day of capture (group 1) and maintained for 30 days in an aquarium (group 2). In all the fish from group 1, the primary and secondary lamellae showed hypertrophy of the respiratory epithelium, lamellar fusion, lifting of the epithelium, aneurysm, hyperemia, and vascular congestion. On the other hand, in all the fish from group 2, restoration of gill integrity was observed, and the primary and secondary lamellae showed a simple epithelium, absence of lamellar fusion, hypertrophy, and aneurysm. Gills of fish from group 1 had higher frequency of cells immunopositive for PCNA, iNOS, HSP70, and Bax than those of fish from group 2 ($p < 0.05$). The molecular and cellular mechanisms from injury to recovery were proposed, with a balance between survival and cell death signals being essential for determining the gill structure. In addition, the findings indicate that recovery of the structural organization of gills is possible if fishes are maintained in good-quality water, indicating the importance of the conservation of aquatic environments.

© 2017 Elsevier Ltd. All rights reserved.

1. Introduction

Rapid population growth and urbanization of extensive areas have resulted in anthropogenic changes in aquatic ecosystems. Therefore, water quality is directly related to the safety of human health and the animals that inhabit these environments [1]. Among aquatic organisms, fishes are directly affected by uncontrolled discharge of domestic and industrial sewage, agricultural

chemicals, heavy metals, and other xenobiotics. In this sense, fishes are sentinel organisms that can be used as bioindicators of environmental stress from abiotic and biotic changes caused by pollutants. The first responses of these organisms to environmental stress are changes at the cellular and tissue levels [2,3].

Because fish gills have a large surface area in contact with water, structural modifications in gills have been widely used as indicators of environmental contamination [4]. Most teleost fishes have four pairs of gill arches. These arches are supported by a cartilage and/or bone associated with the abductor and adductor muscles, facilitating the movement of the gills. From each arch emerge primary lamellae that are subdivided into secondary lamellae, increasing the available surface area for contact with the environment [5]. The

* Corresponding author. Universidade Federal de São João Del Rei, Campus Centro-Oeste Dona Lindu, Rua Sebastião Gonçalves Coelho, 400, Chanadour, 35501-296, Divinópolis, Minas Gerais, Brazil.

E-mail address: ralph@ufsjeu.br (R.G. Thomé).

lamellae are the major sites of oxygen uptake in fishes and are responsible for both active and passive ion fluxes [6]. In addition to the lamellae, there are highly vascularized and diverse cell types in the gills, including pavement epithelial, pillar, immune, mitochondria-rich (MR), and mucous cells (MCs) [5].

Several experimental studies have evaluated gill damage induced by xenobiotics such as heavy metals and pesticides [7–9] as well as the structural and functional recovery of gills, especially the time required for such recovery after the fishes are placed into good-quality water [10–13]. Moreover, gills have been used previously as a biomarker in fishes from impacted environments [14–16]. However, the evaluation of gill recovery after tissue injury and the cellular and molecular mechanisms involved have not yet been reported.

Exposure regimes of pollutants experienced by fish are difficult to determine. Often, there is fluctuation of chemicals in river's water due to variable rates of biodegradation, as well as the physicochemical conditions and water flow rates. These factors might alter dilution levels of discharged effluents and movements of fish between habitats [17]. Chemically induced alterations in tissue histology provide a stronger indication of long-term exposure history [18]. While there are great physiological and biological differences between fishes, the morphological changes in the gills after exposure to xenobiotics or physicochemical alterations in water lead to similar tissue injuries such as hyperplasia, cell hypertrophy, and/or vascular damage, which are independent of the fish species. Moreover, the causes and consequences of these gill changes, particularly the reversibility of the alterations, are not well established.

The armored catfish *Hypostomus* is a typical benthic fish that maintains a close relationship with its environment. Once these fish live at the bottom of rivers and have a detritivorous feeding habit, they come in contact with various pollutants that tend to accumulate on river sediments [14]; these fish have thus become an excellent bioindicator. In addition to the ecological role, the armored catfish are important economically. *H. francisci* has a wide distribution along the São Francisco basin and is often caught in the Itapecerica River, a tributary of the Pará River [19,20].

Hence, we aimed to investigate the molecules linked to proliferation, survival, and cell death in a model of fish gill remodeling, from injury to recovery. For this purpose, we assessed the gill histology and immunohistochemistry in *H. francisci* obtained from a river subjected to chronic anthropic influences and after habitation in good-quality water.

2. Materials and methods

2.1. Experimental design

Thirty adult specimens of *H. francisci* were captured from the Itapecerica River in an urban area of the city of Divinópolis (20°13'09" S; 44°54'51" W and 20°07'80" S; 44°52'83" W), Southeastern Brazil, in July 2014 (dry season). On the day of sampling, the following physicochemical parameters were obtained: temperature = 26 °C, pH = 6.43, conductivity = 71 µs/cm, dissolved oxygen = 5.92 mg/L, and turbidity = 25.34 µt. The Itapecerica River receives generalized pollution from organic and industrial effluents as a result of poorly planned municipal sewage systems. A historical monitoring series (1997–2012) of the water quality of the Itapecerica River evidence a lot of thermotolerant coliforms and ammonium nitrogen, being classified as Water Quality Index (WQI) between medium and poor [21]. Fish were caught alive using casting nets, without injuring their gills. After capture, the fish were quickly carried to the laboratory in plastic tanks supplied with air and then divided into two groups (n = 15 per group). Group 1 was

euthanized with 250 mg/L benzocaine on the day of capture. Group 2 was maintained for 30 days in an aquarium with good-quality water (150 L). Dechlorinated water supply for the aquarium was provided by COPASA (Sanitation Department of the State of Minas Gerais), and the aquarium was maintained at 25 °C, with constant oxygenation, pH 6.8, and a controlled photoperiod. The fish were fed daily with commercial feed for 30 days until euthanasia with 250 mg/L benzocaine. The total length (TL) and body weight (BW) were recorded for each fish. All procedures were performed following the ethical principles established by the National Council of Animal Experimentation (CONCEA), with minimum stress to the fish. The study was approved by the ethics committee of the Universidade Federal de São João Del Rei, n° 49/2010.

2.2. Histology and immunohistochemistry

Gill samples from the right side of the fish were gently dissected and fixed in Bouin fluid. Samples were then stained with hematoxylin and eosin (HE) for routine histological analyses or with periodic acid–Schiff (PAS) and/or alcian blue (AB, pH 2.5) for the staining of carbohydrates.

For transmission electron microscopy, the samples were fixed in modified Karnovsky's solution (2.5% glutaraldehyde and 2% paraformaldehyde) in 0.1 M phosphate-buffered saline (PBS, pH 7.3) for 18–24 h at 4 °C, post-fixed in 1% osmium tetroxide and 1.5% potassium ferrocyanide for 2 h, and embedded in Epon/Araldite plastic resin. Ultrathin sections were stained with uranyl acetate and lead citrate before examination with a Tecnai G2-135 12 Spirit transmission electron microscope at 120 kV.

Histological sections of the gills were maintained in PBS; endogenous peroxidase activity was blocked by the addition of 3% hydrogen peroxide (H₂O₂) in PBS for 30 min at room temperature. The sections were subjected to antigen recovery in 10 mM sodium citrate buffer (pH 6.0) for 20 min at 100 °C. Nonspecific binding was blocked by incubation of sections in 2% bovine serum albumin (BSA) in PBS for 30 min at room temperature. The sections were incubated overnight with primary antibodies for heat-shock protein 70 (HSP70) (sc-373867; 1:1600), proliferating cell nuclear antigen (PCNA) (sc-56; 1:200), Bax (sc-526; 1:200), and inducible nitric oxide synthase (iNOS) (sc-651; 1:200) from Santa Cruz Biotechnology. The antibody reactions were visualized using the LSAB 2 System HRP Kit from Dako Cytomation (K 0675), followed by staining with diaminobenzidine (DAB) and counterstaining with hematoxylin. The negative control slide did not receive primary antibody.

2.3. Morphometry

Morphometry was performed on three fish per group using three representative gill filaments stained with HE. The filaments were photographed and divided into three equal parts, namely basal (proximal region of the primary lamella), intermediate, and apical (distal region of the primary lamella), using a light microscope coupled to Axiovision 4.8 software. For each filament, the following parameters were obtained in micrometers (µm) [22]: secondary lamellar length and width (SLL and SLW, respectively), primary lamellar width (PLW) and interlamellar distance (ID). PAS- and AB-positive cells, as well as, cells immunopositive for PCNA and iNOS were obtained by counting three representative gill filaments per fish.

2.4. Western blot

To evaluate HSP70 and Bax expression, 100 mg of gill samples from three fish per group were sonicated in

radioimmunoprecipitation assay (RIPA) buffer containing protease inhibitors [aprotinin and phenylmethylsulfonyl fluoride (PMSF)]. The homogenate was centrifuged at $15,000\times g$ for 30 min at 4°C , and the supernatant containing the proteins was used for analysis. Total protein concentrations were determined using the Bradford method [23]. An amount of protein corresponding to that present in $100\ \mu\text{g}$ of each sample was mixed with sample buffer, subjected to 10% gel electrophoresis, and subsequently transferred to a nitrocellulose membrane. After transfer, nonspecific reactions were blocked, and the membrane was incubated overnight with primary antibodies (HSP70 1:500 and Bax 1:500). The membrane was incubated for 45 min with secondary antibody conjugated with peroxidase (1:1500). The reactions were visualized by the addition of DAB in PBS containing chloronaphthol, methanol, and H_2O_2 (bands). A membrane stained with Ponceau S was used as a loading control (LC) [24,25]. All tests were performed in triplicate, and the band density obtained was estimated using Image J software. The results were expressed as band density/LC.

2.5. Statistical analysis

The results were expressed as the mean \pm standard deviation (SD) and compared between groups 1 and 2 using Student's *t*-test. The Kolmogorov–Smirnov test was used to assess the normality of data. All statistical tests were performed using Graph Pad software, INSTAT, version 3.00 (Graph Pad Software, San Diego, CA, USA). A *p* value less than 0.05 was considered statistically significant.

3. Results

The total length and body weight ranged, respectively, from 15.0 to 36.0 cm (21.5 ± 3.8) and from 37.5 to 440 g (117.07 ± 72) for G1 and from 20.5 to 25.5 cm (23.2 ± 1.7) and from 63 to 160 g (104.3 ± 31.6) for G2 (*p* > 0.05).

3.1. Structural organization of gills from *H. francisci* under two different conditions

In all the fish from group 1, the gill epithelium was stratified and consisted of several cell types, including cubic or prismatic cells lining the secondary lamellae, mucous (MCs) and mitochondria-rich cells (MRCs) (Fig. 1A and B). In the secondary lamellae, hypertrophy of the respiratory epithelium and pillar cells, complete fusion of several secondary lamellae, lifting of the epithelium, aneurysm, hyperemia, and vascular congestion were observed (Fig. 1A and B). Moreover, an interlamellar cell mass was observed throughout the length of the lamellae (Fig. 1A and B). Marked presence of MCs was observed by strong PAS and AB staining, mainly in the apical and medial regions of the lamellae, respectively (Fig. 1B, E, H). MCs were found in the apical region of primary and secondary lamellae with cytoplasm filled with electron-dense secretory granules, and the Golgi apparatus and endoplasmic reticulum were both well developed. The nucleus was euchromatic and located in the basal region of the cell (Fig. 1F). When PAS and AB stains were used together, we observed two populations of MCs in the apical region of the lamellae: PAS-positive cells and PAS-AB-positive cells (Fig. 1J). Necrosis and inflammatory infiltrate were also observed in few areas (Fig. 1A). MRCs were located at the base of the secondary lamellae, between MCs, and the cytoplasm was strongly stained with eosin (Fig. 1B). Degenerating cartilage, which supports the primary lamellae, and a dilated venous sinus filled with blood were also observed.

In the fish from group 2, the primary and secondary lamellae were lined with a simple epithelium containing pavement cells, MCs, and MRCs (Fig. 1C and D). The restoration of gill integrity was

observed, which was characterized by the appearance of interlamellar distance, absence of lamellar fusion, hypertrophy, and aneurysms in primary and secondary lamellae (Fig. 1C, G, I). Moreover, cellular debris was observed between secondary lamellae, which probably resulted from tissue remodeling (Fig. 1C). Ultrastructural analysis of the gills in the fish from group 2 showed secondary lamellae containing epithelial squamous cells with a euchromatic nucleus and cytoplasm containing mitochondria and various organelles (Fig. 1D). These cells were supported by the basement membrane. Pillar cells showed numerous, irregular extensions, which presented as an electron-dense cytoplasm associated with blood capillaries. MRCs presented as ovoid shapes with cytoplasm rich in mitochondria, endoplasmic reticulum, and electron-dense cytoplasmic inclusions (Fig. 1D). The number of PAS- or AB-positive MCs was significantly decreased in secondary and primary lamellae (Fig. 1G, I). The primary lamellae were supported by an intact cartilage without a dilated venous sinus (Fig. 1C, G, I).

3.2. Immunohistochemistry and western blot

In gills of the fish from group 1, PCNA immunolabeling was observed throughout the length of the primary lamellae (Fig. 2A and B). Several PCNA-positive cells were observed in the hypertrophy of the respiratory epithelium and in the interlamellar cell mass presents in the apical and medial regions. Moreover, PCNA-positive MRCs were noted (Fig. 2A and B). In gills of the fish from group 2, the respiratory epithelium consisted of a simple layer, did not show an interlamellar cell mass, and had scarce PCNA-positive cells (Fig. 2C).

The gill tissues of the fish from group 1, several iNOS-positive cells were dispersed throughout the primary and secondary lamellae (Fig. 2D and E). The labeled cells were associated with blood vessels of nearby pillar cell (Fig. 2E). No iNOS staining was observed in the apical interlamellar cell mass, but some iNOS staining was recorded in the medial region (Fig. 2D). There was no iNOS staining of MCs or MRCs. After 30 days, the simple respiratory epithelium of the gills showed some iNOS-stained cells, which were limited to the internal area of the secondary lamellae (Fig. 2F).

In gills of the fish from group 1, Bax staining was evident throughout the length of the primary lamellae. The labeling was cytoplasmic, without any predominant cell type (Fig. 3A and B). Apoptotic cells were observed throughout the length of the secondary lamellae (Fig. 3A). Bax-stained cells in the interlamellar cell mass were found in the apical region of the primary lamellae (Fig. 3B). Moreover, early degenerating cartilage was observed in several Bax-positive chondrocytes (Fig. 3A inset). In gills of the fish from group 2, the simple respiratory epithelium that lined the primary and secondary lamellae contained few Bax-positive cells (Fig. 3C). Interestingly, the cellular debris present in the interlamellar space was strongly Bax positive (Fig. 3D). In addition, it was possible to identify cells with a typical apoptotic morphology associated with the secondary lamellae or cell debris. These cells had an electron-dense nuclear material that characteristically aggregated along the periphery of the nuclear membrane, had lost cell–cell contact, and formed apoptotic bodies (Fig. 3E).

In gills of the fish from group 1, the cytoplasm of hypertrophic squamous cells was predominantly labeled with HSP70-positive cells throughout the length of the primary lamellae (Fig. 4A). HSP70 was also observed in pillar cells, the interlamellar cell mass, and MRCs (Fig. 4B). In the primary lamellae, strong HSP70 staining was observed in the degenerating cartilage (Fig. 4A). In gill tissues of the fish from group 2, immunostaining for HSP70 decreased

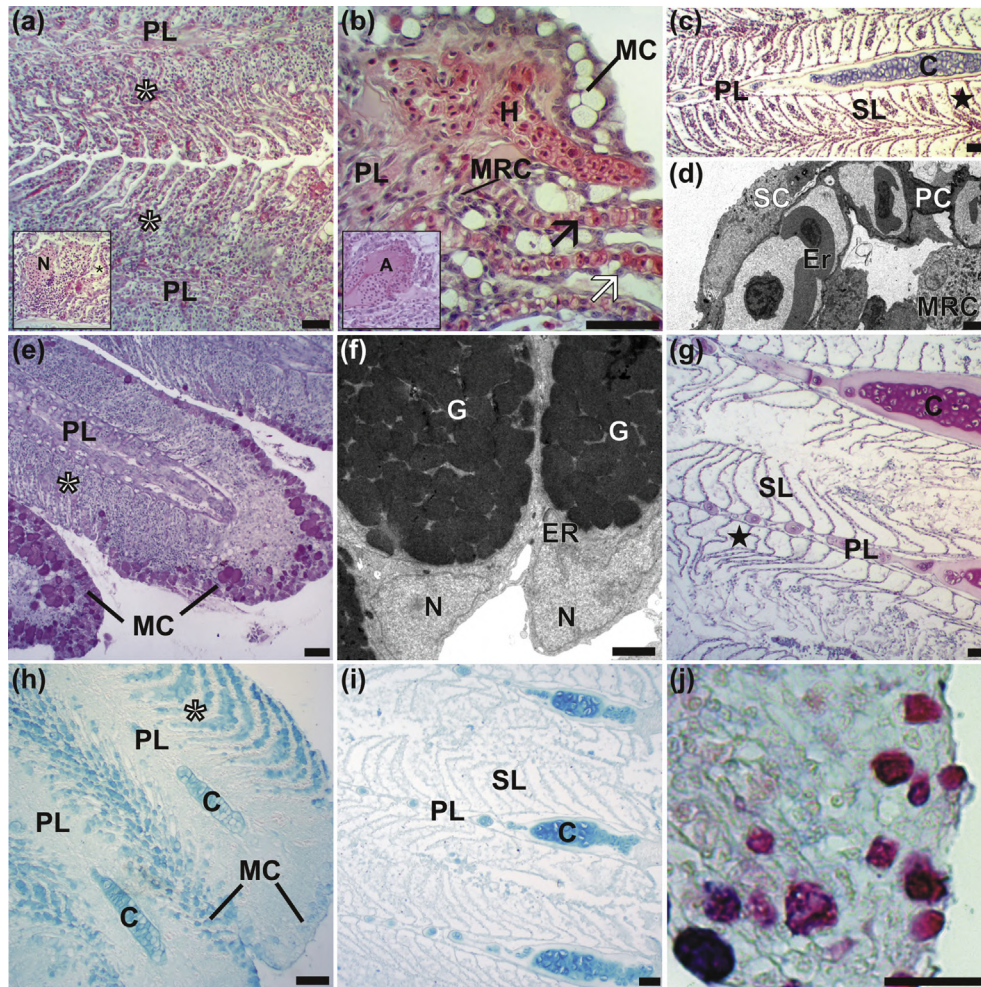


Fig. 1. Light and electron microscopy of histological sections of gills. Hematoxylin and eosin (a–c), Transmission electron microscopy (d and f), Periodic Acid-Schiff (PAS) (e and g) and alcian blue (AB) (h and i) histochemistry, PAS and AB combined in *Hyostomus francisci* (j). Gills from animals 0 h (a–b, e–f, h and j) and 30 days (c–d, g and i). a–b). Interlamellar cell mass (*), hypertrophy of the respiratory epithelium (white arrows) and pillar cells (black arrows), hyperemia (H), mitochondria-rich cells (MRC) and mucous cells (MC) in the medial and apical segments from primary lamellae (PL), respectively. c, g and i) primary lamellae (PL) with cartilage (C), cellular debris (stars) between secondary lamellae (SL) well individualized. d) secondary lamella with squamous cell (SC), pillar cells (PC) and mitochondria-rich cell (MRC). e) apical region of primary lamella with PAS-positive mucous cells organized in layers (MC). f) mucous cells with granules of secretion (G) and basal nucleus (N). h) AB-positive mucous cells were numerous in secondary lamellae and less frequent in the apical region of the primary lamellae (PL). j) PAS-positive mucous cells (magenta) and PAS + AB-positive mucous cells (purple) in the apical segment from primary lamellae showing. Erythrocyte (Er); Endoplasmatic reticulum (ER). Insert: a) Necrosis and inflammation (N) and lifting epithelial (small asterisk). b) Aneurysm (A). Bars: a, c, e, g, h and i 100 μm ; b and j = 50 μm ; d and f = 2 μm . (For interpretation of the references to colour in this figure legend, the reader is referred to the web version of this article.)

(Fig. 4C and D), but the cellular debris located in the interlamellar space was stained with HSP70 (Fig. 4D).

3.3. Gill morphometry

SLW and PLW were significantly higher in the fish from group 1 than in those from group 2. However, SLL and ID were significantly lower in the fish from group 1 fish than in those from group 2 (Table 1). The number of PAS- and AB-positive MCs was higher in gill tissues of the fish from group 1 than in those of the fish from group 2 ($p < 0.001$) (Fig. 5). On the other hand, the number of PAS-positive MCs was higher than the number of AB-positive MCs in gill tissues of the fish from group 1. The number of PCNA- and iNOS-positive cells was higher in the fish from group 1 fish than in those from group 2 ($p < 0.001$) (Fig. 5).

Densitometric analysis of western blot bands was performed for Bax (Fig. 3F and G) and HSP70 (Fig. 4E and F); the results revealed that these proteins were significantly higher in gill tissues of the fish from group 1 than in those of the fish from group 2 ($p < 0.001$).

4. Discussion

The present study showed, for the first time, the immunolocalization of PCNA, iNOS, Bax, and HSP70 during gill remodeling in a fish species caught in a human-perturbed river and subsequently placed into good-quality water. Both molecular and cellular mechanisms from injury to recovery were proposed, with a balance between survival and cell death signals being essential for determining the gill structure (Fig. 6).

Benthic fishes such as *H. francisci* tend to spend less energy and thus require a lesser amount of oxygen than nektonic fishes, leading to morphological differences between their gills [26]. However, it is common to see similar descriptions of gill changes in both benthic and nektonic fishes [14]. This is because gill remodeling is related to oxygen demand and can be considered a defense response that leads to a decrease in the entry of toxic compounds through the gills [27]. Histological changes such as lamellar fusion, hypertrophy of the lamellar epithelium, and increased numbers of MCs were observed in the gills of *H. francisci* from group 1; similar

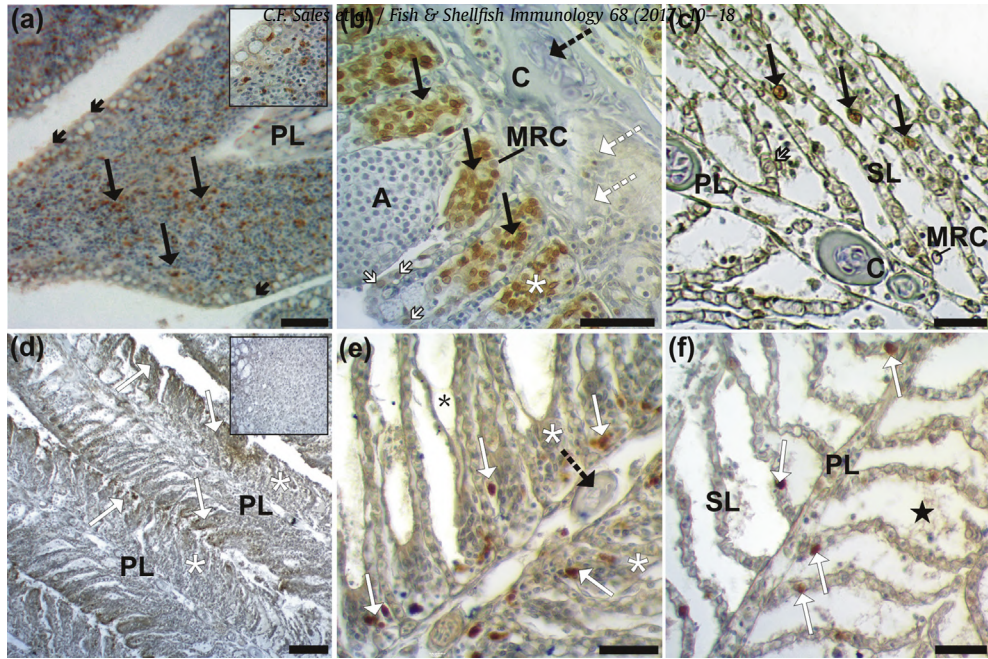


Fig. 2. a-f Immunohistochemical reactions for PCNA (a–c) and iNOS (d–f) in *Hypostomus francisci*. Gills from animals 0 h (a–b and d–e) and 30 days (c and f) evidencing PCNA-positive cells (black arrows) in the apical and medial regions from primary lamellae (PL) and iNOS-positive cells (white arrows) in the medial region from primary lamellae (PL). Observe a few PCNA-positive cells in gills from animals of 30 days (c), PCNA-positive mucous cells (insert a) and absence of iNOS-positive cells in the apical region from primary lamellae (insert d). Interlamellar cell mass (*); aneurysm (A); cartilage (C); chondrocytes (discontinuous black arrows); hypertrophy of the respiratory epithelium (white arrows small); cartilage in degeneration (discontinuous white arrows); lifting epithelial (small asterisk); mitochondria-rich cells (MRC); cellular debris (stars); individualized secondary lamellae (SL). Bars: a, c and d 100 μ m; b, e and f = 50 μ m.

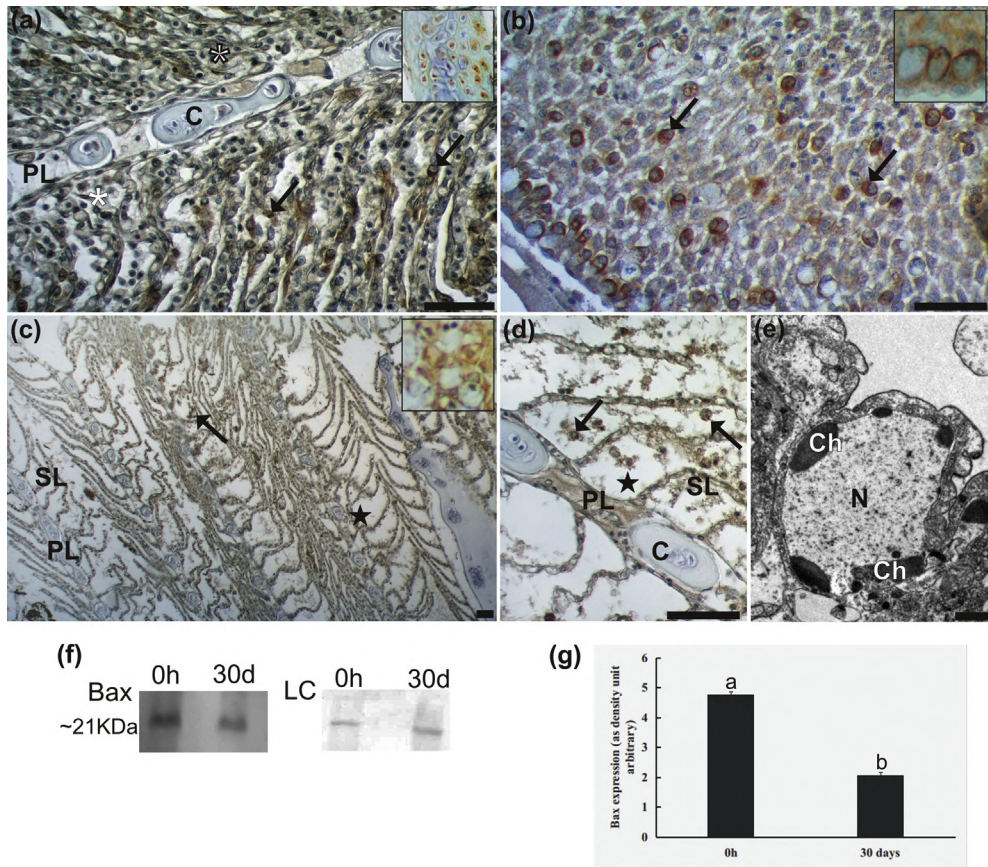


Fig. 3. a-d Immunohistochemical reactions for Bax; e) transmission electron microscopy; f) Representative image of Western blot and a Ponceau S staining for loading control (LC); g) Quantification of Bax expression by densitometry using bands of Western blot in *Hypostomus francisci*. a-b) Medial and apical region from primary lamellae respectively, from animals 0 h showing Bax-positive cells (black arrows), c-d) Gills from animals 30 days showing presenting few Bax-positive cells. e) apoptotic cell in secondary lamella from 30 days. Insert: a) Bax-positive chondrocytes in primary lamellae. b) Bax-positive mucous cells present in apical region from primary lamella. c) Bax-positive cells in apical region from primary lamellae. Interlamellar cell mass (*), primary lamellae (PL), cartilage (C), cellular debris (stars), individualized secondary lamellae (SL), nucleus (N), condensed chromatin (Ch). Bars: a-b and d = 50 μ m; c = 100 μ m; e = 2 μ m. Different letters indicate $p < 0.05$.

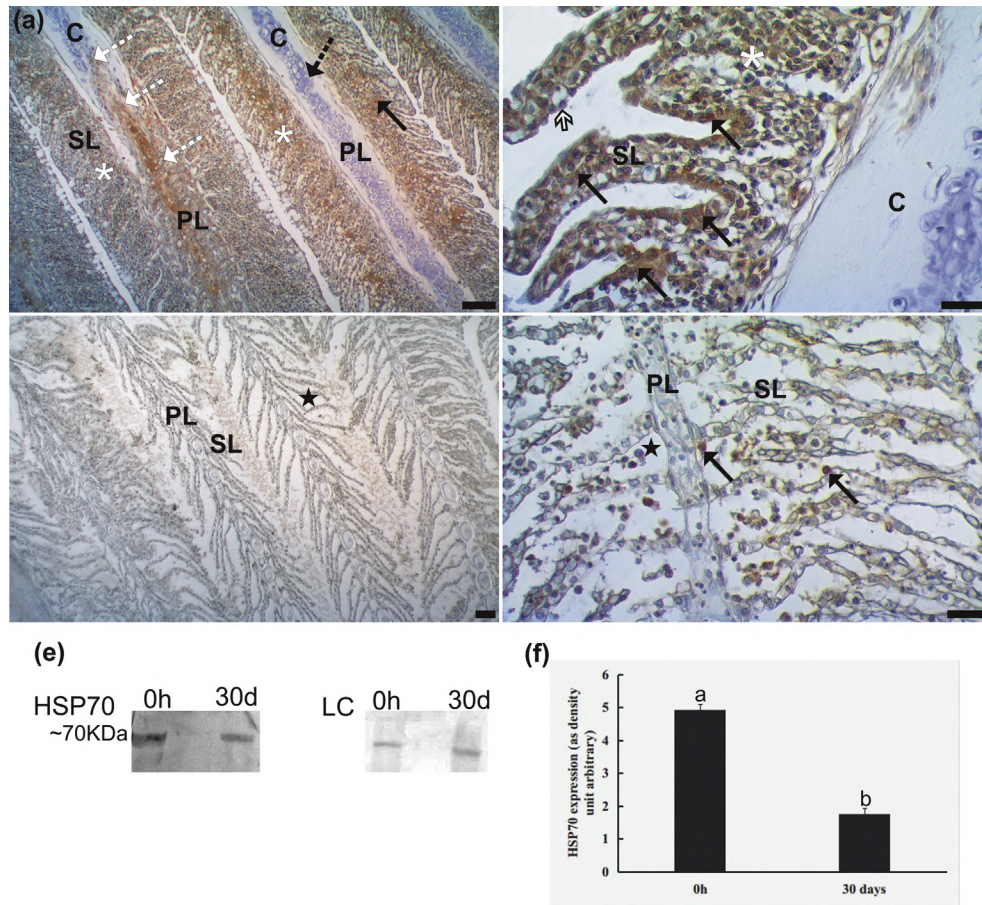


Fig. 4. a-d Immunohistochemical reactions for HSP70; e) Representative image of Western blot and a Ponceau S staining for loading control (LC); f) Quantification of HSP70 expression by densitometry using the bands of Western blot in *Hypostomus francisci*. a-b) Gills from animals 0 h showing HSP70-positive cells (black arrows), interlamellar cell mass (*), primary lamellae (PL) with chondrocytes (discontinuous black arrows), hypertrophy of the respiratory epithelium (small white arrows) and cartilage (C) in degeneration (discontinuous white arrows). c-d) Gills from animals 30 days with cellular debris (stars) between secondary lamellae (SL) well individualized. Bars: a and c 100 μm ; b and d = 50 μm . Different letters indicate $p < 0.05$.

Table 1

Morphometry of the gill structures of each filament region: secondary lamellar length (SLL) and width (SLW), primary lamellar width (PLW) and interlamellar distance (ID).

Groups	Lamellar region	SLL	SLW	ID	PLW
G 1	Apical	127.5 \pm 28.7	25.3 \pm 5.7	15.7 \pm 6.3	207.2 \pm 33.2
	Intermediate	129.9 \pm 23.4	26.2 \pm 5.3	15.6 \pm 3.5	147.6 \pm 32.7
	Basal	124.0 \pm 27.5	25.3 \pm 5.2	15.7 \pm 6.3	128.11 \pm 28.3
G 2	Apical	194.9 \pm 37.8*	7.6 \pm 1.8*	36.9 \pm 6.1*	88.7 \pm 24.5*
	Intermediate	200.3 \pm 24.7*	7.8 \pm 2.0*	35.4 \pm 3.2*	32.0 \pm 9.1*
	Basal	184.0 \pm 28.1*	7.3 \pm 1.2*	36.7 \pm 6.2*	28.3 \pm 4.8*

Data are expressed as mean \pm SD in micrometers (μm), (*) significant difference between G1 and G2, $p < 0.05$.

results were also observed in *Hypotomus auroguttatus* [14]. In nektonic fishes, similar findings were observed in gills of *Squalius vardarensis* captured from three polluted rivers in Macedonia [28] as well as in *Astyanax fasciatus* and *Cyanocharax alburnus*; all these results correlated with environmental degradation [29]. Thus, it is feasible that the histological changes observed in gills follow a common induction pattern that is independent of the type of fish and stressor agent.

The partial or total fusion of the secondary lamellae observed in the medial and apical regions of gills of *H. francisci* from group 1 led to an increase in the thickness of the primary and secondary lamellae and a consequent decrease in ID in these fish. The increased thickness of gill filaments can act as a barrier to xenobiotics present in water since this process could increase the distance between the

capillary and the lamellar surface, reducing the absorption of pollutants [30]. The observed lamellar fusion was associated with hyperplasia (cell proliferation) that results in the reduction of the area in contact with the environmental stressor as well as the formation of an interlamellar cell mass. PCNA is a pleiotropic protein that functions in several vital cellular processes, including chromatin remodeling, DNA repair, and cell cycle control, by interacting with different enzymes and regulatory proteins [31–33]; it is a molecular marker for cellular proliferation [34] and has been used in studies of morphological changes in gills [7]. PCNA immunoreactivity was observed in epithelial cells, MRCs, and MCs; immunopositivity for PCNA was also largely detected in interlamellar cell masses in both medial and apical regions in *H. francisci* from group 1. Interlamellar cell masses are composed of undifferentiated cells [27], justifying

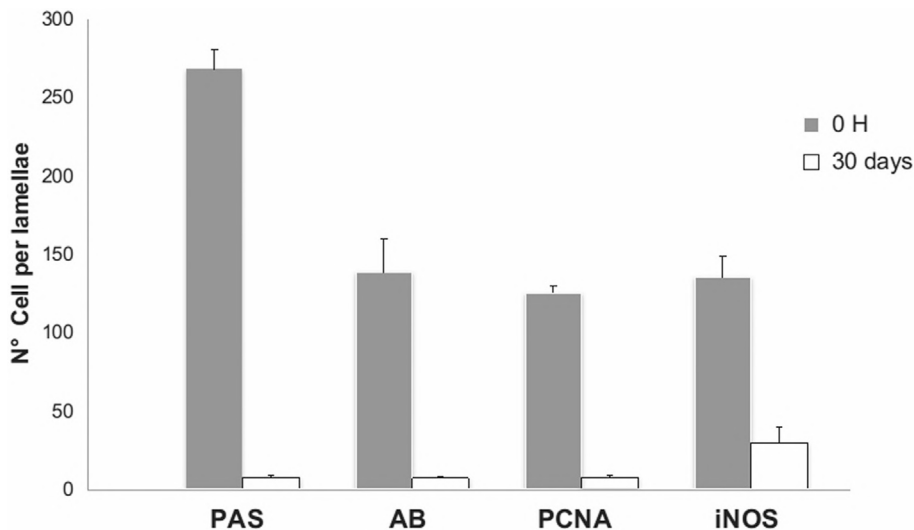


Fig. 5. Number of cells per lamellae stained by periodic acid Schiff (PAS), alcian blue (AB), PCNA and iNOS in gills from animals 0 h and 30 days in *Hypostomus francisci*. Different letters indicate statistical difference for the same stain with $p < 0.05$.

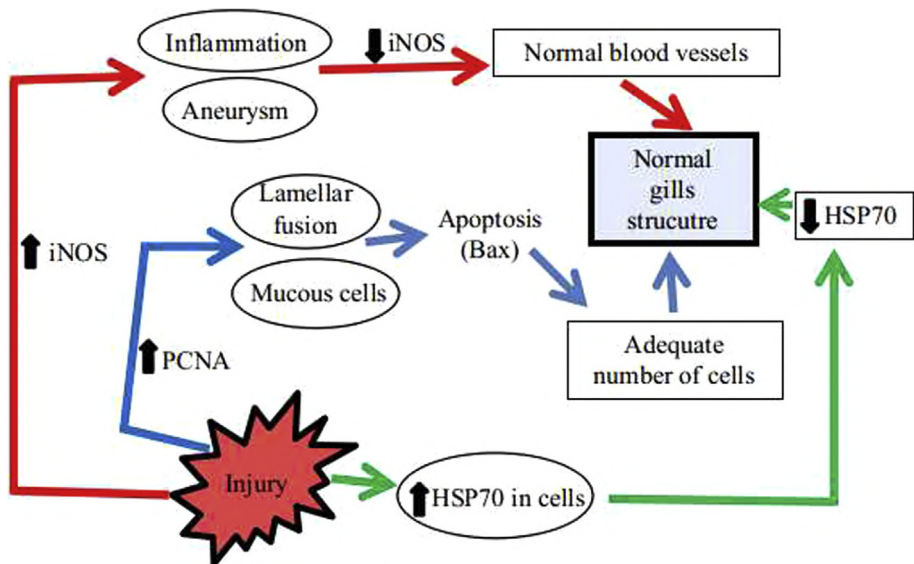


Fig. 6. Proposed model for gills structure recovery. The arrows with the same color color guide the pathway from injury until the normal histology. During the injury, the cell proliferation and the signals of blood vessels change are the primary response, increasing PCNA and iNOS, respectively. The Bax levels support the apoptosis pathway as an important mechanism to lead to normal morphology of gills during the remodeling. At final gill recovery, HSP70 expression decrease. (For interpretation of the references to colour in this figure legend, the reader is referred to the web version of this article.)

their high proliferative rate and supporting the epithelial renewal and proliferation of new MRCs and MCs. In fact, several authors have reported increases in the numbers of these cells caused by exposure to toxins [8,35,36]; however, whether the origin of these histological findings (increase in MRC and MC) is cell division or differentiation remains unclear. Given the functional specialization of MRCs and MCs, it is more likely that PCNA found in these cells is due to DNA repair and cell survival.

Inflammatory processes in gill lamellae could also have contributed to the lamellar remodeling in this study. Nitric oxide (NO) is an important intra- and intercellular signaling molecule involved in the regulation of diverse physiological and pathophysiological mechanisms in cardiovascular, nervous, and immunological systems. NO regulates the vascular tone, inflammatory process, and ion balance in both mammals and fishes [7,37]. It is

also synthesized inside cells by the action of NOS in the presence of oxygen and arginine. Three distinct isoforms of NOS have been described in vertebrates: neuronal NOS (nNOS, iNOS), and endothelial NOS (eNOS). iNOS is a high-output, Ca^{2+} -independent enzyme whose expression can be induced in a wide range of cells and tissues by cytokines and other agents [38]. In this sense, inflammation and most vascular abnormalities observed in gills are likely related to an increase in the number of iNOS-positive cells. Severe vascular disorders such as aneurysms and congestions were frequently observed in *H. francisci* from group 1. Gill aneurysm is a severe pathology resulting from the collapse of the pillar cell system; it affects the vascular integrity and causes disruptions of the lamellar epithelium and subsequent hemorrhage [39]. The occurrence of aneurysms is commonly described in the gills of fishes exposed to stressors [29,40,41], but it could be attributed to iNOS

expression. The possibility of recovery after a gill aneurysm remains controversial. A lamellar aneurysm is always related to a serious and often irreversible pathology in fish gills [14,42,43]. However, in the present study, when fish were placed into good-quality water, we observed a decrease in iNOS expression, with full recovery of lamellar aneurysms after 30 days.

Apoptosis, or programmed cell death, is triggered when cells are exposed to physiological changes or pathogenic or cytotoxic stimuli as well as during tissue homeostasis. Apoptosis is highly regulated by signaling pathways controlled by pro- and antiapoptotic proteins. Members of the Bcl-2 family are important regulators of apoptosis; they are cellular homologs that are either proapoptotic (Bax, Bik, and Bid) or antiapoptotic (Bcl-2 and Bcl-XL) [44]. Bax activates apoptosis under conditions such as growth factor deprivation, DNA damage, and hypoxia [45]. In the present study, the high Bax expression observed in gills of the fish from group 1 occurred in various cell types along the lamellae, as a result of two possible activation mechanisms: 1) cellular damage triggered by environmental stress or 2) control of cell proliferation. The high rate of apoptosis observed in the gills of the fish from group 1 may be related to potential DNA damage caused by direct exposure to contaminants present in the river. Interestingly, Bax expression was observed in cartilaginous cells, supporting the idea of cartilaginous degeneration. In teleost fishes, a significant increase in apoptosis has been used as a biomarker of aquatic environment after exposure to different types of xenobiotics known to damage the liver and gills of aquatic animals [46–49]. However, after 30 days in good-quality water, apoptosis was stimulated in an appropriate number of cells to stimulate gill structure recovery.

Cellular hypertrophy generally indicates an increase in cellular activity and is a very common morphological change related to gill damage; it leads to thickening of the epithelium [27]. Cells respond to stress by adaptive changes that limit or repair damage, thereby preventing cell death [50]. In this sense, the increase in HSP70 expression observed in the lamellar epithelium of the fish from group 1 can be related to protein synthesis required for the maintenance of cell viability and inhibition of apoptosis. HSP70 is known to play an important role in the response to cellular stress. HSP70 synthesis may increase in response to heat shock [51] and various stressors, including hyperosmolarity [52], ischemia [53], and hypoxia [54]. A high expression of HSP70 has been widely used as a biomarker for cellular stress in various species exposed to ambient contamination or specific genotoxic agents [55–60]. In the present study, after the fish were placed in good-quality water, HSP70 expression levels decreased, suggesting a reduction in cellular stress during gill recovery.

In conclusion, gill tissues change under conditions of poor water quality and can be used as a biomarker of nonpoint sources of pollution, as we observed in *H. francisci* from the Itapecerica River. Moreover, the results of the present study suggest that gill tissue recovery is possible if the fishes are maintained in good-quality water, indicating the importance of the conservation of aquatic environments.

Conflict of interest

The authors declare that they have no conflict of interest.

Ethical approval

All procedures performed in studies involving animals were in accordance with the ethical standards of the institution or practice at which the studies were conducted and was approved by the ethic committee of the Universidade Federal de São João Del Rei, nº 49/2010.

Acknowledgments and funding information


We would like to thank the Fundação de Amparo à Pesquisa de Minas Gerais (FAPEMIG-CVZ - APQ-02180-14) and the Conselho Nacional de Desenvolvimento Científico e Tecnológico (CNPq-479535/2013-2) for financial support. The authors also thank the Universidade Federal de São João Del Rei for equipment and undergraduate students scholarship.

References

- [1] M.N. Moore, M.H. Depledge, J.W. Readman, D.R. Paul Leonard, An integrated biomarker-based strategy for ecotoxicological evaluation of risk in environmental management, *Mutat. Res. Fundam. Mol. Mech. Mutagen* 552 (2004) 247–268, <http://dx.doi.org/10.1016/j.mrfmmm.2004.06.028>.
- [2] D.E. Facey, V.S. Blazer, M.M. Gasper, C.L. Turcotte, Using fish biomarkers to monitor improvements in environmental quality, *J. Aquat. Anim. Health* 17 (2005) 265–266, <http://dx.doi.org/10.1577/H04-055.1>.
- [3] T.H. Hutchinson, G.T. Ankley, H. Segner, C.R. Tyler, Screening and testing for endocrine disruption in fish-biomarkers as “signposts,” not “traffic lights,” in risk assessment, *Environ. Health Perspect.* 114 (2006) 106–114, <http://dx.doi.org/10.1289/ehp.8062>.
- [4] P.A. Corbett, C.K. King, J.S. Stark, J.A. Mondon, Direct evidence of histopathological impacts of wastewater discharge on resident Antarctic fish (*Trematomus bernacchii*) at Davis Station, East Antarctica, *Mar. Pollut. Bull.* 87 (2014) 48–56, <http://dx.doi.org/10.1016/j.marpolbul.2014.08.012>.
- [5] F. Genten, E. Terwinghe, A. Danguy, *Atlas of Fish Histology*, Science Publishers, 2009, p. 215.
- [6] G.E. Nilsson, A. Dymowska, J.A.W. Stecyk, New insights into the plasticity of gill structure, *Respir. Physiol. Neurobiol.* (2012) 214–222, <http://dx.doi.org/10.1016/j.resp.2012.07.012>.
- [7] E. Brunelli, A. Mauceri, M. Maisano, I. Bernabo, A. Giannetto, E. De Domenico, B. Corapi, S. Tripepi, S. Fasulo, Ultrastructural and immunohistochemical investigation on the gills of the teleost, *Thalassoma pavo* L., exposed to cadmium, *Acta Histochem.* 113 (2011) 201–213, <http://dx.doi.org/10.1016/j.acthis.2009.10.002>.
- [8] L. Marcon, D.S. Lopes, A.H. Mouteer, A.M.A. Goulart, M.V. Leandro, L. dos Anjos Benjamin, Pathological and histometric analysis of the gills of female *Hypphessobrycon eques* (Teleostei: Characidae) exposed to different concentrations of the insecticide Dimilin®, *Ecotoxicol. Environ. Saf.* 131 (2016) 135–142, <http://dx.doi.org/10.1016/j.ecoenv.2016.05.016>.
- [9] N. Kumar, R. Sharma, G. Tripathi, K. Kumar, R.S. Dalvi, G. Krishna, Cellular metabolic, stress, and histological response on exposure to acute toxicity of endosulfan in Tilapia (*Oreochromis mossambicus*), *Environ. Toxicol.* 31 (2016) 106–115, <http://dx.doi.org/10.1002/tox.22026>.
- [10] C.C.C. Cerqueira, M.N. Fernandes, Gill tissue recovery after copper exposure and blood parameter responses in the tropical fish *Prochilodus scrofa*, *Ecotoxicol. Environ. Saf.* 52 (2002) 83–91, <http://dx.doi.org/10.1006/eesa.2002.2164>.
- [11] M.R. Narra, K. Rajender, R.R. Reddy, U.S. Murty, G. Begum, Insecticides induced stress response and recuperation in fish: biomarkers in blood and tissues related to oxidative damage, *Chemosphere* 168 (2017) 350–357, <http://dx.doi.org/10.1016/j.chemosphere.2016.10.066>.
- [12] T.O. Nilsen, L.O.E. Ebbesson, S.O. Handeland, F. Kroglund, B. Finstad, A.R. Angotzi, S.O. Stefansson, Atlantic salmon (*Salmo salar* L.) smolts require more than two weeks to recover from acidic water and aluminium exposure, *Aquat. Toxicol.* 142 (2013) 33–44, <http://dx.doi.org/10.1016/j.aquatox.2013.07.016>.
- [13] G.L. Galvan, J.R. Lirola, K. Felisbino, T. Vicari, C.I. Yamamoto, M.M. Cestari, Genetic and hematologic endpoints in *Astyanax altiparanae* (Characidae) after exposure and recovery to water-soluble fraction of gasoline (WSFG), *Bull. Environ. Contam. Toxicol.* 97 (2016) 63–70, <http://dx.doi.org/10.1007/s00128-016-1816-5>.
- [14] A.A. Nascimento, F.G. Araújo, I.D. Gomes, R.M.M. Mendes, A. Sales, Fish gills alterations as potential biomarkers of environmental quality in a eutrophized Tropical River in South-Eastern Brazil, *J. Vet. Med. Ser. C Anat. Histol. Embryol.* 41 (2012) 209–216, <http://dx.doi.org/10.1111/j.1439-0264.2011.01125.x>.
- [15] M.S. Procópio, H.J. Ribeiro, L.A. Pereira, G.A. Oliveira Lopes, A.C. Santana Castro, E. Rizzo, Y. Sato, R. Castro Russo, J.D. Corrêa, Sex-response differences of immunological and histopathological biomarkers in gill of *Prochilodus argenteus* from a polluted river in southeast Brazil, *Fish Shellfish Immunol.* 39 (2014) 108–117, <http://dx.doi.org/10.1016/j.fsi.2014.04.010>.
- [16] D.M.S. Santos, M.R.S. Melo, D.C.S. Mendes, I.K.B.S. Rocha, J.P.L. Silva, S.M. Cantanhêde, P.C. Meletti, Histological changes in gills of two fish species as indicators of water Quality in Jansen Lagoon (São Luís, Maranhão State, Brazil), *Int. J. Environ. Res. Public Health* 11 (2014) 12927–12937, <http://dx.doi.org/10.3390/ijerph111212927>.
- [17] B. Vrana, G.A. Mills, I.J. Allan, E. Dominiak, K. Svensson, J. Knutsson, G. Morrison, R. Greenwood, Passive sampling techniques for monitoring pollutants in water, *TrAC Trends Anal. Chem.* 24 (2005) 845–868, <http://dx.doi.org/10.1016/j.trac.2005.06.006>.

- [18] P.B. Hamilton, I.G. Cowx, M.F. Oleksiak, A.M. Griffiths, M. Grahn, J.R. Stevens, G.R. Carvalho, E. Nicol, C.R. Tyler, Population-level consequences for wild fish exposed to sublethal concentrations of chemicals: a critical review, *Fish Fish.* 17 (2016) 545–566, <http://dx.doi.org/10.1111/faf.12125>.
- [19] F.F.T. Domingos, R.G. Thomé, R.I.M.A. Ribeiro, H.A.V. Souza, H.B. Santos, Assessment of fish assemblage in an urban system, Itaipu River, upper São Francisco River basin, Divinópolis, Minas Gerais, Brazil, *Check List* 9 (2013) 482–486.
- [20] C.F. Sales, F.F.T. Domingos, L.S. Brighenti, R.I.M.A. Ribeiro, H.B. Santos, R.G. Thome, Biological variables of *Hyposomus francisci* (Siluriformes: Loricariidae) from Itaipu River, Minas Gerais state, Brazil, *An. Acad. Bras. Cienc.* 88 (2016) 1603–1614, <http://dx.doi.org/10.1590/0001-3765201620150513>.
- [21] Instituto Mineiro de Gestão das Águas, *Identificação de municípios com condição crítica para a qualidade de água na bacia do rio Paraopeba*, 2013, p. 41.
- [22] V. Nero, A. Farwell, A. Lister, G. Van Der Kraak, L.E.J. Lee, T. Van Meer, M.D. MacKinnon, D.G. Dixon, Gill and liver histopathological changes in yellow perch (*Perca flavescens*) and goldfish (*Carassius auratus*) exposed to oil sands process-affected water, *Ecotoxicol. Environ. Saf.* 63 (2006) 365–377, <http://dx.doi.org/10.1016/j.ecoenv.2005.04.014>.
- [23] M.M. Bradford, protein utilizing the principle of protein-dye binding, *Anal. Biochem.* 72 (1976) 248–254, [http://dx.doi.org/10.1016/0003-2697\(76\)90527-3](http://dx.doi.org/10.1016/0003-2697(76)90527-3).
- [24] J.E. Gilda, A.V. Gomes, Stain free total protein staining is a superior loading control to β -actin for western blots, *Anal. Biochem.* 440 (2013) 186–188, <http://dx.doi.org/10.1016/j.ab.2013.05.027>.
- [25] A. Vigelso, R. Dybbøe, C.N. Hansen, F. Dela, J.W. Helge, A. Guadalupe Grau, GAPDH and β -actin protein decreases with aging, making Stain-Free technology a superior loading control in Western blotting of human skeletal muscle, *J. Appl. Physiol.* 118 (2015) 386–394, <http://dx.doi.org/10.1152/jappphysiol.00840.2014>.
- [26] J. Söllid, G.E. Nilsson, Plasticity of respiratory structures - adaptive remodeling of fish gills induced by ambient oxygen and temperature, *Respir. Physiol. Neurobiol.* 154 (2006) 241–251, <http://dx.doi.org/10.1016/j.resp.2006.02.006>.
- [27] E.A. Almeida, C.A. Oliveira Ribeiro, in: *Pollution and Fish Health in Tropical Ecosystems*, vol. 1, CRC Press, Boca Raton, FL, 2014, p. 391.
- [28] J. Barišić, Z. Dragan, S. Ramani, V. Filipović Marijić, N. Krasnići, R. Čož-Rakovac, V. Kostov, K. Rebok, M. Jordanova, Evaluation of histopathological alterations in the gills of Vardar chub (*Squalius vardarensis* Karaman) as an indicator of river pollution, *Ecotoxicol. Environ. Saf.* 118 (2015) 158–166, <http://dx.doi.org/10.1016/j.ecoenv.2015.04.027>.
- [29] F. Flores-Lopes, a T. Thomaz, Histopathologic alterations observed in fish gills as a tool in environmental monitoring, *Braz. J. Biol.* 71 (2011) 179–188, <http://dx.doi.org/10.1590/S1519-698420111000100026>.
- [30] M.M.P. Camargo, C.B.R. Martinez, Histopathology of gills, kidney and liver of a Neotropical fish caged in an urban stream, *Neotrop. Ichthyol.* 5 (2007) 327–336, <http://dx.doi.org/10.1590/S1679-62252007000300013>.
- [31] R. Bravo, R. Frank, P.A. Blundell, H. Macdonald-Bravo, Cyclin/PCNA is the auxiliary protein of DNA polymerase- δ , *Nature* 326 (1987) 515–517, <http://dx.doi.org/10.1038/326515a0>.
- [32] M.K.K. Shivji, M.K. Kenny, R.D. Wood, Proliferating cell nuclear antigen is required for DNA excision repair, *Cell* 69 (1992) 367–374, [http://dx.doi.org/10.1016/0092-8674\(92\)90416-A](http://dx.doi.org/10.1016/0092-8674(92)90416-A).
- [33] D.W. Li, G.R. Li, B.L. Zhang, J.J. Feng, H. Zhao, Damage to dopaminergic neurons is mediated by proliferating cell nuclear antigen through the p53 pathway under conditions of oxidative stress in a cell model of Parkinson's disease, *Int. J. Mol. Med.* 37 (2015) 429–435, <http://dx.doi.org/10.3892/ijmm.2015.2430>.
- [34] R.G. Thomé, F.F.T. Domingos, H.B. Santos, P.M. Martinelli, Y. Sato, E. Rizzo, N. Bazzoli, Apoptosis, cell proliferation and vitellogenesis during the folliculogenesis and follicular growth in teleost fish, *Tissue Cell* 44 (2012) 54–62, <http://dx.doi.org/10.1016/j.tice.2011.11.002>.
- [35] K. Kaur, S. Kaur, A. Kaur, Scanning electron microscopic observations of Basic Violet-1 induced changes in the gill morphology of *Labeo rohita*, *Environ. Sci. Pollut. Res.* 23 (2016) 16579–16588, <http://dx.doi.org/10.1007/s11356-016-6764-4>.
- [36] J.E. Correia, C.A. Christoforetti, A.C.C. Marcato, J.F.U. Marinho, C.S. Fontanetti, Histopathological analysis of tilapia gills (*Oreochromis niloticus* Linnaeus, 1758) exposed to sugarcane vinasse, *Ecotoxicol. Environ. Saf.* 135 (2017) 319–326, <http://dx.doi.org/10.1016/j.ecoenv.2016.10.004>.
- [37] F. Aktan, iNOS-mediated nitric oxide production and its regulation, *Life Sci.* (2004) 639–653, <http://dx.doi.org/10.1016/j.lfs.2003.10.042>.
- [38] H. Kleinert, A. Pautz, K. Linker, P.M. Schwarz, Regulation of the expression of inducible nitric oxide synthase, *Eur. J. Pharmacol.* 500 (2004) 255–266, <http://dx.doi.org/10.1016/j.ejphar.2004.07.030>.
- [39] D.E. Hinton, D.J. Laurén, Integrative histopathological approaches to detecting effects of environmental stressors on fishes, *Am. Fish Soc. Symp. Am. Fish* 8 (1990) 51–66.
- [40] A. Fontáinhas-Fernandes, A. Luzio, S. Garcia-Santos, J. Carrola, S. Monteiro, Gill histopathological alterations in Nile tilapia, *Oreochromis niloticus* exposed to treated sewage water, *Braz. Arch. Biol. Technol.* 51 (2008) 1057–1063, <http://dx.doi.org/10.1590/S1516-89132008000500023>.
- [41] S. Subashkumar, M. Selvanayagam, First report on: acute toxicity and gill histopathology of fresh water fish *Cyprinus carpio* exposed to Zinc oxide (ZnO) nanoparticles, *Int. J. Sci. Res. Publ.* 4 (2014) 10–13, <http://www.ijsrp.org/research-paper-0314/ijsrp-p27123.pdf>.
- [42] S.M. Cantanhêde, A.M. Medeiros, F.S. Ferreira, J.R.C. Ferreira, L.M.C. Alves, M.V.J. Cutrim, D.M.S. Santos, Uso de biomarcador histopatológico em brânquias de *Centropomus undecimalis* (Bloch, 1972) na avaliação da qualidade da água do Parque Ecológico Laguna da Jansen, São Luís-MA, Arq. Bras. Med. Vet. E Zootec. 66 (2014) 593–601, <http://dx.doi.org/10.1590/1678-41626348>.
- [43] J.S. Castro, J.S. Silva, L.C. Freitas, R.N.F. Carvalho-Neta, Biomarcadores histopatológicos na espécie *Hoplias malabaricus* (Pisces, Osteichthyes, Erythrinidae) em uma Unidade de Conservação de São Luís (MA), Arq. Bras. Med. Vet. E Zootec. 66 (2014) 1687–1694, <http://dx.doi.org/10.1590/1678-7414>.
- [44] S. Cory, D.C.S. Huang, J.M. Adams, The Bcl-2 family: roles in cell survival and oncogenesis, *Oncogene* 22 (2003) 8590–8607, <http://dx.doi.org/10.1038/sj.onc.1207102>.
- [45] E. Kratz, P.M. Eimon, K. Mukhyala, H. Stern, J. Zha, A. Strasser, R. Hart, A. Ashkenazi, Functional characterization of the Bcl-2 gene family in the zebrafish, *Cell Death Differ.* 13 (2006) 1631–1640, <http://dx.doi.org/10.1038/sj.cdd.4402016>.
- [46] G. Piechotta, M. Lacorn, T. Lang, U. Kammann, T. Simat, H.S. Jenke, H. Steinhart, Apoptosis in dab (*Limanda limanda*) as possible new biomarker for anthropogenic stress, *Ecotoxicol. Environ. Saf.* 42 (1999) 50–56, <http://dx.doi.org/10.1006/eesa.1998.1725>.
- [47] L.P. Weber, D.M. Janz, Effect of beta-naphthoflavone and dimethylbenz[a]anthracene on apoptosis and HSP70 expression in juvenile channel catfish (*Ictalurus punctatus*) ovary, *Aquat. Toxicol.* 54 (2001) 39–50, [http://dx.doi.org/10.1016/S0166-445X\(00\)00179-X](http://dx.doi.org/10.1016/S0166-445X(00)00179-X).
- [48] L.P. Weber, Y. Kiparissis, G.S. Hwang, A.J. Niimi, D.M. Janz, C.D. Metcalfe, Increased cellular apoptosis after chronic aqueous exposure to nonylphenol and quercetin in adult medaka (*Oryzias latipes*), *Comp. Biochem. Physiol. C Toxicol. Pharmacol.* 131 (2002) 51–59, [http://dx.doi.org/10.1016/S1532-0456\(01\)00276-9](http://dx.doi.org/10.1016/S1532-0456(01)00276-9).
- [49] A. Topal, M. Atamanalp, E. Oruç, M. Kirici, E.M. Kocaman, Apoptotic effects and glucose-6-phosphatase dehydrogenase responses in liver and gill tissues of rainbow trout treated with chlorpyrifos, *Tissue Cell* 46 (2014) 490–496, <http://dx.doi.org/10.1016/j.tice.2014.09.001>.
- [50] D.D. Mosser, a W. Caron, L. Bourget, C. Denis-Larose, B. Massie, Role of the human heat shock protein HSP70 in protection against stress-induced apoptosis, *Mol. Cell. Biol.* 17 (1997) 5317–5327, <http://dx.doi.org/10.1128/MCB.17.9.5317>.
- [51] G.K. Iwama, P.T. Thomas, R.B. Forsyth, M.M. Vijayan, Heat shock protein expression in fish, *Rev. Fish Biol. Fish* 8 (1998) 35–56.
- [52] R. Oehler, M. Zellner, B. Hefel, G. Weingartmann, A. Spittler, H.M. Struse, E. Roth, Influence of heat shock on cell volume regulation: protection from hypertonic challenge in a human monocyte cell line, *FASEB J.* 12 (1998) 553–560, <http://www.scopus.com/inward/record.uri?eid=2-s2.0-0031953857&partnerID=tZotx3y1>.
- [53] B.M. Sanders, J. Nguyen, L.S. Martin, S.R. Howe, S. Coventry, Induction and subcellular localization of two major stress proteins in response to copper in the fathead minnow *Pimephales promelas*, *Comp. Biochem. Physiol. Part C Comp. Comp.* 112 (1995) 335–343, [http://dx.doi.org/10.1016/0742-8413\(95\)02029-2](http://dx.doi.org/10.1016/0742-8413(95)02029-2).
- [54] E. Padmini, J. Tharani, Heat-shock protein 70 modulates apoptosis signal-regulating kinase 1 in stressed hepatocytes of *Mugil cephalus*, *Fish Physiol. Biochem.* 40 (2014) 1573–1585, <http://dx.doi.org/10.1007/s10695-014-9949-0>.
- [55] J.L. Yoo, D.M. Janz, Tissue-specific HSP70 levels and reproductive physiological responses in fishes inhabiting a metal-contaminated creek, *Arch. Environ. Contam. Toxicol.* 45 (2003) 110–120, <http://dx.doi.org/10.1007/s00244-002-0109-7>.
- [56] Y. Wang, J. Xu, L. Sheng, Y. Zheng, Field and laboratory investigations of the thermal influence on tissue-specific Hsp70 levels in common carp (*Cyprinus carpio*), *Comp. Biochem. Physiol. A Mol. Integr. Physiol.* 148 (2007) 821–827, <http://dx.doi.org/10.1016/j.cbpa.2007.08.009>.
- [57] E. Padmini, M. Usha Rani, Impact of seasonal variation on HSP70 expression quantitated in stressed fish hepatocytes, *Comp. Biochem. Physiol. B Biochem. Mol. Biol.* 151 (2008) 278–285, <http://dx.doi.org/10.1016/j.cbpb.2008.07.011>.
- [58] S. Rajeshkumar, N. Munuswamy, Impact of metals on histopathology and expression of HSP70 in different tissues of Milk fish (*Chanos chanos*) of Kaattupalli Island, South East Coast, India, *Chemosphere* 83 (2011) 415–421, <http://dx.doi.org/10.1016/j.chemosphere.2010.12.086>.
- [59] F.F.T. Domingos, R.G. Thomé, P.M. Martinelli, Y. Sato, N. Bazzoli, E. Rizzo, Role of HSP70 in the regulation of the testicular apoptosis in a seasonal breeding teleost *Prochilodus argenteus* from the São Francisco river, Brazil, *Microsc. Res. Tech.* 76 (2013) 350–356, <http://dx.doi.org/10.1002/jemt.22173>.
- [60] J.A. Mosenon, J.M. Eby, C. Hernandez, I.C. Le Poole, A central role for inducible heat-shock protein 70 in autoimmune vitiligo, *Exp. Dermatol.* 22 (2013) 566–569, <http://dx.doi.org/10.1111/exd.12183>.

Thermal stress induces heat shock protein 70 and apoptosis during embryo development in a Neotropical freshwater fish

Camila F. Sales^{A,*}, Flavia S. Lemos^{A,*}, Roberto D. V. S. Morais^A,
Ralph G. Thomé^B, Helio B. Santos^B, Ana P. B. Pinheiro^A, Nilo Bazzoli^C and
Elizete Rizzo^{A,D} 

^AUniversidade Federal de Minas Gerais, Departamento de Morfologia, Instituto de Ciências Biológicas, C. P. 486, 31270-901 Belo Horizonte, Minas Gerais, Brazil.

^BUniversidade Federal de São João Del Rei, Laboratório de Processamento de Tecidos, 35501-296 Divinópolis, Minas Gerais, Brazil.

^CPontifícia Universidade Católica de Minas Gerais, Programa de Pós-graduação em Zoologia de Vertebrados, 30535-610 Belo Horizonte, Minas Gerais, Brazil.

^DCorresponding author. Emails: ictio@icb.ufmg.br; elizeterizzo@gmail.com

Abstract. Fish embryos are particularly vulnerable to temperature changes, with the effects varying with developmental stage. The major aim of the present study was to analyse the relationship between apoptosis and heat shock protein (HSP) 70 during embryo development under thermal stress conditions. To this end, *Prochilodus lineatus* embryos at the blastopore closure stage were subjected to one of three thermal treatments for 1 h (Group 1, 25°C (control); Group 2, 20°C; Group 3, 30°C) and then examined at 0, 4 and 8 h posttreatment (h.p.t.). The viability of embryos was highest in Group 1 (81.33 ± 16.65%), followed by Group 3 and Group 2 (75.33 ± 12.10% and 68.67 ± 16.86% respectively), with significant difference between Groups 1 and 2 ($P < 0.05$). At 0 h.p.t., embryos subjected to thermal stress (Group 3) had a significantly higher number of terminal deoxyribonucleotidyl transferase-mediated dUTP–digoxigenin nick end-labelling (TUNEL)- and caspase-3-labelled cells, and a lower number of HSP70-positive cells than those in the control group. At 4 h.p.t., there was a decrease in the TUNEL reaction and an increase in HSP70 in embryos in Group 3. At 8 h.p.t., the size of Group 3 embryos was significantly smaller than that of Group 1 embryos. The results indicate a cytoprotective role for HSP70, regulating caspase-3-mediated apoptosis during embryo development of *P. lineatus*; however, this mechanism is not effective in controlling embryo viability and larval malformations.

Additional keywords: caspase-3, *Prochilodus lineatus*, terminal deoxyribonucleotidyl transferase-mediated dUTP–digoxigenin nick end-labelling (TUNEL).

Received 9 June 2018, accepted 13 September 2018, published online 30 October 2018

Introduction

Freshwater ecosystems are susceptible to multiple stressors that may change the physicochemical parameters of the water and affect fish populations (Dudgeon *et al.* 2006). Water temperature can undergo circadian fluctuations ranging from 1°C to more than 15°C due to natural causes, climatic changes or human activity (Johnson 2004; Somero 2010). Freshwater fish are particularly vulnerable to temperature fluctuations, which reflect the geographical distribution of the population, community structure, life history and development (Jeppesen *et al.* 2010). Thermal pollution caused by anthropogenic thermal inputs changes water temperatures and affects fish reproduction

(Firkus *et al.* 2018). In fish farming, water temperature is a critical factor because it directly affects the metabolism, oxygen consumption, growth and survival of organisms (Jian *et al.* 2003). Although tolerance to temperature fluctuations is variable among fish species, embryos and larvae are more sensitive relative to adults (Brett 1971). In addition, the effects may be increased depending on the development stage when these organisms are exposed to the thermal stress (Wiegand *et al.* 1989; Ørnstrud *et al.* 2004a, 2004b). In the wolffish *Anarhichas minor*, water temperature affects the speed of yolk mobilisation and changes egg development rates, in addition to affecting the size and survival of larvae (Hansen and Falk-Petersen 2001).

*These authors contributed equally to this work.

The stress caused by temperature fluctuations can stimulate the expression of heat shock proteins (HSPs), which play a fundamental role in the regulation of protein synthesis by acting in the folding and assembly of polypeptide chains (Carpenter and Hofmann 2000; Stefanovic *et al.* 2016; Politis *et al.* 2017). The degree of thermal tolerance is related to the expression of HSPs and, when activated, this mechanism prevents cell damage (Whitehouse *et al.* 2017). Among the HSPs, HSP70 is constitutively expressed during embryonic development, especially during somitogenesis and neurogenesis, but its expression increases under conditions of thermal stress (Santacruz *et al.* 1997).

In addition to HSPs, programmed cell death or apoptosis is also an essential physiological process during embryonic development in vertebrates (Evans *et al.* 2005; Agnello *et al.* 2015) that requires a specialised set of proteins for its activation, including a family of proteases called caspases (Krumshnabel and Podrabsky 2009). Caspase-3 is the major effector protease of apoptosis that activates endonucleases, which are responsible for the breakdown of cytoplasmic structural proteins and DNA, leading to the typical morphological changes of apoptosis (Kerr *et al.* 1972). In teleosts, apoptosis is involved in the morphogenesis of the nervous system and sensory organs, as well as in evolutionary processes such as loss of vision in cavefish and gonadal differentiation (Candal *et al.* 2001; Cole and Ross 2001; Uchida *et al.* 2002; Hooven *et al.* 2004). In general, thermal stress can lead to an apoptotic response essential for organism survival in varying environmental conditions (Li *et al.* 2015; Kvitt *et al.* 2016).

The curimatã *Prochilodus lineatus* (Valenciennes, 1837) (Characiformes, Prochilodontidae), previously known as *Prochilodus scrofa*, is a rheophilic species of commercial importance native to the Paraná–Paraguay and Paraíba do Sul River basins in Brazil whose populations have been drastically affected by pollution and river damming (Viveiros and Godinho 2009). *P. lineatus* exhibits high fecundity (up to 440 000 oocytes per female in the Upper Paraná River basin), provides viable eggs under cultivation conditions and has a short embryonic development time (18–22 h at 24–25°C) (Ninhaus-Silveira *et al.* 2006; Botta *et al.* 2010; Perini *et al.* 2013). Thus, it is an excellent model for the study of development mechanisms under natural and experimental conditions.

Considering that fish eggs and embryos are highly sensitive to environmental stress and that improved management of embryos is a critical step in a hatchery, the goal of the present study was to investigate the effects of thermal stress on *P. lineatus* embryos under culture conditions, with emphasis on the relationship between HSP70 and apoptosis during a critical period of embryo development.

Materials and methods

Experimental procedures

The experiment was performed at the Furnas Hydrobiology and Hatchery Station (20°43'4''S, 46°18'39''W), Minas Gerais state, south-eastern Brazil. *P. lineatus* breeders (five females (48.86 ± 8.04 cm total length (TL) and bodyweight 1.67 ± 0.43 kg) and five males (41.57 ± 8.56 cm TL and 1.41 ± 0.41 kg)) were induced using crude carp (*Cyprinus*

carpo) pituitary extract. The carp pituitary homogenate (CPH) was prepared by macerating dried pituitaries (Agrober) using a 0.9% saline solution as solvent. The females received two doses of CPH injected into the coelomic cavity, with the first dose of 0.5 mg kg⁻¹ bodyweight followed 10 h later by a second dose of 5.0 mg kg⁻¹ (Ninhaus-Silveira *et al.* 2006). Males received a single 1 dose of 0.0 mg kg⁻¹ CPH administered at the time the second dose was given to the females. Stripping of gametes and fertilisation were performed 6 h after the last dose. The fertilised eggs were kept in funnel-type incubators with a capacity of 20 L and under conditions of continuous water flow at 25°C. Embryo development was monitored every hour until hatching. All procedures followed the ethical principles established by the Brazilian College of Animal Experimentation (COBEA), and the study was approved by the Ethics Committee on Animal Use (CEUA Protocol 92/2010) of the Federal University of Minas Gerais.

To evaluate the effect of thermal stress on embryo development, samples of embryos were collected and divided into three groups (200–300 embryos per group) at the blastopore closure stage, 9 h after fertilisation. In Group 1 (control), the embryos were kept at 25°C, without thermal stress. In the treated groups, the embryos were subjected to thermal stress for 1 h at either 20°C (Group 2) or 30°C (Group 3). During treatment, the embryos were kept in 5-L beakers with aerators containing water taken from the incubators of the hatchery, with temperature controlled by a thermostat. Embryos were examined every 10 min. After the 1-h temperature treatment, embryos were transferred to experimental incubators (capacity 1.5 L) with continuous water flow at 25°C and were evaluated at 0, 4 and 8 h posttreatment (h.p.t.). Fertilisation rate was determined after blastopore closure (10 h after fertilisation) and embryo viability was determined at 0, 4 and 8 h.p.t.

Morphology and viability of embryos

For analysis of external morphology and viability of embryos, 50 samples were fixed in neutral formalin and analysed under a stereomicroscope. Embryos that were not viable were opaque with degenerating material in the perivitelline space, whereas viable embryos were intact and had a translucent perivitelline space (Rizzo *et al.* 2003). The TL of embryos and larvae was measured using a micrometer eyepiece coupled with the stereomicroscope. Malformation analyses considered the morphology of the body, tail and trunk.

For histological analysis, samples of 10 viable embryos at each time after treatment (i.e. 0, 4 and 8 h.p.t.) were fixed in Bouin's fluid for 6 h at room temperature. Then, the chorion was manually extracted under a stereomicroscope, samples were embedded in paraffin, sectioned at 5 µm, stained with haematoxylin and eosin (HE) or Toluidine blue and examined under a light microscope.

Apoptosis

Apoptosis was assessed by the terminal deoxyribonucleotidyl transferase-mediated dUTP–digoxigenin nick end-labelling (TUNEL) *in situ* assay and immunofluorescence for caspase-3. To this end, samples of 10 embryos were fixed in 4%

paraformaldehyde 0.1 M phosphate buffer, pH 7.3, for 24 h at 4°C, embedded in Paraplast (Merck) and sectioned at 5 µm. The TUNEL reaction was performed using the Merck Millipore QIA33 DNA fragmentation detection kit following the manufacturer's instructions. For permeabilisation and inactivation of endogenous peroxidase, sections were treated with proteinase K (10 µg mL⁻¹) and 3% hydrogen peroxide respectively. Then, the sections were incubated with a mixture of terminal deoxynucleotide transferase (TdT) and biotin-conjugated deoxynucleotides in a humid chamber at 37°C for 1.5 h. Then, peroxidase-conjugated streptavidin solution was applied to sections in a humid chamber at room temperature for 45 min. The peroxidase reaction was revealed with diaminobenzidine (DAB) for 10 min at room temperature, and the sections were counterstained with haematoxylin. As a negative control, one of the slides did not receive the mixture containing TdT and deoxynucleotides.

For detection of caspase-3 in apoptotic cells, sections were washed with phosphate-buffered saline (PBS) and treated with 2% bovine serum albumin (BSA) to block non-specific reactions. Then, sections were incubated with primary rabbit anti-caspase-3 polyclonal antibody (Sigma-Aldrich; 1 : 300 dilution) overnight at 4°C. After washing with PBS, the blocking buffer was applied again and sections were incubated with the secondary antibody (ALEXA Fluor 488 anti-rabbit IgG; Invitrogen; 1 : 200 dilution). Nuclei were counterstained with 4',6'-diamidino-2-phenylindole (DAPI; Invitrogen; 1 : 500 dilution). As a negative control, primary antibody treatment was omitted.

To assess TUNEL reaction and caspase-3 immunoreaction in apoptotic cells, 25 digital images were chosen at random in the cranial region of the embryo for each time point after treatment and examined at a magnification of ×1000 using Image Pro Plus version 4.0 for Windows (MediaCybernetics). Results are expressed as the number of labelled cells per 100 mm² (Domingos *et al.* 2013).

Immunofluorescence for HSP70

As described above, histological sections were washed with PBS, treated with 2% BSA to block non-specific reactions and then incubated with primary mouse anti-HSP70 monoclonal antibody (Clone BRM-22; Sigma-Aldrich; 1 : 300) overnight at 4°C. After washing with PBS, the blocking buffer was applied again and then sections were incubated with a secondary antibody (ALEXA Fluor 568 anti-mouse; Invitrogen; 1 : 200 dilution) and counterstained with DAPI (1 : 500 dilution) to stain nuclear DNA. As a negative control, primary antibody treatment was omitted. To assess HSP70, 25 digital images were chosen at random in the cranial region of the embryos for each time point after treatment at a magnification of ×400 using Image Pro Plus Demo version 4.0 for Windows. Sections were examined under a Carl Zeiss LSM-510 confocal microscope, and results are expressed as the percentage of the marked area in relation to the total area (Santos *et al.* 2008).

Statistical analysis

Statistical analyses were performed using GraphPad InStat version 5.0 for Windows (GraphPad Software). To compare

different treatments, data were subjected to a normality test, followed by one-way analysis of variance (ANOVA) and Tukey's post test. Results are expressed as the mean ± d.p. (TL, BW, viability) and mean ± s.e.m. (TUNEL, HSP70, caspase-3), and two-tailed $P < 0.05$ was considered significant.

Results

The main stages of embryogenesis in *P. lineatus* and respective developmental times are shown in Fig. 1.

Effects of thermal stress on embryo development

The mean viability of embryos after the blastopore closure stage was higher in Group 1 (control; 81.33 ± 16.65%), followed by Group 3 (75.33 ± 12.10%) and Group 2 (68.67 ± 16.86%), with significant difference in embryo viability between Groups 1 and 2 ($P < 0.05$). Larvae hatched at 18 h postfertilisation (h.p.f.) in Group 1 (control), maintained at 25°C. In embryos subjected to thermal stress, hatching occurred at 17 h.p.f. (Group 3) and 19 h.p.f. (Group 2).

After thermal stress (0 h.p.t.), embryos showed no differences in external morphology relative to the control group (Fig. 2a–c). At 4 h.p.t., embryos in Groups 2 and 3 exhibited changes in body shape and development (Fig. 2d–f), whereas at 8 h.p.t. the newly hatched larvae in Groups 2 and 3 had a greater curvature of the trunk compared with control (Group 1; Fig. 2g–i). The TL of embryos increased significantly at the different sampling times (i.e. 0, 4 and 8 h.p.t.) within each experimental group ($P < 0.001$; Fig. 2j). There was no significant difference in TL between treatment groups ($P > 0.05$), except between Group 1 and 3 at 8 h.p.t. ($P < 0.05$; Fig. 2j).

TUNEL, caspase-3 and HSP70 assays

After treatment (0 h.p.t.), a TUNEL-positive reaction was detected in deep cells (DC) and enveloped cells (EVCs; Fig. 3a–c). At 4 and 8 h.p.t., the TUNEL-positive reaction was predominant in apoptotic cells of the neural tube, notochord and somites in all groups (Fig. 3d–i).

Immunofluorescence for caspase-3 was detected, primarily in the yolk syncytial layer (YSL) and DC at 0 h.p.t. in all experimental groups (Fig. 4a–c). At 4 h.p.t., caspase-3-positive cells occurred in the somites, primitive gut and neural tube, as well as close to the optic cup and in the caudal region of the embryo in Groups 1, 2 and 3 (Fig. 4d–i). Immunostaining for HSP70 was found in most cells of the embryo, primarily in the YSL, EVCs, somites, gut, and neural tube in all groups (Fig. 4). However, in Group 2 at 4 h.p.t., the neural tube cells showed weak labelling for HSP70 compared with other regions of the embryo (Fig. 4e). Colocalisation of caspase-3 and HSP70 was eventually detected at 4 h.p.t. in all groups (Fig. 4f–i).

Morphometric analysis revealed a significant increase in apoptosis, as evidenced by the TUNEL reaction at 4 and 8 h.p.t. in relation to 0 h.p.t. in all three experimental groups ($P < 0.05$; Fig. 5a). Comparing the treatments, the TUNEL reaction was significantly higher in Group 2 and 3 embryos at 0 h.p.t. than in Group 1 embryos, and in Group 1 embryos at 4 h.p.t. than in Group 3 embryos ($P < 0.05$; Fig. 5a). There was no significant difference in caspase-3 expression in Group 1

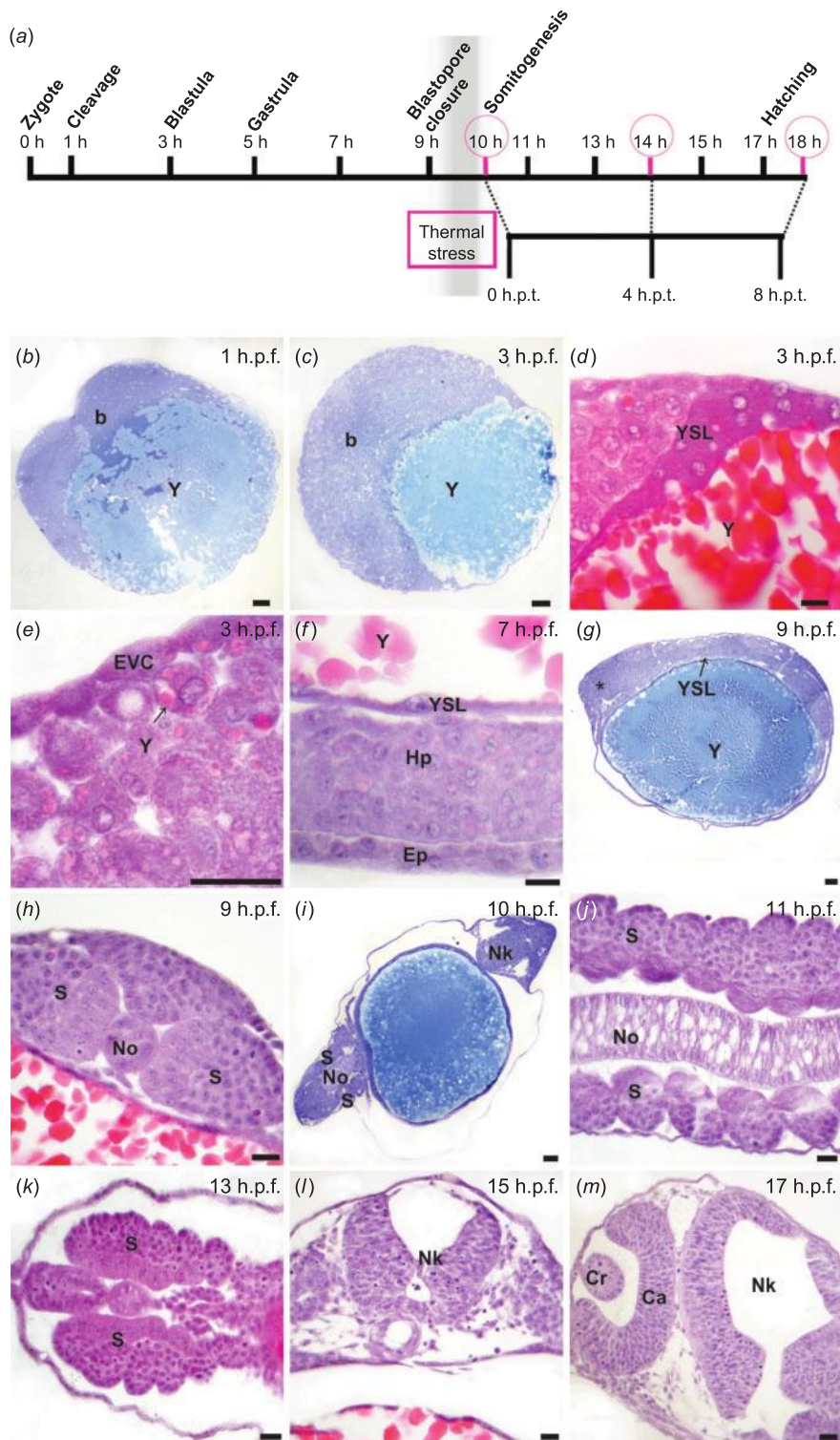


Fig. 1. (a) Time line after fertilisation and (b–m) histological sections of *Prochilodus lineatus* embryos stained with Toluidine blue (b, c, g, i) and hematoxylin-eosin (d–f, h, j–m). (a) Time (h) of the occurrence of the main stages of embryogenesis, from fertilisation to larval hatching (18 h at 25°C), and hours posttreatment (h.p.t.) after application of thermal stress to embryos. (b) Cleavage, embryo with two blastomeres (b) and yolk (Y) concentrated in the vegetative pole. (c) High blastula, with a dome of cells originating from the cell division of the blastoderm on the yolk sac at 3 h postfertilisation (h.p.f.). (d) Presence of yolk syncytial layer (YSL) near high the blastula at 3 h.p.f. (e) Enveloping cells (EVC) and blastomeres (deep cells) in yolk (Y) incorporation activity at 3 h.p.f. (f) Presence of epiblast (Ep) and hypoblast (Hp) layers at 7 h.p.f. (g) YSL completely involving the Y and anterior region of the embryo (asterisk) at 9 h.p.f. (h, i) Presence of the notochord (No), somites (S) and neural tube development (Nk) at 9 and 10 h.p.f. (j, k) Somites (S) in the caudal portion of the embryo at 11 and 13 h.p.f. (l) Note Nk at 15 h.p.f. (m) Optical (Ca) and crystalline (Cr) cups. Scale bars = 20 μ m.

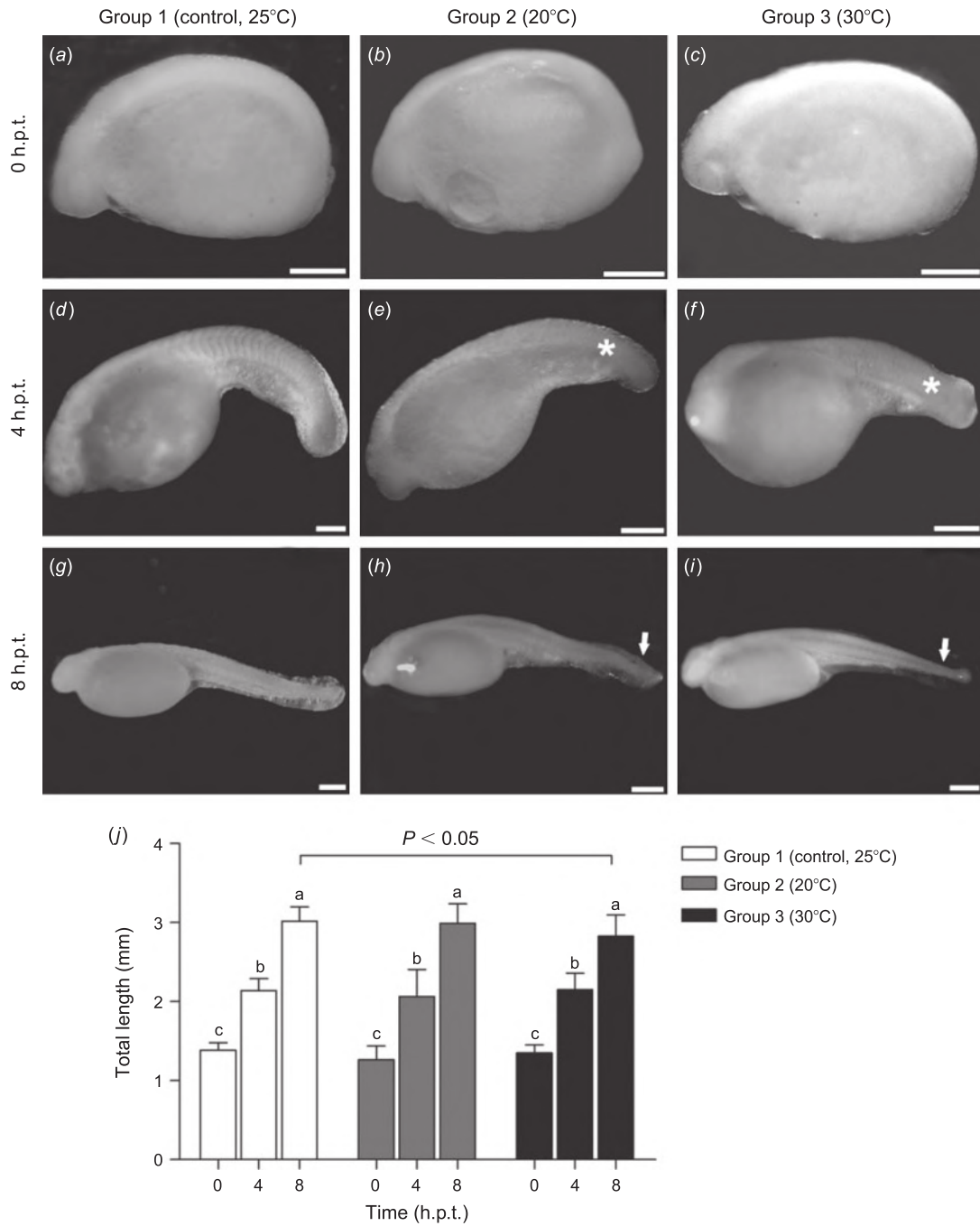


Fig. 2. External morphology at different times (hours posttreatment (h.p.t.)) of *Prochilodus lineatus* embryos kept at 25°C (a, d, g) or subjected to thermal stress for 1 h at either 20°C (b, e, h) or 30°C (c, f, i) at the blastopore closure stage. (e, f) Changes in column curvature (asterisks). (h, i) Caudal degeneration (arrows). Scale bars = 300 μ m. (j) Total length of embryos at different times after treatment. Data are the mean \pm s.e.m. Different letters above columns indicate significant differences between sampling times within each experimental group.

(control) embryos at the different sampling times (0, 4 and 8 h.p.t.), but caspase-3 expression was significantly lower at 4 versus 0 h.p.t. in Group 2 embryos, and at 8 versus 0 h.p.t. in Group 3 embryos ($P < 0.05$; Fig. 5b). Caspase-3 expression was significantly higher at 0 h.p.t. in Group 2 and 3 versus Group 1

embryos, and lower in Group 2 compared with Group 1 and 3 embryos at 4 h.p.t. ($P < 0.05$; Fig. 5b). Expression of HSP70 in Groups 2 and 3 was significantly lower at 0 h.p.t., increased at 4 h.p.t. and then decreased significantly at 8 h.p.t. ($P < 0.05$; Fig. 5c). No significant variation in HSP70 expression was

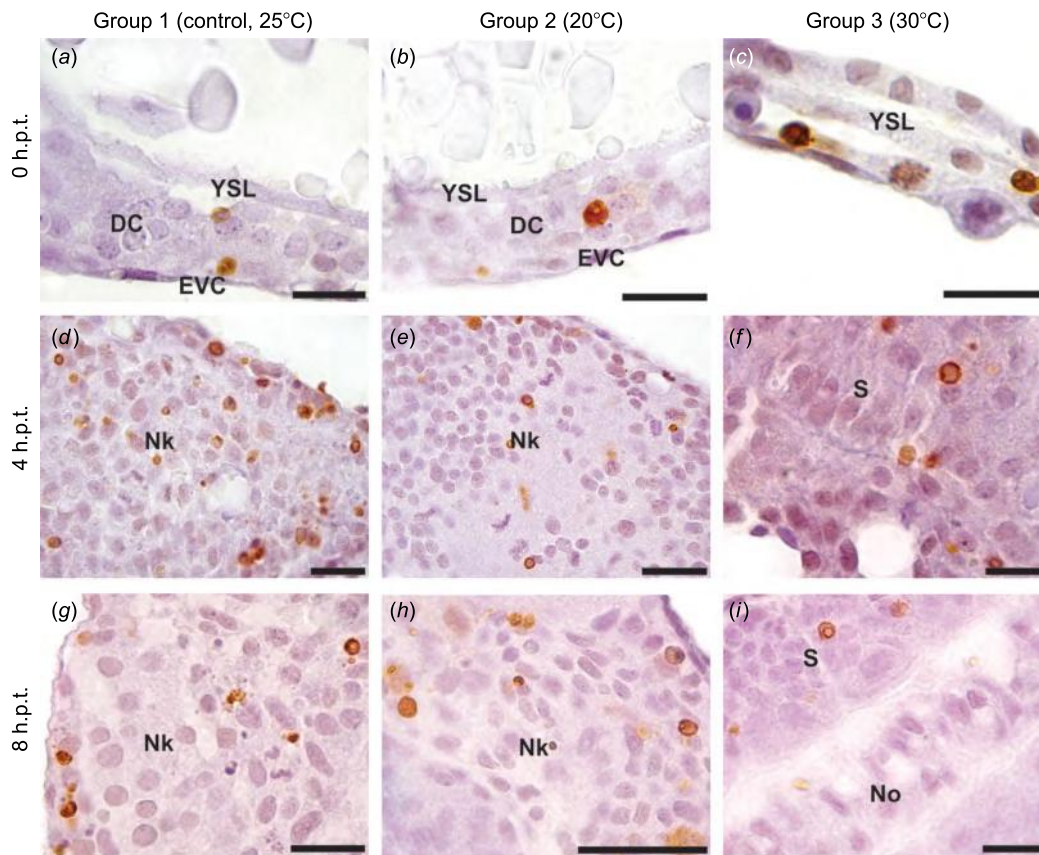


Fig. 3. *In situ* Terminal deoxyribonucleotidyl transferase-mediated dUTP-digoxigenin nick end-labelling (TUNEL) reaction at different times (hours posttreatment (h.p.t.)) in *Prochilodus lineatus* embryos kept at 25°C (a, d, g) or subjected to thermal stress for 1 h at either 20°C (b, e, h) or 30°C (c, f, i) at the blastopore closure stage. Sections were counterstained with haematoxylin. S, somites; YSL, yolk syncytial layer; DC, deep cells; EVC, enveloping cells; No, notochord; Nk, neural tube. Scale bars = 20 µm.

found between sampling times in Group 1 (control, 25°C) embryos. In groups 2 and 3, HSP70 expression was lower at 0 h.p.t. and higher at 4 h.p.t. compared with expression in Group 1 embryos, and lower at 8 h.p.t. in Group 3 versus Group 1 embryos ($P < 0.05$; Fig. 5c).

Discussion

In the present study, we revealed that reduced fish embryo viability and increased larval malformations under thermal stress are probably related to modifications in the expression of caspase-3 during early development, even with increases in HSP70 levels. The thermal stress of 20°C and 30°C used in the present study was below and above the average summer water temperature respectively (i.e. 25°C, which was used as the control), when *P. lineatus* spawn. Industrial thermal pollution and climate change can increase the water temperature of lakes and rivers up to 15°C (Langford 2001; Firkus *et al.* 2018), and these increased changes are a serious threat to freshwater biodiversity, particularly because they affect the early development of aquatic organisms, as demonstrated in the present study. Studies on thermal stress in fish embryos can establish critical thermal limits during development, providing important

parameters for improving the quality of eggs, embryos and larvae in fish farming.

The embryo development of *P. lineatus* follows the general pattern described for other Neotropical fish species (Kimmel *et al.* 1995; Gomes *et al.* 2007; de Amorim *et al.* 2009). The epiboly culminates with blastopore closure, a period in which the embryos of the present study were subjected to thermal stress. In *P. lineatus*, the development of the neural tube, optic cup and vesicle occurred during late somitogenesis, as reported previously (Ninhaus-Silveira *et al.* 2006), which corresponds to the 4 h.p.t. time point in the present study. *P. lineatus* larvae hatched around 18 h.p.f. at 25°C, when vigorous movements of tail contraction culminated in the rupture of the chorion; this period corresponds to 8 h.p.t. in the present study.

Temperature is one of the main environmental factors that affects the duration of embryogenesis, hatching rate and the survival of embryos and larvae (Das *et al.* 2006). In the present study, the duration of *P. lineatus* embryogenesis was 18 h at 25°C (from fertilisation until hatching of larvae); this is similar to the data reported by Botta *et al.* (2010), whereas another study reported a duration of 22 h at 24°C (Ninhaus-Silveira *et al.* 2006). For embryos subjected to thermal stress of 30°C

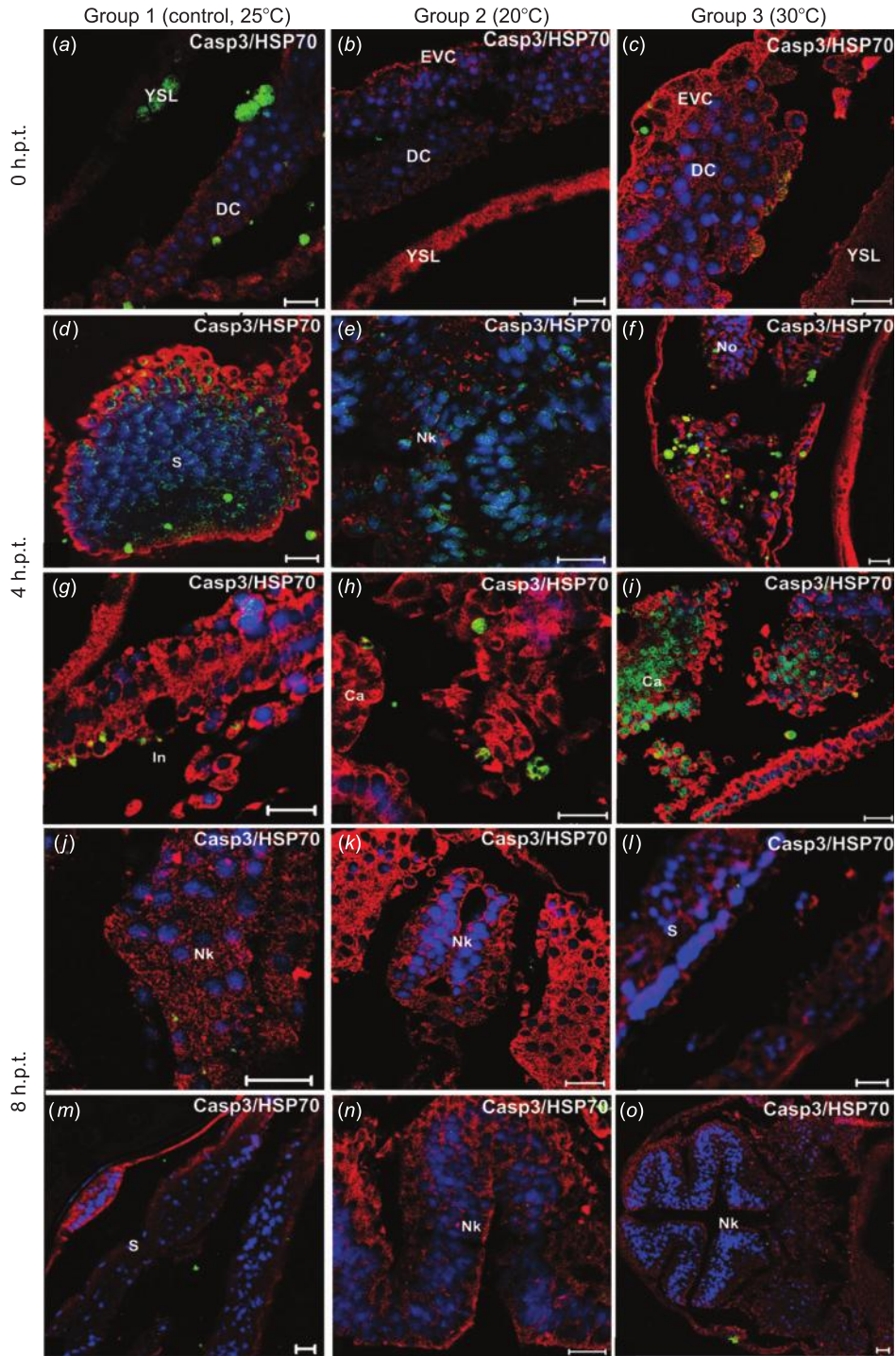


Fig. 4. Immunofluorescence for caspase-3 (green) and HSP-70 (red) at different times (hours posttreatment (h.p.t.) in embryos of *Prochilodus lineatus* kept at 25°C (a, d, g, j, m) or subjected to thermal stress for 1 h at either 20°C (b, e, h, k, n) or 30°C (c, f, i, l, o) at the blastopore closure stage. Nuclei were stained with 4',6'-diamidino-2-phenylindole (blue). S, somites; YSL, yolk syncytial layer; DC, deep cells; EVC, enveloping cells; No, notochord; Nk, neural tube. Scale bars = 20 μm.

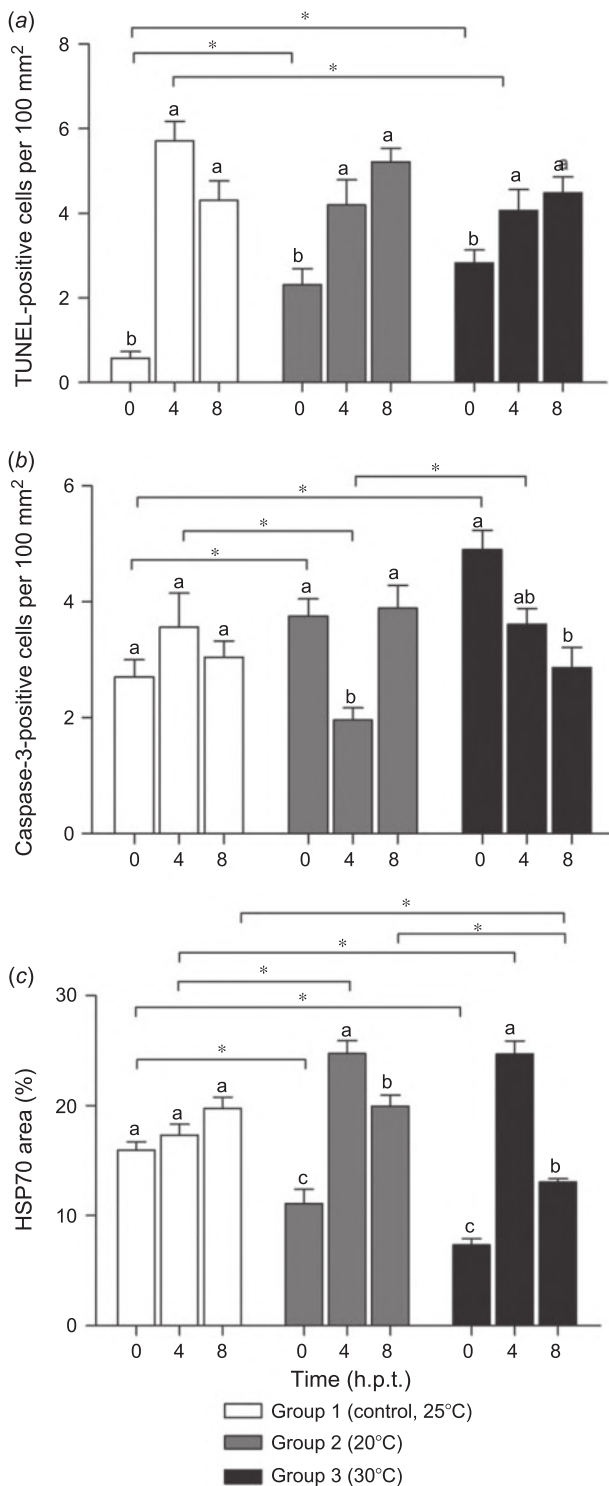


Fig. 5. Morphometry of (a) terminal deoxyribonucleotidyl transferase-mediated dUTP-digoxigenin nick end-labelling (TUNEL) reaction, (b) caspase-3 and (c) heat shock protein (HSP) 70 in the different experimental groups at different times after treatment. h.p.t., hours posttreatment. Data are the mean \pm s.e.m. Different letters above columns indicate significant differences between sampling times within each experimental group. **P* < 0.05.

(Group 3), the water temperature accelerated embryonic development and larvae hatched within 17 h.p.t. In fact, poikilothermic animals show accelerated development at higher temperatures due to changes in enzyme activities (Ojanguren and Braña 2003; Politis *et al.* 2017).

Malformations in embryos and larvae are recurrent problems in fish farming. In general, low abnormality rates are required during larval development, but may increase as a result of different types of stress, such as sudden temperature variations (Hansen and Falk-Petersen 2001; Ørnstrud *et al.* 2004b; Boglione *et al.* 2013). In *P. lineatus*, embryos subjected to thermal stress exhibited skeletal anomalies, spinal curvature and reduced size at 8 h.p.t.; these results are similar to those obtained for Atlantic salmon (*Salmo salar*) embryos (Wargelius *et al.* 2005). In addition, the results of the present study showed that the viability of embryos subjected to thermal stress of 20°C or 30°C was significantly reduced after the blastopore closure stage, when unfertilised eggs had degenerated. Similar results have been reported in zebrafish embryos following the induction of stress by increasing temperature (Krone *et al.* 1997; Yabu *et al.* 2001). Together, the results indicate that abrupt temperature variations during the egg incubation period may accelerate or reduce embryo development, decrease egg viability, increase malformations and reduce growth rates of embryos and larvae.

Unlike mammals, in which apoptosis occurs in the blastocyst stage due to early activation of genes in the zygote, apoptosis in fish is induced only at gastrulation (Agnello *et al.* 2015). Indeed, TUNEL and immunohistochemical reactions for caspase-3 in apoptotic cells were detected in the somites, notochord, developing neural tube, primitive gut and close to the optic cup of *P. lineatus*. Effector caspases (3, 6 and 7) are widely expressed during embryogenesis in vertebrates, including fish, primarily in somitogenesis and during development of the nervous system (Yabu *et al.* 2001; Evans *et al.* 2005; Gashegu *et al.* 2006; Takle *et al.* 2006).

In general, apoptosis gradually increases during development due to organogenesis (Gashegu *et al.* 2006), as found in the present study using the TUNEL assay in *P. lineatus* embryos at different times (0, 4 and 8 h.p.t.). Furthermore, the number of TUNEL- and caspase-3-positive cells was significantly higher soon after thermal stress in relation to the control group, indicating that thermal stress induced caspase-3-mediated apoptosis. This increase in apoptosis indicates an adaptive cell response and a potential beneficial role of apoptosis under adverse developmental conditions (Hashimoto *et al.* 1998; Yabu *et al.* 2001). In addition to apoptosis, HSP70 is induced in response to different types of stress and can directly interact with a variety of cellular proteins. These interactions act as regulatory points of apoptosis by inhibiting both intrinsic and extrinsic pathways (Chatterjee and Burns 2017).

In fish, the onset of embryo genome activation occurs at mid-blastula transition, just before gastrulation, resulting in cell motility and zygotic gene expression (Kane and Kimmel 1993; Pelegri 2003), including proteins related to the cell signalling pathways, such as apoptosis and HSP. In the present study, the lower expression of HSP70 at 0 h.p.t. in groups subjected to thermal stress (Groups 2 and 3) could be related to the increased apoptosis. Under stress conditions, many

proteins undergo unfolding, exposing hydrophobic domains, increasing the likelihood of protein aggregation with loss of cellular functions and finally culminating in cell death (Meimaridou *et al.* 2009). To avoid such effects, HSP70 expression is induced and HSP70 accumulates in the cytoplasm from 2 h after the rise in temperature (Lindquist and Craig 1988; Creagh *et al.* 2000), thus supporting the increase in HSP70 seen at 4 h.p.t. found in the present study. In the group treated with thermal stress at 30°C (Group 3), the increase in HSP70 at 4 h.p.t., the associated subsequent decrease in caspase-3 at 8 h.p.t. may be a consequence of inhibition of apoptotic protease activating factor-1 (Apaf-1) oligomerisation due to its binding to HSP70, preventing subsequent activation of caspase-9 and caspase-3, and thus blocking caspase-3-mediated apoptosis (Parcellier *et al.* 2003). Indeed, HSP70 can inhibit key effectors of apoptosis through its direct association with caspase recruitment domain (CARD) from Apaf-1, with this interaction leading to inhibition of apoptosome formation (Saleh *et al.* 2000; Chatterjee and Burns 2017).

In summary, the findings of the present study indicate that thermal stress at the blastopore closure stage increases caspase-3-mediated apoptosis in *P. lineatus* embryos. These embryos respond to the thermal stress with induction of HSP70 expression as a strategy for cell survival by controlling apoptosis during development. However, this cell stress response is not sufficient to maintain embryo viability and prevent malformations in newly hatched larvae. Thus, the results of this study indicate that *P. lineatus* embryos are highly sensitive to thermal stress during the blastopore closure stage.

Conflicts of interest

The authors declare no conflicts of interest.

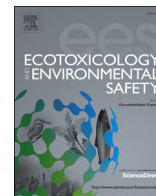
Acknowledgements

The authors are grateful to the team of the Hydrobiology and Hatchery Station of Furnas, Minas Gerais, Brazil, for providing the fish embryos and assistance during the experimental procedures. The authors also thank to Paulo Pimenta and colleagues of the Centro de Pesquisas René Rachou for technical assistance with immunofluorescence image collection, Mônica C. P. Ricardo for preparing the histological sections and Steve Latham for valuable suggestions for improving English language expression. The research was supported by grants from the Brazilian Research Foundations: Conselho Nacional de Desenvolvimento Científico e Tecnológico (CNPq), Coordenação de Aperfeiçoamento de Pessoal de Nível Superior (CAPES) and Fundação de Amparo à Pesquisa do Estado de Minas Gerais (FAPEMIG).

References

- Agnello, M., Bosco, L., Chiarelli, R., Martino, C., and Roccheri, M. C. (2015). The role of autophagy and apoptosis during embryo development. In 'Cell Death – Autophagy, apoptosis and necrosis'. (Ed. T. Ntuli.) pp. 83–112. (IntechOpen: London.)
- Boglione, C., Gisbert, E., Gavaia, P., Witten, P. E., Moren, M., Fontagné, S., and Koumoundouros, G. (2013). Skeletal anomalies in reared European fish larvae and juveniles. Part 2: main typologies, occurrences and causative factors. *Rev. Aquacult.* **5**, S121–S167. doi:10.1111/RAQ.12016
- Botta, P., Sciarra, A., Arranz, S., Murgas, L. D. S., Pereira, G. J. M., and Oberlander, G. (2010). Study of the embryonic development in sábalo (*Prochilodus lineatus*). *Arch. Med. Vet.* **42**, 109–114. doi:10.4067/S0301-732X2010000200014
- Brett, J. R. (1971). Energetic responses of salmon to temperature. A study of some thermal relations in the physiology and freshwater ecology of sockeye salmon (*Oncorhynchus nerka*). *Integr. Comp. Biol.* **11**, 99–113. doi:10.1093/ICB/11.1.99
- Candal, E., Anadón, R., Caruncho, H., and Rodríguez-Moldes, I. (2001). Proliferation, cell death and reelin expression during development of the retina in a teleost, the common trout (*Salmo trutta fario*). *Int. J. Dev. Biol.* **45**, S69–S70.
- Carpenter, C. M., and Hofmann, G. E. (2000). Expression of 70 kDa heat shock proteins in antarctic and New Zealand notothenioid fish. *Comp. Biochem. Physiol. A Mol. Integr. Physiol.* **125**, 229–238. doi:10.1016/S1095-6433(99)00172-5
- Chatterjee, S., and Burns, T. F. (2017). Targeting heat shock proteins in cancer: a promising therapeutic approach. *Int. J. Mol. Sci.* **18**, 1–39.
- Cole, L. K., and Ross, L. S. (2001). Apoptosis in the developing zebrafish embryo. *Dev. Biol.* **240**, 123–142. doi:10.1006/DBIO.2001.0432
- Creagh, E. M., Sheehan, D., and Cotter, T. G. (2000). Heat shock proteins – modulators of apoptosis in tumour cells. *Leukemia* **14**, 1161–1173.
- Das, T., Pal, A. K., Chakraborty, S. K., Manush, S. M., Dalvi, R. S., Sarma, K., and Mukherjee, S. C. (2006). Thermal dependence of embryonic development and hatching rate in *Labeo rohita* (Hamilton, 1822). *Aquaculture* **255**, 536–541. doi:10.1016/J.AQUACULTURE.2006.01.013
- de Amorim, M. P., Gomes, B. V. C., Martins, Y. S., Sato, Y., Rizzo, E., and Bazzoli, N. (2009). Early development of the silver catfish *Rhamdia quelen* (Quoy & Gaimard, 1824) (Pisces: Heptapteridae) from the São Francisco River Basin, Brazil. *Aquacult. Res.* **40**, 172–180. doi:10.1111/J.1365-2109.2008.02079.X
- Domingos, F. F. T., Thomé, R. G., Martinelli, P. M., Sato, Y., Bazzoli, N., and Rizzo, E. (2013). Role of HSP70 in the regulation of the testicular apoptosis in a seasonal breeding teleost *Prochilodus argenteus* from the São Francisco River, Brazil. *Microsc. Res. Tech.* **76**, 350–356. doi:10.1002/JEMT.22173
- Dudgeon, D., Arthington, A. H., Gessner, M. O., Kawabata, Z. I., Knowler, D. J., Lévêque, C., Naiman, R. J., Prieur-Richard, A. H., Soto, D., Stiassny, M. L. J., and Sullivan, C. A. (2006). Freshwater biodiversity: importance, threats, status and conservation challenges. *Biol. Rev. Camb. Philos. Soc.* **81**, 163–182. doi:10.1017/S1464793105006950
- Evans, T. G., Yamamoto, Y., Jeffery, W. R., and Krone, P. H. (2005). Zebrafish Hsp70 is required for embryonic lens formation. *Cell Stress Chaperones* **10**, 66–78. doi:10.1379/CSC-79R.1
- Firkus, T., Rahel, F. J., Bergman, H. L., and Cherrington, B. D. (2018). Warmed winter water temperatures alter reproduction in two fish species. *Environ. Manage.* **61**, 291–303. doi:10.1007/S00267-017-0954-9
- Gashagu, J., Philippson, C., Vanmuylder, N., Choa-Duterte, M., Rooze, M., and Louryan, S. (2006). Correlation of Hsp110 expression with caspase-3 and -9 during apoptosis induced by *in vivo* embryonic exposition to retinoic acid or irradiation in early mouse craniofacial development. *Orthod. Craniofac. Res.* **9**, 84–92. doi:10.1111/J.1601-6343.2006.00361.X
- Gomes, B. V. C., Scarpelli, R. S., Arantes, F. P., Sato, Y., Bazzoli, N., and Rizzo, E. (2007). Comparative oocyte morphology and early development in three species of trahiras from the São Francisco River basin, Brazil. *J. Fish Biol.* **70**, 1412–1429. doi:10.1111/J.1095-8649.2007.01420.X
- Hansen, T. K., and Falk-Petersen, I. B. (2001). The influence of rearing temperature on early development and growth of spotted wolffish *Anarhichas minor* (Olafsen). *Aquacult. Res.* **32**, 369–378. doi:10.1046/J.1365-2109.2001.00567.X
- Hashimoto, H., Toyohara, Y., Women, M. K., and Nishinomiya, I. (1998). Induction of apoptosis in fish cells by hypertonic stress. *Fish. Sci.* **64**, 820–825. doi:10.2331/FISHSCI.64.820
- Hooven, T. A., Yamamoto, Y., and Jeffery, W. R. (2004). Blind cavefish and heat shock protein chaperones: a novel role for hsp90 α in lens apoptosis. *Int. J. Dev. Biol.* **48**, 731–738. doi:10.1387/IJDB.041874TH

- Jeppesen, E., Meerhoff, M., Holmgren, K., González-Bergonzoni, I., Teixeira-de Mello, F., Declerck, S. A. J., De Meester, L., Søndergaard, M., Lauridsen, T. L., Bjerring, R., Conde-Porcuna, J. M., Mazzeo, N., Iglesias, C., Reizenstein, M., Malmquist, H. J., Liu, Z., Balayla, D., and Lazzaro, X. (2010). Impacts of climate warming on lake fish community structure and potential effects on ecosystem function. *Hydrobiologia* **646**, 73–90. doi:10.1007/S10750-010-0171-5
- Jian, C. Y., Cheng, S. Y., and Chen, J. C. (2003). Temperature and salinity tolerances of yellowfin sea bream, *Acanthopagrus latus*, at different salinity and temperature levels. *Aquacult. Res.* **34**, 175–185. doi:10.1046/J.1365-2109.2003.00800.X
- Johnson, S. L. (2004). Factors influencing stream temperatures in small streams: substrate effects and a shading experiment. *Can. J. Fish. Aquat. Sci.* **61**, 913–923. doi:10.1139/F04-040
- Kane, D. A., and Kimmel, C. B. (1993). The zebrafish midblastula transition. *Development* **119**, 447–456.
- Kerr, J. F. R., Wyllie, A. H., and Currie, A. R. (1972). Apoptosis: a basic biological phenomenon with wide-ranging implications in tissue kinetics. *Br. J. Cancer* **26**, 239–257. doi:10.1111/J.1365-2796.2005.01570.X
- Kimmel, C. B., Ballard, W. W., Kimmel, S. R., Ullmann, B., and Schilling, T. F. (1995). Stages of embryonic development of the zebrafish. *Dev. Dyn.* **203**, 253–310. doi:10.1002/AJA.1002030302
- Krone, P. H., Sass, J. B., and Lele, Z. (1997). Heat shock protein gene expression during embryonic development of the zebrafish. *Cell. Mol. Life Sci.* **53**, 122–129. doi:10.1007/PL00000574
- Krumschnabel, G., and Podrabsky, J. E. (2009). Fish as model systems for the study of vertebrate apoptosis. *Apoptosis* **14**, 1–21. doi:10.1007/S10495-008-0281-Y
- Kvitt, H., Rosenfeld, H., and Tchernov, D. (2016). The regulation of thermal stress induced apoptosis in corals reveals high similarities in gene expression and function to higher animals. *Sci. Rep.* **6**, 30359. doi:10.1038/SREP30359
- Langford, T. E. L. (2001). Thermal discharges and pollution. In 'Encyclopedia of Ocean Sciences'. (Eds J. H. Steele, S. A. Thorpe and K. K. Turekian.) pp. 2933–2940. (Academic Press: Amsterdam.)
- Li, A. J., Leung, P. T. Y., Bao, V. W. W., Lui, G. C. S., and Leung, K. M. Y. (2015). Temperature-dependent physiological and biochemical responses of the marine medaka *Oryzias melastigma* with consideration of both low and high thermal extremes. *J. Therm. Biol.* **54**, 98–105. doi:10.1016/J.JTHERBIO.2014.09.011
- Lindquist, S., and Craig, E. (1988). The heat-shock proteins. *Annu. Rev. Genet.* **22**, 631–677. doi:10.1146/ANNUREV.GE.22.120188.003215
- Meimaridou, E., Gooljar, S. B., and Chapple, J. P. (2009). From hatching to dispatching: the multiple cellular roles of the Hsp70 molecular chaperone machinery. *J. Mol. Endocrinol.* **42**, 1–9. doi:10.1677/JME-08-0116
- Ninhaus-Silveira, A., Foresti, F., and De Azevedo, A. (2006). Structural and ultrastructural analysis of embryonic development of *Prochilodus lineatus* (Valenciennes, 1836) (Characiformes; Prochilodontidae). *Zygote* **14**, 217–229. doi:10.1017/S096719940600373X
- Ojanguren, A. F., and Braña, F. (2003). Effects of size and morphology on swimming performance in juvenile brown trout (*Salmo trutta L.*). *Ecol. Freshwat. Fish* **12**, 241–246. doi:10.1046/J.1600-0633.2003.00016.X
- Ørnsrud, R., Gil, L., and Waagbø, R. (2004a). Teratogenicity of elevated egg incubation temperature and egg vitamin A status in Atlantic salmon, *Salmo salar L.* *J. Fish Dis.* **27**, 213–223. doi:10.1111/J.1365-2761.2004.00536.X
- Ørnsrud, R., Wargelius, A., Sæle, Ø., Pittman, K., and Waagbø, R. (2004b). Influence of egg vitamin A status and egg incubation temperature on subsequent development of the early vertebral column in Atlantic salmon fry. *J. Fish Biol.* **64**, 399–417. doi:10.1111/J.0022-1112.2004.00304.X
- Parcellier, A., Gurbuxani, S., Schmitt, E., Solary, E., and Garrido, C. (2003). Heat shock proteins, cellular chaperones that modulate mitochondrial cell death pathways. *Biochem. Biophys. Res. Commun.* **304**, 505–512. doi:10.1016/S0006-291X(03)00623-5
- Pelegri, F. (2003). Maternal factors in zebrafish development. *Dev. Dyn.* **228**, 535–554. doi:10.1002/DVDY.10390
- Perini, Vda R., Paschoalini, A. L., Cruz, C. K., Rocha Rde, C., Senhorini, J. A., Ribeiro, D. M., Formagio, P. S., Bazzoli, N., and Rizzo, E. (2013). Profiles of sex steroids, fecundity and spawning of a migratory characiform fish from the Paraguay–Paraná basin: a comparative study in a three-river system. *Fish Physiol. Biochem.* **39**, 1473–1484. doi:10.1007/S10695-013-9800-Z
- Politis, S. N., Mazurais, D., Servili, A., Zambonino-Infante, J.-L., Miest, J. J., Sørensen, S. R., Tomkiewicz, J., and Butts, I. A. E. (2017). Temperature effects on gene expression and morphological development of European eel, *Anguilla anguilla* larvae. *PLoS One* **12**, e0182726. doi:10.1371/JOURNAL.PONE.0182726
- Rizzo, E., Godinho, H. P., and Sato, Y. (2003). Short-term storage of oocytes from the neotropical teleost fish *Prochilodus marggravii*. *Theriogenology* **60**, 1059–1070. doi:10.1016/S0093-691X(03)00108-0
- Saleh, A., Srinivasula, S. M., Balkir, L., Robbins, P. D., and Alnemri, E. S. (2000). Negative regulation of the Apaf-1 apoptosome by Hsp70. *Nat. Cell Biol.* **2**, 476–483. doi:10.1038/35019510
- Santacruz, H., Vriz, S., and Angelier, N. (1997). Molecular characterization of a heat shock cognate cDNA of zebrafish, hsc70, and developmental expression of the corresponding transcripts. *Dev. Genet.* **21**, 223–233. doi:10.1002/(SICI)1520-6408(1997)21:3<223::AID-DVG5>3.0.CO;2-9
- Santos, H. B., Sato, Y., Moro, L., Bazzoli, N., and Rizzo, E. (2008). Relationship among follicular apoptosis, integrin β_1 and collagen type IV during early ovarian regression in the teleost *Prochilodus argenteus* after induced spawning. *Cell Tissue Res.* **332**, 159–170. doi:10.1007/S00441-007-0540-1
- Somero, G. N. (2010). The physiology of climate change: how potentials for acclimatization and genetic adaptation will determine 'winners' and 'losers'. *J. Exp. Biol.* **213**, 912–920. doi:10.1242/JEB.037473
- Stefanovic, D. I., Manzon, L. A., McDougall, C. S., Boreham, D. R., Somers, C. M., Wilson, J. Y., and Manzon, R. G. (2016). Thermal stress and the heat shock response in embryonic and young of the year juvenile lake whitefish. *Comp. Biochem. Physiol. A Mol. Integr. Physiol.* **193**, 1–10. doi:10.1016/J.CBPA.2015.12.001
- Takle, H., McLeod, A., and Andersen, O. (2006). Cloning and characterization of the executioner caspases 3, 6, 7 and Hsp70 in hyperthermic Atlantic salmon (*Salmo salar*) embryos. *Comp. Biochem. Physiol. B Biochem. Mol. Biol.* **144**, 188–198. doi:10.1016/J.CBPA.2006.02.006
- Uchida, D., Yamashita, M., Kitano, T., and Iguchi, T. (2002). Oocyte apoptosis during the transition from ovary-like tissue to testes during sex differentiation of juvenile zebrafish. *J. Exp. Biol.* **205**, 711–718.
- Viveiros, A. T. M., and Godinho, H. P. (2009). Sperm quality and cryopreservation of Brazilian freshwater fish species: a review. *Fish Physiol. Biochem.* **35**, 137–150. doi:10.1007/S10695-008-9240-3
- Wargelius, A., Fjellidal, P. G., and Hansen, T. (2005). Heat shock during early somitogenesis induces caudal vertebral column defects in Atlantic salmon (*Salmo salar*). *Dev. Genes Evol.* **215**, 350–357. doi:10.1007/S00427-005-0482-0
- Whitehouse, L. M., McDougall, C. S., Stefanovic, D. I., Boreham, D. R., Somers, C. M., Wilson, J. Y., and Manzon, R. G. (2017). Development of the embryonic heat shock response and the impact of repeated thermal stress in early stage lake whitefish (*Coregonus clupeaformis*) embryos. *J. Therm. Biol.* **69**, 294–301. doi:10.1016/J.JTHERBIO.2017.08.013
- Wiegand, M. D., Hataley, J. M., Kitchen, C. L., and Buchanan, L. G. (1989). Induction of developmental abnormalities in larval goldfish, *Carassius auratus L.*, under cool incubation conditions. *J. Fish Biol.* **35**, 85–95. doi:10.1111/J.1095-8649.1989.TB03395.X
- Yabu, T., Todoriki, S., and Yamashita, M. (2001). Stress-induced apoptosis by heat shock, UV and γ -ray irradiation in zebrafish embryos detected by increased caspase activity and whole-mount TUNEL staining. *Fish. Sci.* **67**, 333–340. doi:10.1046/J.1444-2906.2001.00233.X



Effects of metal contamination on liver in two fish species from a highly impacted neotropical river: A case study of the Fundão dam, Brazil

André Alberto Weber^a, Camila Ferreira Sales^a, Francisco de Souza Faria^a,
Rafael Magno Costa Melo^a, Nilo Bazzoli^b, Elizete Rizzo^{a,*}

^a Departamento de Morfologia, Instituto de Ciências Biológicas, Universidade Federal de Minas Gerais, UFMG, Belo Horizonte, C.P.486, 30161-970, Minas Gerais, Brazil

^b Programa de Pós-graduação em Zoologia de Vertebrados, Pontifícia Universidade Católica de Minas Gerais, PUC Minas, Belo Horizonte, 30535-610, Minas Gerais, Brazil

ARTICLE INFO

Keywords:

Hoplias intermedius
Hypostomus affinis
Metallothionein
Oxidative stress
Doce river

ABSTRACT

Environmental disasters such as the rupturing of mine tailings dams are a major concern worldwide. In the present study, we assess the effects of the release of mine waste due to the rupture of the Fundão dam on two native fish species (*Hoplias intermedius* and *Hypostomus affinis*) from the Doce River basin. Two sampling sites were chosen: S1, a reference site, and S2, contaminated by mining waste. Water and sediment were collected to evaluate metals concentration. Adult fish were caught to analyse biological parameters, hepatic histopathology, and biomarkers of metal contamination. Compared to site S1, the concentration of manganese was statistically higher in water while lead, nickel, and arsenic were statistically higher in the sediment from site S2, and iron had no significant difference between sites. At site S1, fish of both species presented hepatic tissue with normal architecture. At site S2, hepatic alterations, such as cytoplasmic vacuolization and necrosis were frequently found in both species. Regarding the histopathological index, higher values were found in both species from site S2. The positive antibody reactions for cytochrome P450 1A (CYP1A) and metallothionein (MT) were statistically greater in site S2 for both species. The oxidative stress biomarkers, superoxide dismutase (SOD) and catalase (CAT) were statistically higher in *H. intermedius* from site S2, but only CAT was statistically greater in *H. affinis* at site S2. These results demonstrate that the release of mineral residues from the rupture of the Samarco mine dam is provoking hepatic damage in the fish from the Doce River besides inducing the expression of proteins and enzymes related to metal contamination.

1. Introduction

The disaster of mine tailings that occurred in the Doce River basin in November 2015, due to the rupture of the Fundão dam owned by Samarco S.A., was one of the largest mining disasters in the world (Cordeiro et al., 2019). It has been estimated that 43–60 million m³ of mining waste reached Doce River basin, contaminating more than 650 km of rivers until the Atlantic Ocean (Andrade et al., 2018; Segura et al., 2016).

Wild fish are continually exposed to different types of contaminants, so they are considered excellent models for assessing health status of aquatic ecosystems (Dane and Sisman, 2015; Paschoalini et al., 2019). Heavy metals may enter in the aquatic environment either naturally (e.g. geological processes) or anthropogenic (e.g. mining). The release of metals to aquatic environments by anthropogenic activities is much higher than those observed by natural processes (AnvariFar et al., 2018). To evaluate the effects of these metals on fish liver, several

biomarkers are frequently used including metallothionein (MT), cytochrome P450 (CYP1A), superoxide dismutase (SOD), catalase (CAT), and reduced glutathione (GSH) (Hermenean et al., 2015; Linde-Arias et al., 2008a, 2008b; Rajeshkumar et al., 2013; Rajeshkumar and Li, 2018).

The liver is the most important organ in drug metabolism and detoxification of different environmental contaminants (Bernet et al., 1999). Heavy metals can alter lipid and carbohydrate metabolism by binding or blocking nuclear receptors and can also activate cell death mechanisms, like caspases or some kinases involved with necrosis in liver (AnvariFar et al., 2018). Field studies demonstrate an association between metals contamination with steatosis and necrosis in fish liver (AnvariFar et al., 2018; Hermenean et al., 2015; Rajeshkumar et al., 2013).

The exposure of fish to metals promotes the induction of hepatic proteins, including metallothionein (MT) and cytochrome P450 1A (CYP1A) (Almeida et al., 2014). Metallothioneins are small proteins

* Corresponding author.

E-mail address: ictio@icb.ufmg.br (E. Rizzo).

involved in the binding and regulation of essential metals such as copper and zinc, and in the detoxification of toxic metals such as arsenic (As) (Coyle et al., 2002). For this reason, MT expression is an important biomarker to evaluate heavy metal exposure, both under laboratory and field conditions (Bervoets et al., 2013). Further, CYP1A is an enzyme that plays a role in the biotransformation of environmental toxicants and carcinogens, including heavy metals and is widely used in ecotoxicological field studies (Anjos et al., 2011; Lewis et al., 2006; Trídico et al., 2010).

Exposure to metals promotes changes in enzyme levels involved oxidative stress and antioxidant systems (Valavanidis et al., 2006). The accumulation of heavy metals leads to formation of free radicals and causing histological alterations on liver and other metabolic organs. Biomarkers at different levels of biological organization (molecules to populations) are important tools for assessing environmental pollution (Bernet et al., 1999).

The trahira *Hoplias intermedius* and the armoured catfish *Hypostomus affinis* are fish species widely distributed in the Doce River basin. These species are considered ecologically resistant to environmental changes because they are capable of living in highly impacted rivers (Vieira et al., 2015). *H. intermedius* is a large-sized characiform fish from the Erythrinidae family that has a piscivorous feeding habit (Oyakawa and Mattox, 2009), while *H. affinis* is a medium-sized siluriform fish of the Loricaridae family, which has a benthic habit and feeds on periphyton (Duarte et al., 2012). Both species are sedentary and do not migrate and have commercial importance for the riverine populations from the Doce River basin (Vieira et al., 2015).

Since the accident involving the dam rupture of Samarco mine at the end of 2015, no study has been carried out on fish contamination in the Doce River. Thus, the present study aims to evaluate, through histological, immunohistochemical, and enzymatic approaches, the impact of mine tailings on the liver of two fish species from the Doce River basin, south-eastern Brazil.

2. Material and methods

2.1. Sampling sites

Due to the high impact of the spill on the Doce River, fish populations in the impacted stretch are greatly reduced or absent. Initially a site was also proposed at Carmo River, however after some samplings no fish were caught due to the high level of contamination of this river. After some sampling trials, a site was defined in the Doce River that could capture species that were also found in the reference site, for comparative purposes. Two sampling sites along the Doce River basin were investigated (Fig. 1): (S1) situated on the Piranga River (20°20'5.95"S; 42°53'55.14"W) was chosen as a reference site because it was unaffected by the mine waste from the Fundão dam, and (S2) located on the Doce River (20°15'20.20"S; 42°54'3.49"W) that directly received the waste discharge from the Samarco dam by way of the Carmo River. Two samplings were carried out, March (rainy season) and June (dry season), 2018. For fish samplings, was used 80 m gillnets (eight gillnets of 10 m each), with a 4–8 cm stretched mesh size, deployed for about 12 h at each sampling site. Only alive fish were used in the present study, and euthanasia procedures followed the ethical principles established by the Brazilian College of Animal Experimentation (COBEA), and the study was approved by the Ethics Committee on Animal Use (CEUA, protocol N°189, 2016) of the Federal University of Minas Gerais, Brazil. A total of 12 *H. intermedius* (S1 – four and S2 - eight) and 14 *H. affinis* (S1 – eight and S2 - six) were analysed in the present study. Biometric data, total length (TL, 0.01 cm), body weight (BW, 0.01 g), and liver weight (LW, 0.001 g) were measured to calculate biological indices like, hepatosomatic index ($HSI = 100 LW/BW$) and Fulton condition factor ($K = 100 BW/TL^3$). All handling and euthanasia steps followed the standards established by Brazilian College of Animal Experimentation (COBEA), and Ethics Committee on

Animal Use of the Federal University of Minas Gerais, Brazil approved the conduct of the study (CEUA, protocol N°189, 2016).

2.2. Water and sediment samplings and metal analysis

The physico-chemical water parameters of the sampling sites were obtained from Institute of Water Management from Minas Gerais (IGAM, 2018), at same sampling sites that fish were collected.

Concentrations of iron (Fe), manganese (Mn), lead (Pb), nickel (Ni), and arsenic (As) were determined in water and sediment. Five samples of water and sediment were collected from each site. For water, 50 ml of sample was digested in 5 ml of nitric acid (HNO₃) in a microwave oven at a temperature of 160 °C for 10 min, and after cooling heated for a further 10 min. The preparation steps of the sediment samples followed the protocol described by Paschoalini et al. (2019). After that, samples and blank solutions were determined by an AA-680 Shimadzu (Kyoto, Japan) flame atomic absorption spectrometer (FAAS) in an air-acetylene flame, according to the user's manual, provided by the manufacturer. The concentrations of metals in the water and sediment were expressed in µg/L and 10 µg/g, respectively.

2.3. Histopathology and morphometry

Liver samples were fixed in Bouin's fluid for 24 h and then transferred to 70% ethanol. Then, the samples were submitted to routine histological techniques, i.e. dehydration in ethanol, embedded in paraffin, sectioned at 5 µm thickness, and stained with haematoxylin-eosin (HE).

The histopathological alterations were evaluated in 10 random fields per animal at 400× magnification. To calculate the histopathological alteration index (HAI), the hepatic alterations were classified in three progressive stages according the impairment of the organ functions: I (low severity: hepatocytes showing cellular hypertrophy, peripheral nucleus, cytoplasmic vacuolization and deformation of the cellular contour), II (middle severity: hepatocyte with pyknotic nucleus, presence of hyperemia and inflammatory infiltrate), and III (great severity: presence of focal or total necrosis and fibrosis. For each animal, an HAI value was calculated using the formula: $HAI = (1 \times S1) + (10 \times S2) + (100 \times S3)$, where I, II and III correspond to the number of alteration stages 1, 2 and 3 and S represents the sum of alterations in each stage (Poleksic and Mitrovic-Tutundzic, 1994). The mean HAI was classified as: normal tissue functioning (0–10), slight to moderate tissue damage (11–20), moderate to severe modification of tissue (21–100), and irreparable tissue damage (> 100) (Poleksic and Mitrovic-Tutundzic, 1994).

2.4. Metallothionein and cytochrome P450 (CYP1A)

Liver samples (n = 4 fish per species/site) were submitted to immunoperoxidase, using the primary polyclonal antibody rabbit anti-fish CYP1A (CP-226) and polyclonal rabbit anti-cod metallothionein (KH-1) from Biosense Laboratories AS, Bergen, Norway. Paraffin-embedded liver sections were submitted to xylene, ethanol and PBS washings. The slides were submitted to antigen retrieval in microwave for 45 min and incubate in 3% H₂O₂ for 10 min to inactivate the endogenous peroxidase. BSA 2% was used to block the unspecific staining. After that, the primary antibodies were applied overnight 4 °C. The biotinylated secondary antibody (Dako EnVision™ + Sistema Dual Link-HRP) was applied for 30 min and then 3'3'-diaminobenzidine (DAB) was utilized for the immunohistochemistry reactions and the sections were counterstained with haematoxylin. For each biomarker, 10 fields per slide were randomly chosen at 100× magnification, giving a total of 80 analysed fields (40 each site) per species. The results were expressed by stained area (%).

The specificity of the antibodies was confirmed by western blotting and in one slide primary antibody was omitted for negative control. All

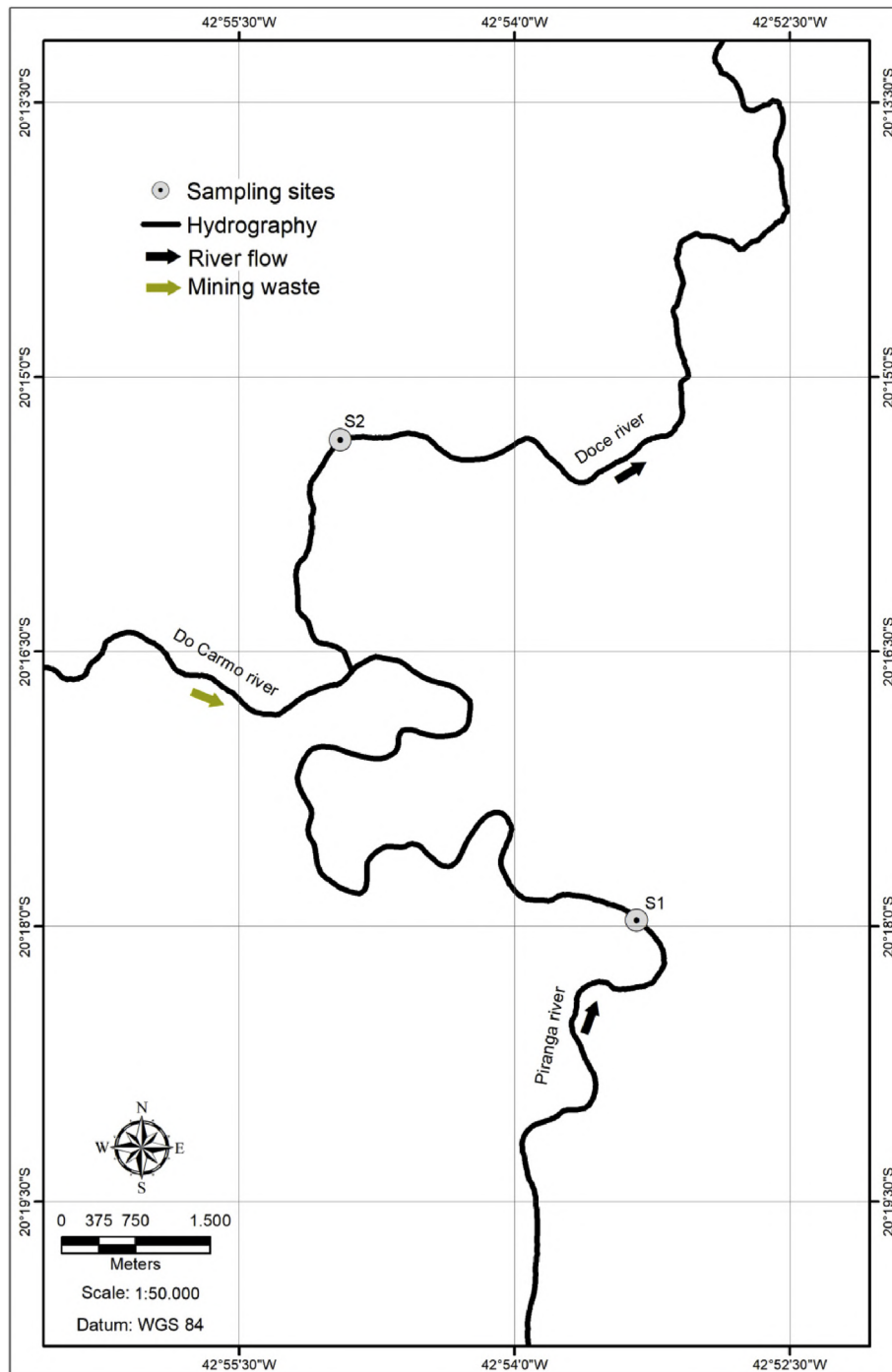


Fig. 1. Location of sampling sites, reference site (S1) at Piranga River and impacted site (S2) at Doce River after the confluence with Carmo River, Doce River basin, southeastern Brazil.

the steps of immunohistochemistry protocol and quantification were previously described by Paschoalini et al. (2019).

2.5. Oxidative stress biomarkers

Liver samples were immediately frozen in liquid nitrogen in field and then transferred to $-80\text{ }^{\circ}\text{C}$ freezer. Samples (0.1 g tissue) were homogenized with protease inhibitors cocktail, aprotinin and phenylmethanesulfonyl fluoride (Sigma-Aldrich) following the protocol described by Prado et al. (2014) at 1:2 ratio of tissue (m:v). After centrifugation for 1 h at 15,000 g at $4\text{ }^{\circ}\text{C}$ in an Eppendorf™ Centrifuge 5427 R, the supernatants were stored in aliquots at $-80\text{ }^{\circ}\text{C}$ until

analysis. The determination of superoxide dismutase (SOD), catalase (CAT), and reduced glutathione (GSH) levels were performed on duplicate samples by using commercial ELISA kits following the manufacturer's instructions (Cayman Chemicals, Ann Arbor). The SOD and CAT levels were expressed as U/ml and nmol/min/ml, respectively. For glutathione assay, the homogenates were previously deproteinized following manufacturer's protocol. The reduced glutathione (GSH) concentration was obtained by subtracting the oxidized glutathione (GSSG) level from the total glutathione. The GSH levels were calculated and were expressed as μM . The ELISA dilution curves for catalase ($y = 0.001x + 0.0175$, $R^2 = 0.9954$), superoxide dismutase ($y = 72.669x + 1.1513$, $R^2 = 0.9791$), total glutathione

($y = 0.0541x + 0.0156$, $R^2 = 0.9984$) and oxidized glutathione ($y = 0.1082x + 0.0156$, $R^2 = 0.9984$) showed high correlation with absorbance.

2.6. Statistical analysis

Prism Graph Pad 5.0 (Graph Pad software, San Diego, USA) was used in the statistical analyses. To check data normality was used Lillifors test. A non-paired T-student test was used to compare data obtained between sampling sites. Data were expressed as means \pm SD. P values < 0.05 were considered statistically significant, and statistically significant differences are indicated with * $p < 0.05$; ** $p < 0.01$; *** $p < 0.001$.

3. Results

3.1. Water quality parameters

The water temperature dissolved oxygen and pH varied from 18.4 to 26.7 °C, 6.7–8.4 mg/L and 6.0 to 7.7, respectively, with no significant differences between sampling sites ($p = 0.49$, $p = 0.18$ and $p = 0.93$, respectively). Conductivity ($p = 0.001$), total dissolved solids ($p = 0.04$), and turbidity ($p = 0.05$) had statistically higher values at site S2 (Table 1).

3.2. Metals concentrations in water and sediments

The metal loads of Fe, Pb, Ni, and As in the water showed no statistical differences between sites, ($p > 0.05$), but Mn was higher in S2 site ($p = 0.001$). Regarding sediment, Ni ($p = 0.001$), Pb ($p = 0.001$), and As ($p = 0.001$) were statistically higher in S2, but Fe and Mn showed no significant differences among sites ($p > 0.05$) (Table 2).

3.3. Liver histopathology

Both species had no significant differences in length, weight and biological indices ($p > 0.05$) (Table 3). Both species collected at site S1 presented hepatic tissue with normal architecture, showing hepatocytes with central nucleus forming cords around blood capillaries (Fig. 2A and C). Hepatic damage was mild and infrequent in fish from S1. For S2, fish from both species frequently presented cellular and tissue alterations, such as cytoplasmic vacuolization (Fig. 2E), disarrangement of hepatic cords, and flat nucleus in cell periphery, as well as hyperemia (Fig. 2G), inflammatory infiltrate (Fig. 2F), and tissue necrosis (Fig. 2D and H). Regarding the histopathological index, higher values were observed in fish captured at site S2 for *H. affinis* ($p = 0.001$) and *H. intermedius* ($p = 0.001$). Fish caught at site S2 presented a mean HAI greater than 100 for both species. However, fish caught at site S1 demonstrated an average HAI of 40 (Fig. 2).

Table 1

Water physico-chemical parameters in two sampling sites from the Doce River basin, south-eastern Brazil: (S1) Piranga River and (S2) Doce River.

Parameters	S1	S2
Temperature (°C)	22.2 \pm 2.8 ^a	23.2 \pm 2.3 ^a
Dissolved oxygen (mg/L)	7.6 \pm 0.5 ^a	8.0 \pm 0.3 ^a
pH	6.8 \pm 0.7 ^a	6.8 \pm 0.5 ^a
Conductivity (μ S/cm at 25 °C)	44.6 \pm 6.8 ^a	57.0 \pm 3.7 ^b
Dissolved solids (mg/L)	44.4 \pm 5.1 ^a	52.3 \pm 7.4 ^b
Turbidity (NTU)	15.4 \pm 19.0 ^a	66.1 \pm 75.1 ^b

Data represent a mean \pm standard deviation (SD) of samples per site. Different letters in the same row indicate significant differences among sampling sites.

Table 2

Concentrations of heavy metals in the water (μ g/L) and sediment (10 μ g/g) from Piranga River (S1) and Doce River (S2), Doce River basin, south-eastern Brazil.

Heavy metal	Site	Water (μ g/L)	Sediment (10 μ g/g)
Ni	S1	7.2 \pm 1.5 ^a	7.94 \pm 1.11 ^a
	S2	8.2 \pm 2.8 ^a	10.94 \pm 1.39 ^b
Fe	S1	458.2 \pm 72.9 ^a	847.8 \pm 55.8 ^a
	S2	455.6 \pm 167.3 ^a	775.9 \pm 102.7 ^a
Mn	S1	50 \pm 10.6 ^a	15.4 \pm 4.1 ^a
	S2	132.8 \pm 14.9 ^b	16.4 \pm 2.4 ^a
Pb	S1	50.4 \pm 18.7 ^a	1.3 \pm 0.1 ^a
	S2	22.2 \pm 23.7 ^a	1.8 \pm 0.1 ^a
As	S1	< LQ	0.04 \pm 0.02 ^a
	S2	< LQ	0.12 \pm 0.01 ^a

Data represent mean \pm standard deviation (SD) of 5 samples per site. Different letters between sites indicate significant differences. (Ni) nickel, (Fe) iron, (Mn) manganese, (Pb) lead and (As) arsenic. < LQ, limit on quantification.

Table 3

Biological indices of *Hoplias intermedius* and *Hypostomus affinis* from the Piranga River (S1) and Doce River (S2), Doce River basin, south-eastern Brazil.

	<i>Hoplias intermedius</i>		<i>Hypostomus affinis</i>	
	S1	S2	S1	S2
TL (cm)	34.5 \pm 6.3 ^a	36.4 \pm 2.2 ^a	24.9 \pm 1.2 ^a	27.8 \pm 2.1 ^a
BW (kg)	0.57 \pm 0.31 ^a	0.58 \pm 0.12 ^a	0.16 \pm 0.03 ^a	0.17 \pm 0.04 ^a
IHS	1.36 \pm 0.6 ^a	1.05 \pm 0.24 ^a	0.2 \pm 0.02 ^a	1.38 \pm 0.12 ^a
K	1.1 \pm 0.01 ^a	1.04 \pm 0.04 ^a	0.94 \pm 0.04 ^a	0.74 \pm 0.02 ^b

Data represent mean \pm standard deviation of 4–11 measures. In each line, different letters in the same row indicate significant differences between sites ($p < 0.05$). (TL) total length, (BW) body weight, (HSI) hepatosomatic index and (K) Fulton condition factor.

3.4. Cytochrome P450 1A (CYP1A) and metallothionein (MT)

The immunolabelling for CYP1A was cytoplasmic and spread through the hepatic parenchyma (Fig. 3A, E, C and G). Positive reactions for CYP1A were statistically higher for both species in site S2. For *H. intermedius*, the mean labelled area (%) was 9.18 \pm 0.56 in fish from S2, while it was 3.60 \pm 0.30 in fish from S1 ($p = 0.001$) (Fig. 3). Regarding *H. affinis*, the mean marked area (%) was 7.67 \pm 0.43 for S2 and 1.99 \pm 0.17 for S1 ($p = 0.001$) (Fig. 3).

Similar to CYP1A, MT positive reactions were statistically higher in fish from S2 for both species (Fig. 3B, F, D and H). For *H. affinis*, the mean marked area (%) was 5.04 \pm 0.27 for S2 and 0.88 \pm 0.13 for S1 ($p = 0.001$) (Fig. 3). Regarding *H. intermedius*, the mean positive area (%) for MT was 4.49 \pm 0.30 for S2 while it was 1.86 \pm 0.19 for S1 ($p = 0.001$) (Fig. 3).

3.5. Levels of oxidative stress biomarkers

The SOD activity in *H. intermedius* was statically higher in fish from S2 ($p = 0.04$) but no statistical difference was observed in *H. affinis* ($p = 0.65$). The CAT activity in *H. intermedius* and *H. affinis* from site S2 was statically higher ($p = 0.001$ and $p = 0.04$, respectively). Regarding GSH, *H. intermedius* and *H. affinis* showed no statistical differences between sites S1 and S2 ($p > 0.05$) (Fig. 4).

4. Discussion

The Doce River is one of the most important Brazilian rivers for fish biodiversity and urban water supply. It is located inside the Atlantic Rainforest biome and has a high degree of fish species endemism (Myers et al., 2000). The Samarco dam disaster drastically affected the landscape and the aquatic environments such as Doce River and

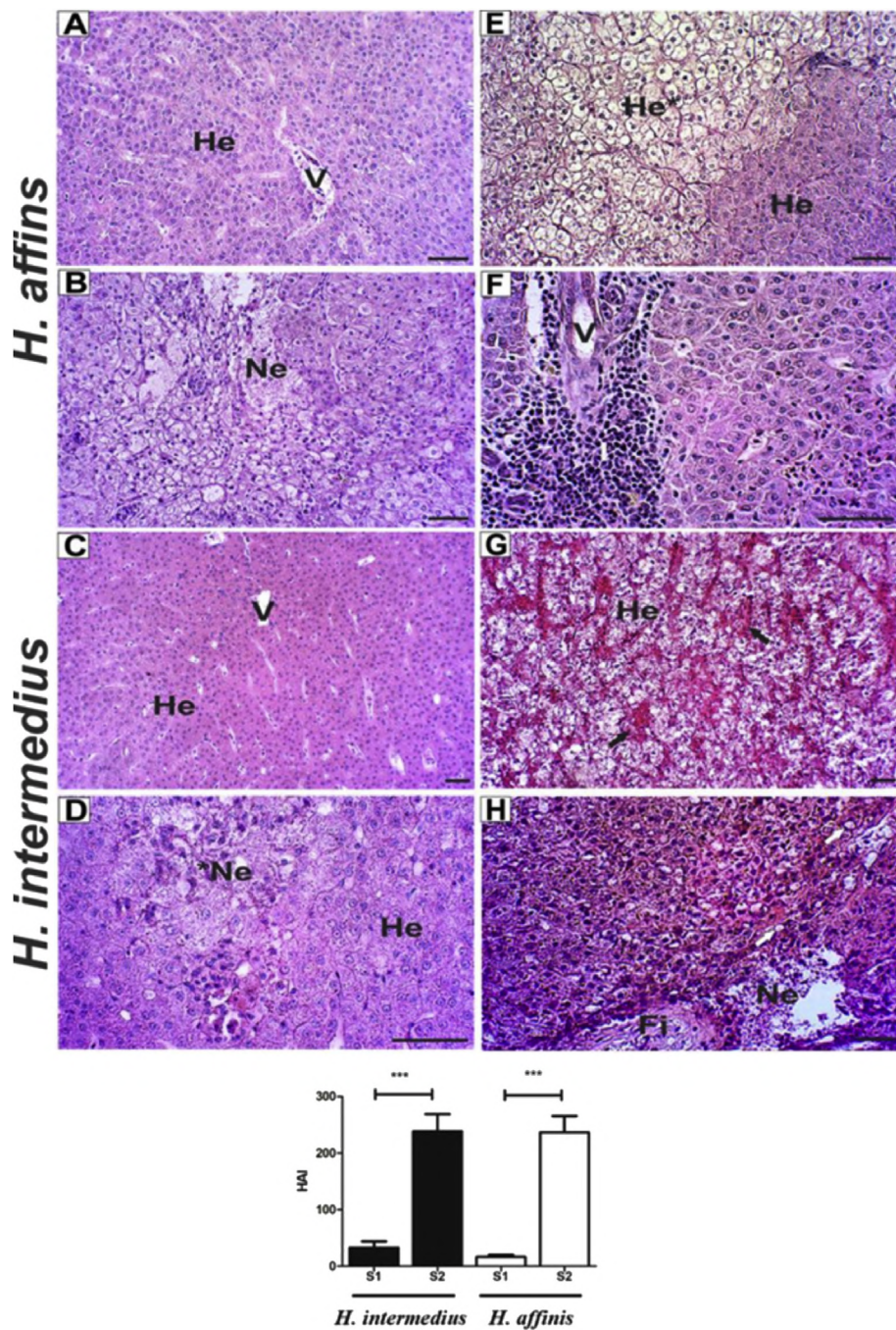


Fig. 2. Histological sections of hepatic tissue of *H. intermedius* and *H. affinis*. (A and C) normal liver of fish collected in S1, hepatocytes with the central nucleus arranged in cords and located around blood capillaries; (B) *H. affinis* necrotic hepatic tissue of fish collected in S2 (E and H) Pathological processes such as cytoplasmic vacuolization, cell contour deformation, inflammatory infiltrate, disruption of hepatic cords and nucleus at the periphery of the cell were found more frequently in fish collected at site S2. (F) Inflammatory infiltrate; (G) Hyperemia with enlarged blood vessels, (D and H) focal and multifocal necrosis were also observed in both species collected in S2. He – normal hepatic tissue, Ne – necrotic hepatic tissue and I – inflammatory infiltrate, Fi-fibrosis, V – vessel. Scale bars: 50 μ m (A, B, C, E, G and H) and 20 μ m (F and D). (Graph) Histopathology index (HAI) of both species. The values were measured as means and standard deviation (SD). (***) statistical difference ($p = 0.001$).

Atlantic Ocean (Cordeiro et al., 2019; do Carmo et al., 2017; Segura et al., 2016). In the present study, it was shown for the first time the effects of the release of mine tailings on liver histopathology and different biomarkers of metal contamination in two native fish species from the Doce River basin.

The concentrations of As, Ni, and Pb in the sediment and higher values of conductivity, total dissolved solids and turbidity at site S2 (Doce River) were statistically higher than site S1 (Piranga River), with these differences possibly being related to the rupture of the Fundão dam that has affected site S2 but not influenced site S1. The concentrations of Ni and Pb at site S2 have similar concentrations when compared to highly polluted rivers, such as the Ganges River in India, the Buriganga River in Bangladesh, and the Tur River in Romania (Ahmad et al., 2010; Hermenean et al., 2015; Singh et al., 2005). The iron (Fe) levels at both sites were high because this region of the iron quadrangle has high levels

of iron in the soil (Vicq et al., 2015). Manganese, which is an essential metal, was found in high concentrations in waters at Doce River. A study with *Oreochromis niloticus* showed that fishes exposed to manganese at high concentrations can promote DNA damage and activates oxidative stress in the liver (Coppo et al., 2018). Metal studies after the Fundão dam collapse were performed on sediments of the Doce River estuary (Espírito Santo state, Brazil) seven days after the arrival of the contamination plume and were found in large concentrations: Fe: $45,200 \pm 2850$; Mn: 433.0 ± 110.0 ; Ni: 24.7 ± 10.4 ; Pb: 20.2 ± 4.6 (μ g/g) (Queiroz et al., 2018). The present study demonstrated a lower concentration of Fe and Mn and higher Ni when compared to the study carried out when the disaster occurred, probably indicating a sedimentation of these metals over time.

Fish caught at site S2 presented greater hepatic histopathological alteration indices, with a higher frequency of vacuolization and

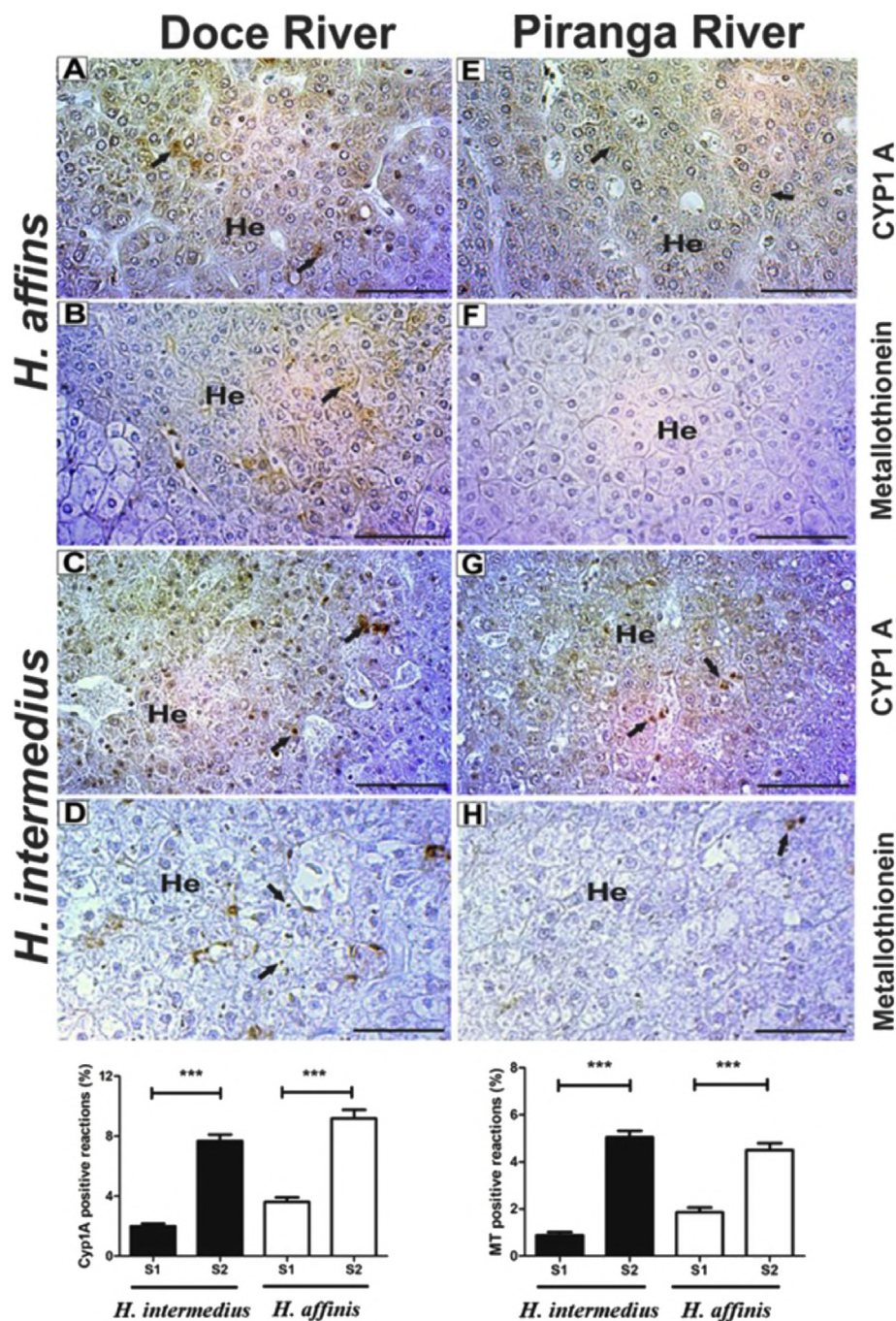


Fig. 3. (A-H) Immunoperoxidase reaction for cytochrome P450 (CYP1A) and metallothionein (MT) in the liver of *H. intermedius* and *H. affinis* from Piranga River (S1) and Doce River (S2), south-eastern Brazil. Black arrows = positive reactions. Scale bars: 40 μ m. Quantification of reactions to (left graph) cytochrome P450 (CYP1A) and (right graph) metallothionein (MT). The values were measured as means and standard deviation (SD). (***) statistical difference ($p = 0.001$).

hypertrophy of hepatocytes and areas of necrosis, than fish from site S1. Studies have shown that exposure to metals affects the development of these histopathology (Dane and Sisman, 2015; Wolf and Wheeler, 2018). The hypertrophy of hepatocytes can be associate with an increase of metabolic activity and accumulation of lipid droplets in the cytoplasm (Braunbeck et al., 1990). Studies with *Oreochromis mossambicus* exposed to As (Ahmed et al., 2013), *Hypophthalmichthys molitrix* exposed to Ni (Athikesavan et al., 2006), and *Clarias gariepinus* exposed to Pb (Olojo et al., 2005). However in present study no lipid infiltration was observed in liver sections. The oxidation of fatty acids is an important source of reactive oxygen species (ROS) (Mannaerts et al., 2000). Some of the consequences of increased ROS include cell death

processes (necrosis/apoptosis), pro-inflammatory cytokines release and lipid accumulation (Bergamini et al., 2005; Robertson et al., 2001). A study using HepG2 and *Allium cepa* cells in contact with contaminated water from the Doce River after the Samarco accident demonstrated DNA damage and reduced mitotic index (Segura et al., 2016). In this sense, necrosis and inflammatory infiltrate frequently found in fish from site S2 may be related to the increase of oxidative stress in the hepatocytes.

The liver is the most important organ for metal contamination analysis in aquatic environments due to its high level of binding proteins (e.g. metallothioneins) (Marijić and Raspur, 2007). The expression of hepatic metallothionein in *H. affinis* and *H. intermedius* at site S2 were

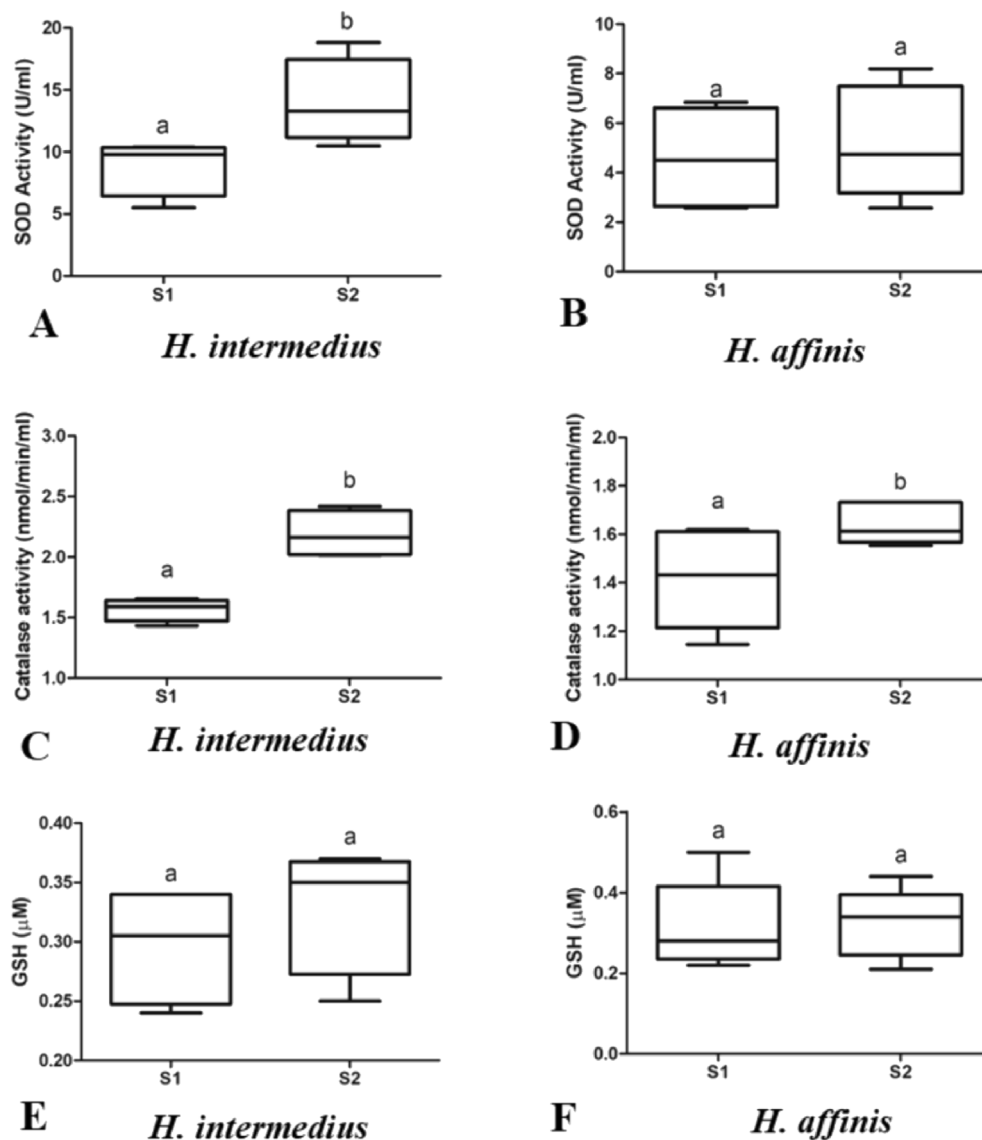


Fig. 4. Box plots graphs indicating levels of oxidative stress biomarkers in the liver. Superoxide dismutase, catalase and glutathione reduced in *H. intermedius* (A, C and E) and in *H. affinis* (B, D and F). Central bar indicates the median, the box represents the interquartile range and the whiskers are the minimum and maximum values. Different letters indicate statistical differences among groups ($p < 0.05$).

3.8-fold and 2.5-fold higher, respectively, than the levels expressed in the specimens from site S1, a reference site in this study. Studies with As, Ni, and Pb, metals with higher concentrations in site S2 of the present study, demonstrate a significant increase in the levels of hepatic metallothionein (Campana et al., 2003; Ptashynski et al., 2001; Roy and Bhattacharya, 2006). Fe and Mg, which exhibited similar concentrations between sites, do not appear to induce the expression of metallothionein (Sevcikova et al., 2011). The high levels of hepatic metallothionein in the two species of the present study may be related to the action of several metals acting together, as observed in some rivers polluted by metals (Linde-Arias et al., 2008b, 2008a; Paschoalini et al., 2019).

Some metals promote the activation of nuclear receptors in hepatocytes, such as the aryl hydrocarbon receptor (AhR) triggering the expression of CYP1A (Schlenk et al., 2008). Most studies with CYP1A report the activation of this enzyme only through contamination by organic pollutants, such polycyclic aromatic hydrocarbons (PAHs). However, this monooxygenase can be induced by several metals such as zinc (Zn), lead (Pb), and cadmium (Cd) (Faverney et al., 2000; Huang et al., 2014).

Antioxidant enzymes are important in decreasing oxidative stress induced by environmental contaminants (Saglam et al., 2014). Some metals like Pb may increase the production of superoxide radicals. The role of SOD is to eliminate free radicals by converting them to hydrogen peroxide (Ni et al., 2004). In the present study, only *H. intermedius* presented a significant increase in SOD. On the other hand, catalase is the enzyme responsible for neutralizing hydrogen peroxide formed by SOD. This enzyme was observed at high levels in the two species analysed at impacted site S2. Reduced glutathione (GSH) reacts with various environmental contaminants as well as metals (Bussolaro et al., 2010; Hermenean et al., 2015; Rajeshkumar and Li, 2018). However, the GSH levels did not change between sites for both species. Some authors suggest that the liver of herbivorous bottom fish such as *H. commersoni*, possess an antioxidant defence mechanism that is more efficient than piscivorous fish like *H. malabaricus*, since the antioxidant enzymes were less altered in *H. commersoni* exposed to DDT and methylmercury (Bussolaro et al., 2010). In this sense, our data indicate that *H. intermedius*, a piscivorous species, has a greater oxidative stress response than *H. affinis*, and it is therefore a more appropriate species for studies of aquatic contamination.

5. Conclusion

In summary, this study demonstrated for the first time the effects of the release of mine waste on two fish species from the Doce River. The results demonstrate that the two species analysed presented great damage to the liver and the induction of proteins and enzymes associated with metal contamination at impacted site. The two species of the present study were chosen because of their ability to inhabit highly altered environments (Parente et al., 2009; Vicari et al., 2018). Thus, species more sensitive to environmental modifications may not resist this highly contaminated aquatic environment. In the reference site (S1) were also captured other fish species, i.e. two characiforms (*Astyanax bimaculatus* and *Oligosarcus argenteus*), one perciform (*Geophagus brasiliensis*) and two siluriforms (*Hypostomus auroguttatus* and *Rhamdia quelen*). However, the site impacted by the spill was captured only *H. intermedius* and *H. affinis*. This reinforces the plasticity of the two species utilized in this study to inhabit places with a high degree of contamination. The biomarkers used in this study were efficient in the detection of metals contamination in the Doce River, and their use is recommended in environmental monitoring programs. In addition, this study points out the need to carry out restoration and decontamination programs for the Doce River.

Author contribution section

André A. Weber: Conceptualization, Methodology, Investigation, Formal Analysis, Writing-original draft, Writing - Review & Editing. Camila F. Sales: Methodology, Formal analysis, Methodology, Writing - Review & Editing. Francisco S. Faria: Methodology, Formal Analysis. Rafael M. C. Melo: Conceptualization, Investigation, Methodology, Formal Analysis. Nilo Bazzoli: Funding Acquisition, Supervision, Project Administration. Elizete Rizzo: Supervision, Conceptualization, Funding Acquisition, Writing-original draft, Writing - Review & Editing.

Acknowledgments

The study was supported by Brazilian funding agencies: Conselho Nacional Científico e Tecnológico (CNPq 407778/2016-0 and 305132/2015-6), Fundação de Amparo a Pesquisa do Estado de Minas Gerais (FAPEMIG 01/2015 - CVZ-APQ-00898-15). This study was partially financed by the Coordenação de Aperfeiçoamento de Pessoal de Nível Superior - Brasil (CAPES) - Finance Code 001.

References

- Ahmad, M.K., Islam, S., Rahman, S., Haque, M.R., Islam, M.M., 2010. Heavy metals in water, sediment and some fishes of buriganga river, Bangladesh. *Int. J. Environ. Res.* 4, 321–332. <https://doi.org/10.1016/j.aquatox.2018.01.013>.
- Ahmed, M.K., Habibullah-Al-Mamun, M., Parvin, E., Akter, M.S., Khan, M.S., 2013. Arsenic induced toxicity and histopathological changes in gill and liver tissue of freshwater fish, tilapia (*Oreochromis mossambicus*). *Exp. Toxicol. Pathol.* 65, 903–909. <https://doi.org/10.1016/j.etp.2013.01.003>.
- Almeida, E.A. De, Rodrigues, A.C.F., de Oliveira Ribeiro, C.A., Almeida, E.A. De, de Oliveira Ribeiro, C.A., 2014. Introduction—pollution and fish health in tropical ecosystems: a brief summary on current challenges and perspectives. In: *Pollution and Fish Health in Tropical Ecosystems*. Taylor & Francis, London, pp. 1–14.
- Andrade, G.F., Paniz Jr., F.P., Martins, A.C., Rocha, B.A., Lobato, A.K. da S., Rodrigues, J.L., Cardoso-Gustavson, P., Masuda, H.P., Batista, B.L., 2018. Agricultural use of Samarco's spilled mud assessed by rice cultivation: a promising residue use? *Chemosphere* 193, 892–902. <https://doi.org/10.1016/j.chemosphere.2017.11.099>.
- Anjos, N.A., Schulze, T., Brack, W., Val, A.L., Schirmer, K., Scholz, S., 2011. Identification and evaluation of cyp1a transcript expression in fish as molecular biomarker for petroleum contamination in tropical fresh water ecosystems. *Aquat. Toxicol.* 103, 46–52. <https://doi.org/10.1016/j.aquatox.2011.02.004>.
- AnvariFar, H., Amirkolaie, A.K., Jalali, A.M., Miandare, H.K., Sayed, A.E.D.H., Üçüncü, S., Ouraji, H., Ceci, M., Romano, N., 2018. Environmental pollution and toxic substances: cellular apoptosis as a key parameter in a sensible model like fish. *Aquat. Toxicol.* 204, 144–159. <https://doi.org/10.1016/j.aquatox.2018.09.010>.
- Athikesavan, S., Vincent, S., Ambrose, T., Velmurugan, B., 2006. Nickel induced histopathological changes in the different tissues of freshwater fish, *Hypophthalmichthys molitrix* (Valenciennes). *J. Environ. Biol.* 27, 391–395.
- Bergamini, C., Gambetti, S., Dondi, A., Cervellati, C., 2005. Oxygen, reactive oxygen species and tissue damage. *Curr. Pharmaceut. Des.* 10, 1611–1626. <https://doi.org/10.2174/1381612043384664>.
- Bernet, D., Schmidt, H., Meier, W., Burkhardt-Holm, P., Wahli, T., 1999. Histopathology in fish: proposal for a protocol to assess aquatic pollution. *J. Fish Dis.* 22, 25–34. <https://doi.org/10.1046/j.1365-2761.1999.00134.x>.
- Bervoets, L., Knapen, D., De Jonge, M., Van Campenhout, K., Blust, R., 2013. Differential hepatic metal and metallothionein levels in three feral fish species along a metal pollution gradient. *PLoS One* 8, e60805. <https://doi.org/10.1371/journal.pone.0060805>.
- Braunbeck, T., Storch, V., Bresch, H., 1990. Species-specific reaction of liver ultra-structure in zebrafish (*Brachydanio rerio*) and trout (*Salmo gairdneri*) after prolonged exposure to 4-chloroaniline. *Arch. Environ. Contam. Toxicol.* 19, 405–418. <https://doi.org/10.1007/BF01054986>.
- Bussolaro, D., Filipak Neto, F., Oliveira Ribeiro, C.A., 2010. Responses of hepatocytes to DDT and methyl mercury exposure. *Toxicol. In Vitro* 24, 1491–1497. <https://doi.org/10.1016/j.tiv.2010.07.016>.
- Campana, O., Sarasquete, C., Blasco, J., 2003. Effect of lead on ALA-D activity, metallothionein levels, and lipid peroxidation in blood, kidney, and liver of the toadfish *Halobatrachus didactylus*. *Ecotoxicol. Environ. Saf.* 55, 116–125. [https://doi.org/10.1016/S0147-6513\(02\)00093-3](https://doi.org/10.1016/S0147-6513(02)00093-3).
- Coppo, G.C., Passos, L.S., Lopes, T.O.M., Pereira, T.M., Merçon, J., Cabral, D.S., Barbosa, B.V., Caetano, L.S., Kampke, E.H., Chippari-Gomes, A.R., 2018. Genotoxic, biochemical and bioconcentration effects of manganese on *Oreochromis niloticus* (Cichlidae). *Ecotoxicology* 27, 1150–1160. <https://doi.org/10.1007/s10646-018-1970-0>.
- Cordeiro, M.C., Garcia, G.D., Rocha, A.M., Tschöcke, D.A., Campeão, M.E., Appolinario, L.R., Soares, A.C., Leomil, L., Froes, A., Bahiense, L., Rezende, C.E., de Almeida, M.G., Rangel, T.P., De Oliveira, B.C.V., de Almeida, D.Q.R., Thompson, M.C., Thompson, C.C., Thompson, F.L., 2019. Insights on the freshwater microbiomes metabolic changes associated with the world's largest mining disaster. *Sci. Total Environ.* 654, 1209–1217. <https://doi.org/10.1016/j.scitotenv.2018.11.112>.
- Coyle, P., Philcox, J.C., Carey, L.C., Rofe, A.M., 2002. Metallothionein: the multipurpose protein. *Cell. Mol. Life Sci.* 59, 627–647. <https://doi.org/10.1007/s00018-002-8454-2>.
- Dane, H., Sisman, T., 2015. Histopathological changes in gill and liver of capoeta capoeta living in the karasu river, erzurum. *Environ. Toxicol.* 30, 904–917. <https://doi.org/10.1002/tox.21965>.
- do Carmo, Flávio Fonseca, Kamino, L.H.Y., Junior, R.T., de Campos, I.C., do Carmo, Fonseca, Felipe, Silvino, G., de Castro, K.J., da, S.X., Mauro, M.L., Rodrigues, N.U.A., Miranda, M.P., Pinto, C.E.F., 2017. Fundão tailings dam failures: the environment tragedy of the largest technological disaster of Brazilian mining in global context. *Perspect. Ecol. Conserv.* 15, 145–151. <https://doi.org/10.1016/j.pecon.2017.06.002>.
- Duarte, S., Araújo, F.G., Bazzoli, N., 2012. Reproductive plasticity of *Hypostomus affinis* (Siluriformes: loriciidae) as a mechanism to adapt to a reservoir with poor habitat complexity. *Zool* 28, 577–586. <https://doi.org/10.1590/s1984-46702011000500005>.
- Faverney, C.R., Lafaurie, M., Girard, J.P., Rahmani, R., 2000. Effects of heavy metals and 3-methylcholanthrene on expression and induction of CYP1A1 and metallothionein levels in trout (*Oncorhynchus mykiss*) hepatocyte cultures. *Environ. Toxicol. Chem.* 19, 2239–2248. <https://doi.org/10.1002/etc.5620190914>.
- Hermenean, A., Damache, G., Albu, P., Ardelean, A., Ardelean, G., Puiu Ardelean, D., Horge, M., Nagy, T., Braun, M., Zsuga, M., Kéki, S., Costache, M., Dinischiotu, A., 2015. Histopathological alterations and oxidative stress in liver and kidney of *Leuciscus cephalus* following exposure to heavy metals in the Tur River, North Western Romania. *Ecotoxicol. Environ. Saf.* 119, 198–205. <https://doi.org/10.1016/j.ecoenv.2015.05.029>.
- Huang, G.Y., Ying, G.G., Liang, Y.Q., Liu, S.S., Liu, Y.S., 2014. Expression patterns of metallothionein, cytochrome P450 1A and vitellogenin genes in western mosquitofish (*Gambusia affinis*) in response to heavy metals. *Ecotoxicol. Environ. Saf.* 105, 97–102. <https://doi.org/10.1016/j.ecoenv.2014.04.012>.
- IGAM, 2018. Qualidade Das Águas Superficiais em Minas Gerais em 2018. MG Institute of Water management, pp. 1–19. <http://www.igam.mg.gov.br/>.
- Lewis, N.A., Williams, T.D., Chipman, J.K., 2006. Functional analysis of a metal response element in the regulatory region of flounder cytochrome P450 1A and implications for environmental monitoring of pollutants. *Toxicol. Sci.* 92, 387–393. <https://doi.org/10.1093/toxsci/kfl023>.
- Linde-Arias, A.R., Inácio, A.F., de Albuquerque, C., Freire, M.M., Moreira, J.C., 2008a. Biomarkers in an invasive fish species, *Oreochromis niloticus*, to assess the effects of pollution in a highly degraded Brazilian River. *Sci. Total Environ.* 399, 186–192. <https://doi.org/10.1016/j.scitotenv.2008.03.028>.
- Linde-Arias, A.R., Inácio, A.F., Novo, L.A., de Albuquerque, C., Moreira, J.C., 2008b. Multi-biomarker approach in fish to assess the impact of pollution in a large Brazilian river, Paraíba do Sul. *Environ. Pollut.* 156, 974–979. <https://doi.org/10.1016/j.envpol.2008.05.006>.
- Mannaerts, G.P., Van Veldhoven, P.P., Casteels, M., 2000. Peroxisomal lipid degradation via beta- and alpha-oxidation in mammals. *Cell Biochem. Biophys.* 32, 73–87.
- Marijić, V.F., Raspor, B., 2007. Metal exposure assessment in native fish, *Mullus barbatus* L., from the Eastern Adriatic Sea. *Toxicol. Lett.* 168, 292–301. <https://doi.org/10.1016/j.toxlet.2006.10.026>.
- Myers, N., Mittermeier, R.A., Mittermeier, C.G., da Fonseca, G.A., Kent, J., 2000. Biodiversity hotspots for conservation priorities. *Nature* 403, 853–858. <https://doi.org/10.1038/35002501>.
- Ni, Z., Hou, S., Barton, C.H., Vaziri, N.D., 2004. Lead exposure raises superoxide and hydrogen peroxide in human endothelial and vascular smooth muscle cells. *Kidney Int.* 66, 2329–2336. <https://doi.org/10.1111/j.1523-1755.2004.66032.x>.
- Olojo, E.A.A., Mbaka, G., Oluwemimo, 2005. Histopathology of the gill and liver tissues

- of the African catfish *Clarias gariepinus* exposed to lead. *Afr. J. Biotechnol.* 4, 117–122.
- Oyakawa, O.T., Mattox, G.M.T., 2009. Revision of the Neotropical trahiras of the Hoplias lacerdae species-group (Ostariophysi: characiformes: Erythrinidae) with descriptions of two new species. *Neotrop. Ichthyol.* <https://doi.org/10.1590/s1679-62252009000200001>.
- Parente, T.E.M., De-Oliveira, A.C.A.X., Beghini, D.G., Chapeaurouge, D.A., Perales, J., Paumgarten, F.J.R., 2009. Lack of constitutive and inducible ethoxyresorufin-O-deethylase activity in the liver of suckermouth armored catfish (*Hypostomus affinis* and *Hypostomus auroguttatus*, Loricariidae). *Comp. Biochem. Physiol. C Toxicol. Pharmacol.* 150, 252–260. <https://doi.org/10.1016/j.cbpc.2009.05.006>.
- Paschoalini, A.L., Savassi, L.A., Arantes, F.P., Rizzo, E., Bazzoli, N., 2019. Heavy metals accumulation and endocrine disruption in *Prochilodus argenteus* from a polluted neotropical river. *Ecotoxicol. Environ. Saf.* 169, 539–550. <https://doi.org/10.1016/j.ecoenv.2018.11.047>.
- Poleksic, V., Mitrovic-Tutundzic, V., 1994. Sublethal and chronic effects of pollutants on freshwater fish. In: Müller, R., Lody, R. (Eds.), *Fish Gills as a Monitor of Sublethal and Chronic Effects of Pollution*. Cambridge University Press, Cambridge, pp. 339–352.
- Prado, P.S., Pinheiro, A.P.B., Bazzoli, N., Rizzo, E., 2014. Reproductive biomarkers responses induced by xenoestrogens in the characid fish *Astyanax fasciatus* inhabiting a South American reservoir: an integrated field and laboratory approach. *Environ. Res.* 131, 165–173. <https://doi.org/10.1016/j.envres.2014.03.002>.
- Ptashynski, M.D., Pedlar, R.M., Evans, R.E., Wautier, K.G., Baron, C.L., Klaverkamp, J.F., 2001. Accumulation, distribution and toxicology of dietary nickel in lake whitefish (*Coregonus clupeaformis*) and lake trout (*Salvelinus namaycush*). *Comp. Biochem. Physiol. C Toxicol. Pharmacol.* 130, 145–162. [https://doi.org/10.1016/S1532-0456\(01\)00228-9](https://doi.org/10.1016/S1532-0456(01)00228-9).
- Queiroz, H.M., Nóbrega, G.N., Ferreira, T.O., Almeida, L.S., Romero, T.B., Santaella, S.T., Bernardino, A.F., Otero, X.L., 2018. The Samarco mine tailing disaster: a possible time-bomb for heavy metals contamination? *Sci. Total Environ.* 637–638. <https://doi.org/10.1016/j.scitotenv.2018.04.370>.
- Rajeshkumar, S., Li, X., 2018. Bioaccumulation of heavy metals in fish species from the meiliang bay, taihu lake, China. *Toxicol. Reports* 5, 288–295. <https://doi.org/10.1016/j.toxrep.2018.01.007>.
- Rajeshkumar, S., Mini, J., Munuswamy, N., 2013. Effects of heavy metals on antioxidants and expression of HSP70 in different tissues of Milk fish (*Chanos chanos*) of Kaattuppalli Island, Chennai, India. *Ecotoxicol. Environ. Saf.* 98, 8–18. <https://doi.org/10.1016/j.ecoenv.2013.07.029>.
- Robertson, G., Leclercq, I., Farrell, G.C., Konstandi, M., Cheng, J., Gonzalez, F.J., Savransky, V., Reinke, C., Jun, J., Bevans-fonti, S., Li, J., Myers, A.C., Torbenson, M.S., Polotsky, V.Y., 2001. Nonalcoholic Steatosis and Steatohepatitis: II. Cytochrome P-450 enzymes and oxidative stress. *Am. J. Physiol. Gastrointest. Liver Physiol.* 281, G1135–G1139.
- Roy, S., Bhattacharya, S., 2006. Arsenic-induced histopathology and synthesis of stress proteins in liver and kidney of *Channa punctatus*. *Ecotoxicol. Environ. Saf.* <https://doi.org/10.1016/j.ecoenv.2005.07.005>.
- Saglam, D., Guluzar, A., Dogan, Z., Baysoy, E., Gurler, C., Eroglu, A., Canli, M., 2014. Response of the antioxidant system of freshwater fish (*Oreochromis niloticus*) exposed to metals (Cd, Cu) in differing hardness. *Turk. J. Fish. Aquat. Sci.* 14, 43–52. https://doi.org/10.4194/1303-2712-v14_1_06.
- Schlenk, D., Celander, M., Gallagher, E.P., George, S., James, M., Kullman, S.W., Van Den Hurk, P., Willett, K., 2008. Biotransformation in fishes. *The Toxicology of Fishes*. <https://doi.org/10.1201/9780203647295>.
- Segura, F.R., Nunes, E.A., Paniz, F.P., Paulelli, A.C.C., Rodrigues, G.B., Braga, G.Ú.L., dos Reis Pedreira Filho, W., Barbosa, F., Cerchiaro, G., Silva, F.F., Batista, B.L., 2016. Potential risks of the residue from Samarco's mine dam burst (Bento Rodrigues, Brazil). *Environ. Pollut.* 218, 813–825. <https://doi.org/10.1016/j.envpol.2016.08.005>.
- Sevcikova, M., Modra, H., Slaninova, A., Svobodova, Z., 2011. Metals as a cause of oxidative stress in fish: a review. *Vet. Med. (Praha)*. 56, 537–546. <https://doi.org/10.17221/4272-VETMED>.
- Singh, K.P., Mohan, D., Singh, V.K., Malik, A., 2005. Studies on distribution and fractionation of heavy metals in Gomti river sediments - a tributary of the Ganges, India. *J. Hydrol.* 312, 14–27. <https://doi.org/10.1016/j.jhydrol.2005.01.021>.
- Trídico, C.P., Ferreira, A.C.R., Nogueira, L., da Silva, D.C., Moreira, A.B., de Almeida, E.A., 2010. Biochemical biomarkers in *Oreochromis niloticus* exposed to mixtures of benzo[a]pyrene and diazinon. *Ecotoxicol. Environ. Saf.* 73, 858–863. <https://doi.org/10.1016/j.ecoenv.2010.01.016>.
- Valavanidis, A., Vlahogianni, T., Dassenakis, M., Scoullou, M., 2006. Molecular biomarkers of oxidative stress in aquatic organisms in relation to toxic environmental pollutants. *Ecotoxicol. Environ. Saf.* 64, 178–189. <https://doi.org/10.1016/j.ecoenv.2005.03.013>.
- Vicari, T., Dagostim, A.C., Klingelfus, T., Galvan, G.L., Monteiro, P.S., da Silva Pereira, L., Silva de Assis, H.C., Cestari, M.M., 2018. Co-exposure to titanium dioxide nanoparticles (NpTiO₂) and lead at environmentally relevant concentrations in the Neotropical fish species *Hoplias intermedius*. *Toxicol. Reports* 5, 1032–1043. <https://doi.org/10.1016/j.toxrep.2018.09.001>.
- Vicq, R., Matschullat, J., Leite, M.G.P., Nalini Junior, H.A., Mendonça, F.P.C., 2015. Iron Quadrangle stream sediments, Brazil: geochemical maps and reference values. *Environ. Earth Sci.* 74, 4407–4417.
- Vieira, F., Gomes, J.P., Maia, B.P., Silva, L.G., 2015. *Peixes do quadrilátero ferrífero - guia de identificação*. Fundação biodiversitas. Belo Horizonte.
- Wolf, J.C., Wheeler, J.R., 2018. A critical review of histopathological findings associated with endocrine and non-endocrine hepatic toxicity in fish models. *Aquat. Toxicol.* 197, 60–78. <https://doi.org/10.1016/j.aquatox.2018.01.013>.